A study of near-ultraviolet radiation-induced damage in Escherichia coli.

Kelland, Lloyd R.

Award date:
1984

Awarding institution:
University of Bath

A STUDY OF NEAR-ULTRAVIOLET RADIATION - INDUCED DAMAGE IN ESCHERICHIA COLI.

THESIS

Submitted by Lloyd R. Kelland, B. Pharm., M.P.S.

for the degree of Doctor of Philosophy

of the University of Bath.

1984

This research has been carried out in the School of Pharmacy and Pharmacology of the University of Bath under the supervision of S. H. Moss, M.Sc., PhD., M.P.S. and D.J.G. Davies, M.Sc., PhD., F.P.S.

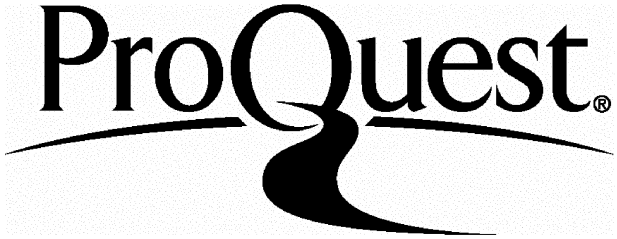

TO MY MOTHER AND FATHER,

for their foresight, encouragement

and sacrifice when it mattered most.

Iamque opus exegi, quod nec Iovis ira, nec ignis,

Nec poterit ferrum, nec edax abolere vetustas.

Ovid.

ACKNOWLEDGEMENTS.

The author wishes to express his gratitude for the encouragement and guidance received from Dr. S. H. Moss and Dr. D. J. G. Davies throughout all stages of this work.

His sincere thanks are also due to Professor J. E. Rees for providing facilities for this research, and to Mr. D. A. Vinicombe for invaluable technical assistance and help with the figures.

This research was funded by the Science and Engineering Research Council to which the author also wishes to express his gratitude.

His thanks are also due to Miss Karen Butler for typing the manuscript and to Mrs Sally Kelland for her diligent proof-reading of the manuscript.

SUMMARY

The introduction consists of a review of the current evidence concerning the effects of near-ultraviolet radiation on cells, with particular emphasis placed upon possible effects on cell membranes.

The experimental work, the broad aim of which is to expand existing knowledge of the effects of near-ultraviolet radiation that may lead to cell lethality, has centred upon the irradiation of a DNA repair-proficient Escherichia coli K-12 strain, SR385, using both monochromatic and broad-band sources. The work is divided into five parts. Chapter 1 indicates that broad-band near-ultraviolet irradiation of SR385 induces a sensitivity to inorganic salt, which is largely recoverable by holding treated cells in a complex recovery medium. By using various metabolic inhibitors, the recovery process has been related to a return of normal membrane functions. Chapter 2 describes an action spectrum, from 254-405nm, for ultraviolet radiation-induced salt sensitivity, and shows that this effect is important only at wavelengths above 310nm. The third part of the experimental section describes a more direct means of measuring ultraviolet radiation-induced membrane damage by the detection of leakage of radioactive labels from treated cells. An action spectrum, from 254-405nm, determined for ^{86} rubidium leakage, indicates that membrane damage may be important in near-ultraviolet (but not far-ultraviolet) radiation-induced cell lethality. Chapter 4 describes the effect of the phase of growth of the cell in determining its senstivity to near-ultraviolet radiation. The final chapter comprises a preliminary investigation into the effects of membrane damage in influencing the assessment of mutagenesis by near-ultraviolet

radiation, by reversion to prototrophy.

The data obtained in each section have been discussed in the context of current published concepts regarding the induction and repair of damage in cells by ultraviolet radiation.

Table of Contents

I N T R O D U C T I O N

Ultraviolet (UV) radiation, as a component of terrestrial sunlight, forms a part of the natural environment of most organisms. The range of wavelengths within the UV part of the electromagnetic radiation spectrum may be considered to extend from about 190 nm, below which, atoms and molecules may be ionized, to 400 nm, above which, the radiations may be detected by the human eye. UV radiation, unlike X rays and γ rays, may therefore be considered as a non-ionizing radiation.

The relationship between the energy and the wavelength of radiations is given by the following expression:

$E = \frac{h.c}{\lambda}$ (i) where E is the energy of the quantum in Joules

h = Planck's constant (which has a value of 6.624×10^{-34} J. sec.)

c = velocity of light (3×10^{10} cm^2. $sec.^{-1}$)

and λ = the wavelength in cm.

The energy of a quantum (or photon) is therefore, inversely proportional to the wavelength of the radiation.

The range of wavelengths within the UV region itself may be subdivided according to physical and biological properties as follows:

far-UV	(UVC)	190 - 290 nm
mid-UV	(UVB)	290 - 320 nm
near-UV	(UVA)	320 - 400 nm
(visible		400 - 750 nm)

The nomenclature far, mid and near - UV radiation will be used throughout this thesis, the alternative nomenclature UVA, UVB and UVC is used in the literature, particularly in dermatology. The division between far- and mid- UV radiation arises as a result of the absorption of solar - UV radiation by atmospheric ozone which cuts off all

radiation reaching the surface of the earth below 290 nm. Therefore, the environmentally relevant UV radiation within solar - UV radiation may be considered to consist of wavelengths from 290 to 400 nm, and thus does not include the higher energy far- UV radiation region. As shown above, solar - UV radiation may be further divided, according to its effects on human skin, into mid- UV radiation, where erythemal effects on the skin are apparent, and near- UV radiation.

The effects of UV radiation on cells.

The first observation of an effect of UV radiation on living systems occurred in 1877 when Downes and Blunt reported the inactivation of bacteria. In 1930, F.I. Gates published an observation regarding the wavelength dependence for bacterial inactivation (i.e. an action spectrum for killing) by UV radiation of wavelengths 230 - 302 nm, showing that a peak in the killing of Staphylococcus aureus and a Bacillus species occurred around a wavelength of 265 nm. This observation contradicted previous ideas that the shorter the wavelength the more marked the bactericidal action and introduced the idea of a specific 'vital' target being involved for inactivation.

Since Gates' observations, the production of action spectra has proven to be a most useful tool in attempting to identify possible cellular 'targets', or chromophores, for the effects of UV radiation on cells. An action spectrum is defined as a plot of the reciprocal of the number of incident photons required to produce a given effect against wavelength - the most efficient wavelength producing the effects at the lowest doses. The chosen end-points for the production of action spectra are generally those considered to be related by a common cellular target to the effect of interest in the whole organism. For UV radiation studies in bacteria this has generally

meant inactivation or mutation induction, defined as an alteration in the phenotypic characteristics of the resulting progeny.

We now know that action spectra for inactivation, by far- UV radiation, of a wide variety of cells, show a close correspondence to the absorption spectrum of DNA, which has a peak absorbance at around 260 nm, implicating DNA as the chromophore for the effects observed. The nature of the DNA damage induced by far- UV radiation has largely been elucidated; the primary lesion being the pyrimidine dimer. The main dimer involved is one between two adjacent thymine molecules on the DNA strand, as shown in Figure 1, where the molecules are linked between their respective 5 and 6 carbons, thus forming a cyclobutane ring between. The photochemical formation of the thymine dimer was discovered by Beukers and Berends in 1960.

Figure 1.
A cyclobutane-type thymine dimer.

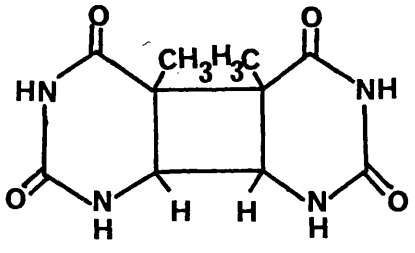

Cytosine-cytosine, uracil-uracil, thymine-cytosine, uracil-thymine and uracil-cytosine dimers may also be produced but in much lower yields than the thymine-thymine dimer. Although the thymine-thymine dimer DNA photoproduct has been the one most extensively studied, due to its unique chemical stability and ease of isolation and assay, other lesions in DNA have also be identified as being of possible importance in far- UV radiation - induced cell lethality. These other lesions include the formation of cross-links between DNA and protein or between two DNA strands, the hydration of pyrimidine molecules, the oxidation or reduction of pyrimidines especially to form 5, 6 - dihydroxythymine, chain breaks, and possibly reactions involving the purines although they are about 10-fold more resistant to photo-

chemical alteration than are the pyrimidines. The effects of far-UV radiation on cells have been the subject of a number of reviews (e.g. Swenson, 1976; Smith, 1977).

Much of the evidence of the importance of DNA as a target in far- UV radiation - induced cell lethality and in the elucidation of the lesions involved, has been obtained by isolating and using bacteria found to be particularly sensitive to far- UV radiation. These 'sensitive' bacteria have since been found to be lacking one or a number of gene products concerned with the repair of damaged DNA. Three such repair processes have thus far been recognized; photoreactivation, excision and postreplication.

(a) Photoreactivation.

This repair process, first recognized by Kelner in 1949, and under the control of the phr gene in Escherichia coli, involves the photoenzymatic removal of pyrimidine dimers from DNA. In the dark, the photoreactivating enzyme specifically recognizes and attaches to cyclobutane-type, pyrimidine dimers in DNA to form an enzyme substrate complex. This complex is then activated by the absorption of light between 320 - 420 nm, the pyrimidine dimers are converted back to monomeric pyrimidine bases, and the enzyme is released.

(b) Excision repair.

Evidence of this repair pathway, the first of the two 'dark' repair processes to be understood, arose from the observations of Setlow and Carrier (1964) and Boyce and Howard-Flanders (1964). They found that thymine dimers were removed from the DNA of wild-type E. coli during post-irradiation incubation but not from the DNA of UV-sensitive strains such as E. coli B_{s-1}. The loci conferring this

sensitivity were mapped and designated uvrA, uvrB and uvrC. An early model for excision repair is shown in figure 2.

The pathway is proposed to occur by four basic steps: (1) an endonuclease, coded for by the uvrA or uvrB genes recognizes the lesion and makes an incision in the DNA strand. This initiation step can occur by two methods termed nucleotide excision repair, where the whole damaged region of DNA is excised, or more recently by the process termed base excision repair, where an altered base is recognized and cut off the DNA chain by a N- glycosidase leaving an apyrimidinic or apurinic site in the DNA that is then susceptible to attack by a specific endonuclease. (2) Repair replication is then initiated by the action of a DNA polymerase, coded for by the pol A, B or C genes, using the opposite strand of DNA as the template. (3) The damaged section of DNA is excised by an exonuclease. (4) The break in the DNA strand is sealed enzymatically by polynucleotide ligase.

This has proven to be the major pathway for excision repair, but another minor one can proceed but only when the cells are in complete growth medium. The major growth medium - independent pathway appears to be error free and to make short patches of repair replication, while the growth medium - dependent pathway makes long patches and appears to be error prone and hence may lead to mutations.

(c) Postreplication repair.

The evidence for another dark repair pathway arose from work by Rupp and Howard - Flanders (1968) who showed that newly synthesized DNA in UV- irradiated excision-deficient strains of E. coli was smaller than in unirradiated cells. They interpreted their results as evidence for the existence in the daughter DNA strands of gaps,

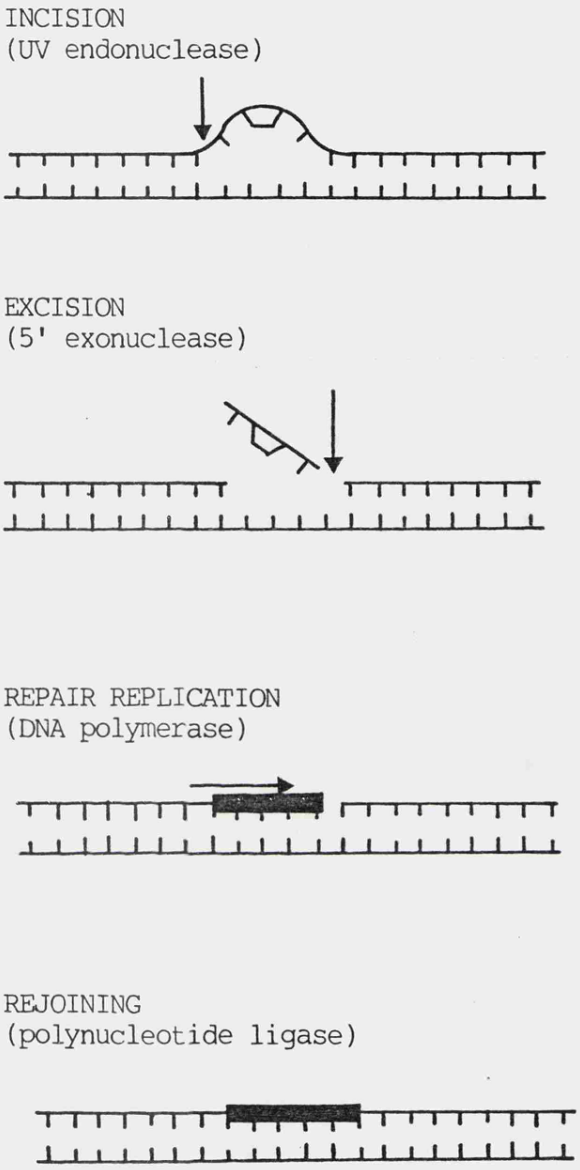

Figure 2. The excision repair process.

which they presumed were opposite the pyrimidine dimers in the parental strands. The subsequent sealing of these gaps has been shown to be a very complex process but it does occur, probably by utilizing material from the parental strands by a recombinational process, and it has been shown to be absolutely dependent on the rec A gene product. A number of independent biochemical pathways have been proposed for this repair in E. coli, including pathways controlled by the rec B, lex A, uvr D and rec F genes (Youngs and Smith, 1976). The pathways involving the lex A gene product are thought to be error prone, and hence mutagenic, as rec A, lex A mutant strains are totally refractory to UV - induced mutagenesis. Extensive and detailed reviews on these DNA repair processes are available (Lehmann and Bridges, 1977; Hanawalt et al., 1978; Lehmann and Karran, 1981; and specifically on photoreactivation; Sutherland, 1977).

The effects of near-UV radiation on cells.

Although it is well established that far-UV radiation - induced cell lethality, as outlined above, is primarily due to damage in DNA, the cellular effects of radiations above 320 nm are less clear. Furthermore, as it is these wavelengths that are present in the solar spectrum reaching the surface of the earth and are thus environmentally relevant, it is thus essential that the largely ill-defined effects of near-UV radiation on cells are elucidated.

Hollaender (1943) was the first to establish that high fluences of near-UV radiation can kill bacteria in the absence of added sensitizers. Using E. coli he observed that it required 10^3 to 10^4 times as much incident energy to kill to the same extent at 350 - 490 nm as at 265 nm. Luckiesh (1946) published a preliminary action spectrum for lethality in E. coli extending from 200 - 700 nm. Further to Luckiesh's original

data, action spectra for cell killing extending into the near-UV radiation region have been published for a variety of organisms. For a review see Webb (1977). The sensitivity to each wavelength has generally been expressed, as quantum units, in terms of either the inactivation constant (k), derived from the final slope of the survivor curve, or the reciprocal of the fluence required to reduce the surviving fraction to 37 or 10% (F_{37} or F_{10} values respectively). The derivation of these parameters and the reasons behind the choice of any particular one in preference to another for use in action spectrum determinations is discussed in the treatment of data section of the general methodology.

A typical action spectrum for lethality in E. coli B/r Hcr, a strain lacking the ability to repair DNA by the excision pathway, under aerobic or anaerobic conditions, is shown in Figure 3. Also included in Figure 3, is the absorption spectrum for thymidine which acts as a close approximation for the DNA absorption curve. Some striking observations can be made from this action spectrum for cell killing. First, at wavelengths longer than 320 nm, cell inactivation is more effective under aerobic than under anaerobic conditions. Second, the cell sensitivity closely follows the curve for the absorbance of DNA over the range of 240 - 313 nm, but at longer wavelengths, a deviation from the curve occurs. Third, a significant shoulder in the cell inactivation curve under aerobic conditions is apparent around 340 nm. There is also a small shoulder around 365 nm and shoulders at 410 and 500 nm in the visible region of the spectrum. The sensitivity is expressed in terms of the inactivation constant (k). However, similar shoulders were apparent at the same wavelengths for an action spectrum of E. coli B/r Hcr based on $^{1}/F_{37}$ values (Webb and Brown, 1976).

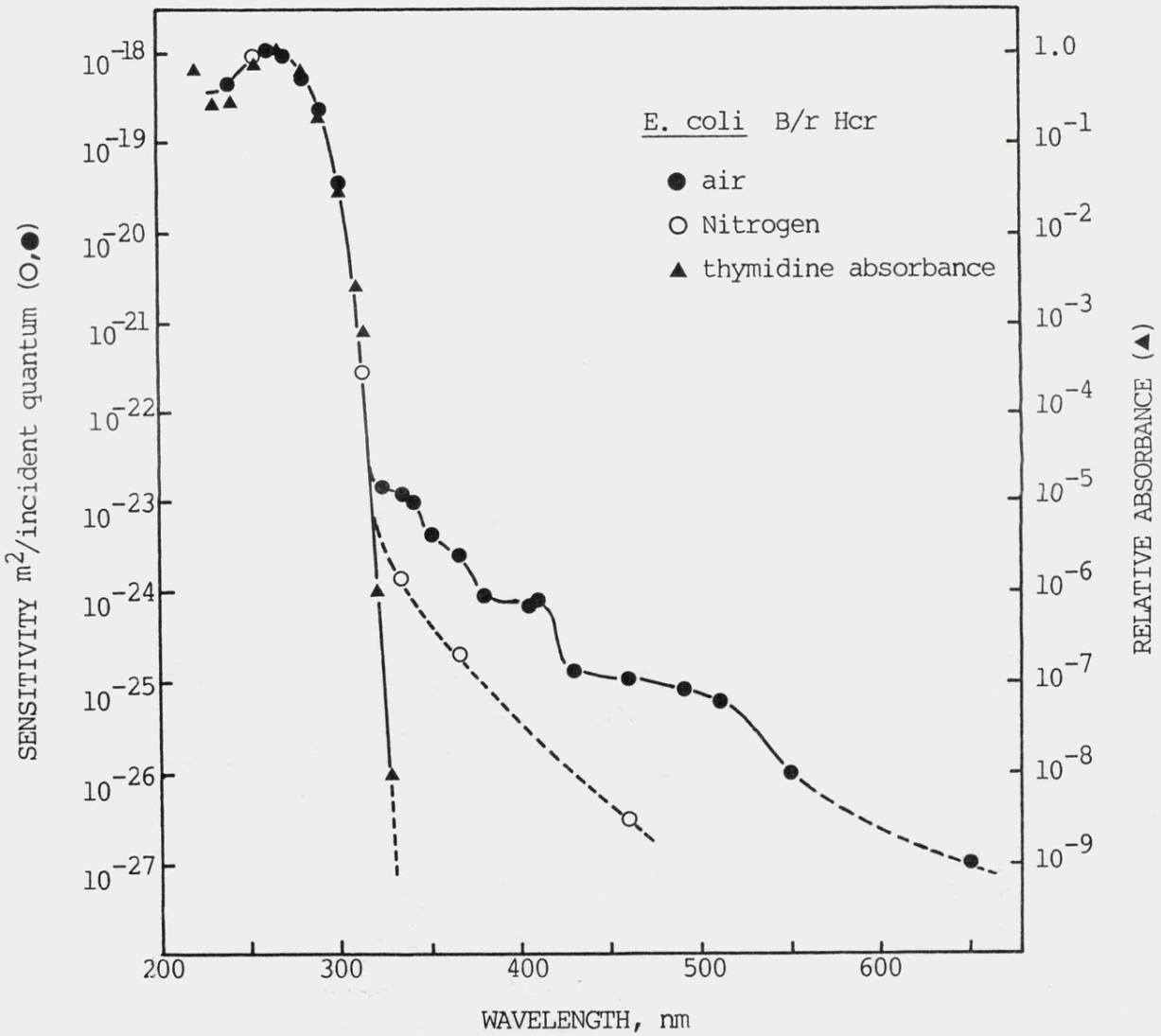

Figure 3

Action spectra for the inactivation of stationary phase cells of E. coli B/r Hcr. The inactivation constant is the final slope k. Cell suspensions were irradiated at 25°C.
(reprinted from Webb, 1977).

An oxygen dependence for near- UV irradiated cells also has been shown in other microorganisms; in a carotenoid - deficient colourless mutant of Sarcina lutea (Mathews and Sistrom, 1959); in a Salmonella typhimurium strain (Eisenstark, 1970); and in two series of DNA deficient E. coli K12 mutants in which all showed oxygen dependence at 365 nm except the uvr A, rec A double mutant (Tyrrell, 1976). This oxygen dependence provides a clear distinction between cells irradiated with wavelengths less than 320 nm, which do not show such a response (Webb and Lorenz, 1970), and formed one of the first pieces of evidence that their biological effects may be different. Oxygen dependence suggests that the lethal effects at wavelengths longer than 320 nm may involve photodynamic processes mediated by endogenous sensitizers. Moreover, further evidence to suggest the differing biological effects of far and near- UV radiations, which is not readily apparent from Figure 3, is that the near-UV survival curves exhibited larger shoulders compared to the far - UV survival curves.

It is difficult to measure the absorbance of DNA at wavelengths longer than 320 nm because of light scatter i.e. turbidity effects (Sutherland and Griffin, 1981). However, by using procedures that subtract contributions due to light scattering they have shown that DNA absorption is significant, but very low, up to 350 nm. Also Webb (1977) has calculated that the absorbance of thymidine at 330 nm is 1×10^{-8} of its absorbance at 260 nm, whereas the sensitivity ratios based on quantum units in E. coli B/r Hcr are 1.9×10^{8} for 260 nm vs. 550 nm, and 1.3×10^{9} for 260 nm vs. 650 nm. Therefore, while some of the lethal and mutagenic actions of near - UV radiation may be due to direct absorption in DNA, the majority of the aerobic lethal response is probably due to absorption by other molecules causing either DNA molecular alterations or other effects lethal to

the cell. The presence of the shoulders around 340 and 365 nm may well indicate the involvement of a chromophore or chromophores conferring sensitivity under aerobic conditions at this near - UV radiation wavelength region.

Thus effects on cells, other than DNA damage, may be of importance in our understanding of near - UV radiation-induced effects. A number of different effects have been recognized involving different cellular components. They may be broadly divided into sublethal effects and effects leading to cell death or mutation.

Sublethal effects.

Sublethal effects normally occur in E. coli at fluences about one order of magnitude lower than lethal fluences. The first effect to be recognized was the phenomenon of growth inhibition, which consists of a 'growth delay', on average of about 90 minutes, plus a small growth rate-depression (see Jagger, 1972 for a review). Action spectra for near - UV radiation-induced growth delay show a narrow range from 300 to 380 nm with a peak effect around 340 nm (Jagger et al., 1964; Kubitschek and Peak, 1980). The probable chromophore for this effect was determined from observations that rel strains of E. coli, which show no immediate cessation in RNA synthesis on deprival of a required amino acid, show no such growth inhibition after near - UV irradiation, whereas normal 'stringent' rel^+ strains do exhibit growth inhibition. Further studies showed that near - UV radiation simulates this amino acid starvation due to absorption by 4 thiouridine (^{4}Srd), an unusual base occurring in the 8-position of many tRNAs of E. coli (Ramabhadran et al., 1976; Thomas and Favre, 1975). Absorption of near - UV radiation by this chromophore results in the production of adducts in the tRNA's which prevents RNA synthesis

and subsequent protein synthesis, with resultant growth delay. This evidence has been substantiated by the isolation and use of ^{4} Srd^{-} mutants lacking 4-thiouridine, the production of which is controlled by the nuv gene in E. coli (Ryals et al., 1982) which show no growth inhibition. Moreover, the two other sublethal effects thus far observed in E. coli, the reduction of bacterial capacity for phage development (Wingo et al., 1980) and inhibition of induced-enzyme (tryptophanase) synthesis (Sharma et al., 1981) have recently been shown to also involve ^{4}Srd as the primary chromophore. However, growth delay in Bacillus subtilis seems to involve another chromophore, menaquinone (Taber et al., 1978). An extensive review of these effects is available (Jagger, 1981).

Effects leading to cell death and mutation induction.

i) Damage to DNA.

As for far- UV radiation studies, damage to DNA is one of the main causes of near - UV radiation-induced cell lethality. Indeed the current interpretation of near - UV radiation survival curves is generally based on the assumption that inactivation is due to DNA damage (Webb and Brown, 1976; Webb et al., 1976), in some cases amplified by damage to DNA repair enzymes (Tyrrell, 1976). However, while the evidence implicating cellular DNA damage after near - UV irradiation is unequivocal, the direct absorption of the radiation by DNA in unlikely (as explained above) and the importance of this damage in producing cell lethality is questionable. In some cases (Harrison, 1967; Peak, 1970) results have shown that two E. coli strains differing in DNA repair capability, B/r and Bs-1 (uvr B, lex A,) exhibit the same sensitivity in exponential phase to broad-band (330-380 nm) or 365 nm radiation. In contrast, other reports have shown that the repair capability of the organism does influence near - UV radiation

survival. Eisenstark (1970) showed sensitivity differences between recombination-deficient S.typhimurium and E. coli strains and wild-type and excision-deficient strains. Also, E. coli B/r Hcr was 2.5 times more sensitive than B/r at 365 nm (Webb and Lorenz, 1970) but the difference was not as great as at wavelengths below 313 nm (Webb and Brown, 1976). Further evidence has been reported by Webb et al. (1976) who, while using a series of five E. coli K12 strains, obtained the following sensitivity value ratios (in terms of $^{1}/F_{37}$) : AB 2480 (rec A, uvr A) being most sensitive was assigned a value of 1.0; AB 2463 (rec A), 23; AB 1886 (uvr A), 35; P3478 (pol A), 22; AB 1157 (repair-competent), 67. However, these ratios are less than the corresponding values at 254 nm, indicating the reduced importance of DNA repair capability at 365 nm.

As for far - UV radiation, pyrimidine dimers have been identified as one of the main types of near - UV radiation-induced lesion in DNA (Brown and Webb, 1972; Tyrrell, 1973). By way of contrast, different ratios of dimer type are observed at 254 and 365 nm; the ratio of thymine-thymine (T>T) to uracil-thymine (U>T) dimers at 254 nm is 1.1 - 1.2* whereas at 365 nm it is 5 (Webb, 1977). However, dimers are not thought to be important in terms of lethality for repair competent strains, except under anaerobic conditions, as under normal conditions the inactivating light itself will photoreactivate the majority of the dimers (concomitant photoreactivation). Indeed, it has been shown that no significant photoreactivation is observed after 365 nm irradiation of uvr A or repair proficient strains of E. coli K12. Under aerobic irradiation pyrimidine dimers appear to be lethal only in completely repair-deficient cells (e.g. AB 2480 rec A uvr A) or in cells that have photoreactivating enzyme but are irradiated at 0°C (Webb et al., 1976).

* Webb (1977) has misquoted Setlow & Carrier (1966) J. Mol. Biol. 17 , 237-254. The actual value of T>T:U>T dimers is 3.3.

Near - UV radiation can also induce single-strand breaks in DNA (Tyrrell et al., 1974). Action spectra for DNA strand-break induction have been obtained by Peak and Peak (1982) for B. subtilis and by Rosenstein and Ducore (1983) for normal human fibroblasts. The increased importance of strand-breaks compared to dimers after near - UV irradiation was shown by Webb (1977) who calculated the ratio of dimers to breaks at 254 nm to be 800, at 313 nm the ratio declined to 21, at 365 nm it was 1.8 and at 405 nm it was less than 0.1. Single-strand breaks are now thought to be the major lethal lesion in DNA under aerobic 365 nm irradiation as no detectable breaks are induced under anaerobic (nitrogen) conditions (Tyrrell et al., 1974). Also a reduction in breaks is observed in the presence of AET (2-aminoethylisothiouronium.bromide - HBr), a free radical scavenger, suggesting a free radical involvement in DNA strand-break induction by 365 nm radiation (Webb, 1977). In addition, the rate of single-strand break induction has been implicated as the reason for the increase in resistance to 334 nm radiation shown by $^{4}Srd^{-}$ mutants after Tsai and Jagger (1981) reported $^{4}Srd^{-}$ mutants to be about twice as resistant to 334 nm radiation as wild-type cells, hence suggesting 4-thiouridine as a possible chromophore for near - UV radiation-induced cell lethality as well as for growth delay. Peak et al. (1983a) have correlated this with a slower induction of single-strand breaks in $^{4}Srd^{-}$ mutants. A repair of strand-breaks was observed by Ley et al. (1978) who showed that post-irradiation incubation of wild-type cells in buffer results in rapid repair (up to 80% in 10 minutes), with repair dependent on the pol A gene.

Other lesions in DNA may also be important in near - UV radiation-induced cell lethality. Cabrera-Juárez and Setlow (1977) found a thymine containing photoproduct that is similar but not identical to

the spore photoproduct 5-thyminyl - 5,6-dihydrothymine, after near - UV irradiation of purified DNA. This finding has been supported in HeLa cells by Hariharan and Cerutti (1977). Hartman et al., (1979) have found DNA - protein cross-linking to be important in the combined near - UV radiation plus H_2O_2 inactivation of phage T7.

As a consequence of the presence of these lesions in DNA and the existence of error prone repair systems, mutation induction after near - UV irradiation might be expected. However, early efforts to induce mutations with wavelengths longer than 320 nm were either unsuccessful or of doubtful validity (see Eisenstark, 1971 for a review), one exception being that Kubitschek (1967) unequivocally demonstrated mutation to bacteriophage T5 in chemostat cultures of E. coli by wavelengths between 320 - 400 nm. Webb and Malina (1970) then confirmed this finding and extended it to the visible region of the spectrum.

A proposal regarding the nature of the premutational lesion has been put forward by Webb (1978). He showed, using photoreactivation as an indicator, that mutation, measured by reversion to tryptophan independence, but not killing, in a uvr A mutant of E. coli WP2 is caused by pyrimidine dimers. However, subsequent large differences shown between mutant and dimer yields in different strains with 254 and 365 nm radiation demonstrate that non-dimer factors may also be important in near - UV radiation mutagenesis (Webb and Turner, 1981). These non-dimer lesions maybe single-strand breaks or pyrimidine adducts. Therefore the current interpretation of near - UV radiation mutagenesis involves a multiple component mechanism. This may possibly be an interaction of nondimer oxygen-dependent lesions and pyrimidine dimers.

Near - UV radiation mutagenesis has been consistently difficult to observe in wild-type E. coli strains. In a series of E. coli strains differing in repair capability, after 254 nm radiation, mutants were observed in all strains except the lex A and rec A strains thus confirming the role of error prone repair in mutagenesis. In contrast, after broad spectrum near - UV radiation, in addition to the lex A and rec A strains, no significant induction of mutants was observed in wild-type or pol A strains (Turner and Webb, 1981). They have suggested that this is due to a relative enhancement of error-free repair that results from the inhibition of error-prone rec A^+, lex^+ - mediated pathways by the broad-band radiation. In addition, Tyrrell (1980) observed, that with exponential phase cells, monochromatic 365 nm radiation did not induce mutants (reversion to tryptophan independence) in the repair proficient strains B/r and AB 1157. He interpreted this to be due to near - UV radiation induced-growth delay allowing more time for constitutive, primarily error-free, repair to occur.

Conversely, with monochromatic 365 nm radiation, Webb and Turner (1981) using the same strains as for their broad-spectrum data, observed mutation induction in stationary phase wild-type and pol A strains, but only at fluences where more than 90% of the cell population had been inactivated. Therefore, Turner and Webb have concluded that monochromatic and broad-band near - UV radiation sources provide differing responses toward mutagenesis. Also, the failure to observe significant mutagenesis after near - UV irradiation, under some cultural conditions (e.g. Cabrera-Juárez and Espinosa-Lara, 1974 with Haemophilus influenzae) may be due to a greater susceptibility of the error - prone rec A^+ lex^+ dependent repair system.

Webb (1978) also found that the type of agar plate used to assess

mutagenesis influenced the number of mutants obtained. After 365 nm radiation, many more mutants were observed on minimal plates supplemented with 2% nutrient broth (semi-enriched medium, SEM) than on minimal agar supplemented with tryptophan only, whereas at 254 nm, the opposite effect occurred. He attributed this 365 nm radiation-effect to selective damage to repair systems or selective recovery on SEM of repair systems involved in mutagenesis.

ii) Damage to DNA repair systems.

In addition to the induction of lesions in DNA, near - UV radiation has been shown to inhibit the full functioning of DNA repair systems. Tyrrell et al. (1973) reported that cells which were damaged by fluences of 365 nm radiation, sufficient to inactivate repair - proficient strains of E. coli, and then exposed to 254 nm radiation, show a reduction in their capacity to photoreactivate 254 nm-induced dimers. The extent of this reduction increases with increasing dose. He proposed that this is due to the inactivation of the photoenzymatic repair system by near - UV radiation. Tyrrell (1976) then supported his hypothesis by observing the in vitro oxygen-dependent 365 nm inactivation of the yeast photoreactivating enzyme.

The capacity to excise pyrimidine dimers is also impaired by fluences of 365 nm radiation in the biological range (Tyrrell and Webb, 1973). After a 365 nm fluence of 1.5×10^6 Jm^{-2}, only 15% of the capacity to excise pyrimidine dimers remained. The rate of inactivation of the same repair-proficient strain increased sharply at fluences greater than 1.5×10^6 Jm^{-2} indicating that damage to the excision repair system may be the cause of the sharp increase in 365 nm inactivation at higher fluences. Finally, Webb et al. (1978) have suggested that both excision and recombination repair processes are

significantly impaired by fluences of 365 nm radiation greater than 1×10^6 Jm^{-2} as both exponential and stationary phase wild-type and uvrA (excisionless) E. coli strains were strongly sensitized to 254 nm radiation by a prior exposure to 365 nm radiation.

iii) Growth phase effects.

Bacterial sensitivity to near - UV radiation depends greatly upon the growth phase. Harrison (1967) and Peak (1970 - as shown in Figure 4) reported that cells of repair-proficient strains of E. coli show a greater sensitivity to near - UV radiation in the rapidly growing (exponential) phase than in stationary phase. Subsequently this result has been shown for other repair - proficient E. coli strains (Tuveson and Jonas, 1979 for AB 1157; Hartman and Eisenstark, 1978 for W 3110) and for the human urogenitalparasite Trichomonas vaginalis (Daly et al., 1981). In addition, Tuveson and Jonas (1979) showed a greater sensitivity to near - UV radiation in exponential-phase cultures for recA, relA and recA, nur strains of E. coli. Eisenstark (1970) and Mackay et al., (1976) have also reported that recA strains of S. typhimurium and E. coli are readily inactivated by broad-band near - UV radiation in exponential growth phase but not inactivated by even greater fluences in stationary phase. However, sensitivity differences between exponential - and stationary-phase cells for some repair-deficient strains are not as clearcut. Webb and Peak (unpublished but cited by Webb, 1977) tested the 365 nm sensitivity of four E. coli strains at different stages of the growth cycle. AB 1157 (wild-type) and AB 2463 (rec A) showed much greater sensitivity in exponential phase, whereas strains deficient in excision repair, AB 1886 (uvr A) and AB 2480 (uvr A, rec A), were approximately equal in sensitivity in exponential and stationary phase.

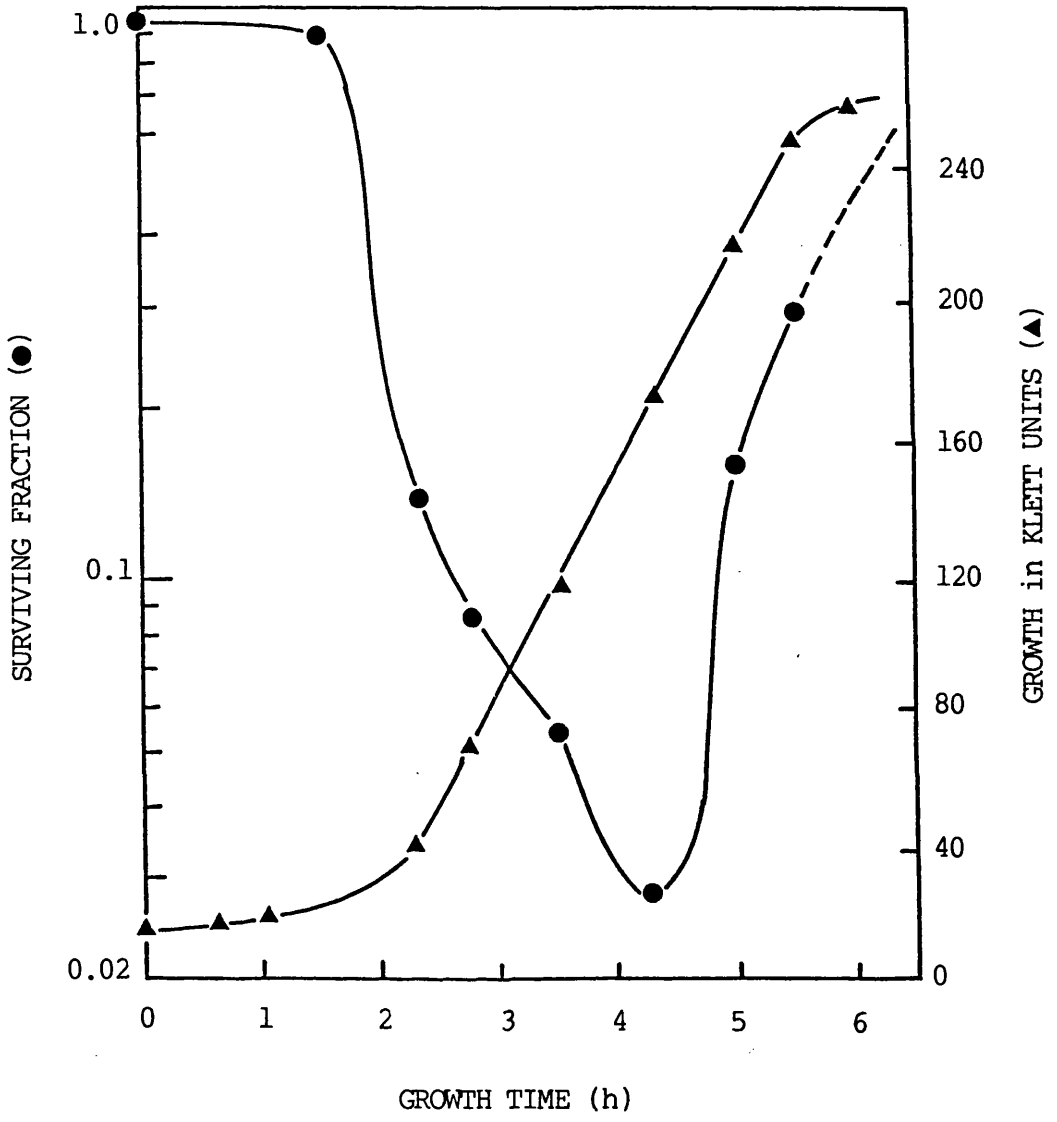

Figure 4

Inactivation of E. coli B/r at 365 nm at a constant fluence (1.44×10^{6} Jm^{-2}) throughout the growth cycle.

Modified from Peak, 1970.

This finding for excisionless strains is also observed at 254 nm (Tyrrell et al., 1972) and may account for the failure of some workers to observe a greater near - UV radiation sensitivity of repair-deficient strains than repair-proficient strains (Peak, 1970; Harrison, 1967). Also, Eisenstark (1970) and Mackay et al. (1976) have reported the difference in sensitivity of exponential - and stationary-phase strains to be considerably greater for inactivation by broad-band near - UV radiation than for monochromatic radiation.

A possible mechanism for the increased sensitivity of exponential-phase cells was suggested by Peters (1977) who implicated the photo-inactivation of the ribonucleoside diphosphate reductase complex in the killing of exponentially growing E. coli by near - UV radiation. More recently, Peters and Jagger (1981) have suggested that exponential-phase cells may also possess additional mechanisms for the repair of near - UV radiation-induced damage. They described a new inducible repair system which repairs a major proportion (about 90%) of the damage produced at 365 nm. These findings emphasize the importance of carrying out near - UV radiation lethality studies with cells that are clearly in a particular growth phase.

(iv) Additional genetic factors.

In addition to the numerous genes controlling the repair of damaged DNA, Tuveson and Jonas (1979) have isolated a gene product (nur) of E. coli K-12 that specifically confers near - UV radiation sensitivity in stationary-phase cells. On isolation of isogenic strains representing all four combinations of the recA and nur genes (RT-1, nur, recA;RT-2,nur; RT-3, recA: RT-4, repair-competent), the recA and wild-type strains showed little difference in sensitivity to near - UV radiation whereas the strains containing the nur mutation

showed increased sensitivity. However, after 254 nm irradiation, the nur and the wild-type strains showed approximately the same sensitivity while the recA strains showed a much greater sensitivity. This suggests that the nur gene and not the recA gene produces near - UV sensitivity. Subsequently, the nur gene has been shown to occur in the 50-53 min region of the chromosome which is near the position of the recA gene at 58 min. This finding may explain some of the variable results found for near - UV radiation sensitivity dependence upon the recA gene since the recA and nur genes may easily be cotransduced. Furthermore, on isolation of all four combinations involving the nur and uvr A genes, a similar result to the recA / nur observation was obtained (Tuveson, 1980) indicating that, as was true for recombination deficiency, an excision repair defect (uvr A6) does not lead to near - UV radiation sensitivity for stationary phase cells. Finally, Tuveson (1981) has isolated the four polA/nur combinations and shown that the polA gene also sensitizes cells to near - UV radiation, but only in a nur^+ strain, suggesting that these two mutations may sensitize by an equivalent mechanism. This may also explain the frequent failure of polA strains to provide near - UV radiation sensitization.

Webb and Tuveson (1982) have presented evidence that the nur mutation sensitizes cells to inactivation by monochromatic 365 nm radiation as well as broad spectrum near - UV radiation. They observed a nur sensitization from 313 - 405 nm with a broad maximum effect occurring at 334 and 365 nm; with no sensitization being observed at wavelengths below 300 nm. More recently, Peak et al. (1983b) have determined action spectra for the aerobic and anaerobic inactivation of nur^+ and nur^- strains of E. coli which showed negligible oxygen dependence below 315 nm and a large peak oxygen enhancement ratio at 365 nm.

Various mechanisms for the sensitization of cells to near - UV radiation by the nur gene, including cell membrane damage and the accumulation of endogenous photosensitizers, have been proposed (Webb and Tuveson, 1982) but the current interpretation involves a correlation with an enhancement of single-strand breaks in DNA in nur strains (Tuveson et al., 1983).

(v) Wavelength interactions.

These experiments, which involve an exposure to radiation of one wavelength before subsequent survival or mutation assessment with radiation of another wavelength, have been performed between wavelengths in the near - UV range or between wavelengths in the near and far - UV range. A strong lethal interaction between various monochromatic near - UV wavelengths has been demonstrated for 334, 365 and 405 nm in repair-proficient E. coli K-12, with the exception of pre-exposure to 405 nm, which protects cells from the lethal effects of 365 nm radiation (Tyrrell and Peak, 1978; Webb et al., 1982). They suggest that, this synergism is due to the wavelengths producing a common type of sublethal damage, possibly damage to repair enzymes. These interactions illustrate the difficulty of interpreting experiments carried out with broad-band near - UV radiation sources.

Near - UV/far - UV wavelength interactions generally involve antagonisms such as photoreactivation, where irradiation with near - UV light after irradiation with far - UV reduces the biological effects of the far - UV radiation, or photoprotection, where irradiation with near - UV light before irradiation with far - UV reduces the effects of the far - UV radiation. Photoprotection is thought to occur by means of growth delay induced by near - UV radiation and so allowing more time for DNA repair to occur (Tsai and Jagger, 1981).

However, some synergistic lethal interactions may occur between near and far - UV radiations at much higher fluences than those used in photoprotection experiments. These synergisms are generally thought to be due to damage to DNA repair enzymes (Webb et al., 1978; Webb and Brown, 1979a).

The number of mutants measured as reversion to tryptophan independence, induced by far - UV radiation is also affected by pre-treatment with near - UV radiation. A progressive decline in far - UV radiation-induced mutants was observed after pre-exposure with increasing fluences of near - UV radiation (wavelengths 334, 365 and 405 nm) in a wild-type E. coli strain. However, in a uvr A strain, an increase in the number of far - UV radiation-induced mutants was observed (Tyrrell,1978b; Tyrrell, 1980; Turner and Webb, 1981). This mutational antagonism in wild-type cells may be due to growth delay induced by near - UV radiation, as $^{4}Srd^{-}$ mutants show no such interaction (Tyrrell, 1980; De Moraes and Tyrrell, 1983), the growth delay allowing more time for error-free excision repair to occur.

(vi) Effects on cell membranes.

The possibility of near - UV radiation inducing a damaging effect on bacterial cell membranes was first proposed by Hollaender (1943). However, membrane damage as a possible factor in near - UV radiation-induced cell killing has been largely overlooked since the realization of the importance of DNA to cells, and indeed, the discovery that near - UV radiation exerts a damaging effect on DNA. Recently though, several papers have proposed that near - UV radiation-induced cell lethality in E. coli also may include membrane - related components. As this thesis is concerned with near - UV radiation effects on membranes, before discussing these

observations in detail, an appreciation of the structure and functions of the cell membrane in E. coli is included to assist in making predictions as to the chromophores or mechanisms involved in these effects.

The generally accepted structure of the cell envelope of E. coli is shown in Figure 5. The envelope is composed of three regions; an inner cytoplasmic (or plasma) membrane, of thickness 7.5 nm, and two regions which constitute the cell wall; a cytoplasmic space containing a very thin layer of peptidoglycan (1 nm) and an outer membrane region, of thickness 7.5 nm. This is in contrast to gram-positive organisms which possess a similar inner cytoplasmic membrane but this is surrounded by a thick cell wall composed of peptidoglycan (20 to 80 nm) and no outer membrane.

(a) The cytoplasmic membrane.

The cytoplasmic membrane (CM) is a site of high enzyme activity making this cell component of paramount importance in the maintenance of the integrity of cells. The CM is composed of 60-70% protein, 20 to 30% lipid and small amounts of carbohydrate. The proteins, which constitute as much as 20% of the total protein of a bacterium, are known to be of two types; 'peripheral' or 'extrinsic' proteins which are easily removed by altering the ionic strength of the suspending fluid or by the use of chelating agents such as EDTA; and 'intrinsic' or 'integral' proteins which cannot easily be removed except by agents breaking hydrophobic bonds, such as detergents and some organic solvents. Extrinsic proteins are attached principally by ionic bonds, probably with the involvement of divalent cations, such as Mg^{2+}.

Membrane lipids are amphipathic molecules, i.e. they are structurally asymmetric having one highly polar region while the other end is strongly non-polar. This realization led to the now widely accepted 'fluid mosaic' model (Singer and Nicolson, 1972) for the arrangement of the proteins and lipids of the CM. The model, which

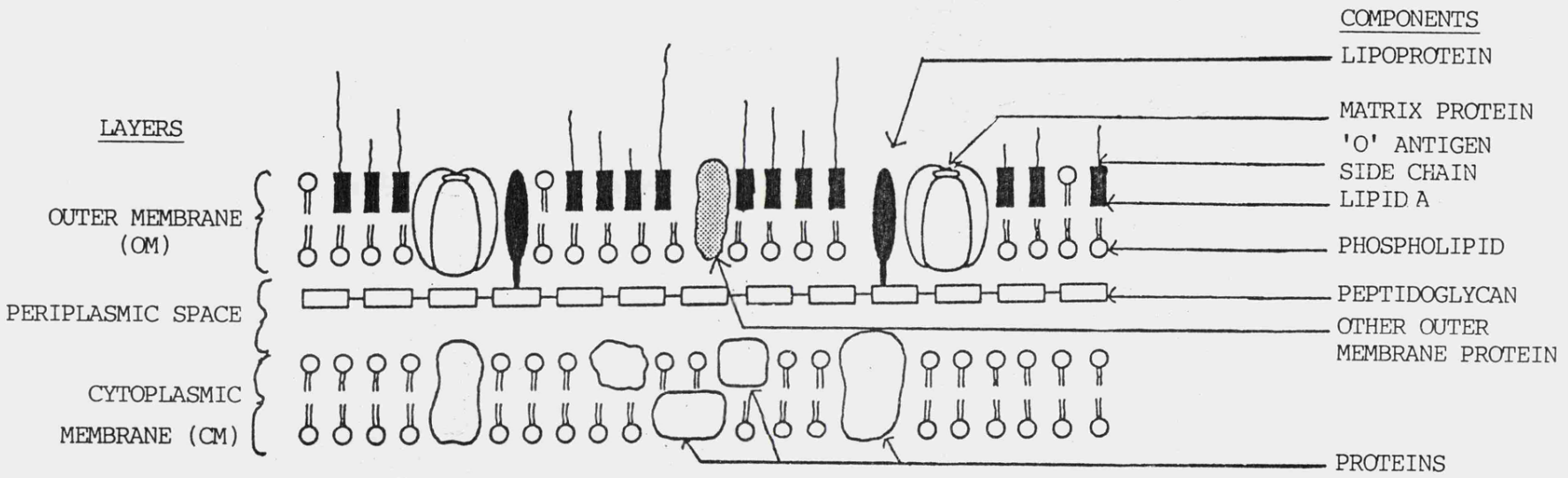

Figure 5

Diagram of the cell envelope of Escherichia coli.

From Davis et al., 1980.

assumes the proteins and lipids to be linked not by strong covalent bonds but by many weaker hydrophobic and hydrophilic linkages working co-operatively, is shown in Figure 6. The figure shows that the lipids largely arrange themselves in a bilayer in such a way as to minimize the free energy of the structure, i.e. with the non-polar hydrocarbon chains of the fatty acids facing inwards towards each other and the polar regions facing outwards towards the aqueous environment. About 70 - 80% of the membrane area is thought to be arranged in this way. The integral proteins, some of which pass completely through the bilayer, are then interspersed into the lipid matrix as shown. This model does not take into account the easily removed peripheral proteins. Therefore the membrane may be regarded as a viscous lipid fluid with protein molecules floating in it to various depths. Both the lipids and proteins are capable of rather rapid lateral movements; there is general agreement that lipids can redistribute over the surface of a membrane at a rate of about $10^{-8} cm^2\ sec^{-1}$, with proteins moving at a rate approximately 100 times slower (Rogers et al., 1980). Other evidence has shown that the bilayer is asymmetric; the components of the two leaflets making up the bilayer may be different (Rogers et al., 1980).

The lipids are mainly phosphatides with traces (<1%) of undecaprenol-phosphate. In E. coli membranes, three main phosphatides have been recognized; phosphatidylethanolamine (constituting about 77% of the total lipid phosphorus), phosphatidylglycerol (11%) and diphosphatidyl-glycerol (7%) which is also known as cardiolipin (Rogers et al., 1980). The basic structure of these molecules is shown in Figure 7.

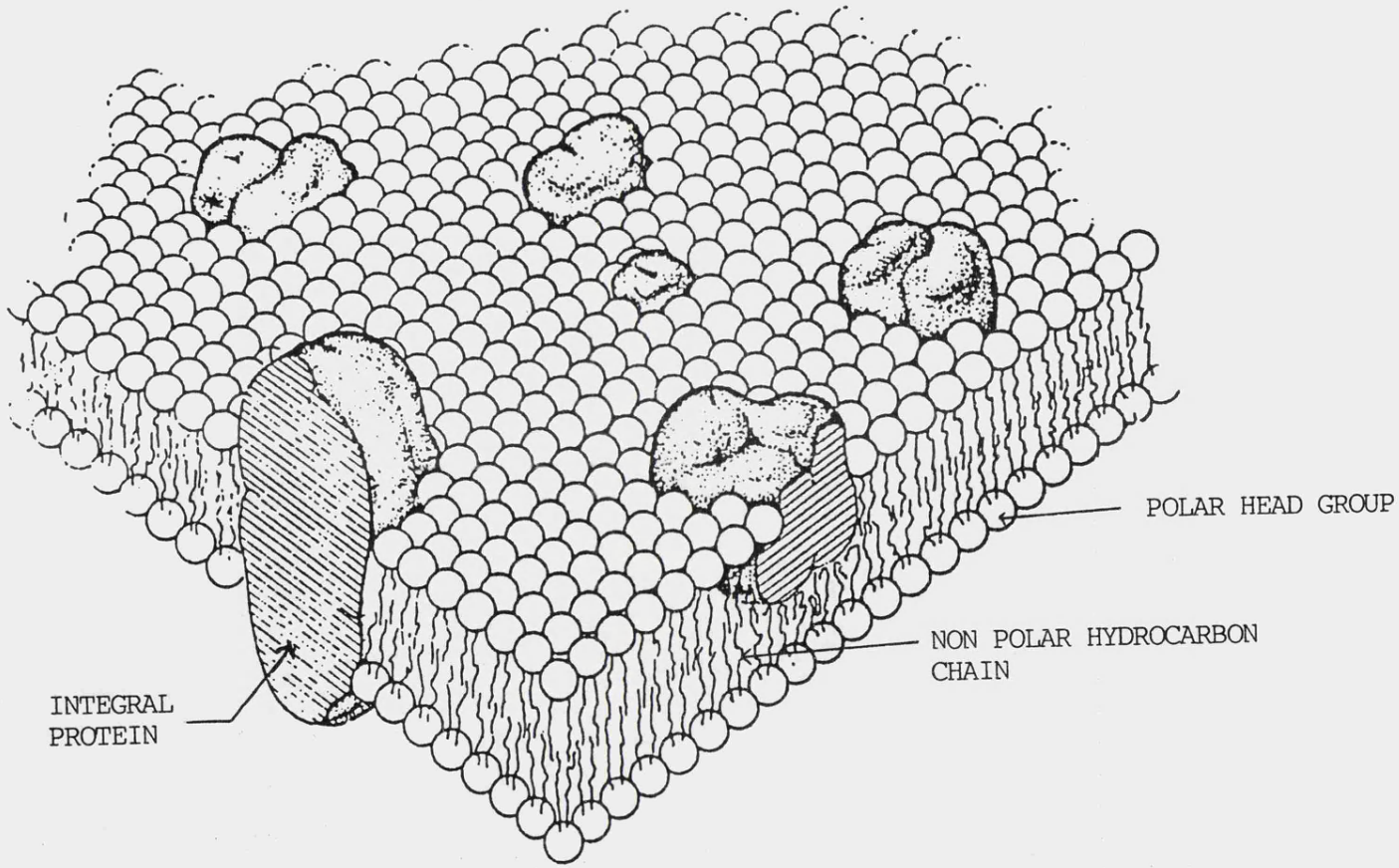

Figure 6 Fluid mosaic model for membrane structure.

From Singer and Nicolson, 1972

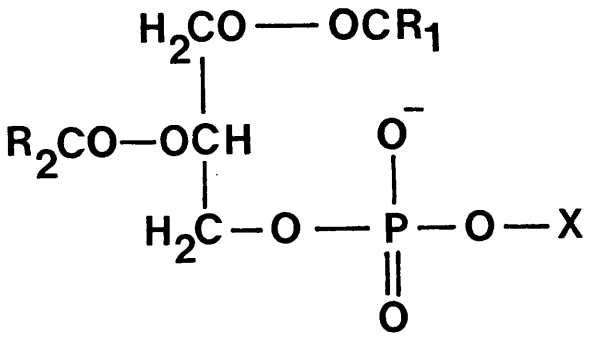

R_1 & R_2 = fatty acid hydrocarbon residues

X = the differing groups in the three phosphatides

e.g. $-CH_2-CH_2-NH_2$

phosphatidyl ethanolamine

$-CH_2-CHOH\ -CH_2OH$

phosphatidyl glycerol

Figure 7 General structure of membrane phospholipids.

The fatty acids of the phospholipids.

Although unique acyl groups may be required for certain biochemical processes in the membrane, the bulk of the evidence indicates that the physical attributes of the hydrocarbon residues in the phospholipids are the important determinants. These hydrocarbon chains forming the interior of the lipid bilayer perform a vital role in determining the fluidity of the bilayer. Moreover, membrane fluidity has been recognized as being of particular importance as the lipids must be in a liquid state for normal membrane function (Cronan and Gelmann, 1975). Therefore, since bilayers with only saturated fatty acids are rigid at physiological temperature, some of the fatty acids must be unsaturated. Indeed, mutants unable to make unsaturated fatty acids, require them and on deprival die when the membrane reaches a composition incompatible with fluidity.

Considerable and deliberate manipulation of the unsaturated fatty acid content of membranes can be achieved by the use of various mutants. Indeed, much of the current understanding regarding the importance of unsaturated fatty acids in membrane function has been obtained by the use of these mutants. The fab mutants lack the ability to synthesize unsaturated fatty acids, the gps and pls mutants block phospholipid synthesis and the fad mutants block the degradation of fatty acids prior to incorporation into the phospholipid. One E. coli mutant designated K1060 (Overath et al., 1970) is incapable of synthesizing or degrading unsaturated fatty acids as it contains mutations in the fab and fad genes. This strain has proved particularly useful in membrane studies as the total unsaturated fatty acid content of its membrane may be controlled. A review of these mutants is available (Silbert, 1975).

The unsaturated fatty acid content of the membrane is known to be affected by various nutritional factors making detailed analyses of fatty acid composition in E. coli difficult. For instance, as cells approach the stationary phase of growth there is a conversion of unsaturated fatty acids to cyclopropane fatty acids by addition of a methylene group across the double bond (Cronan, 1968). This 'toughening' of the lipid bilayer of the membrane increases the cell's chances of survival through the period of starvation associated with stationary growth phase. Also, the proportion of unsaturated fatty acids in E. coli increases in an inverse relationship to the growth temperature over a range 10° to 40°C (Marr and Ingraham, 1962). Finally, the proportion of cyclopropane fatty acids increases when the growth of E. coli is limited by the supply of oxygen. A review of these effects is available (Cronan, 1978).

Whereas in membranes of other cell types, polyunsaturated fatty acids are common and cyclopropane acids are missing, the reverse is true in E. coli. The common fatty acid residues in E. coli have 15 - 19 carbon chains and are of four types: straight chain saturated (e.g. palmitic or stearic); straight chain monounsaturated (e.g. palmitoleic, cis-vaccenic or oleic); cyclopropane (e.g. lactobacillic); and branched chain.

The synthesis and regulation of membrane phospholipids.

Phospholipids are synthesized in the cytoplasmic membrane itself from fatty acids and an intermediate of glycolysis, dihydroxy-acetone - phosphate. The dihydroxyacetone - phosphate is first reduced to glycerol 3-phosphate which is subsequently esterified by two fatty acid residues. The resulting diglyceride (phosphatidic acid) is then activated by CTP which then undergoes transfer reactions with serine

(which by subsequent decarboxylation leads to phosphatidylethanolamine) and α-glycerol 3-phosphate (which leads to cardiolipin and phosphatidyl-glycerol) releasing CMP.

Fatty acid synthesis proceeds by successive additions of acetyl residues to the chain at its carboxyl end. Briefly, it starts with the transfer of an acetyl group from acetyl CoA to a special protein known as acyl carrier protein (ACP). This complex then serves as an acceptor to which successive C_2 units are transferred. The C_2 donor is malonyl-ACP which is formed, in turn, by carboxylation of acetyl CoA; during transfer of the C_2 unit, Co_2 is released and free ACP is regenerated.

Phospholipid synthesis in E. coli appears to be coupled to protein synthesis by the stringent control mechanism (see Silbert, 1975 for a review). There is excellent correlation between the accumulation of intracellular guanosine tetraphosphate (ppGpp), a mediator in the stringent control mechanism,and the reduction in phospholipid synthesis (Merlie and Pizer, 1973). Moreover, this seems to affect fatty acid as well as phospholipid synthesis, as a 60% reduction in fatty acid content of rel^+ but not rel^- strains was observed after amino acid starvation (Polakis et al., 1973). Also, the regulation of the phospholipid content of membranes has been shown to involve catabolic as well as anabolic processes (Albright et al., 1973). This catabolism is thought to involve the hydrolytic activities of phospholipases A_1 and A_2 within the cell envelope which remove the apolar hydrophobic fatty acid residue. Subsequent action involving a phosphodiesterase on the residual 'backbone' would then complete the degradation.

Functions of the cytoplasmic membrane.

The cytoplasmic membrane primarily provides an osmotic barrier, traversed at intervals by specific transport systems. This barrier retains metabolites and macromolecules while excluding external compounds. Thus ions, and non-ionized molecules larger than glycerol, can only penetrate very slowly except by utilization of specific transport systems. It also contains the enzymes involved in respiration (i.e. electron transport coupled with oxidative phosphorylation), complex lipid synthesis, synthesis of wall constituents (e.g. peptidoglycan), and DNA replication. In addition, various proteins involved in active transport and motility and associated chemotaxis are present. Finally, the membrane is involved in protein secretion and, much like the endoplasmic reticulum of eucaryotes it binds a considerable fraction of the ribosomes in the cell. Thus the cytoplasmic membrane is truly multifunctional and indeed can be considered to be self-generating as it contains many of the enzymes concerned with the synthesis of the lipid bilayer itself.

(b) The periplasmic space.

This space between the outer and cytoplasmic membranes in E. coli contains a thin layer of peptidoglycan, also called glycopeptide, mucopeptide or murein, which is responsible for the rigidity of the cell and for its resistance to osmotic lysis. Peptidoglycan may be dissolved by the enzyme lysozyme in a hypertonic medium (thus preventing osmotic lysis) to render spheroplasts. These are osmotically sensitive spheres which retain the outer membrane and have proven useful in the study of membrane functions. Peptidoglycan is a covalently linked polymer consisting of a backbone of alternating N-acetylmuramic acid (Mur NAc) and N-acetylglucosamine (Glc NAc) residues in β-1, 4 linkage, a tetrapeptide substituent with alternating L and D residues,

and a peptide bridge from the terminal COOH of one tetrapeptide to an available group (most often a free NH_2 group) of a neighbouring tetrapeptide. This tetrapeptide substituent in E. coli is composed of L-alanine linked to the Mur NAc residues, D-glutamic acid, mesodiaminopimelic acid and D-alanine.

The biosynthesis of peptidoglycan occurs in four stages : synthesis of water-soluble complex precursors; attachment to a membrane lipid carrier, followed by further additions; formation of linear polymers outside the CM; and cross-linking of these polymers. The initial stages of this biosynthesis and the sites of action of various antibiotics affecting it, are shown in Figure 8. The figure shows the initial attachment of the uridine nucleotide of Mur NAc (UDP-MurNAc-pentapeptide), which acts as a precursor, to the membrane carrier lipid (represented as P-lipid) which has been identified as undecaprenol - P:

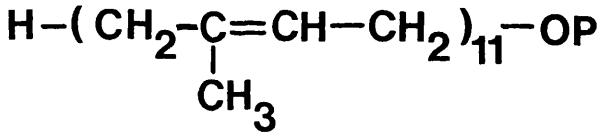

Figure 9 Structure of undecaprenol-P.

GlcNAc is then added from its UDP derivative, and any future polypeptide is built up at this stage on the pentapeptide. In the polymerization reaction, a completed disaccharide subunit on a lipid carrier accepts the growing end of a polysaccharide chain from another molecule of carrier, releasing the latter as undecaprenol-PP This compound then loses a P and is ready again to accept a precursor. It should be noted that the final cross-linking reaction (not shown in Figure 8) occurs outside the CM, and involves a transpeptidation in which a free NH_2 group displaces a terminal D-alanine, releasing that residue, and forming a bridge to the subterminal D-alanine.

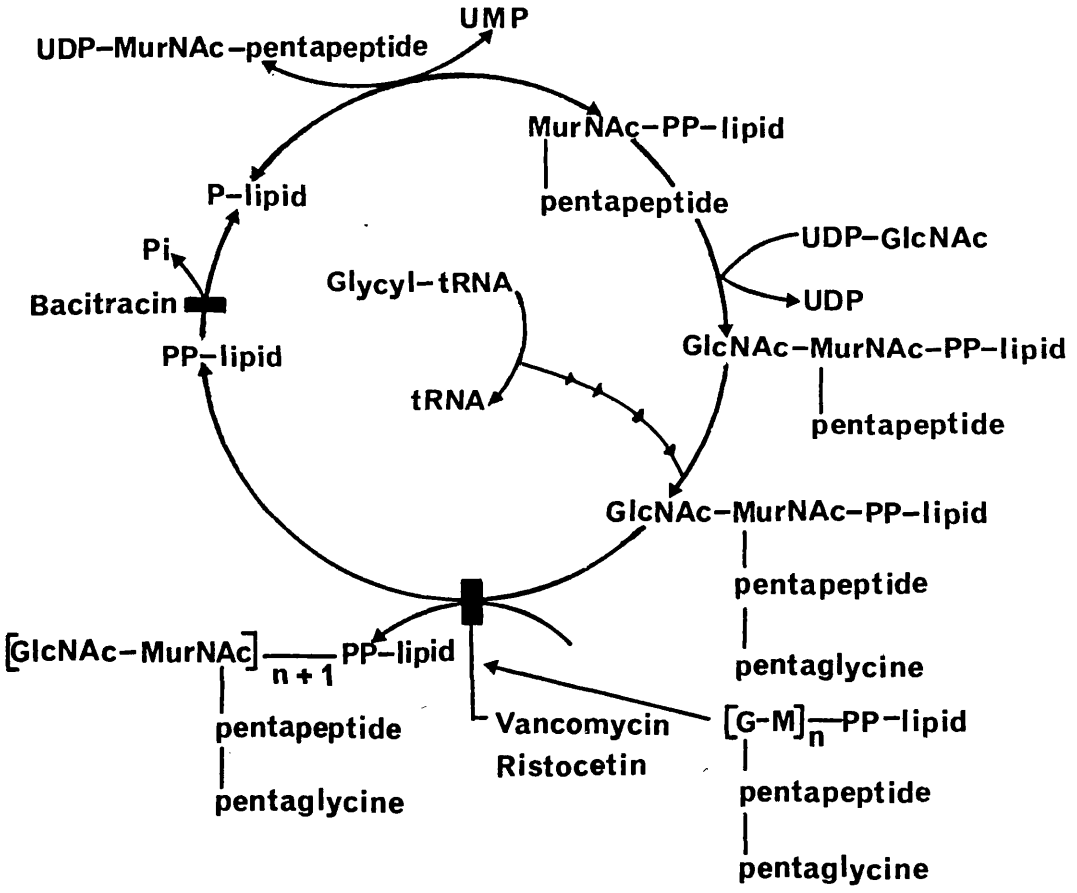

Figure 8

The involvement of the lipid carrier cycle in peptidoglycan synthesis.

It is this final stage which is inhibited by the penicillins.

In addition, bacteria themselves contain enzymes (autolysins) which are capable of attacking peptidoglycan. These include glycosidases, such as lysozyme, which are specific for one or other of the glycoside bonds between the alternating sugars in the backbone; an amidase, which releases the tetrapeptide from MurNAc; and endopeptidases, which attack various bonds in the bridge. Their main role is probably in the splitting and reshaping of the cell wall in the region of a dividing septum.

Finally, whereas gram-positive organisms excrete various exoenzymes such as proteases, nucleases and penicillinase into the medium, in gram-negative organisms, the periplasmic space acts as a store for these potentially destructive enzymes. The periplasmic space is also thought to contain enzymes important for cell growth and other proteins, such as specific amino acid and sugar transport binding proteins.

(c) The outer membrane.

The outer membrane (OM) is largely composed of lipids and proteins and has a similar structure to the cytoplasmic membrane. It is firmly attached to the peptidoglycan layer by two types of proteins; small lipoproteins (Mwt 7,200) and matrix proteins (Mwt 36,000) present as trimers. However, it is different from the CM in first containing lipopolysaccharide (LPS) and second by exhibiting a much lower enzymatic activity. The presence of the long polysaccharide side-chains of the LPS enables the OM to serve as a carrier of surface antigens and receptors for phages and colicins, although its main role appears to be the provision of specific and non-specific channels for those nutrients and ions required for growth. These nutrients are transported

through the OM pores by passive diffusion. In this function, it allows diffusion of molecules up to about 800 Mwt., which can then pass via the loose underlying peptidoglycan, thereby acting as a coarse molecular sieve. In comparison, the CM excludes almost all hydrophilic molecules except water itself. In addition, the OM plays an important role in cell-cell interactions (e.g. conjugation) as well as an indirect role in chemotaxis. A thorough review of the OM properties and functions is available (Inouye, 1979).

The evidence for near - UV radiation-induced damage to membranes.

Until recently, in the light of the overwhelming evidence that near - UV radiation exerts a damaging effect either directly, or more probably, indirectly on cellular DNA, with obvious lethal consequences, damage to membranes as a factor in near - UV radiation-induced cell lethality has been largely overlooked. Indeed, in a 1977 review on the lethal and mutagenic effects of near - UV radiation, Webb stated that published data on near - UV radiation-produced membrane damage have not been interpreted as "convincing evidence that such damage contributes to near - UV radiation cell lethality under usual growth conditions." However, he does mention the early observations of Hollaender (1943) involving the inactivation of E. coli in physiological saline immediately after near - UV irradiation (350 - 490 nm broadband) which did not occur after 254 nm irradiation.

It is now apparent, that near - UV irradiation of a number of cell types, both procaryote and eucaryote, over a wide range of fluences, i.e. sublethal, lethal or much greater than lethal, may exert some inhibitory or damaging effect on the normal functioning of the cytoplasmic membrane. In some of these cases it is possible that the effects may contribute significantly to near - UV radiation-induced

lethality. The effects thus far observed may be broadly grouped as follows; (i) effects on membrane active uptake, (ii) effects on bacterial respiration; (iii) effects correlated with membrane lipid composition; and (iv) effects leading to cell lysis or changes in the membrane permeability barrier.

(i) Effects on membrane active uptake.

These effects normally occur at near - UV radiation fluences that cause no detectable killing of repair proficient strains, and so are not thought to contribute significantly towards cell lethality. An inhibitory effect by near - UV irradiation on several membrane transport systems in E. coli was first observed by Sprott et al. (1976). Previous observations in the same laboratory with sublethal fluences of visible light had shown an inhibition of active uptake of several amino acids and methyl thio- β - galactoside (TMG) (Barran et al., 1974; D'Aoust et al., 1974). Sprott and co-workers extended this work to include near - UV radiation, and showed an increase in the efficiency of inhibition of uptake of various amino acids (proline, alanine, glycine, threonine, methionine, phenylalanine, tryptophan and tyrosine) and glucose and TMG with decreasing wavelength from 578 to 366 nm. However, no data below 366 nm was included. They concluded that four photosensitizers were involved, three active under aerobic conditions and one in anaerobic conditions.

Also, in 1976, Koch et al., observed that sublethal fluences of near - UV light (primarily 365 nm but contaminated with 334 and 313 nm) could inhibit sugar (galactoside) transport in E. coli. This could occur by either inactivation of the permease system itself or by interfering with metabolic energy production. In addition, Doyle and Kubitschek (1976) described a near - UV radiation-induced inhibition

of an energy independent membrane transport system (L-Sorbose uptake) into yeast cells.

The first action spectrum covering the far and mid - UV radiation region for inhibition of membrane transport was described by Robb et al. (1978) who showed two similar spectra, with a peak at 290 nm in the far - UV region and another, two orders of magnitude lower, around 365 nm, for the inhibition of both the leucine and the leucine-isoleucine systems in E. coli K-12. They concluded that the inhibition was due to an inactivation of an essential component or components of the active uptake mechanism itself and not the result of generalized leakage. Subsequently, other action spectra for membrane transport inhibition, have been obtained. Robb and Peak (1979) described an action spectrum similar to that for the leucine system, with a major far - UV radiation peak at 290 nm, but with a minor component around 405 nm, for the inactivation of the lactose permease in E. coli. Also, Ascenzi and Jagger (1979) extended the visible action spectrum of Sprott et al. (1976) for the inhibition of glycine uptake in E. coli B/r and showed maxima at 280 and 334 nm and minima at 260 and 313 nm. These studies showed a negligible effect above 405 nm whereas Sprott et al., (1976) showed nearly equal effects at 366 and 405 nm and a significant effect at 435 nm. However, Sharma and Jagger (1981), while describing similar action spectra for the inhibition of alanine and glycine uptake, found the same peak at 280 nm but could not reproduce the Ascenzi and Jagger (1979) findings regarding a minimum at 313 nm and a peak at 334 nm.

In summary, these action spectra show evidence of a near - UV chromophore, or chromophores, absorbing at 334, 366 or possibly, in the case of the lactose permease system, 405 nm. The chromophores

are, as yet, unknown but may be components of the electron transport chain, e.g. quinonesas suggested by Ascenzi and Jagger, 1979.

Finally, some workers have implicated the inhibition of membrane transport in the induction of near - UV radiation-induced growth delay (Kubitschek and Doyle, 1981). They have shown that rates of uptake of carbon sources, glucose and succinate, in E. coli B/r are proportional to growth rate at all times during near - UV radiation-induced growth delay and recovery from this growth delay. In addition, the rate of leucine uptake did not show such a correlation. However, the evidence suggesting 4-thiouridine as the chromophore involved is substantial (see previous section on sublethal effects of near - UV radiation on cells).

(ii) Effects on bacterial respiration.

A transient inhibition of respiration at fluences of near - UV radiation causing little cell killing was first observed by Kashket and Brodie (1962). This was observed as a failure of an irradiated culture of E. coli, which is a facultative anaerobe, to grow on media where energy was obtainable solely by oxidative phosphorylation (succinate medium), while growth took place in the presence of a fermentable carbon source (glucose) albeit with a lower yield of cells as compared to unirradiated control cultures. They proposed that this effect was due to a near - UV radiation-induced destruction of the quinones within the electron transport chain. Subsequently, equivocal data has been produced concerning the actual targets (within the electron transport chain) for this effect. Bragg (1971), while supporting the general mechanism of respiratory inhibition by near - UV radiation being due to a destruction event in the electron transport chain, proposed cytochrome a2 to be the main target with ubiquinone

having a much less important role. However, Lakchaura et al. (1976) obtained an action spectrum for the inhibition of ATP synthesis in E. coli and concluded from its shape that ubiquinone Q_8 or menaquinone were the most likely targets for the effect. Also, Madden et al. (1981) have shown, by means of an action spectrum, the extreme near - UV radiation sensitivity of menaquinone. It shows a F_{37} at 334 nm of 1.3 kJm^{-2}, a value 15 times lower than that required for growth delay, and 150 times lower than that for killing a DNA repair-proficient E. coli strain.

However, it is now apparent that, in some cases, an inhibition of respiration may contribute to near - UV radiation-induced cell lethality. For instance, Fong et al. (1975) reported that respiration failure may be a factor in the near - UV radiation sensitivity in actively growing cultures of a haploid strain of Saccharomyces cerevisiae. They showed that cell death occurred by two distinct mechanisms : at low fluences ($\sim 3x10^3 Jm^{-2}$) due to a reversible inactivation of the respiratory capacity of the cell (possibly due to quinone destruction); and at high fluences ($\sim 2x10^4 Jm^{-2}$) by an unknown irreversible reaction. In addition, at higher fluences, components of the electron-transport chain have been definitely shown to be involved in near - UV radiation-induced biological effects. For example, Sprott and Usher (1977) have shown that at fluences of about $1x10^6 Jm^{-2}$ and greater, at 366 nm, where 80% inhibition of respiration is apparent, there is a rapid loss of the electrochemical proton gradient in E. coli.

Finally, it is also apparent that in some cases, far - UV irradiation (254 nm) of cells (e.g. when grown on minimal medium with glycerol as the carbon source) may cause a cessation of respiration and growth about one hour after irradiation (Swenson & Schenley, 1974).

(iii) Effects correlated with membrane lipid composition.

The use of the E. coli mutant strain K1060, which cannot synthesize or degrade unsaturated fatty acids (Overath et al., 1970) enables workers to vary the unsaturated fatty acid content and hence the fluidity properties of membranes by means of adding fatty acid supplements with varying degrees of unsaturation or by manipulation of growth temperature and medium composition. Studies with γ rays have clearly shown that membrane fluidity influences survival, - increased degrees of fatty acid unsaturation leading to increased sensitivity (Yatvin, 1976; Redpath and Patterson, 1978). These studies implicate membrane damage in γ ray - induced cell lethality.

To date, one report has shown a similar effect to occur after near - UV irradiation of this E. coli mutant strain (Klamen and Tuveson, 1982). They observed that the near - UV radiation (300-400 nm) sensitivity, particularly of logarithmically growing cells, increased with the number of carbon-carbon double bonds, i.e. the degree of unsaturation, in the fatty acid used as a supplement. However, no such effect was observed for stationary phase cells grown at 30, 37 or 39°C except that the use of oleic acid as a supplement led to a decrease in sensitivity in all three cases compared to the other four supplements used. Oleic acid is an 18 carbon chain monounsaturated fatty acid while the others were all 20 carbon chain with varying degrees of unsaturation from 1 to 4, suggesting that, for stationary phase populations, the fatty acid carbon chain length rather than the degree of unsaturation may be important for sensitivity to near - UV radiation. Moreover, growth at lower temperatures would be expected to increase the percentage of unsaturated fatty acids in the membrane of E. coli K1060 (Cronan, 1968) but they found that the near - UV radiation survival curves for these stationary phase cells appeared

approximately the same. However, when the fluence resulting in 10^{-2} survival was plotted as a function of the number of carbon-carbon double bonds in the membrane, there was a tendency for increasing double bonds to enhance the sensitivity of stationary as well as log phase cell populations. This observation is shown in Figure 10. It is obvious from this that the increase in sensitivity with increasing degrees of unsaturation is more pronounced for log phase cells than for stationary phase cells although all the curves show some tendency to this effect. They suggest that, in part, the greater sensitivity of log phase cells to near - UV radiation compared to stationary phase cells, may reflect the importance of unsaturated sites in the fatty acid components of the membrane as targets for singlet oxygen ($^1O_2$). They have speculated that, for log phase cells, $^1O_2$ attacks the double bonds of the unsaturated fatty acids forming peroxides and hydroperoxides, altering the hydrophobic character of the membrane, resulting in membrane destruction. It is suggested that $^1O_2$ is generated following absorption of near - UV wavelengths by an endogenous photosensitizer, or photosensitizers, yielding a triplet state photosensitizer which in turn interacts with molecular oxygen.

However, as K1060 does not efficiently convert the double bonds in its membrane fatty acids to saturated cyclopropane analogues (13% vs. the expected 25 - 30%) then stationary phase cell populations should be as sensitive as log phase cultures if these double bonds are important in determining sensitivity. They have interpreted the fact that log and stationary phase cell populations of strain K1060 are not equally sensitive as meaning that these unsaturated sites are not as important near - UV radiation targets in stationary phase cells of strain K1060 compared to log phase cells. Furthermore, as the stationary phase cells of strain K1060 are about as resistant to

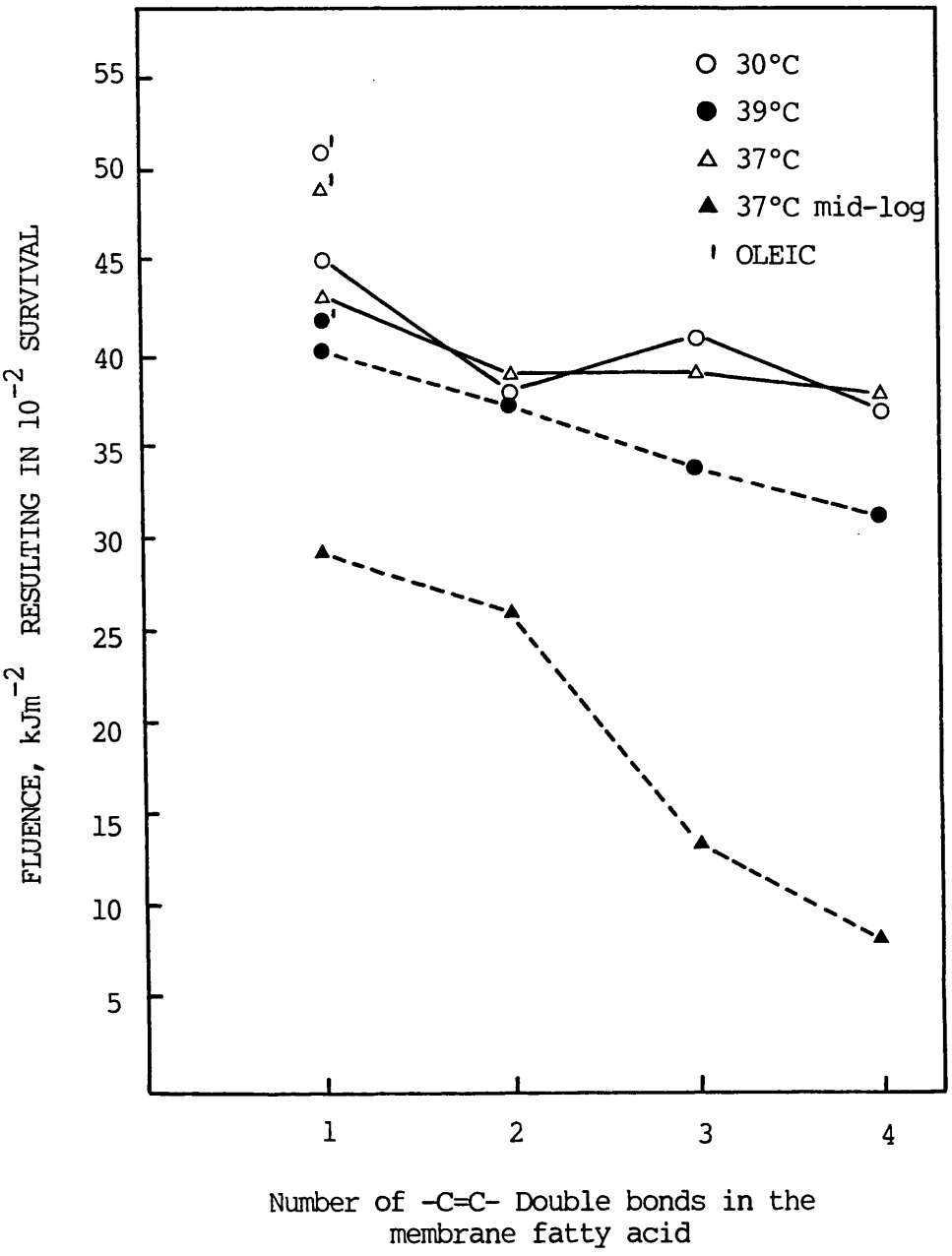

Figure 10

Dependence of fluence to give 1% survival for E. coli K1060 on the number of double bonds in the supplemented unsaturated fatty acids.

From Klamen and Tuveson, 1982.

near - UV radiation as are stationary phase cells of *nur*$^+$ strains, they have implied that, as stationary phase populations of *nur*$^-$ strains are near - UV radiation sensitive, this must be unrelated to the fact that *nur*$^-$ strains also inefficiently convert unsaturated fatty acids in their membranes to cyclopropane analogues (*nur*$^+$ 35.5%; *nur*$^-$ 5.5% conversions). Therefore, the suggestion made by Tuveson (1980) that the stationary phase near - UV sensitivity due to the *nur* gene is due to inefficient conversion to cyclopropane fatty acids and, is thus a membrane effect, must be wrong. Indeed, subsequently, it has been concluded that the *nur* sensitivity is due to an enhancement of single-strand breaks in DNA (Tuveson *et al.*, 1983).

Finally however, Wagner *et al.* (1980) have used acridine as a photosensitizer of near - UV radiation, and shown that log phase cells of K1060 are extremely resistant when grown in the presence of linoleic acid (18 carbons, 2 C=C) while being more sensitive when grown in the presence of elaidic acid (18 carbons, 1C=C). They explained this result by assuming a more fluid membrane, when growing with linoleic acid, would be less susceptible to disruption. This is in direct contradiction to the results of Klamen and Tuveson, although they did use 18 carbon rather than 20 carbon fatty acids and employed an exogenous photosensitizer compared to depending on endogenous photosensitizers.

(iv) Effects leading to cell lysis or changes in the membrane permeability barrier.

The majority of these effects, which have been observed in both eucaryotic and procaryotic cell types, occur at substantially higher fluences than is required to kill DNA repair proficient cells, suggesting these effects not to be important in near - UV radiation-

induced cell lethality.

In 1958 Bruce reported that X rays, 254 nm and near - UV/ visible (350 - 490 nm) irradiations of yeast cells resulted in a loss of K^+ retentivity. The near - UV radiation source used and the method of dosimetry does not permit a useful estimate of the absolute fluence of near - UV radiation employed. However, it is apparent from the relative effect on survival and K^+ retentivity that, whereas far - UV radiation requires an approximately 16-fold higher fluence to affect K^+ retentivity compared with survival, after near - UV irradiation, survival and K^+ retentivity are influenced by similar fluences.

Indirect evidence of near - UV radiation-induced membrane damaged was proposed by Mathews and Krinsky (1965). They observed that carotenoidless mutants of Sarcina lutea were much more sensitive to near - UV radiation than wild-type pigmented cells. Cell membrane damage was proposed as the basis of this cell killing because these pigments are localized in the cell membrane and certain enzymes associated with the membrane are preferentially destroyed in carotenoidless mutants. In addition, Burchard and Dworkin (1966) observed that carotenoidless forms of Myxococcus xanthus underwent lysis upon near - UV irradiation; whereas the wild-type pigmented cells did not. Nevertheless, a genetic basis for these effects has not been excluded.

Some other studies have shown a leakage of material through membranes after near - UV irradiation of cells, but at fluences somewhat greater than those required to kill wild-type cells under the usual growth conditions. Koch et al., (1976) used cells of E. coli, in which galactosidase transport was rendered inoperative, which became

'leaky' after exposure to 365 nm radiation (contaminated with 1-2% of 313 and 334 nm wavelengths) at a fluence of $1.2 \times 10^{6} Jm^{-2}$, a fluence somewhat greater than that required to kill 99.9% of the cells under the conditions of the experiment. A fluence of $6 \times 10^{5} Jm^{-2}$ of near - UV radiation had no effect on the generalized permeability of E. coli. Robb et al. (1978) observed a 'similar' leakage of radioactively labelled leucine from cells of an E. coli strain at high fluences of 365 nm radiation where 90% of the uptake ability had been destroyed.

End points that have been used for the detection of radiation-induced membrane damage are lipid peroxidation and erythrocyte haemolysis. Cook (in a 1975 review) described an action spectrum for erythrocyte haemolysis; it resembledthat of a typical protein containing aromatic amino acids, showing a peak in effectiveness at 280 nm and a minimum at 265 nm. Some effects were observed above 300 nm but these were oxygen dependent and required very high radiation fluences compared to the far - UV radiation fluences, unless photosensitizers such as photoporphyrin were added. He proposed that the UV haemolysis was due to an increase in ionic permeability as a result of photochemical damage to cell membranes.

Also, Roshchupkin et al. (1975), using liposomes and rat erythrocytes, have shown UV radiation (254, 313 and 365 nm) - induced haemolysis to correlate with lipid peroxidation. They observed that detectable 365 nm induced lipid peroxidation required a fluence in the region of $2.5 \times 10^{4} Jm^{-2}$, and was much less efficient than either 313 nm, or 254 nm radiations, where about $8 \times 10^{3} Jm^{-2}$ and $1.5 \times 10^{3} Jm^{-2}$ respectively, were required to produce a similar amount of lipid peroxidation. This may be compared with the fluences at 254, 313 and 365 nm required

to produce a survival level of 37% in a DNA repair - proficient E. coli strain, (E. coli B/r irradiated at 25°C in stationary growth phase) which are about 40, $3x10^4$, and $2x10^6 Jm^{-2}$ respectively (Webb 1977). However, such a correlation with lethality in E. coli is difficult as the liposomal and erythrocyte membranes contain higher concentrations of polyunsaturated fatty acids than found naturally in E. coli, containing only monounsaturated fatty acids, which would make the liposomal and erythrocyte membranes more prone to lipid peroxidation and leakage effects. A review of the photodegradation of biomembranes, which includes the Cook and Roshchupkin papers, is available (Lamola, 1977).

In agreement with the results of Roshchupkin et al., Mandal and Chatterjee(1980) observed that near - UV radiation and sunlight caused lipid peroxidation of liposomes and erythrocyte membranes which made the membrane leaky, measured as a release of chromate ions. However, their data indicated that 365 nm radiation was more efficient than 254 nm radiation in producing these effects, the 365 nm radiation effects occurring at a fluence of about $1.2x10^3 Jm^{-2}$ while an equal amount of lipid peroxidation occurred at a fluence of $6x10^3 Jm^{-2}$ of 254 nm radiation.

An alternative approach to investigate UV - radiation-induced damage of membranes is to introduce irradiated cells into conditions of increased osmotic stress. Under these conditions membrane damage may be seen to relate to cell death. This approach has been used by Ito and Ito (1983) who exposed irradiated yeast cells to hypotonic conditions, and also by Hollaender (1943) and Moss and Smith (1981) who exposed near - UV irradiated E. coli to hypertonic conditions.

Ito and Ito (1983) have shown that, for exponentially growing cultures of a diploid strain of the yeast Saccharomyces cerevisiae, in the case of near - UV irradiated cells placed in water, inactivation is closely related to a disruption of the permeability barrier, whereas near - UV irradiated cells suspended in 0.1M potassium phosphate buffer and stationary phase cells suspended in water showed no such disruption. Furthermore, no such effect was observed after 254 nm irradiation. Their results are shown replotted in Figure 11, where the disruption of the permeability barrier is represented by the spectrophotometric detection of p-nitrophenol. The procedure involved adding the normally impermeable substance PNPG to the irradiated cell suspension, then if any permeated into the cell, due to membrane damage, it was hydrolyzed by intracellular maltase yielding the p-nitrophenol.

These studies showed exponential-phase cells to be much more sensitive to membrane damage than stationary-phase cells and the membrane damage to be oxygen-dependent with a low temperature dependence. These findings are consistent with the view that the effects are caused by photosensitization rather than enzymatic processes. The absence of maltase in the suspension medium of irradiated cells indicated that such presumed damage in the membrane only allowed small molecules to go through.

Ito and Ito have also suggested a possible mechanism for this disruption of the permeability barrier and for the apparent 'tailing' off in the yield of p-nitrophenol after fluences of $100 kJm^{-2}$ (see Fig. 11). Previous work in their laboratory (Watanabe et al., 1982) showed a drastic shrinkage of yeast cells almost immediately after a lethal fluence of near - UV radiation (less than 30 minutes after

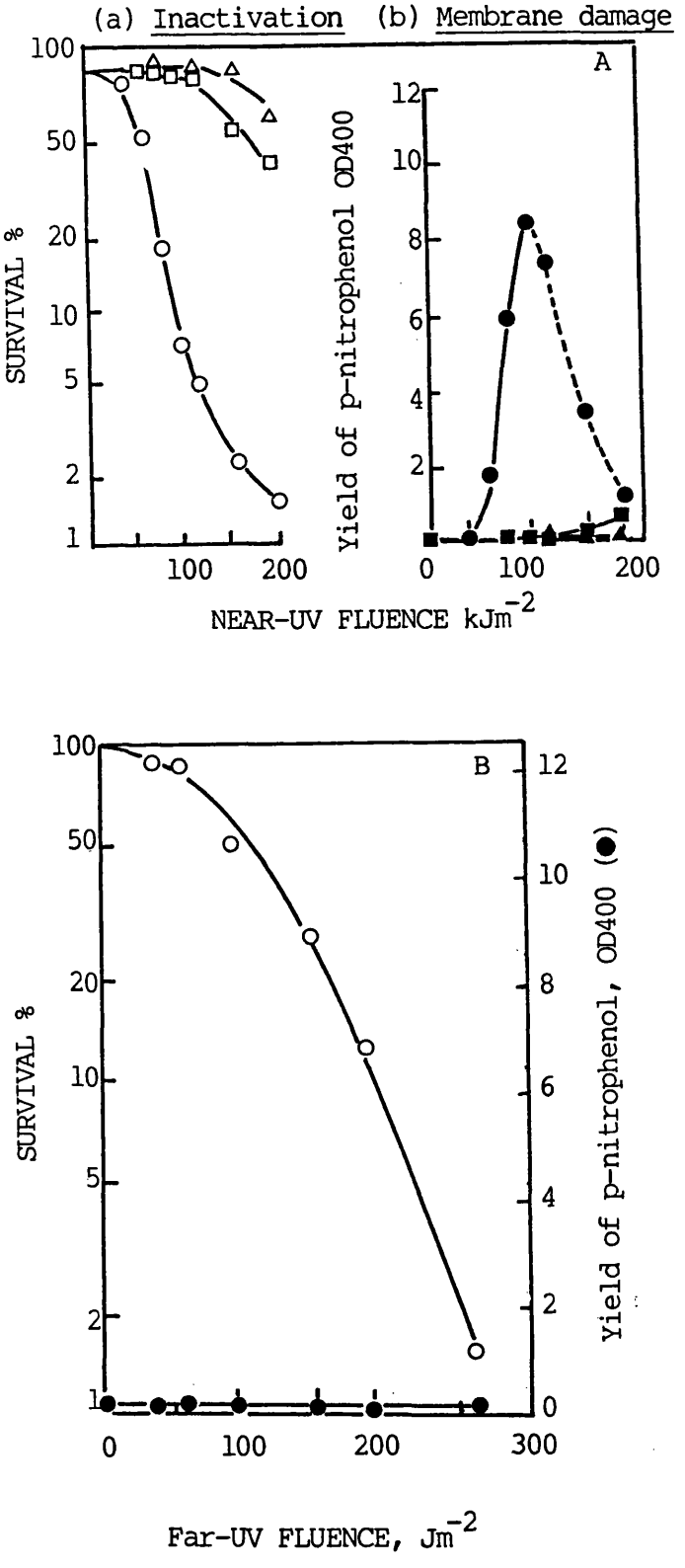

Figure 11

Inactivation (open symbols) and membrane damage (closed symbols) in A) near-UV irradiated and B) far-UV irradiated yeast cells in either exponential growth phase, suspended in water (○,●) or 0.1M phosphate buffer (□,■), or stationary phase cells, suspended in water (△,▲).

Redrawn from Ito and Ito, 1983.

irradiation). According to this work the cell volume is maximally reduced by a factor of more than 2 at a fluence of $100kJm^{-2}$. Also, the shrinkage was first observed at a fluence of about $100kJm^{-2}$ where the survival enters a region of exponential decline after a large shoulder. As this fluence coincides with the beginning of the decline of the yield of p-nitrophenol they have correlated this decline to be due to a major structural change occurring in the cell which suppresses the maltase function in hydrolyzing PNPG. They have suggested that other cytoplasmic enzymes may suffer in the same way, ultimately leading to cell death. Moreover, they have suggested that the increased resistance of the stationary phase cells could be due to the thickened cell wall giving more mechanical tolerance to this tendency of cell shrinkage.

In E. coli, the pioneering work of Hollaender (1943) showed that inactivation may occur when cells are held in physiological saline after near - UV irradiation. Hollaender's observations implicating physiological damage after near - UV irradiation in lethality were largely overlooked in favour of damage to DNA until recently, and in particular, until the observations of Moss and Smith (1981). Using a DNA repair-competent strain of E. coli K-12 they observed an increased sensitivity when plating on minimal media after irradiation with broad-spectrum near - UV radiation (320 - 405 nm) at fluences that caused little inactivation when plated on nutrient agar or other complex media. A reproduction of this result is shown in Figure 12.

Figure 12 also shows that this minimal medium sensitivity effect was not apparent after far - UV irradiation, where DNA damage is known to be the principal cause of lethality. In fact, the far - UV radiation observation exhibits a 'minimal medium recovery' phenomenon

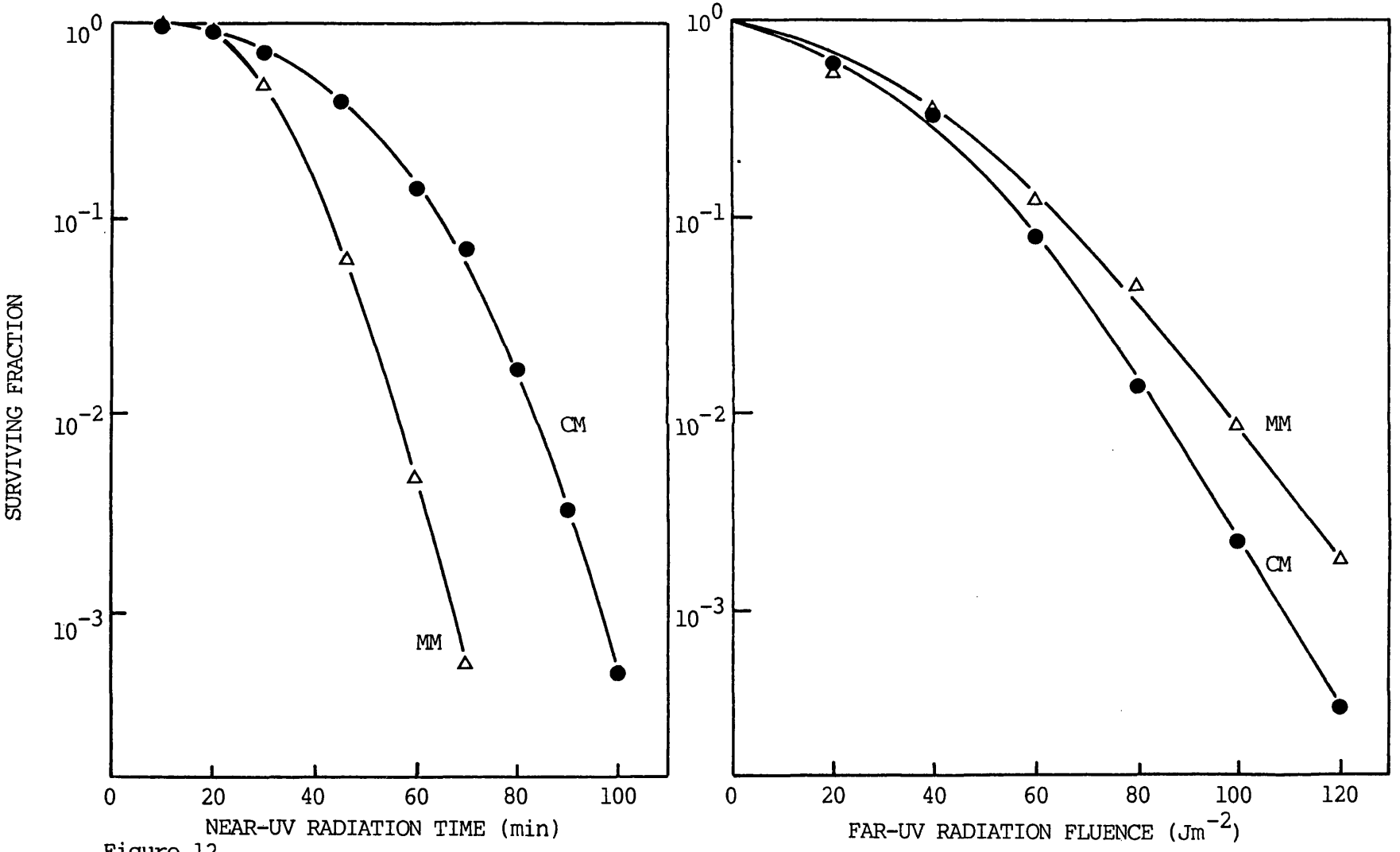

Figure 12
Survival curves for E. coli K-12 (SR 385) with viability assessed using either complex medium (CM) plates (●) or minimal medium (MM) plates (△). Redrawn from Moss and Smith, 1981

which is characteristically shown to a small extent by repair competent strains, and to a greater extent by excision-repair deficient strains.

Subsequent studies, where irradiated and unirradiated controls were held either in minimal or complex liquid medium at 37°C, helped determine the time course of the inactivation in minimal medium. On holding near - UV irradiated cells in either complex or minimal medium they observed that, in complex medium, with increasing time of irradiation, as expected, an increased growth delay occurred; while in minimal medium, with increasing time of irradiation an increasing sensitivity to minimal medium over the time of holding was observed. For subsequent experiments a single irradiation time was chosen which produced a significant decrease in survival in liquid minimal medium relative to complex growth medium.

Moss and Smith related the different responses on complex and minimal medium to the presence of relatively high concentrations or inorganic salts in the latter. Their minimal medium contained inorganic salts with a total molarity of 64mM, and other frequently used minimal media contain up to 160mM (Neidhardt et al., 1974). They have shown that by increasing the concentration of inorganic salt in the minimal medium an increased sensitivity to near - UV radiation resulted. This observation is shown in Figure 13.

In order to determine if the effects of salt concentration were a property of the particular inorganic salts in the formulation of the minimal medium, they added sodium chloride at various concentrations to tenfold-diluted minimal medium and repeated the experiment. The results are shown in Figure 14.

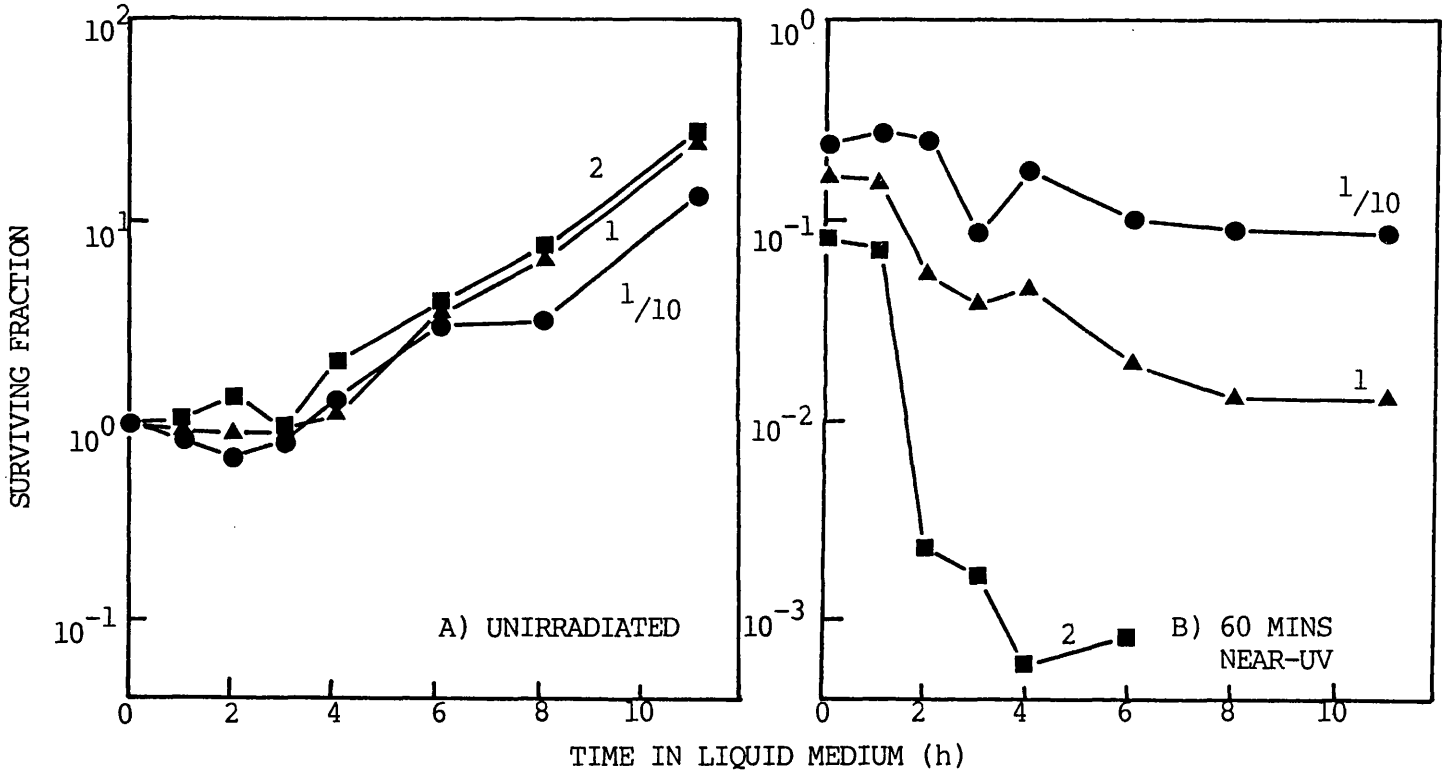

Figure 13

The surviving fraction of E. coli K-12 (SR 385) in different holding media. Samples were held at 37°C in minimal medium with tenfold-diluted salts (●), single strength minimal medium (▲), or minimal medium with double strength salts (■). Viability was assessed on complex medium. Redrawn from Moss and Smith, 1981.

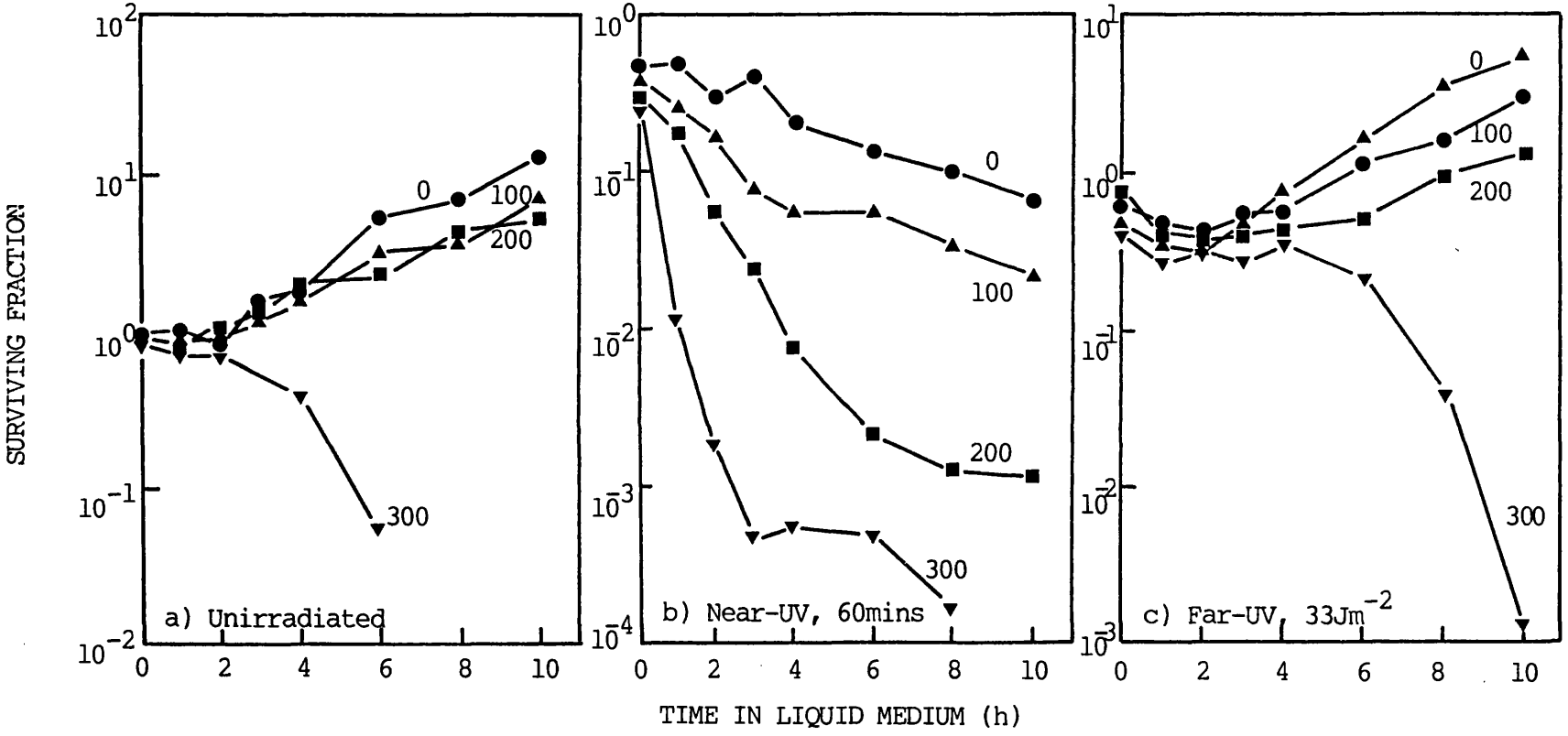

Figure 14

The surviving fraction of E. coli K-12 (SR 385). Samples were held at 37°C in minimal medium with tenfold-diluted salts (●), or in minimal medium with tenfold-diluted salts with sodium chloride added at 100mM (▲), 200mM (■), or 300mM (▼). Viability was assessed on complex medium. Redrawn from Moss and Smith, 1981.

It can be seen that increasing the concentration of sodium chloride in the minimal medium (100 and 200mM), while causing no significant effect on the growth of unirradiated cells, caused increased sensitivity to near - UV radiation. Such an effect is not shown after 254 nm irradiation. Addition of 300mM NaCl is seen to cause lethality effects in unirradiated as well as 254 nm and near - UV irradiated cells. They then performed experiments where full near and far - UV radiation survival curves were constructed from the data using corresponding solid minimal and complex medium agar plates. The reduced inorganic salt concentration was sufficient to permit colony formation and did not result in decreased survival. The presence of 200mM sodium chloride corresponded well with the decreased survival seen on normal strength minimal medium (shown in Figure 13). In addition they showed that sensitivity was increased by increasing the pH of the medium, and greatly increased by adding a low concentration (1μg/ml) of commercial glassware detergent (which had no lethal effect on unirradiated or far - UV irradiated cells) to the medium. Also, this salt sensitivity effect appeared to be largely oxygen-dependent.

They attempted to correlate this sensitivity of near - UV irradiated cells to inorganic salts, to similar effects observed with treating *E. coli* with mild-heat. Clark and Ordal (1969), while studying the inactivation of *S. typhimurium* heated at 48°C, observed a higher viability for heated cells on a complex medium (Trypticase Soy Broth) than on a medium (Levine Eosin Methylene Blue Agar) containing 2% sodium chloride (342 mM). Other workers had shown that this difference in survival between the two plate types was due to 'sublethally injured' cells, the lesions having been identified as a loss of membrane integrity, observed as a leakage of cell components that absorb at 260 nm (Iandolo and Ordal, 1966; Russell and Harries, 1967). Therefore,

by analogy with these data, they suggested that the increase in lethality of near - UV irradiated cells on minimal medium, compared with that on complex medium, is due to the death of cells with damaged membranes.

G E N E R A L M E T H O D O L O G Y

Test organisms.

The main organism used in this study was SR 385 which is K-12 JG 139, a DNA repair-competent strain requiring thymine as a growth supplement. A list describing SR 385 and the other organisms used in this study with their respective genotypes and source is given in Table 1. A full description of the derivation of strain K-12 SR 385, including a comparison with K-12 AB 1157, is given in the Appendix A1.

Storage of organisms.

Master cultures of each organism were kept in plastic vials and stored in the vapour phase of a liquid nitrogen refrigerator (Union Carbide Ltd.) at approximately - 196°C. These were subcultured into nutrient agar stabs (5ml of molten nutrient agar poured into 8ml screw-capped glass vials obtained from Wheaton Scientific, New Jersey, USA). The nutrient agar was prepared by adding 22.4g Oxoid CM3 nutrient agar to 800 ml of glass distilled water in a flat-bottomed 1 litre flask and allowing to stand for 15 minutes. The agar was then dissolved by bringing to the boil, and 5ml aliquots poured into the vials. These were then sterilized by autoclaving for 15 min at 121°C. After allowing to set, the stabs were inoculated and incubated for 24 h at 37°C in an incubator. One ml of sterile liquid paraffin B.P. (B.D.H. Ltd.) was then aseptically added to each stab to limit evaporation. The liquid paraffin was sterilized in sealed glass 10ml ampoules by heating at 160°C in a hot air oven for 1 hour. These stabs were then kept at room temperature and used routinely for the storage of organisms.

For the day to day use of organisms, a stab was taken from the

Table 1. List of strains used.

STRAIN	LAB CODE NO.	RELEVANT GENOTYPE	OTHER GENOTYPE	REFERENCE
K-12 JG139 (SR 385)	DV 66	+	F^-, rha-5, lacZ53, rpsL151, thyA36, deo(C2?).	see Appendix A1
K-12 AB 1157	DV 4	+	F^-, thr, leu, arg, his, pro, ara, lac, gal, mtl, thi, xyl, tsx^r, str^r.	Adelberg and Burns (1960)
K-12 AB 1886	DV 3	uvr A6	as for AB 1157.	Howard-Flanders et al., 1966
K-12 SR 362	DV 65	uvrA, uvrB, recA, phr.	F^-, leu, thyR, met, rha, lacZ, str.	Constructed at Stanford University
K-12 SR 246	DV 51	polB100	F^-, thyA, thyR, lys, lacZ, Su^-, str.	Constructed at Stanford University
B/r	DV 132	+	lon, sul.	Hill, 1964
NCTC 86	DV 33	+	wild-type.	-

Table 1 (contd...)

STRAIN	LAB CODE NO.	RELEVANT GENOTYPE	OTHER GENOTYPE	REFERENCE
Bacillus subtilis spores UVSSP 42-1	DV 28	uvrA 42 SSP-1	thy, trpC2, met-14, sul.	Munakata, 1972 Tyrrell, 1978a

Strain K-12 SR 385 was obtained from J. Gross via Prof. Kendric Smith, Stanford University, USA.

Strains SR 362 and SR 246 were obtained from Professor Kendric Smith, Stanford University, USA.

Strains AB 1157 and AB 1886 were obtained from Dr. B.A. Bridges while at the MRC. Radiobiology Unit, Harwell, UK.

Strain B/r was obtained from Dr. N. Gillies, The Middlesex Hospital Medical School, London.

Strain NCTC 86 was obtained from the National Collection of Type Cultures.

The *B. subtilis* spores were obtained from Dr. R. M. Tyrrell while at the Institute de Biofisica, Rio de Janeiro, Brazil.

master stab and subcultured onto a nutrient agar plate and streaked for single colonies using a sterile wire loop. The agar for these plates was prepared as above and sterilized as 800ml batches, in the same way as above. Twenty ml volumes of molten agar were then poured into 9cm diameter sterile petri dishes (Sterilin Ltd., England) using sterile Kipp's burettes. After inoculation and incubation as above, the plates were sealed with adhesive tape and stored in an inverted position at 4°C for up to 3 weeks before discarding. Subsequent plates were obtained from further subculturing from the agar stab. Before use, the strains were routinely tested on defined media for their growth requirements, to verify their phenotypes.

Glassware.

Unless otherwise stated, all glassware was washed with tap water followed by 3 rinses with glass distilled water, and dried overnight in an oven. Sterilization of glassware was then performed as required by heating in a hot air oven at 160°C for at least 1 hour. This washing of glassware was strictly adhered to and involved the use of no detergent in order to eliminate any possible damage to the bacterial membranes due to trace amounts of detergent present during the experiments (as shown by Moss and Smith, 1981).

Water.

The water used throughout this study for the preparation of media was single glass distilled.

Media used for the growth of organisms.

Unless otherwise stated, the organisms were grown up in a minimal growth medium. This was essentially M9 salts solution (Anderson, 1946)

plus the growth requirements for each particular strain. M9 salts solution was made up as two concentrates as follows:-

M9 A

NH_4Cl	50g	
$MgSO_4.7H_2O$	10g	This is a 50 X concentrate.
water to	1 litre	

M9 B

KH_2PO_4	37.5g	
$Na_2HPO_4.2H_2O$	75g	
NaCl	6.25g	This is a 12.5 X concentrate.
water to	1 litre	

All chemicals were 'Analar' grade obtained from B.D.H. Ltd. These stock concentrates were autoclaved in 500ml M.R.C. bottles at 121°C for 20 minutes. For use as a diluting fluid and for washing and resuspending cells for treatment, M9 salts solution (subsequently referred to as M9) was prepared by mixing 180ml M9 A concentrate, 720ml M9 B concentrate and making up to 9 litres with glass distilled water. Approximately 250 ml volumes of this solution were transferred to 300ml flasks, capped with aluminium foil and sterilized by autoclaving at 121°C for 15 minutes. The final pH of this solution was 6.9.

For preparing the minimal growth medium, 20ml of M9 A and 80ml of M9 B concentrates were mixed with an accurately measured amount of water (as shown in Table 2). The solution was then divided equally into ten x 250ml pyrex screw-top conical flasks, sealed and sterilized by autoclaving at 121°C for 15 minutes. Immediately prior to use for the growth of organisms, the sterile growth supplement solutions for

Table 2. Composition of minimal media used for growth of organisms.

Strain	M9A vol(ml)	M9B vol(ml)	distilled water vol(ml) for batch of 10	vol per 100ml batch of M9A/B plus water	Glucose 40% vol(ml)	thymine 1mg/ml vol(ml)	thiamine 1mg/ml vol(ml)	amino acid solution 10^{-1}M vol(ml)
SR 385	20	80	879.5	97.95	1.0	1.0	0.05	-
SR 246	20	80	869.5	96.95	1.0	1.0	0.05	1.0 lysine
SR 362	20	80	859.5	95.95	1.0	1.0	0.05	1.0 lysine 1.0 Methionine
B/r and NCTC 86	20	80	889.5	98.95	1.0	-	0.05	-
AB 1157 and AB 1886	20	80	875.0	97.5	1.0	-	0.5	1.0 leu/pro/ arg/his/thr solution.

N.B. Other strains in Table 1 were only grown in nutrient broth.

the particular strain were aseptically added, using laminar flow conditions, as shown in Table 2.

Preparation of growth requirements.

a) Glucose.

This was made up as a 40% stock solution by dissolving 200g D-glucose ('Analar' Grade B.D.H. Ltd.) in approximately 300ml of water and then making up to a final volume of 500ml in a volumetric flask. The resulting solution was clarified by filtration via a 3.0μm pore-size filter and then sterilized under aseptic conditions using a horizontal laminar flow unit (Microflow products), by negative pressure filtration through a 47mm diameter 0.2 μm pore-size Sartorius membrane. The sterilized solution was then stored at 4°C in pre-sterilized screw cap 150ml flat bottles. This concentrate was diluted 100-fold to give the required final concentration of 0.4%.

b) Thymine.

A 1mg/ml stock solution was prepared by dissolving 500mg thymine (Sigma chemical company) in 400ml warm glass distilled water. On allowing to cool this was made up to a final volume of 500ml in a volumetric flask, sterilized by filtration,and stored as above for the glucose solution. This concentrate was diluted 100-fold to give the required final concentration of 10μg/ml.

c) Thiamine hydrochloride.

A 1mg/ml stock solution was prepared by dissolving 100mg thiamine HCl (Sigma Chemical Company) in about 90ml of glass distilled water and making up to a final volume of 100ml in a volumetric flask. This was sterilized through a 25mm Swinnex unit (Millipore U.K., Ltd., London), sterilized by moist heat at 121°C for 15 minutes), fitted

with a 0.2 μm pore-size Sartorius membrane filter disc (V.A. Howe and Co. Ltd., London). This final solution was stored at 4°C in pre-sterilized 50ml flat screw-cap bottles and protected from light by wrapping in aluminium foil. To give a final concentration of 0.5 μg/ml for strain SR 385, this stock solution requires dilution by X 2000. Note, for thiamine requiring strains, e.g. E. coli K-12 AB strains, a final concentration of 5 μg/ml was required; and the stock solution is a 200 X concentrate.

d) Amino acid solutions.

In most cases a 0.1 M solution was prepared, which, to give a final concentration of 10^{-3} M, requires a 100 X dilution. For the E. coli K-12 AB strains used, a stock solution containing 0.1M of the required amino acids was prepared as follows:
L - threonine 5.955g, L - proline 5.755g, L - histidine 7.760g, L - arginine 10.535g and L - leucine 6.560g were dissolved in about 400 ml of water. All chemicals were obtained from Sigma Chemical Company. This solution was made up to a final volume of 500ml in a volumetric flask and sterilized and stored as for the glucose 40% solution. For use with other strains, 7.4605g of methionine to 500ml, 9.135g of lysine to 500ml and 5.106g of tryptophan to 500ml (i.e. a 0.05 M solution) were prepared in the same manner.

Composition of nutrient broth medium.

Occasionally, where indicated, nutrient broth was used as the growth medium. This was prepared by dissolving 13g of powdered nutrient broth (Oxoid CM1) in glass distilled water and making the final solution up to 1 litre. 100ml volumes of the broth were transferred to 250ml pyrex screw-top conical flasks which were then sealed and sterilized by autoclaving at 121°C for 15 minutes. The final pH of

the broth media was 7.2 - 7.4.

Incubation water bath.

This was a Gallenkamp water immersion bath set at a temperature of 37°C$^{+}_{-}$ 0.5°C and shaking at 100 cycles per minute. It was protected by a Grant "safety cut out" set at 50°C. The bath temperature and number of cycles per minute were checked regularly as small differences are known to affect membrane lipid composition (Cronan, 1978).

Aeration apparatus.

This was a forced aeration system devised to standardise the amount of air introduced into the culture vessels. Atmospheric air was drawn through a coarse cotton wool filter by a 40 watt Reciprotor piston pump (Edwards High Vacuum Ltd., Sussex, England) and fed into a 5 litre bell jar. This was connected to a Rotameter flow meter (Rotameter, Croydon, England) which monitored the flow rate of the air at 10ml per minute to a given culture vessel. The air was sterilized by passing it through a 25mm diameter Sartorius membrane (Sartorius membrane filters, G.M.B.H., West Germany) with a nominal pore size of 0.45 µm. The filter was positioned immediately before the entrance port of the culture vessel. The apparatus used for providing aeration has been described by Hodges, (1979).

Method.

A loopful of surface-grown culture from the agar plate (note, not a single colony but from an area of denser growth) was inoculated into a 250ml flask containing 100ml of prewarmed growth medium. This was connected to the aeration apparatus, set at 10ml per minute, and incubated in the shaking water bath for 24 hours. A secondary liquid

subculture was performed by transferring 1ml of the first (primary) liquid culture into 100ml of prewarmed growth medium and incubating in the same manner. From growth curves determined under the same conditions, log or stationary phase cultures were then obtained by growth for the necessary period of time. Such a growth curve for SR 385 is included in the Appendix A2. These culture conditions were used, unless otherwise specified, to ensure that cells were always in a defined phase of growth before irradiation, especially as it is known that membrane fatty acid composition alters during the transition from log to stationary phase cultures (Cronan, 1968).

Harvesting of organisms.

Two methods were routinely used; a filtration method when suspensions for irradiation were required at concentrations of 10^7 colony forming units (CFU) ml^{-1} or less, and a centrifugation method, when the concentration required was more than 10^7 CFU ml^{-1}.

i) Filtration method.

Apparatus : This was a negative pressure Sartorius apparatus incorporating a sintered glass supporting bed (Sartorius, G.M.B.H. West Germany). The filters used were 25mm diameter Sartorius membranes with a pore size of 0.45 μm. The filter was rinsed three times prior to and three times after filtration of the cell suspension with 10ml volumes of M9 salts solution. A measured amount of cell suspension, normally 1.0 ml, was filtered. The pressure was then released and the filter aseptically transferred to a sterile 100ml flask containing a volume of M9 sufficient to give the required concentration. The cells were then resuspended by gentle agitation. In this way over 95% of the cells are recovered (Moss and Davies, 1974).

ii) Centrifugation method.

Apparatus: This was either a Chilspin centrifuge or a M.S.E. minor model S-61 bench centrifuge (both from M.S.E. scientific instruments. Crawley, Sussex.) Both were operated at 1500 X g. The centrifugation tubes were disposable 25ml Sterilin universal containers (Sterilin Middlesex, England).

Method: The experimental culture was transferred in equal volumes into the universal tubes which were then sealed and centrifuged for 20 min. The supernatant liquid was then carefully poured off and the cell pellets for each tube were resuspended in 20ml of M9 salts solution by agitation and centrifuged again for 20 min. This washing procedure was repeated twice, then finally the cells were suspended in ice-cold M9 ready for experimentation.

After harvesting, an estimation of the initial viability of the culture was provided by measurement of the optical density of the culture and referring to a previously determined calibration curve for the particular organism. The optical density : viable count calibration curve for strain SR 385 is shown in the Appendix A3. The optical density of the bacterial suspension was measured using M9 salts solution as a blank in one of 2 matched glass cuvettes in a Unicam S.P. 600 spectrophotometer set at a wavelength of 470 nm. It was found that the Beer-Lambert relationship only held for optical densities of less than 0.35 so dilutions of cell suspensions with optical densities greater than this value were performed before reading.

Assessment of viability.

Cell viability was determined by relative colony forming ability

on various solid agar plates.

Materials:

a) pipettes.

Three Gilson pipettes (Gilson Medical Electronics, France) with volume ranges 20 - 200µl, 0.2 - 1.0ml and 1.0 - 5ml were used, each fitted with appropriate matching plastic changeable tips. The tips were washed in running water, boiled in glass distilled water, dried, and packed into D.H.S.S. specification bags (J. Dickenson and Sons Ltd.) before sterilization at 132°C for 5 minutes in a Drayton Castle high vacuum autoclave.

b) dilution tubes.

All serial dilutions were performed in 6" x ¾" rimless thick walled tubes of pyrex glass, fitted with Oxoid metal caps. The tubes were washed with tap water and rinsed with glass distilled water (3 times as described previously under glassware) while the metal caps were boiled in glass distilled water. After drying in an oven, sterilization was achieved by heating at 160°C in a hot air oven for at least one hour.

c) spreaders.

These were prepared by sealing both ends of glass quill and making a 60° bend two thirds along its length. After washing and drying as above, the spreaders were placed into glass beakers, aluminium foil placed on top, and sterilized by dry heat at 160°C for at least one hour.

d) dilution medium.

All dilutions, unless otherwise stated, were carried out

in M9 minimal salts solution.

Plating Media.

Essentially two types of plating medium were used in this study; complex medium and minimal medium.

a) Complex medium.

For the majority of experiments the complex medium used was YENB medium. This was prepared by adding 800ml of glass distilled water to 18.4g Difco Bacto nutrient agar (Difco Laboratories, Detroit, USA) and 6.0g Difco Bacto yeast extract in a 1 litre flat-bottomed flask and thoroughly mixing until all the powder had dissolved. This was allowed to stand for 10 minutes before sterilization by autoclaving at 121°C for 20 minutes. 20ml volumes of the molten agar were dispensed into 9cm diameter sterile petri dishes (Sterilin Ltd., England) using sterile Kipp's burettes.

Occasionally, where indicated, Oxoid nutrient agar (as described under storage of strains section) was used as a complex medium.

b) Minimal medium.

Essentially, this was the minimal growth medium, for the particular strain, solidified using 1.2% Oxoid agar No. 3. This is described subsequently as 'normal strength' minimal medium.

However, where specified, the concentration of inorganic salts was decreased 10-fold (= 'Low salt' minimal medium) or decreased 10-fold and supplemented with NaCl at 200mM (= 'high salt' minimal medium). A sodium chloride stock solution was prepared by dissolving 93.504 g

in 700ml of glass distilled water and making up to 1 litre in a volumetric flask. 10 x 100ml volumes were then dispensed into 150ml flat bottles and sterilization was carried out by autoclaving at 121°C for 15 minutes. One x 100ml bottle of this (1.6M) solution in each 800ml agar batch then provides a total of 200mM NaCl. The sodium chloride was 'analar' grade obtained from B.D.H. Ltd.

Preparation of minimal medium plates.

In all cases, 800ml batches were prepared by dissolving 9.6g of Oxoid agar No. 3 in an accurately measured volume of glass distilled water (see Table 3), pertaining to the particular plate type or organism used, in a flat-bottomed 1 litre flask. This mixture was then sterilized by autoclaving at 121°C for 20 minutes. The sterile molten agar was then allowed to cool to approximately 60°C and transferred to a laminar flow hood where the appropriate M9 salts solutions (concentrates), NaCl and growth supplements were all added as sterile solutions. Mixing was achieved by gentle rotation of the flask. 20ml aliquots were then poured as for the complex medium.

All plates were stored at 4°C in the dark for up to 4 days. Immediately before use they were dried in an open inverted position at 37°C for 75 minutes under ventilated conditions.

Method of viability assessment.

For the determination of the viable count of bacteria, generally an initial 20-fold dilution was made by transferring 0.2ml of the test suspension into 3.8ml of M9 solution in a dilution tube. Occasionally, when sample volumes were low, a 100-fold initial dilution (0.05ml + 4.95ml M9) was performed. A subsequent series of 10-fold dilutions

Table 3. Composition of minimal medium plates for strain SR 385.

All weights (in grams) and volumes (in mls) refer to a 800ml agar batch.

Plate Type	Oxoid agar No. 3	distilled water	M9A concentrate	M9B concentrate	NaCl solution 1.6M/100ml	Glucose 40%	Thymine 1mg/ml	Thiamine 1mg/ml
'Normal' strength	9.6	703.6	16	64	-	8	8	0.4
'Low salt' (Tenfold-diluted inorganic salts)	9.6	775.6	1.6	6.4	-	8	8	0.4
'high salt' (Tenfold-diluted plus NaCl at 200mM)	9.6	675.6	1.6	6.4	100	8	8	0.4

For other strains, the appropriate amino acid solutions (8ml of 0.1M solution) etc. were added and the volume of distilled water adjusted accordingly. Note: for the thiamine requiring strains (K-12 AB strains) 4.0ml is required per 800ml batch.

(0.5ml + 4.5ml) was then performed as required. At each dilution stage the suspension was thoroughly mixed using a whirlimix (Fisons Ltd.). A 0.2ml sample (or occasionally 0.1ml) of the required dilution was then pipetted onto the surface of the agar plates, 3 of each of the types used in the particular experiment, and spread evenly over the surface using a sterile glass spreader, a different spreader being used for each plate type. The plates were then incubated in an inverted position at 37°C for 48 hours for the complex medium and 72 hours for the minimal medium. The number of colonies visible, without magnification, on each plate was counted. From the mean value of the three plates, and the known dilution factor, the number of viable bacteria in the original suspension was determined.

The optimum number of colonies for counting by this method is between 30 - 300 colonies per plate. A range of dilutions were plated to yield colony counts within this range.

Estimation of the errors involved in viable count assessment by this technique.

Errors may be introduced in two ways; the pipettes may not deliver accurate or precise volumes, and the mixing of the suspension at each dilution stage may be insufficient to provide a count which truly represents the viability of the original suspension.

The error involved in the pipetted volumes was determined periodically by weighing the volumes of glass distilled water delivered under experimental conditions. The conditions employed simulate the worst encountered; the pipettes were reset on each separate occasion and a fresh tip fitted. The glass-distilled water was equilibrated to temperature (22°C) in a Dewar flask. The results, which are shown

in Table 4, show that in all cases the coefficient of variation obtained was not greater than 0.72% and the deviation from the theoretical weight was a maximum of 2.77% for the 0.05ml volume. It was considered that this method of volume measurement gave satisfactory results and was thus employed.

The error associated with the homogeneity of the suspension was determined by performing viable counts on a typical experimental suspension using separate series of dilution series. These results are described in Table 4 and show that this error is the major contributing factor to the overall experimental error. The coefficient of variation is shown to be 3.55%. This was considered acceptable.

IRRADIATION PROCEDURES.

General.

All experiments involving irradiation with ultraviolet light were carried out in a 'dark room' under illumination from red fluorescent tubes (Atlas Ltd. 80W) which do not emit at wavelengths below 540 nm (thus preventing concurrent photoreactivation of damage to DNA).

Radiation Sources.

a) Near - UV radiation.

This was provided either as broad-band wavelength radiation from Black-Light Blue fluorescent lamps, or monochromatic wavelength radiation from a 200-W super pressure Hg lamp or a 1-kW Hg-Xe arc lamp.

i) Broad-band radiation.

This apparatus, shown diagrammatically in Figure 15,

Table 4. Summary of errors introduced in viable count assessment.

a) accuracy of Gilson pipettes.

volume (ml)	pipette	Mean (g)	Standard deviation from mean	Coefficient of variation	% difference from theoretical value
0.05	P200	0.0513	3.682×10^{-4}	0.718	-2.77
0.2	P1000	0.1975	9.982×10^{-4}	0.505	+1.01
0.5	P1000	0.4972	3.3698×10^{-3}	0.678	+0.22
3.8	P5000	3.8177	1.586×10^{-2}	0.415	-0.71
4.5	P5000	4.5039	1.113×10^{-2}	0.251	-0.40
4.95	P5000	4.9840	1.883×10^{-2}	0.378	-1.03

Each volume of glass distilled water was weighed fifteen times using an analytical balance at constant humidity.

Table 4.

b) homogeneity of the suspension. (Strain SR 385)

Series No.	Plate Counts	Mean viable count (10^7/ml)
1	151 205 191 182	1.82
2	203 191 178 190	1.90
3	165 175 180 157	1.69
4	163 193 207 188	1.88
5	202 167 196 185	1.87
6	179 196 196 173	1.86
7	196 186 186 189	1.89
8	189 201 177 189	1.89
9	208 188 161 186	1.86
10	200 185 198 189	1.93

Overall mean viable count = 1.859×10^7.

Standard deviation = 6.607×10^5.

Overall coefficient of variation = 3.55%.

A 10^5 dilution was performed ten times, using separate dilution tubes, on the original bacterial suspension.

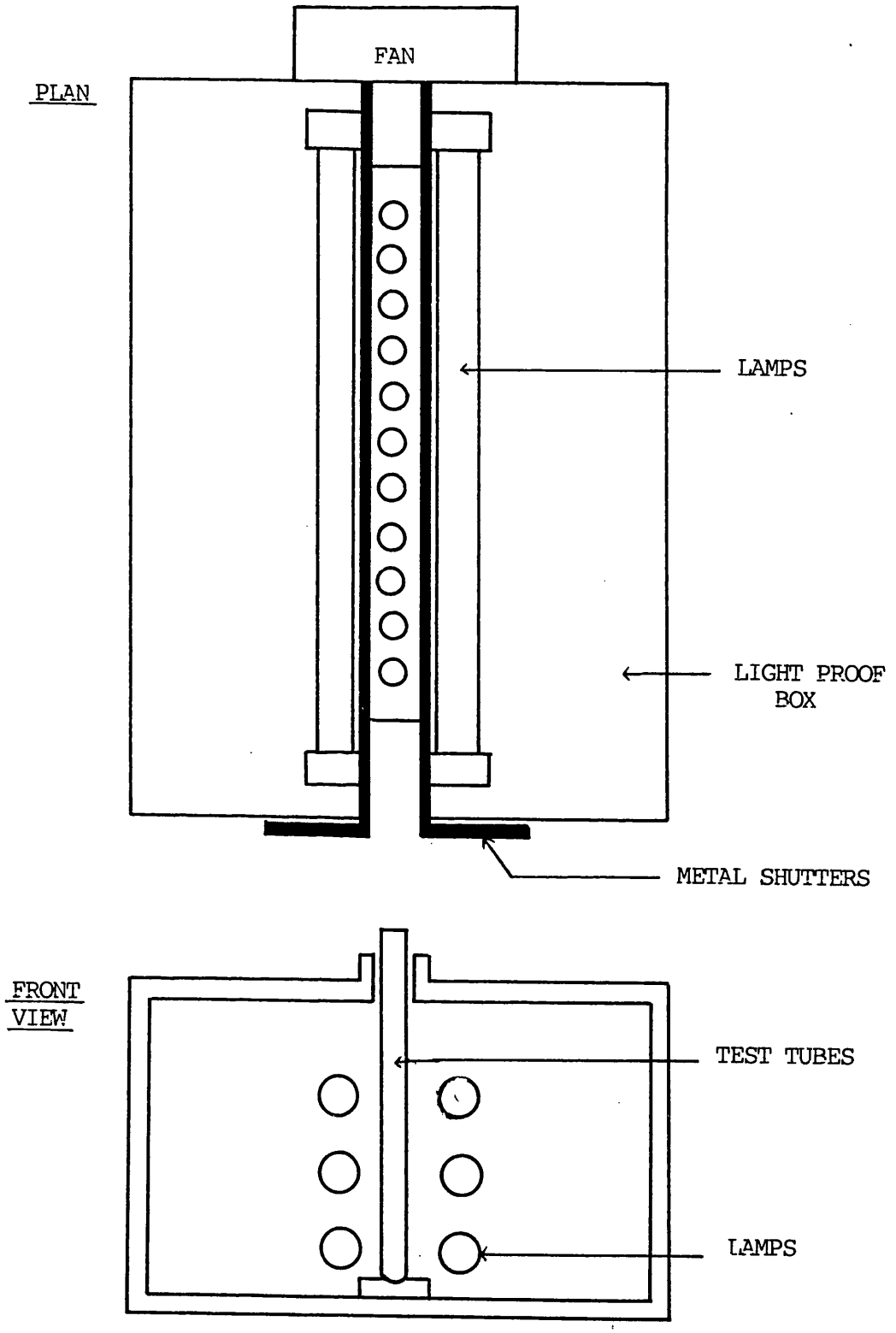

Figure 15 Diagram of near ultraviolet light source.

consisted of six Sylvania F15T8 'Black-Light Blue' lamps (Sylvania Electric Products Inc., Danvers, Mass. USA) mounted as two vertical banks of three lamps. The emission spectrum of these lamps is shown in Figure 16. This was determined by the detection of radiation through a monochromator, set at 5 nm steps, using a microvoltmeter. Figure 16 shows the emission of these lamps to be from 320 to 405 nm with an emission peak at 355 nm. To overcome fluence output variations, the lamps were run for 100 hours before use in an experiment, it was found that after this time the output is steady. Twelve glass test tubes (Oxoid) were held vertically, spaced 1.5cm apart and centred between the lamps. The distance between the front surface of the lamps and the tubes was fixed at 4cm. The apparatus contained two metal shutters between the tubes and the lamps, and a fan at one end. Five millilitres bacterial suspensions in M9 salts solution, in the positions used, were found to remain at 28°±1°C throughout irradiation. When not in use, positions were fitted with tubes containing 5ml of M9 salts solution to keep reflected light constant. For 15 minutes prior to and during irradiation, samples were bubbled with filtered humidified air using Pasteur pipettes, which provided a means of stirring the irradiation suspensions.

This fluorescent lamp housing was constructed to strict specification, as outlined above, because it was intended to provide a near replica of the apparatus used by Moss and Smith (1981) in order that meaningful comparisons of results could be made.

ii) Monochromatic radiation.

Unless otherwise stated, the source of radiation was a Bausch and Lomb SP 200 super pressure mercury lamp (Bausch and Lomb Rochester, New York). This was a 200-W super pressure Hg vapour lamp

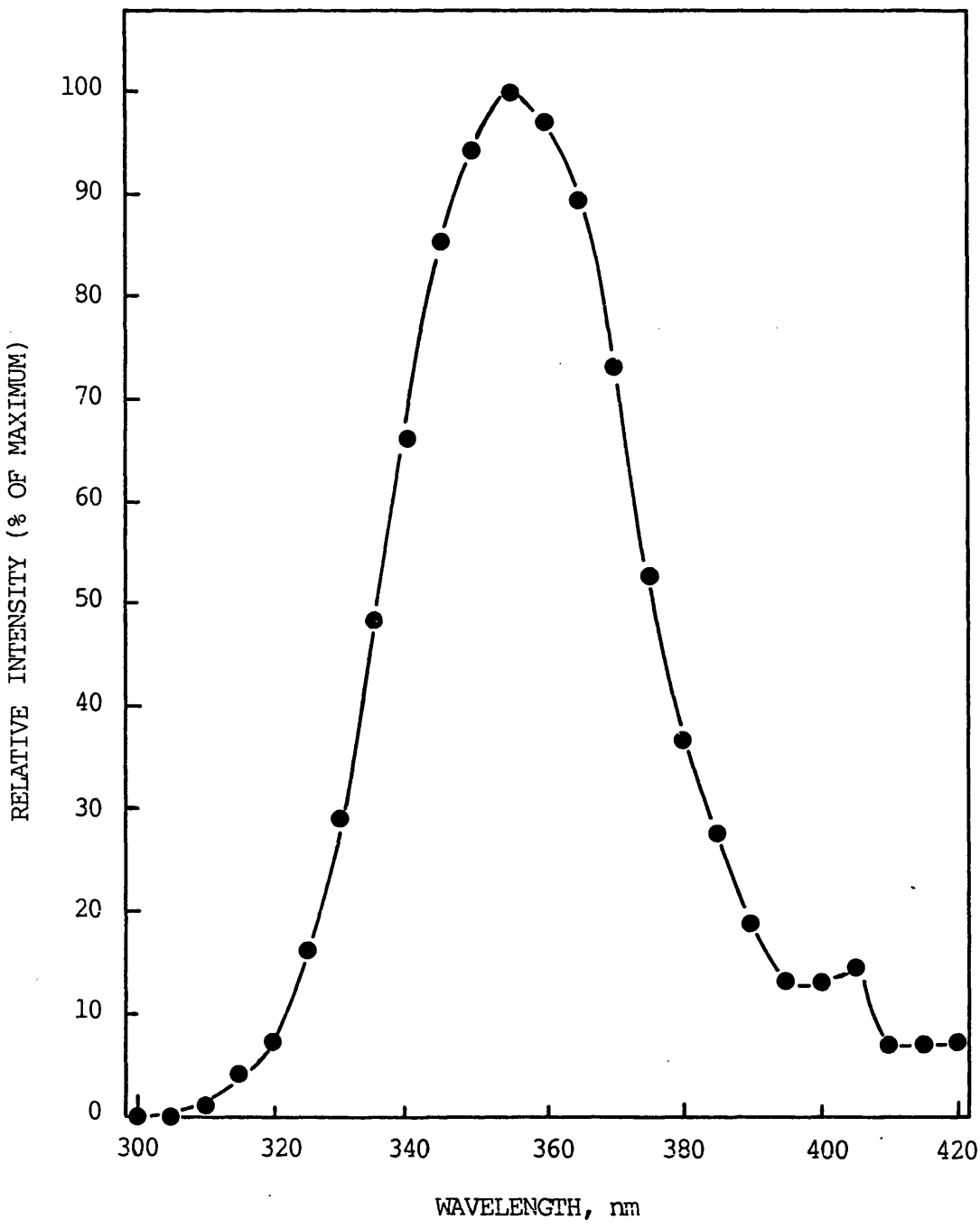

Figure 16 : Emission spectrum of near-ultraviolet Black-Light Blue fluorescent light source.

with a fused silica envelope and an appropriate fused silica condensing lens system. Lamps were replaced after 100 hours use (after which time output had dropped considerably and was unstable) and a 2 hour burn off of newly fitted lamps was allowed prior to use for irradiation. This light source was used in conjunction with a Bausch and Lomb high intensity grating monochromator, which was fitted with a UV-visible diffraction grating of 1350.0 lines per mm blazed for maximum efficiency at 300 nm. Operation is over a wavelength of 200 - 800 nm with a stated reciprocal dispersion of 6.4 nm/mm. Matched fixed slit discs were used; the entrance and exit slits being 2.68mm and 1.5mm respectively.

Arrangement of optical bench for monochromatic irradiation of cells.

All optical components were arranged in a horizontal plane on an Ealing Beck optical bench and associated supports, allowing vertical and horizontal adjustment. The general arrangement of apparatus is shown in Figure 17.

The shutter : This was an iris camera shutter (G.B. Kershaw 630) with a 2cm aperture. This was fitted with a cable release and exposures were timed using a stopwatch. Where exposure times below 10 seconds were required, the shutter opening time was electronically controlled and the exact exposure recorded on a millisecond timer (Venner Electronics Ltd.).

The focusing lens : This was a 40mm diameter Spectrosil biconvex lens having a focal length of 55mm. This produced an inverted magnified image of the exit slit of the monochromator 3cm high and 1cm wide allowing full illumination of the irradiation cuvette.

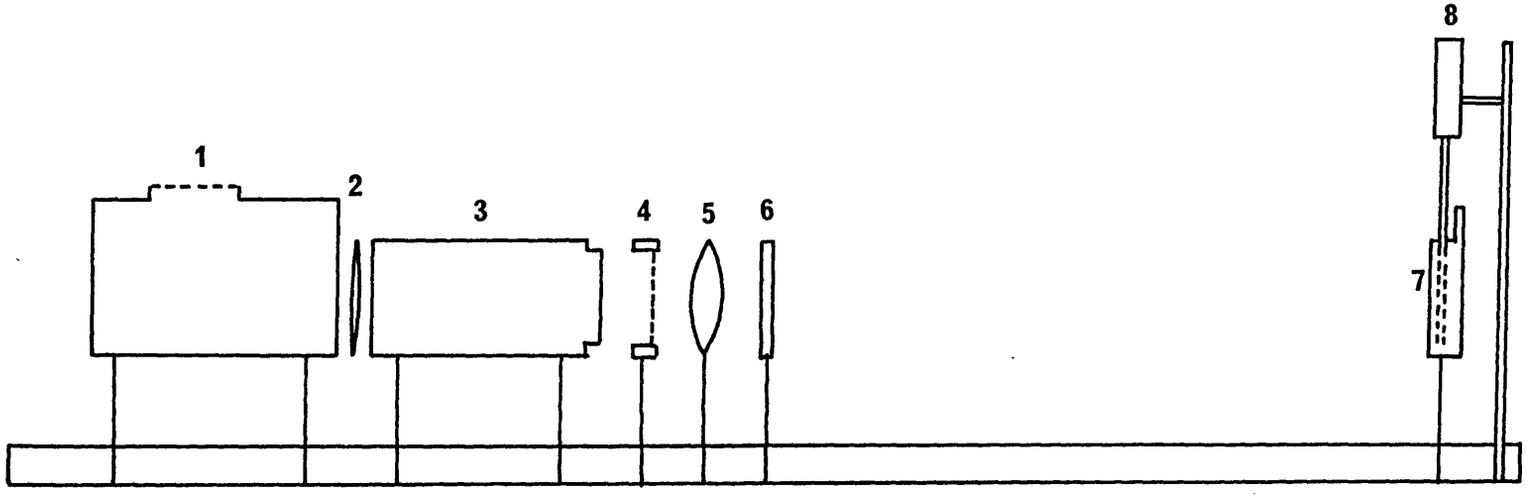

Figure 17 Diagram of apparatus for UV irradiation of cells in suspension.

1. Mercury UV Source (SP200)
2. Quartz Collective Lens
3. Monochromator
4. Shutter
5. Focusing Lens
6. Stray Light Filter
7. Irradiation Cuvette (see Figure 19)
8. Stirrer

Stray light filters : During irradiation with near - UV monochromatic wavelength radiation produced using a monochromator, it is essential that any stray light of shorter wavelength be removed from the radiation beam as this would contribute significantly to inactivation due to its higher energy properties. The introduction of a corresponding error in determination of the biological sensitivity would also result. Therefore, an appropriate UV - absorbing filter was positioned between monochromator and the irradiation cuvette. Details of the filters used at each wavelength studied are given in Table 5 and the cut off of each filter is shown in Figure 18. The choice of stray light filter at each wavelength was generally taken from published work involving action spectra for lethality determinations (e.g. Webb and Brown, 1976; Webb and Peak, 1981). The spectral properties of the filters were determined upon receipt from the suppliers by construction of UV transmission spectra, relative to air, using a Pye-Unicam SP 1800 scanning spectrophotometer in order to ensure that their specification was met.

For irradiation at 313 nm, a film of Mylar C 2.5μm (Dupont Ltd.) was employed as a stray light filter. This material required a period of about 2 hours exposure to the 313 nm radiation before use in an experiment, to 'age' it. During this time the transmission of the filter at 313 nm fell initially and then remained stable.

The irradiation cuvette : A jacketed 10mm internal width, 10mm pathlength quartz cuvette was used (Thermal Syndicate Ltd.). This is illustrated in Figure 19. Control of the temperature of cell suspensions during irradiation was achieved by the circulation of a 50% ethylene glycol solution through the jacketed cuvette. For irradiation

Table 5. Details of stray light filters, band widths and approx. fluence rates used in irradiation experiments.

	Wave-length (nm)	SOURCE	STRAY LIGHT FILTER	Wavelength 1% transmission on Low side (nm)	% transmission at designated wavelength	Band width at 50% maximum (nm)	Approx. fluence rate $Jm^{-2}sec^{-1}$
*	254	Penray	G-275	252	92 without filter (Child's 1962)	4.0	0.05
*	254	B&L	-	-	95 with filter	12.0	0.98
	260	"	-	-	-	12.0	0.22
	270	"	-	-	-	12.0	0.24
	280	"	-	-	-	12.0	0.73
	290	"	CORNING 0-56	240	60	13.0	2.2
	300	"	CORNING 0-53	268	47.9	10.0	4.5
	305	"	CORNING 0-53	268	56.2	13.5	7.0
	310	"	CORNING 0-54	302	20	8.5	7.0
*	313	"	Mylar 2.5 μm	301	54	7.0	25
	317	"	WG 320	296	72.4	9.5	20
	325	"	CORNING 0-54	302	84	12.5	16
	328	"	WG 335	314	50	13.0	18
*	334	"	WG 335	314	68	7.25	14
*	365	"	CORNING 0-52 (HALF THICKNESS)	332	75	7.0	60
*	365	Oriel	"	330	72	10.0	95
*	405	B&L	CORNING 0-51	362	66	7.0	160
*	405	Oriel	"	360	62	10.0	210

* denotes mercury resonance line.

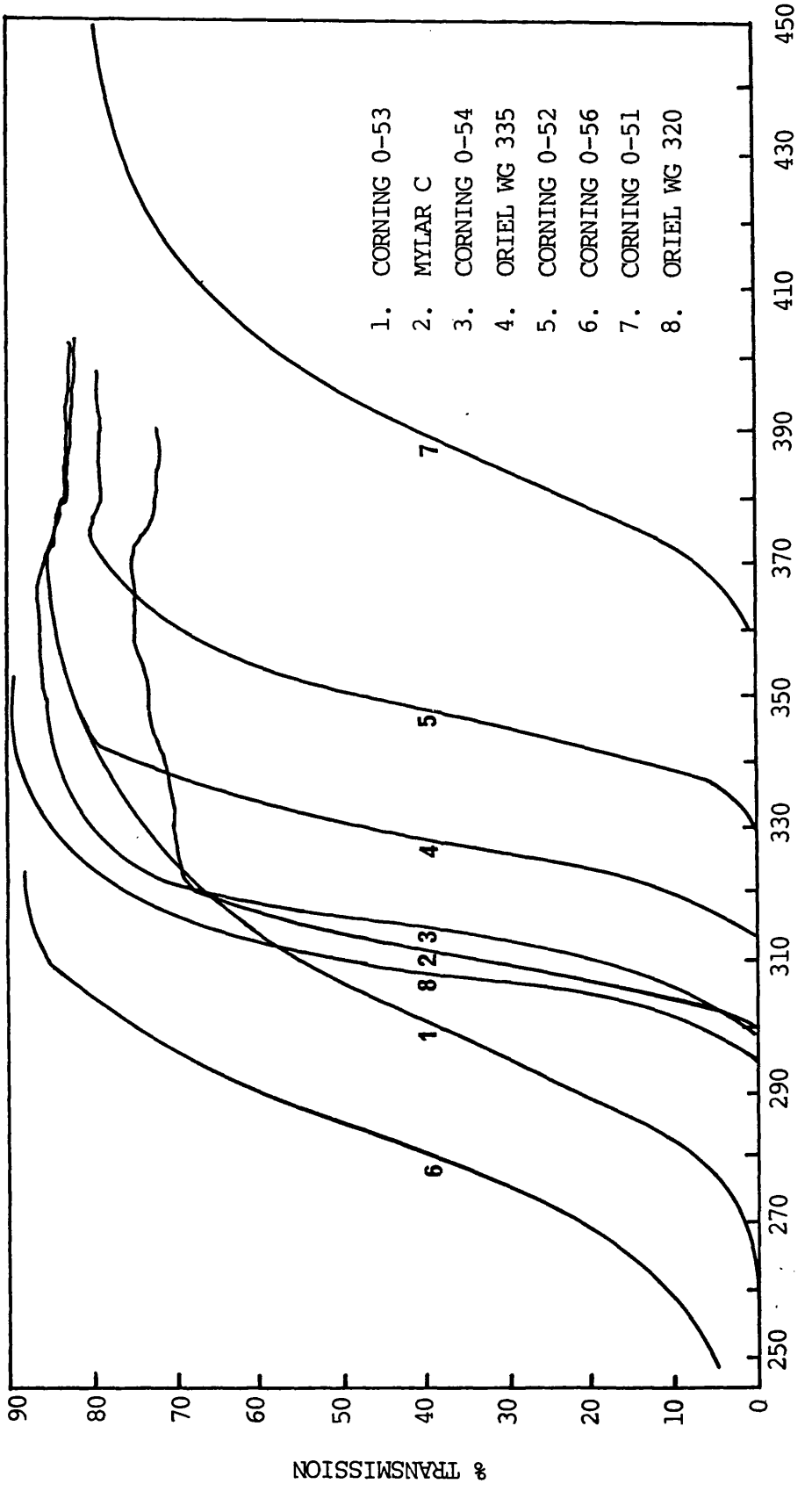

Figure 18 Transmission characteristics of stray light filters.

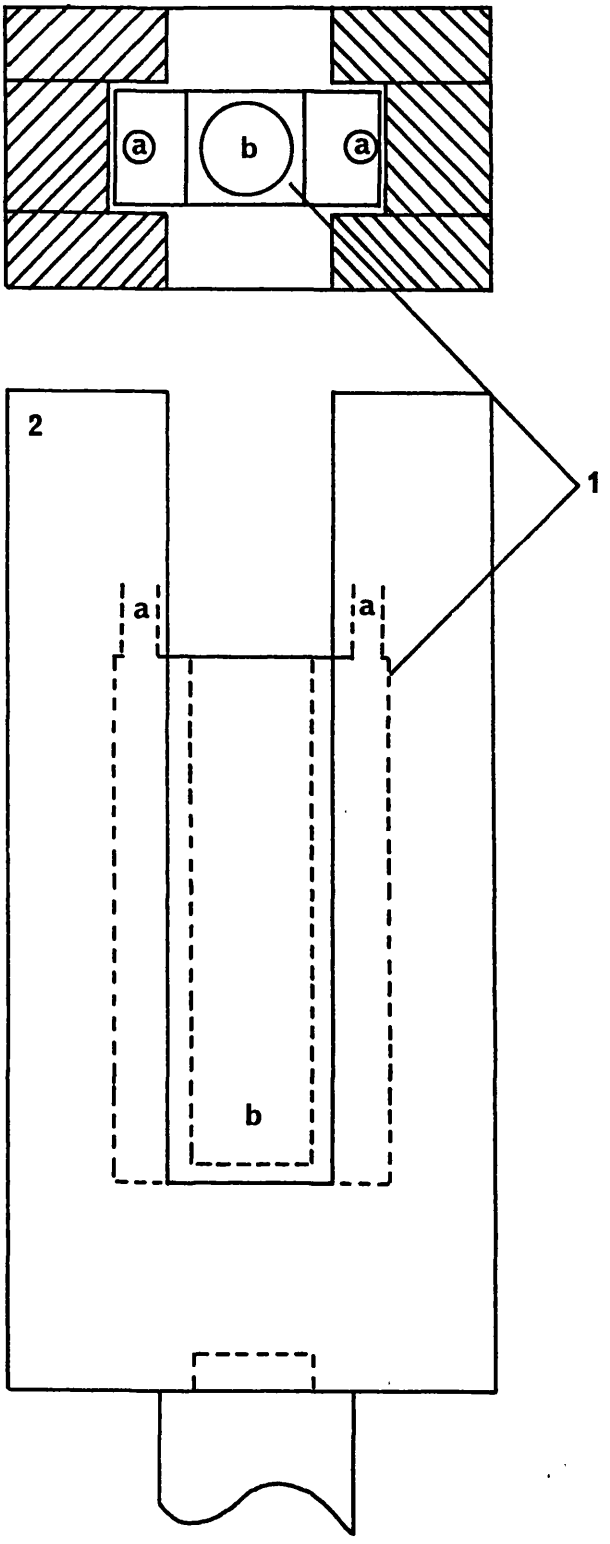

Scale 1: 1.5

Figure 19 Diagram of Irradiation Cuvette.

1. Irradiation Cuvette.
   a. Entrance and Exit ports for cooling solution.
   b. Position of suspension for Irradiation.
2. Perspex holder.

at 0°C, an insulated bath of the glycol solution was cooled by a U-cool refrigeration unit (Neslab Instruments Inc.). Thermostatic regulation was achieved by a heating coil pump (Grant Instruments Ltd.). The solution was then circulated at high flow rate through lagged rubber tubing by a peristaltic pump (Watson Marlow Ltd.). Periodic monitoring of the cuvette temperature, achieved using a probe thermometer (Comark Ltd), showed that a temperature of 0°C ± 0.5°C was maintained. Condensation which formed on the cuvette faces during irradiation was removed at the sampling intervals with a clean tissue. Normally a 3.0ml suspension of bacteria was irradiated.

The stirrer : Cell suspensions were stirred during irradiation by means of a quartz paddle rotating in a laboratory stirrer (Stanhope Seta Ltd.) at approximately 1200 rpm.

At longer wavelengths (e.g. 365 and 405 nm), where higher fluences are necessary to cause inactivation, the Bausch and Lomb Hg source and monochromator was replaced, where indicated, with a 1-kW Hg-Xe arc lamp (Oriel Scientific Ltd., Kingston Upon Thames) and an Oriel (Model 7240) grating monochromator with 2400 lines per mm. The optical bench arrangement was the same as described previously. The monochromator was operated with entrance and exit slits at 3mm providing band-widths at half maximum as given in Table 5.

Analysis of emitted radiation.

Analysis of the radiation emitted from the monochromator system, with the appropriate stray light filter in place, was performed routinely. The procedure involved the use of a second Bausch and Lomb high intensity monochromator to scan the emitted spectrum. The second 'analyzing' monochromator was fitted with half-width slit discs; the

entrance and exit slits being 1.34mm and 0.75mm respectively. It was interposed between the irradiation cuvette and the stray light filter. Emitted radiation was focused onto its entrance slit and dosimetry measurements of the light passing through it were made using a calibrated thermopile (see under dosimetry section). The measurements were made at one nm intervals at $\pm$ approximately 12 nm from the maximum emission wavelength. The data obtained were plotted as relative intensity against wavelength and used to determine the bandwidths in nm at half the maximum intensity (the most common parameter used to portray the degree of monochromaticity of the source). A typical emission spectrum is shown in Figure 20 and the data for the radiations employed are given in Table 5.

b) Far - UV radiation (254 nm).

The source used, unless otherwise indicated, was a 5cm Penray lamp (UV Products Inc. JnC SC-1) fitted with a G-275 filter, which isolates the 254 nm line to the extent that 95% of the emission is at this wavelength. The lamp was either used in a vertical position on an optical bench in conjunction with a shutter and irradiation cuvette (as described previously), or in a horizontal position in the apparatus illustrated diagrammatically in Figure 21. This is shown to consist of an irradiation vessel positioned at a distance of 15cm directly beneath the UV source, with a shutter regulating exposure, positioned between. The shutter was of the same type as previously described. The irradiation vessel was a straight-sided glass bowl, with an internal diameter of 5cm. For adequate mixing, filtered humidified air was blown on to the surface of the test suspension through a side jet. Ten ml of bacterial suspension was normally irradiated. Even though the distance between the source and the surface of the suspension fractionally increased after the removal of

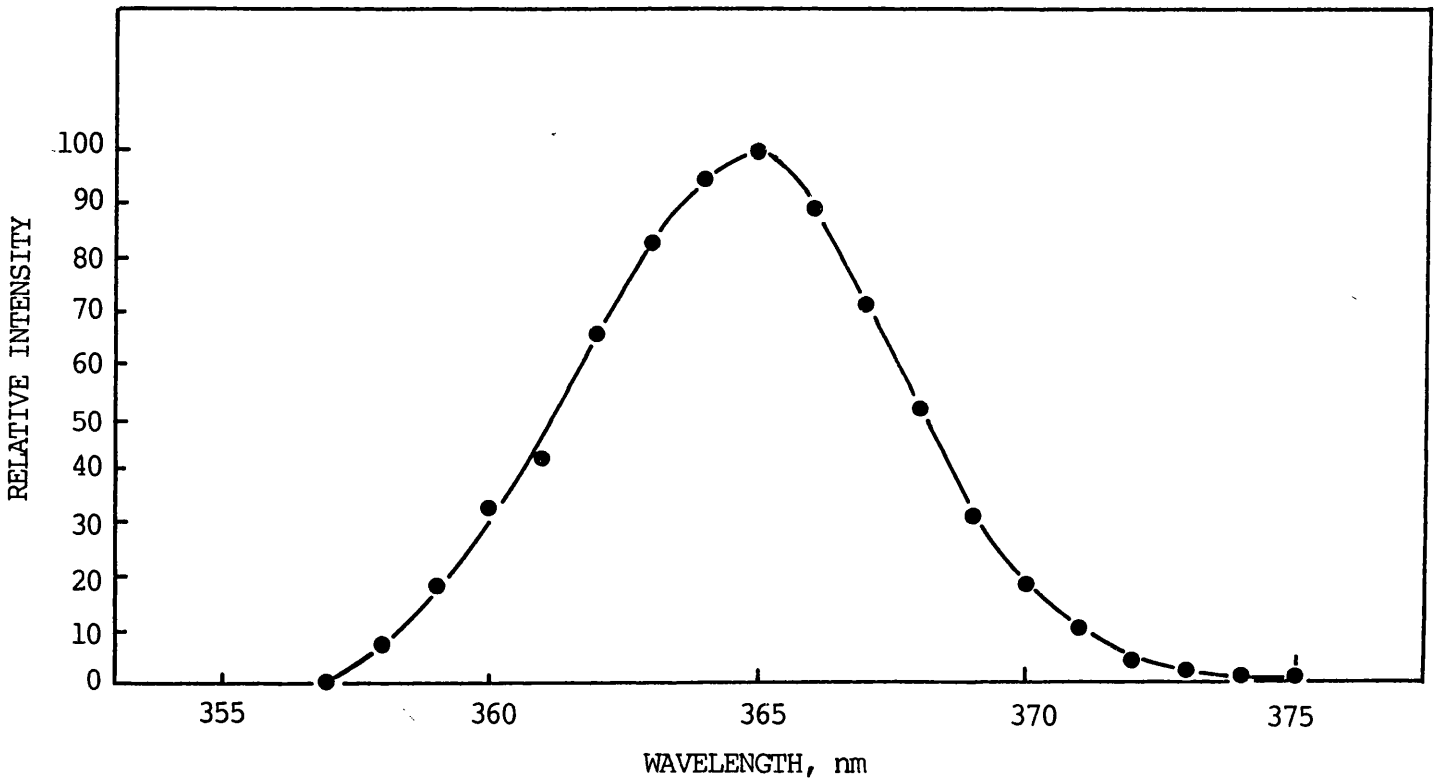

Figure 20 Typical analysis spectrum of emitted 365 nm radiation from Bausch and Lomb source (plus 0-52 filter)

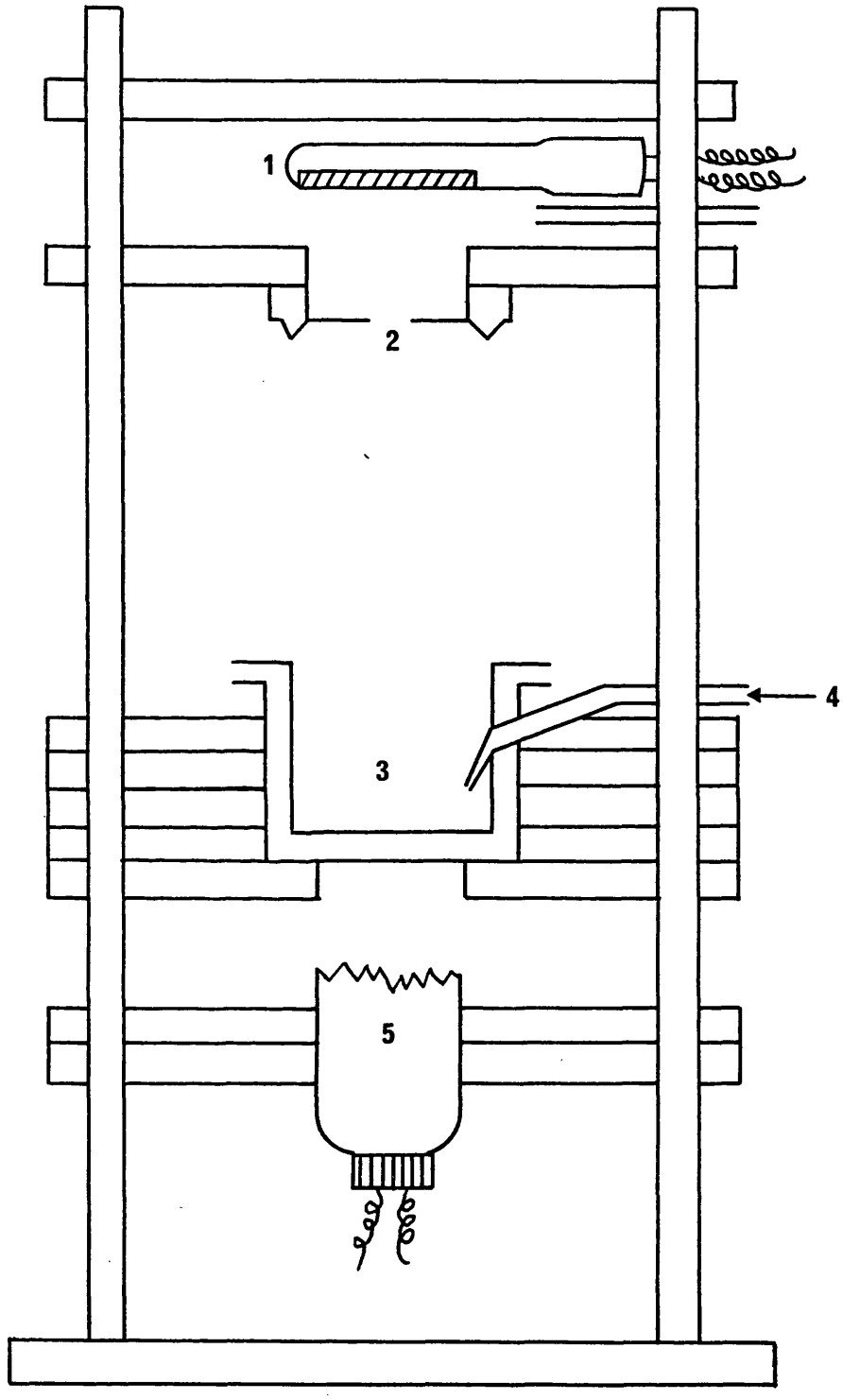

Figure 21. Diagram of apparatus for 254 nm irradiation.

1. UV Source.
2. Shutter.
3. Irradiation Vessel.
4. Air Inlet.
5. Position of Thermopile.

each 0.05ml aliquot, this was considered to be insignificant. In order to prevent any build up of ozone and to maintain steady experimental conditions, a flow of compressed air was blown over the surface of the source filter and mains electricity to the lamp was supplied through a voltage stabiliser (Advance Electronics CV 100A). No temperature control was used with this 'horizontal' 254 nm apparatus during this study, the irradiations proceeding at room temperature. However, temperature control was, of course, possible using the Penray lamp in position on the optical bench and using 254 nm radiation from the Bausch and Lomb Hg source.

General procedure for UV irradiation of cells.

In all cases the lamp was allowed to 'warm up' for a standard time (20 minutes for the Black-Light Blue source and the Penray lamps, and at least 30 - 60 minutes for the Bausch and Lomb and Oriel lamps). Precision alignment of the irradiation cuvette along the optical bench was then carried out for the monochromatic irradiation of cells. This involved positioning the cuvette at a height and distance from the source such that the front face of the cuvette was entirely within the field of illumination. A thermopile (Oriel products Model 7102) was then moved into the radiation beam, and using the focal plane shutter, a number of microvolt readings were taken. These were used to calculate the incident fluence by application of the calibration factor appropriate to the detector (see under dosimetry section). If, as sometimes occurred with these arc lamps, the microvolt readings showed significant variation, the lamp was allowed to burn until a stable reading could be taken. The irradiation cuvette was then moved back into position, rinsed twice with M9 salts solution, the stirring paddle introduced and switched on, and the apparatus sterilized by 15minutes exposure to the 254 nm output of a Penray lamp either by

placing this a few centimetres in front of the cuvette or, if this was the radiation source in use, simply by opening the shutter. A 3ml volume of the cell suspension, usually at a concentration of $1x10^7$ CFU/ml was then transferred to the sterile irradiation cuvette, the circulation of cooling liquid through the water jacket surrounding the cuvette started, and the suspension allowed a 5 minute period to reach the desired temperature.

In the case of irradiation with the broad-band near - UV radiation source, a sterile test tube in a fixed position in front of the lamps was used, at which point the fluence had been previously determined (see under dosimetry section). In all cases involving single irradiation procedures, the sample was placed in position 7 of the lamp box. Where more than one position was required during an experiment, a maximum of four positions was used, those being the central ones (tubes 5, 6, 7 and 8). Stirring was achieved by bubbling filtered humidified air via sterile Pasteur pipettes. A 5 minute period was allowed for equilibration of the test suspension to ambient temperature. The cell suspension was then exposed to graded fluences of UV radiation and a sample removed from the tube both as a control and after each fluence for the assessment of viability.

Determination of fluence rate for ultraviolet radiations.

a) Broad-band near - UV source.

The general method of fluence determination using a thermopile calibrated by chemical actinometry was found to be inappropriate for this source. First, a thermopile could not be inserted into the narrow central position between the lamps in such a way as to detect the entire field of radiation reaching the bacterial suspension, and

second, chemical actinometry itself, involving the use of potassium ferrioxalate required exposure times that were too short (<5 seconds) to measure accurately in order to obtain a conversion value within the limits of the calibration curve (see later under actinometry section).

Therefore, an approximate fluence rate was determined by biological means by a comparison of sensitivity of various organisms with published work. First, as up to a maximum of 4 positions in the lamp box were used during any one experiment, survival curves for the normal test organism used in this study, K-12 SR 385, were determined in various positions in the lamp box, in order to ascertain whether the tubes used throughout this study, by a comparison of lethal effects, received equal fluence rates. The survival curves obtained are shown in Figure 22. This result was obtained using the same stationary-phase bacterial suspension and as one experiment. Figure 22 shows that the tubes 5, 6, 7 and 8 used throughout this study received approximately equal fluence rates. It may be noted that significantly lower fluences were received in the outer positions of 1 and 12.

In order to make a comparison of strain sensitivity with published work it was necessary to assume that the Black-Light Blue lamps emitted radiation which could be approximated, in terms of biological effectiveness, to 365 nm monochromatic radiation. This is because of the relatively few survival curves published using such sources, and variations in their emission spectra due to differences in their phosphors (as shown by Forbes et al., 1976) making comparisons impossible. Although not ideal (due to possible wavelength interactions) no other method was available for use and, from the emission

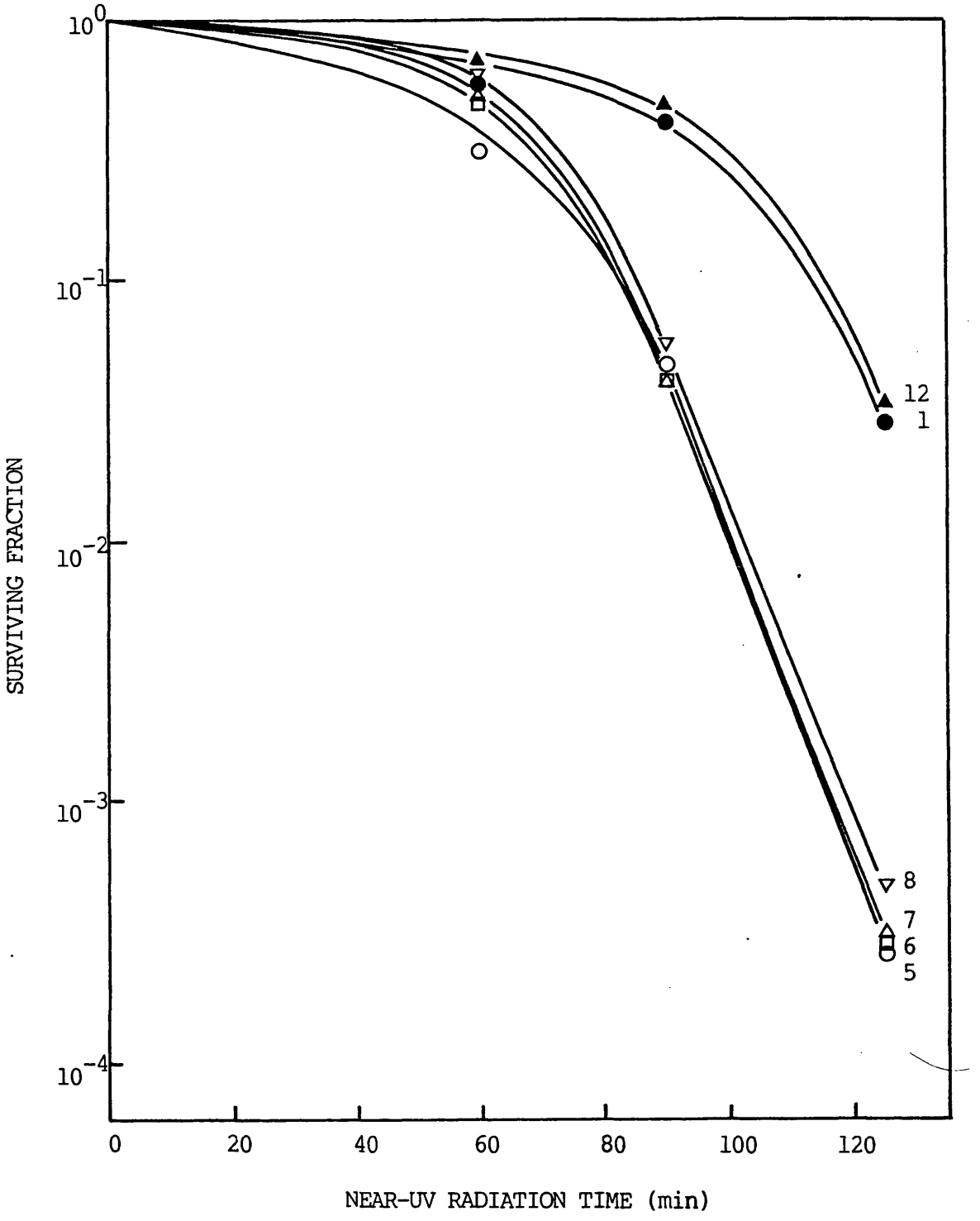

Figure 22 Survival curves for E. coli K-12 SR 385 after broad-band near-UV irradiation at various positions (as numbered) in Black-Light Blue Lamp source.

spectrum shown in Figure 16, this approximation was considered to be appropriate.

For the first dosimetric comparison with published work (e.g. Tyrrell, 1978a), a survival curve was obtained for Bacillus subtilis UV SSP 42-1 spores. As a second comparison, a survival curve was obtained using E. coli K-12 SR 362 uvrA, uvrB, recA, phr, which was then compared with the published sensitivity of E. coli K-12 AB 2480 (uvrA, recA) at 0°C (where no photoreactivation could occur) to 365 nm radiation (e.g. Brown and Webb, 1972).

These survival curves (both published and those obtained with the broad-band source) are shown in Figure 23 and a summary of the comparisons and calculated fluence rates is shown in Table 6.

Table 6 indicates that the fluence rate of the Black-Light Blue lamps, used in this study, is approximately 1.08×10^{3} $Jm^{-2}sec^{-1}$. However, as these experiments only provide an approximate fluence rate, all survival curves involving this source are expressed in terms of the time of exposure (in minutes). From routinely determined survival curves, using strain SR 385, it was found that inactivation did not alter significantly, suggesting a constant fluence rate emitted by the lamps throughout this study.

b) Monochromatic radiation.

For both near and far - UV radiation, the fluence rate was determined using an Oriel 7102 thermopile (Oriel Scientific Ltd., Kingston upon Thames). For use on the optical bench, thermopiles were mounted in a sliding bench saddle beside the cuvette such that the detector was coincident with the inside front face of the cuvette

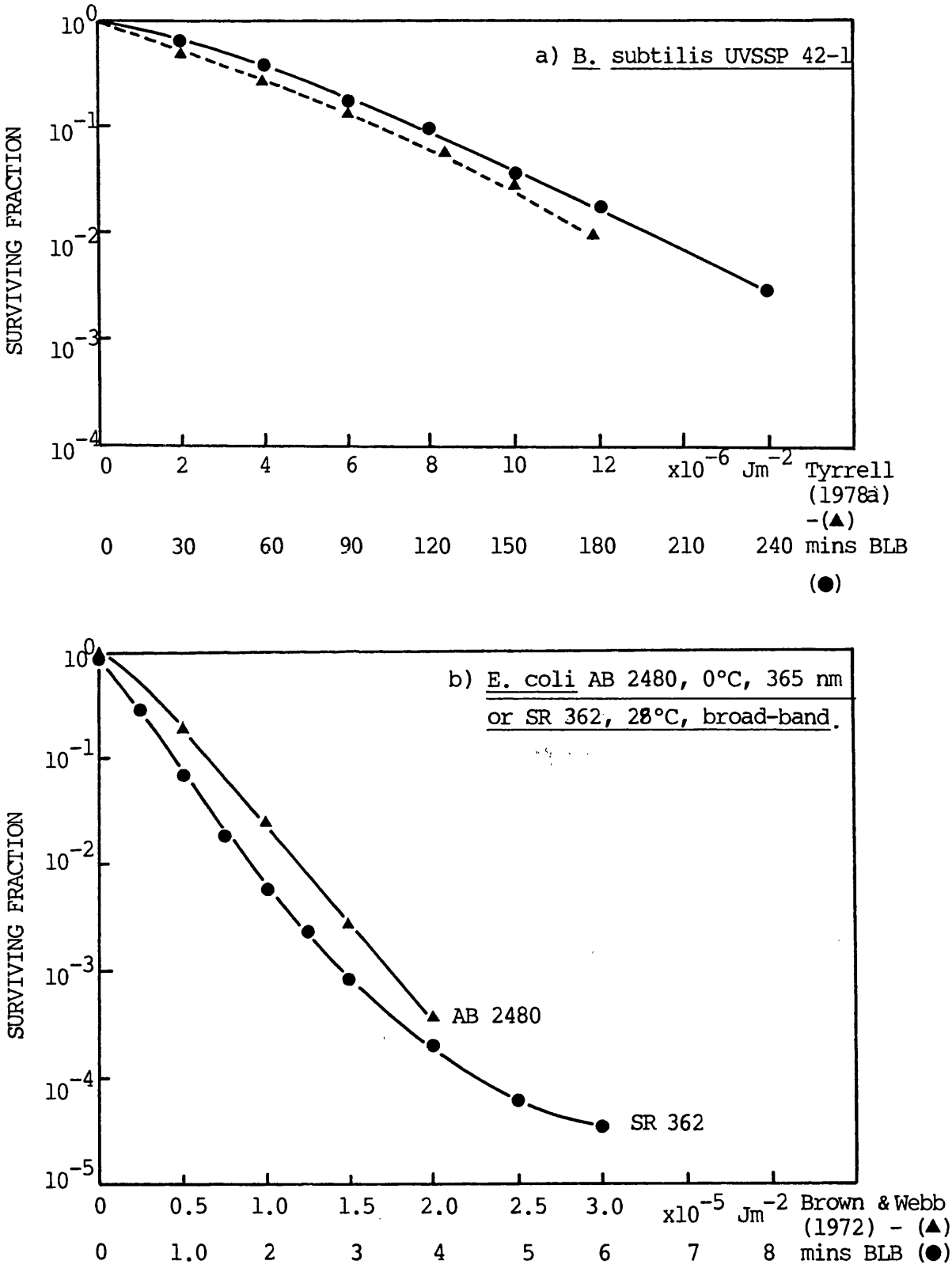

Figure 23 Biological dosimetry comparisons for Black-Light Blue lamp source.

Table 6. Summary of fluence rate determinations for the Black-Light Blue source by biological dosimetry.

Strain.	Time of exposure to broad-band near-UV radiation for inactivation to 10% survival.	365nm radiation fluence (Jm^{-2}) for inactivation to 10% survival.	Calculated fluence rate $Jm^{-2}sec^{-1}$
B. subtilis UVSSP 42-1 spores.	120 mins	$6.9x10^6$ (Tyrrell, 1978a)	$9.58x10^2$
E. coli AB 2480 (0°C) or SR 362 (28°C).	54 seconds	$6.5x10^4$ (Brown & Webb, 1972)	$1.20x10^3$

Mean calculated fluence = 1.08×10^3 $Jm^{-2}sec^{-1}$.

when moved across into the radiation beam. Output voltages were measured on a microvoltmeter (Keithley Instruments Model 150B). In measuring the output of Penray lamps, an error is introduced due to the radiant heat detected by the thermopile. To correct this, the lamp was allowed to warm up for 20 minutes, a reading taken, the lamp switched off, and a second reading taken. This when subtracted from the first gives the UV output of the lamp. For the 254 nm apparatus the thermopile was positioned, as shown in Figure 21, immediately below the irradiation vessel, and the fluence rate determined by removing the irradiation vessel and moving the thermopile up so that the detector was level with the surface of the 10ml bacterial test suspension in the vessel.

Calibration of thermopiles.

Conversion of the incident energy from microvolts to Joules $m^{-2}sec^{-1}$ was made with reference to the calibration factor of the thermopile obtained by chemical actinometry (Hatchard and Parker, 1956). Potassium ferrioxalate actinometry relies on the light catalysed production of Fe^{2+} ions in a solution of $K_3 Fe (C_2O_4)_3$. The solution absorbs light completely in the UV region, the quantum yield of the reaction is practically constant throughout the UV region and the yield is independent of the fluence rate.

Actinometry was performed under red light according to the method of Jagger (1967). A calibration curve of optical density at 510 nm against amount of ferrous ion (shown in the Appendix A4) was determined and used to ascertain the amount of ferrous ion formed by the radiation. From this, a fluence rate was calculated by application of the constants pertaining to the wavelength chosen (see Jagger, 1967).

Then a number of fluence rates obtained at different distances from a Penray 254nm UV source were plotted against the corrected thermopile reading for the Oriel 7102 detector. This graph is shown in Figure 24. The slope of this line was obtained by linear regression analysis and yielded a calibration factor for microvolts to Jm^{-2} sec^{-1} of 0.0316.

TREATMENT OF DATA.

The survival of irradiated bacteria was expressed graphically by plotting the surviving fraction ($^{N}/No$), on a logarithmic scale, against some measure of the amount of radiation received (F) which was either the time of exposure or the fluence. For single 'hit' kinetics where, according to the 'target' theory (see Lea, 1955; and Clayton, 1971 for a review) a cell can be killed by hitting just one target, survival curves may be described by the following equation:-

$$^{N}/No = e^{-kF} \qquad (i)$$

Therefore, a plot of Log $^{N}/No$ against F produces a straight line relationship of slope $-\frac{k}{2.303}$

However, in most cases, the survival curves obtained in this study consisted of an initial shoulder at high survival levels, followed by an exponential portion over at least one log cycle. Such curves have been described by the following 'multi-target' expressions:

$$^{N}/No = 1-(1-e^{-kF})^{n} \qquad (ii)$$

or

$$^{N}/No = ne^{-kF} \qquad (iii)$$

where k is the slope of the linear portion of the survival curve in reciprocal fluence units (often termed the inactivation constant) and n is the extrapolation number or shoulder constant, numerically equal

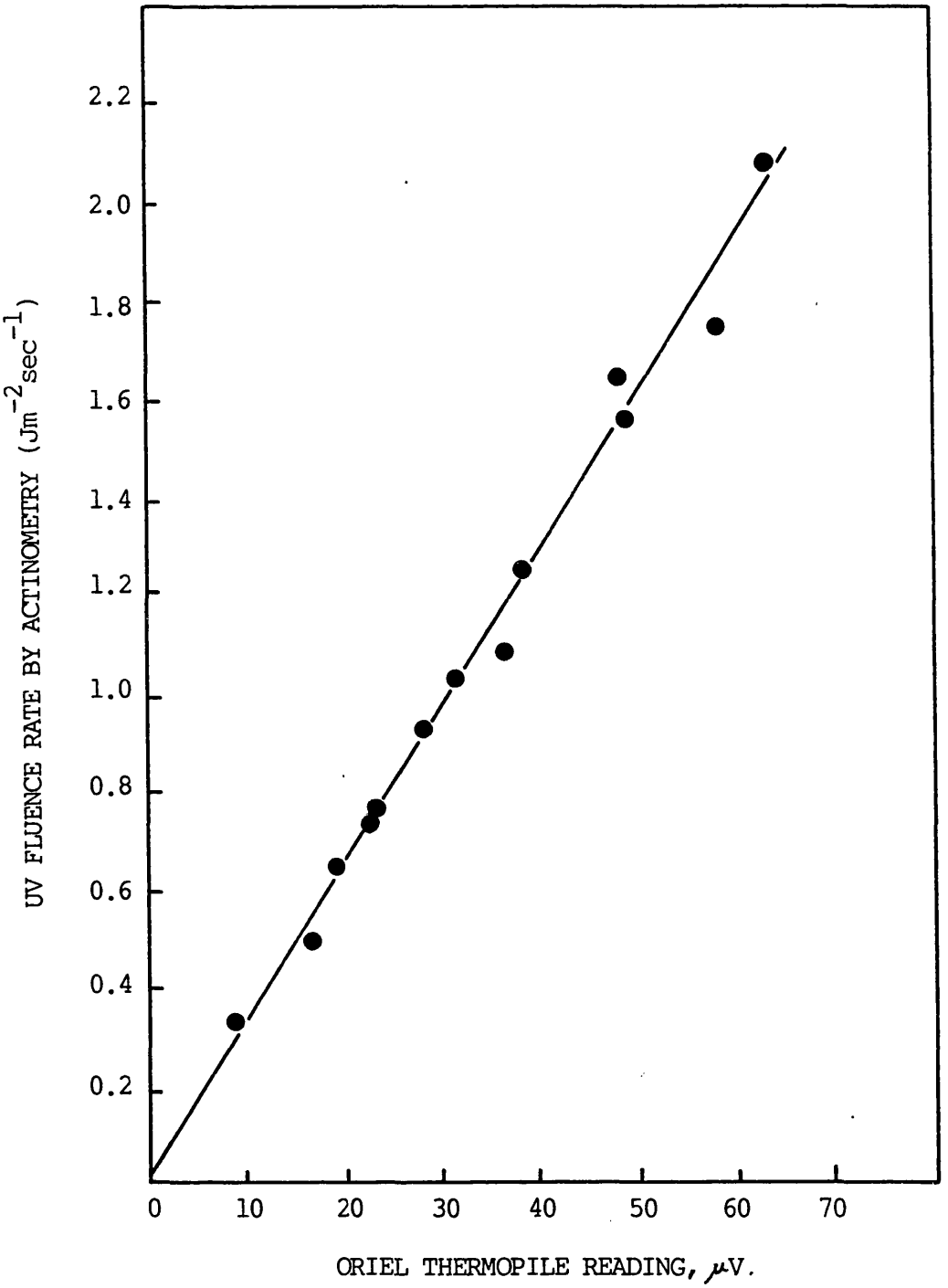

Figure 24 Thermopile reading (Oriel 7102) in microvolts, plotted against UV FLUENCE RATE OBTAINED BY POTASSIUM FERRIOXALATE ACTINOMETRY.

SLOPE BY LINEAR REGRESSION ANALYSIS = 0.03161

CORRELATION COEFFICIENT = 0.994

to the y-axis intercept of the extrapolation of the exponential part of the survival curve. While the mechanistic interpretation of shouldered survival curves no longer relies on classical target theory, the parameters 'k' and 'n' are often usefully used to describe empirically the inactivation efficiency of a particular radiation treatment.

In addition to the use of k and n values to quantify radiation survival curves, other approaches have been employed (e.g. Webb and Brown, 1976). These include the expression of radiation sensitivity by the empirical use of the reciprocal of fluences that yield surviving fractions of 0.5, 0.37 and 0.1 ($^1/F_{50}$ and $^1/F_{37}$ and $^1/F_{10}$ values respectively). Another parameter which has been used is the D_Q value; the fluence resulting from extrapolation of the straight-line portion of the survival curve to the 100% survival level and extrapolating to the x - fluence - axis intercept.

Action spectra described in this study were based on the parameter considered most appropriate from the particular survival curves obtained. The choice of parameter is discussed under the appropriate experimental section.

Each result described in the experimental section of this thesis is represented by a single 'typical' experimental result, from a set of two to four repeat experiments. Action spectra are based on the mean of at least two 'complete' survival curves for each wavelength studied. Statistical analyses were performed, as indicated, by one of the procedures outlined in the Appendix B.

E X P E R I M E N T A L

CHAPTER 1

PRELIMINARY INVESTIGATIONS INTO NEAR-UV RADIATION - INDUCED SENSITIVITY TO INORGANIC SALT IN A DNA REPAIR - COMPETENT *E. coli* K-12 STRAIN : PROTECTION AND RECOVERY.

This chapter describes some preliminary investigations, using the broad-band near-UV radiation source, which were carried out firstly, to determine whether the findings of Moss and Smith (1981), regarding sensitivity to inorganic salt after near-UV irradiation of a DNA repair - competent E. coli K-12 strain, were obtainable in this laboratory. Secondly, some preliminary findings of Moss and Smith (unpublished) suggested that a protection from near-UV radiation-induced salt sensitivity could be gained by addition of Casamino Acids to the minimal media. This chapter describes findings re this protection phenomenon, using strain K-12 SR 385, with Casamino Acids and yeast extract added to the plating media. Thirdly, studies with mild-heat, which showed a similar sensitivity to inorganic salts occurring in treated cells (Busta and Jezeski, 1963), also showed that a return to salt tolerance was observed if treated cells were held in a rich growth medium (Iandolo and Ordal, 1966; Clark and Ordal, 1969). This chapter describes experiments, with strain SR 385, that determine whether a recovery from salt sensitivity occurred with near-UV radiation-treated cells.

For the particular group of experiments described in this chapter, some additional media and methods were used which were not included in the general methodology section.

Media.

(a) Casamino Acids solution.

This was prepared as a 20% $^{W}/_{V}$ stock solution by dissolving 20g Casamino Acids (Difco Laboratories, Detroit, USA) in 70mls of pre-warmed glass distilled water and, after allowing to cool, making up to 100ml with glass distilled water. This solution was then sterilized by being passed through a 0.2 μm pore-size membrane filter contained

in a sterile swinnex unit (Millipore UK Ltd., London). A final concentration of 2mg/ml, obtained by a one hundred-fold dilution of the stock solution, was used unless otherwise indicated.

(b) Tryptone Soya agar plates (TSA).

These were prepared by adding 29.6g Tryptone Soya agar (Lab M Ltd., Salford) to 800ml of glass distilled water, which was then sterilized by autoclaving at 121°C for 15 minutes. Twenty ml volumes were then distributed into plates and stored as described in the general methodology section.

(c) Complex holding medium (For recovery experiments).

This was Difco YENB broth, prepared by dissolving 8.0g of Difco nutrient broth and 7.5g of Difco yeast extract in 900ml of glass distilled water and then making up to 1 litre. Ten 100ml batches were then prepared and sterilized by autoclaving at 121°C for 15 minutes. Twenty ml aliquots of this medium were then used as the holding medium.

(d) Chemicals used in recovery experiments .

(i) Chloramphenicol.

A 1mg/ml solution was prepared by dissolving 100mg chloramphenicol (Sigma Chemical Company) in, and making up to 100ml with, glass distilled water. Sterilization was achieved by filtration via a 0.2 μm pore-size membrane filter. The stock solution, which was stored at 4°C and protected from light, was then diluted to produce the required concentration of 40 μg/ml by adding 0.8ml to each 20ml of holding medium. The stock solution was kept for up to one week before discarding.

(ii) Penicillin G.

A stock solution was prepared immediately prior to each experiment in which it was required, by dissolving the contents of one vial (containing 1 mega unit of sterile penicillin G powder - obtained from Glaxo Laboratories Ltd.) in 90ml of sterile M9 salts solution and then making up to 100ml; the solution being prepared under aseptic conditions in a laminar flow cabinet. A ten-fold dilution of this solution in sterile M9 salts solution then produced the stock solution [containing 1000 units ml^{-1} (U/ml) penicillin G]. Appropriate dilutions were then performed to produce the required concentration in the 20ml holding medium.

(iii) Bacitracin.

As for penicillin G, due to its instability in aqueous solution, a separate stock solution was prepared immediately prior to use, in each experiment where this agent was required. A stock solution of 29.7 U/ml was prepared by dissolving 50mg bacitracin (obtained as a 59,400 U/g powder from Sigma Chemical Company) in M9 salts solution and making up to 100ml in a volumetric flask. Sterilization was achieved by filtering via a 0.2μm pore-size membrane filter. Appropriate dilutions were then made to produce the required concentration in the 20ml holding medium.

RESULTS.

The experimental results described in this chapter were all obtained using 24 hour (i.e. stationary growth phase) secondary cultures of E. coli K-12 SR 385, unless otherwise stated. The cells were irradiated as a $1x10^7$ CFU/ml suspension in M9 salts solution in either position 6 or 7 (i.e. central) of the Black-Light Blue lamp box, in which positions it had been previously shown that the fluence rates were not significantly different (see Fig. 22 general methodology).

Initially, strain SR 385 was irradiated, and its viability assessed on Oxoid nutrient agar (the complex medium) and on 'low', 'normal' and 'high' salt minimal media (see general methodology for the composition of these media). These observations are shown in Figure 25, with the corresponding data presented in Appendix B, Table 1.

Table 1 (Appendix B) shows a full presentation of the data pertaining to Figure 25, in order to emphasize some important points. It is apparent that, for the unirradiated cells, the initial mean plate count for each of the types of media used to assess viability is similar. This indicates that the viability of the control, unirradiated cells was not affected to any large extent by the differences in inorganic salt concentration within the minimal media, or by plating on complex medium. Unless otherwise indicated, this was found to be the case throughout this study and agrees with the findings of Moss and Smith (1981). Although no consistent difference in the viability of the unirradiated cells on the various media used was observed, for the purpose of calculating the surviving fraction, the viability of the unirradiated cells on the corresponding medium was used.

These points having been illustrated for Figure 25; all subsequent tables pertaining to experimental data (presented in Appendix B) only contain a measure of the radiation fluence and the corresponding surviving fractions on each type of medium used to assess viability. However, an indication of any initial variation in viable count between the types of plating medium used, is presented for the unirradiated cells.

It should also be noted that, although the initial viability of unirradiated cells was not affected significantly by the type of medium

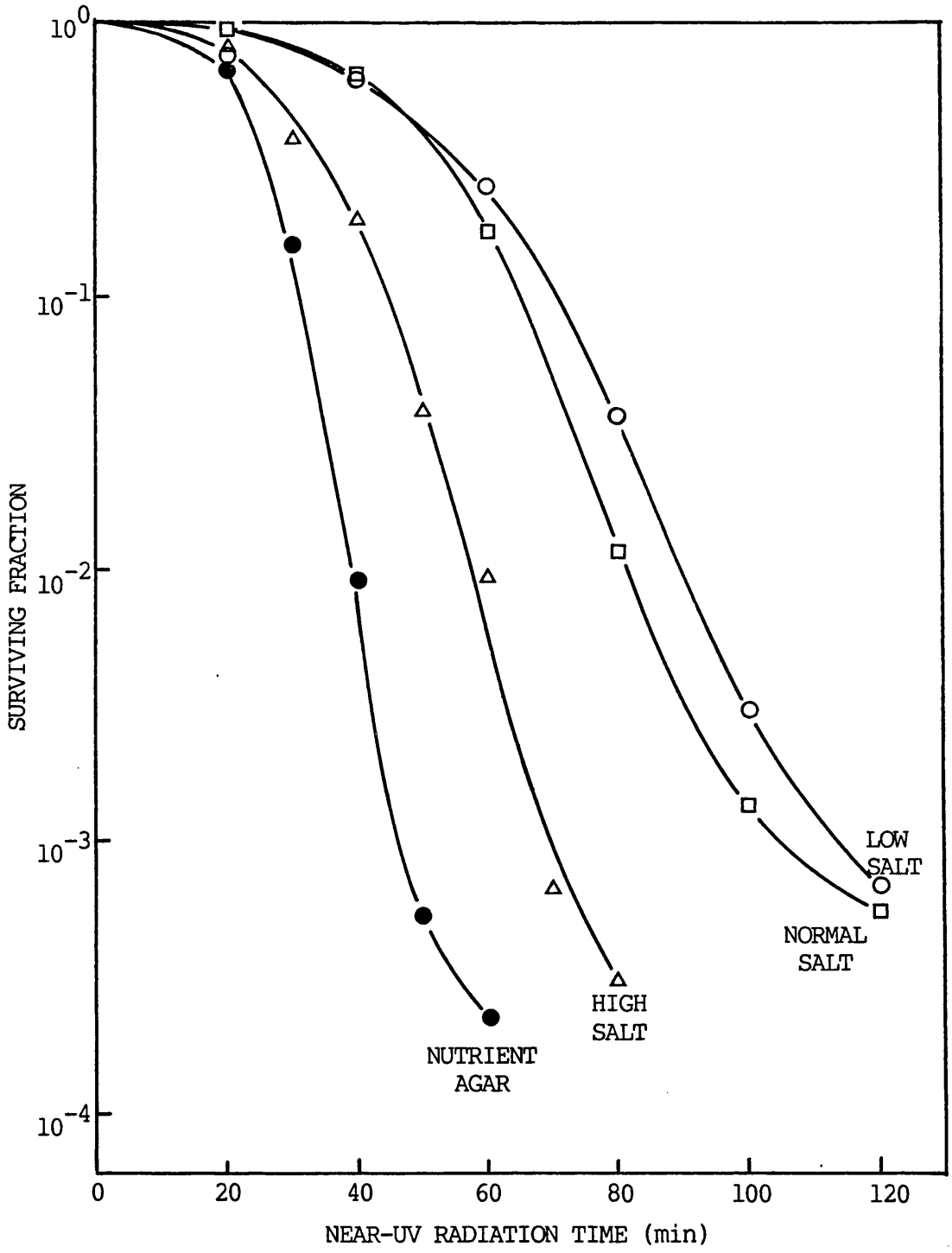

Figure 25 Survival curves for E. coli K-12 (SR 385) after broad-band near-UV irradiation, with viability assessed on Oxoid nutrient agar (●), Low salt minimal medium (O), normal salt minimal medium (□) and high salt minimal medium (△).

used to assess viability, the colonies themselves did differ in their appearance, particularly with reference to their size. The colonies appeared later on the minimal media (counting being carried out after 72 hours compared to 48 hours for the complex media) but, even after maximum growth, they appeared to be smaller. Furthermore, within the three types of minimal media, the colonies on the normal and low salt media appeared larger and somewhat irregular whereas, with the high salt medium, they appeared small, compact and circular.

Figure 25 shows that, when viability is assessed on minimal media, the resulting survival curves exhibit a response similar to the observations reported by Moss and Smith (1981); that is, as the concentration of inorganic salt in the medium is increased, from one-tenth of normal to the normal concentration (85mM), and then to one-tenth of the normal concentration plus sodium chloride added at 200mM, there is a corresponding increase in cell sensitivity to near-UV radiation. However, the sensitivity of the irradiated cells, when plated on Oxoid complex medium, was markedly different from the published data of Moss and Smith. Whereas their data showed that cell sensitivity to near-UV radiation was decreased by plating on a complex medium (Difco YENB) relative to minimal media, Fig. 25 shows the opposite result.

As the nature of the complex medium routinely used in the two laboratories was different, near-UV radiation survival curves were obtained, comparing viability assessed on Oxoid nutrient agar and Difco YENB agar. The result obtained is shown in Figure 26. The figure shows that the survival curves for this strain on the minimal media and the Oxoid complex medium bear a similar relationship to those shown in Fig. 25. However, when viability is assessed on Difco YENB

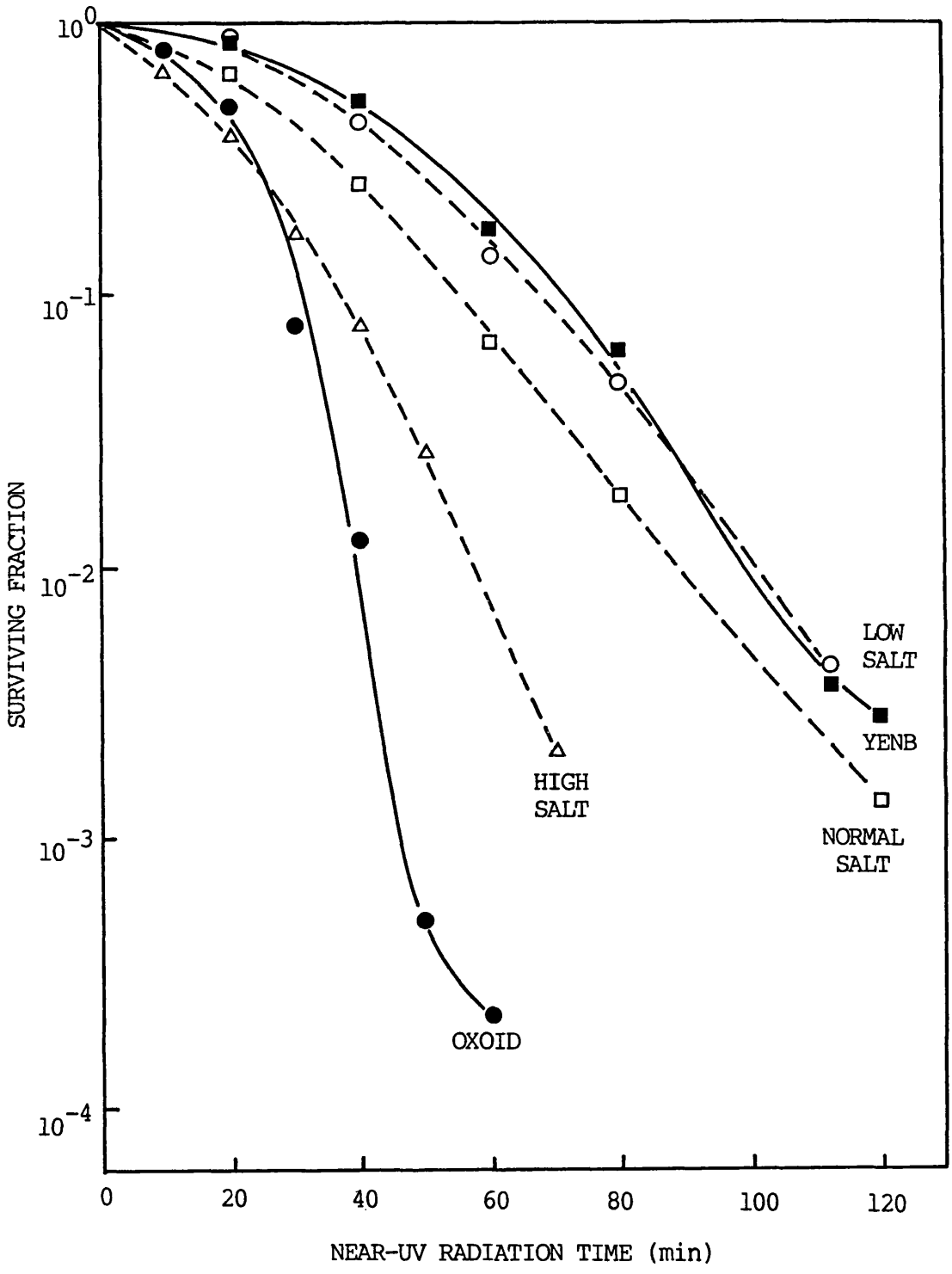

Figure 26 Survival curves for E. coli K-12 (SR 385) after broad-band near-UV irradiation, with viability assessed on Oxoid nutrient agar (●), Difco YENB agar (■) and minimal medium - Low salt (○), normal salt (□) and high salt (△).

medium, the strain shows the greatest resistance to the radiation.

In order to ascertain the cause of this unexpected difference in sensitivity between the two complex media, the composition of these commonly used media was investigated. The compositions of the three main complex media used in UV-radiation studies are shown in Table 7. The table shows one of the most obvious differences between the Oxoid and the Difco media to be the presence of 5g/l sodium chloride in the former. Therefore it was decided to determine whether the presence of sodium chloride (at 85mM) in the Oxoid and Tryptone Soya agars was the cause of these differences in sensitivity. To this end, an Oxoid nutrient agar was prepared by dissolving its individual ingredients, as shown in Table 7, but omitting the sodium chloride. In addition, plates of Difco YENB medium with sodium chloride at 5g/l added, were prepared. It should be noted that no colonies were visible on any of the TSA plates (i.e. neither unirradiated nor irradiated cells). However, on adding thymine at a concentration of 10µg/ml to the sterilized molten agar before pouring, colonies were then visible and, as shown in Table 3, (Appendix B) in the same initial numbers as for the other types of plate used.

The results obtained by assessing cell viability, after near-UV irradiation, with these various complex media are shown in Figure 27. The figure illustrates that, when cell viability was assessed on the TSA (+ thymine), a similar sensitivity to that for Oxoid nutrient agar was exhibited. When sodium chloride was omitted from the Oxoid complex medium, the survival curve roughly corresponded to that for the Difco complex medium. Finally, the addition of sodium chloride (5g/l) to Difco complex medium did increase near-UV radiation sensitivity, but not to the same extent as observed for the TSA and Oxoid media.

TABLE 7.

The composition of commonly used nutrient agars.

Ingredient	YENB (per litre)	Oxoid (per litre)	Tryptone Soya (per litre)
Peptone	5.0g	5.0g	5.0g
Sodium Chloride	-	5.0g	5.0g
Beef extract	3.0g	-	-
Tryptone	-	-	15.0g
Yeast extract	7.5g*	2.0g	-
'Lab Lemco' powder	-	1.0g	-
Agar	15.0g	15.0g	12.0g
(pH) approx.	6.8	7.4	7.3

* added separately

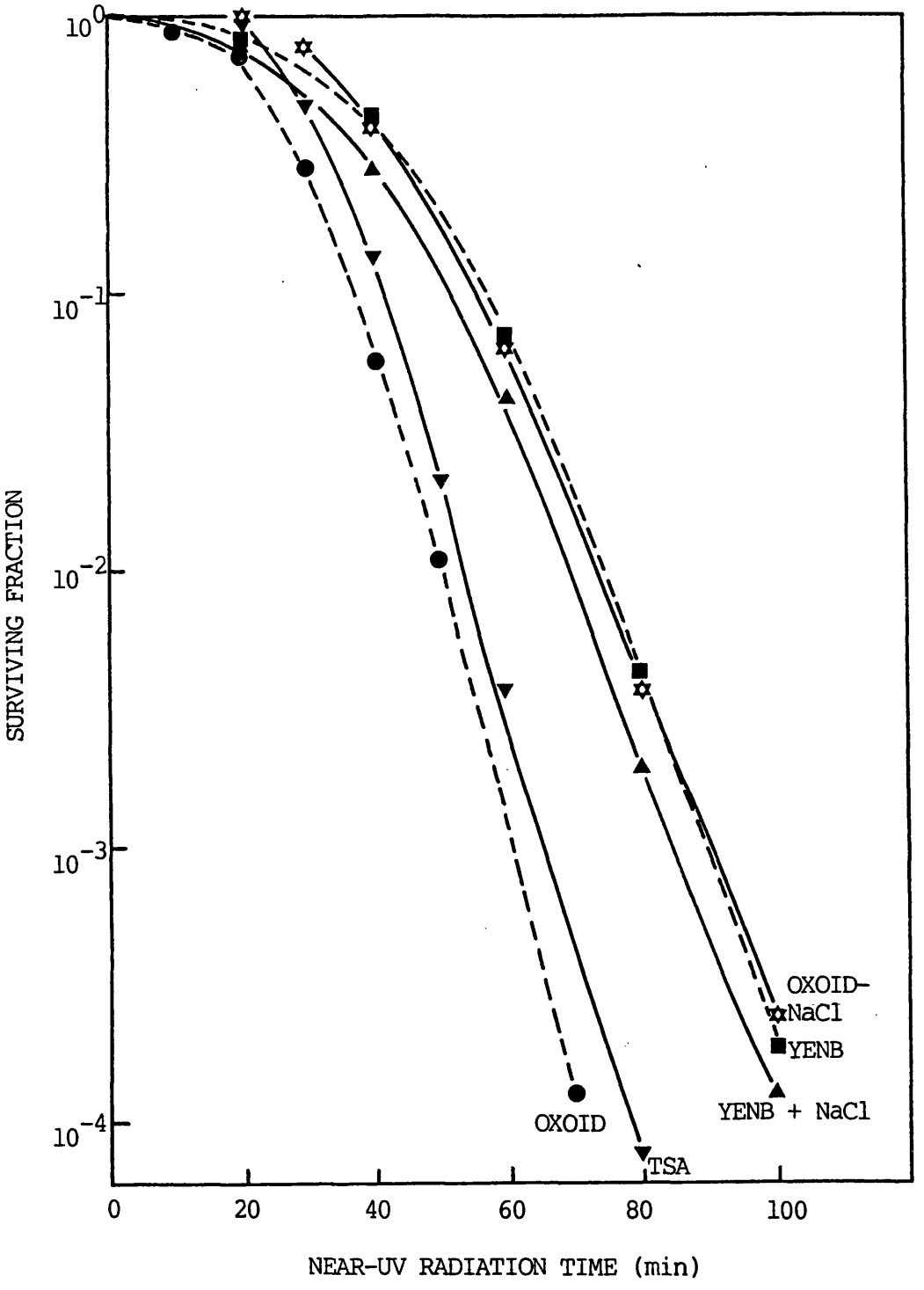

Figure 27 Survival curves for E. coli K-12 (SR 385) after broad-band near-UV radiation, with viability assessed on Oxoid nutrient agar (●), Tryptone Soya agar plus 10μg/ml thymine (▼), Difco YENB nutrient agar (■), Oxoid nutrient agar minus NaCl (✡) and Difco YENB nutrient agar plus NaCl (5g/l) (▲).

In an attempt to show that the salt sensitivity effects were not limited to strain SR 385, an experiment was carried out using E. coli K-12 AB 1157, another DNA repair-competent organism. Figure 28 shows near-UV radiation survival curves on low, normal and high salt minimal plating media, for strain AB 1157. The figure shows that a near-UV radiation-induced sensitivity to inorganic salt is also apparent for strain AB 1157, with the survival curves exhibiting a similar pattern to Figure 25 for strain SR 385.

Preliminary observations of Moss and Smith (unpublished) showed that a protection from near-UV radiation-induced salt sensitivity may be obtained by adding Casamino Acids (2mg/ml) to the plating media. Casamino Acids is an acid hydrolyzed casein containing the essential amino acids plus small amounts of some vitamins (pyridoxine, biotin, thiamine, nicotinic acid and riboflavin). Yeast extract also contains similar amounts of amino acids and much higher concentrations of the vitamins. A detailed analysis of these two media is given in the Difco Manual. Therefore, as the Difco YENB medium contains a much higher concentration of yeast extract than does Oxoid nutrient agar (7.5g/l to 2g/l as shown in Table 7), the possible protective effect of yeast extract was also investigated.

Near-UV irradiation experiments were performed using strain K-12 SR 385 and viability was assessed on Oxoid nutrient agar (where, as shown in Fig. 26, a large degree of salt sensitivity was exhibited) and on Oxoid nutrient agar containing either Casamino Acids (2mg/ml) or yeast extract (7.5 g/l); i.e. the same concentration of yeast extract was added to that contained in Difco YENB medium. In addition, as a

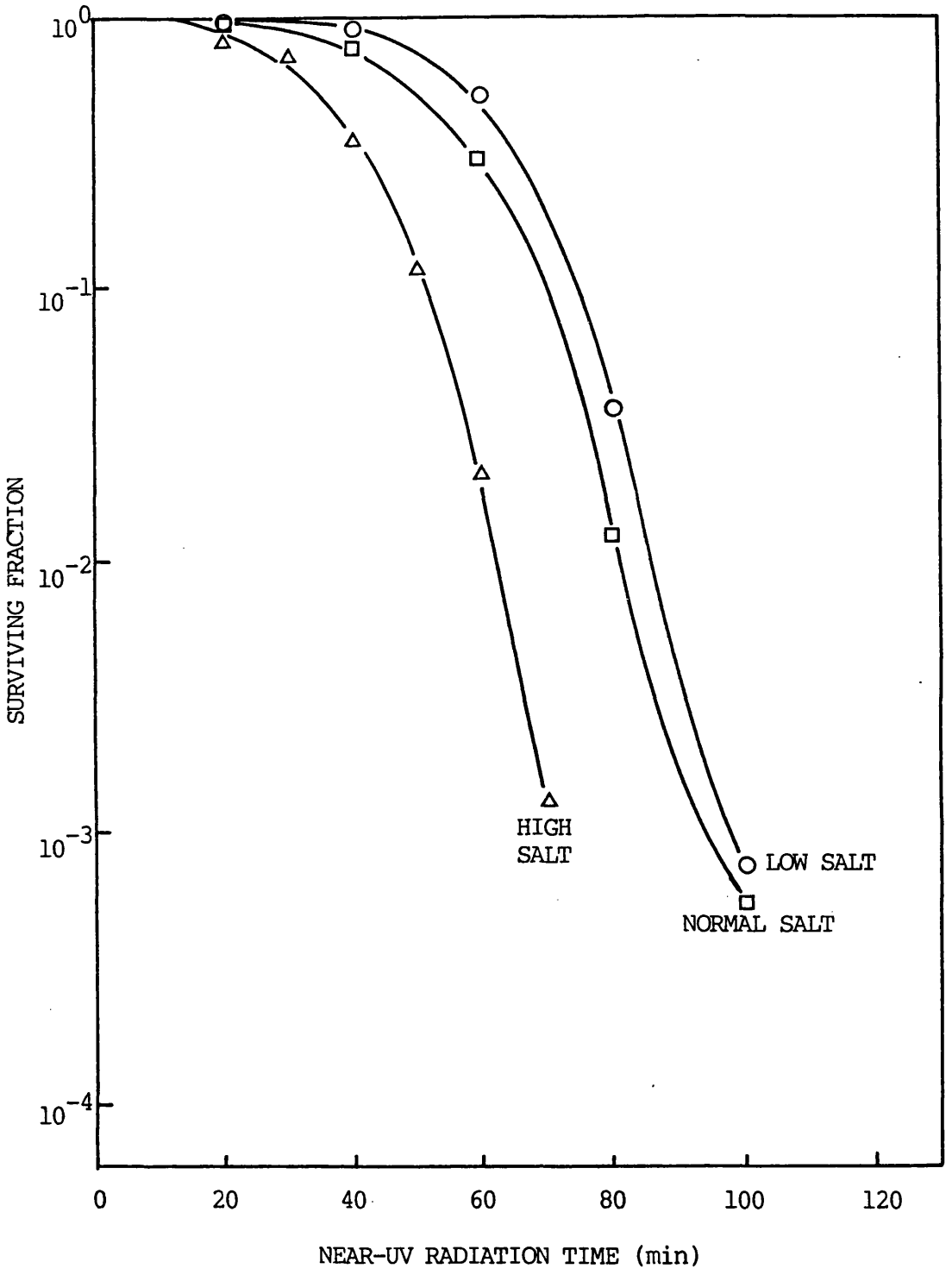

Figure 28 Survival curves for E. coli K-12 AB 1157 after broad-band near- UV radiation, with viability assessed on Low salt (O), normal salt (□) and high salt (△) minimal media.

means of providing a comparison with previous observations (Figs. 26 and 27), survival was determined using YENB and Difco nutrient agar containing sodium chloride added at 100mM (i.e. no yeast extract added). The results obtained are shown in Figure 29.

Figure 29 shows that the addition of Casamino Acids at a concentration of 2mg/ml to Oxoid nutrient agar offered a small, but always obtainable, protection from salt sensitivity, whereas the addition of yeast extract at a concentration of 7.5g/l (identical to that present in YENB medium) offered a much larger protection from salt sensitivity. Finally, the survival on plates of Difco nutrient agar with sodium chloride added at 100mM (with no yeast extract present) was similar to that obtained on the Oxoid nutrient agar plus yeast extract plates.

In order to determine whether any recovery from near-UV radiation-induced salt sensitivity was possible, an experimental protocol adapted from the mild-heat studies of Iandolo and Ordal (1966) and the X-ray studies of Gillies et al. (1979) was used. After irradiation with broad-band near-UV radiation for a time where, from previously determined survival curves, survival levels of about 10% on the YENB plates (and thus about 1% on the high salt minimal medium) were apparent, samples of the irradiated and unirradiated cells were transferred to a liquid recovery medium. This was YENB growth medium, pre-warmed to 37°C. Control and irradiated samples were diluted in M9 salts solution prior to holding to give an initial cell concentration of approximately 10^5 CFU/ml in 20ml of recovery medium. Then, after incubation at 37°C in a shaking water bath (operated at a constant 100 cycles per minute),

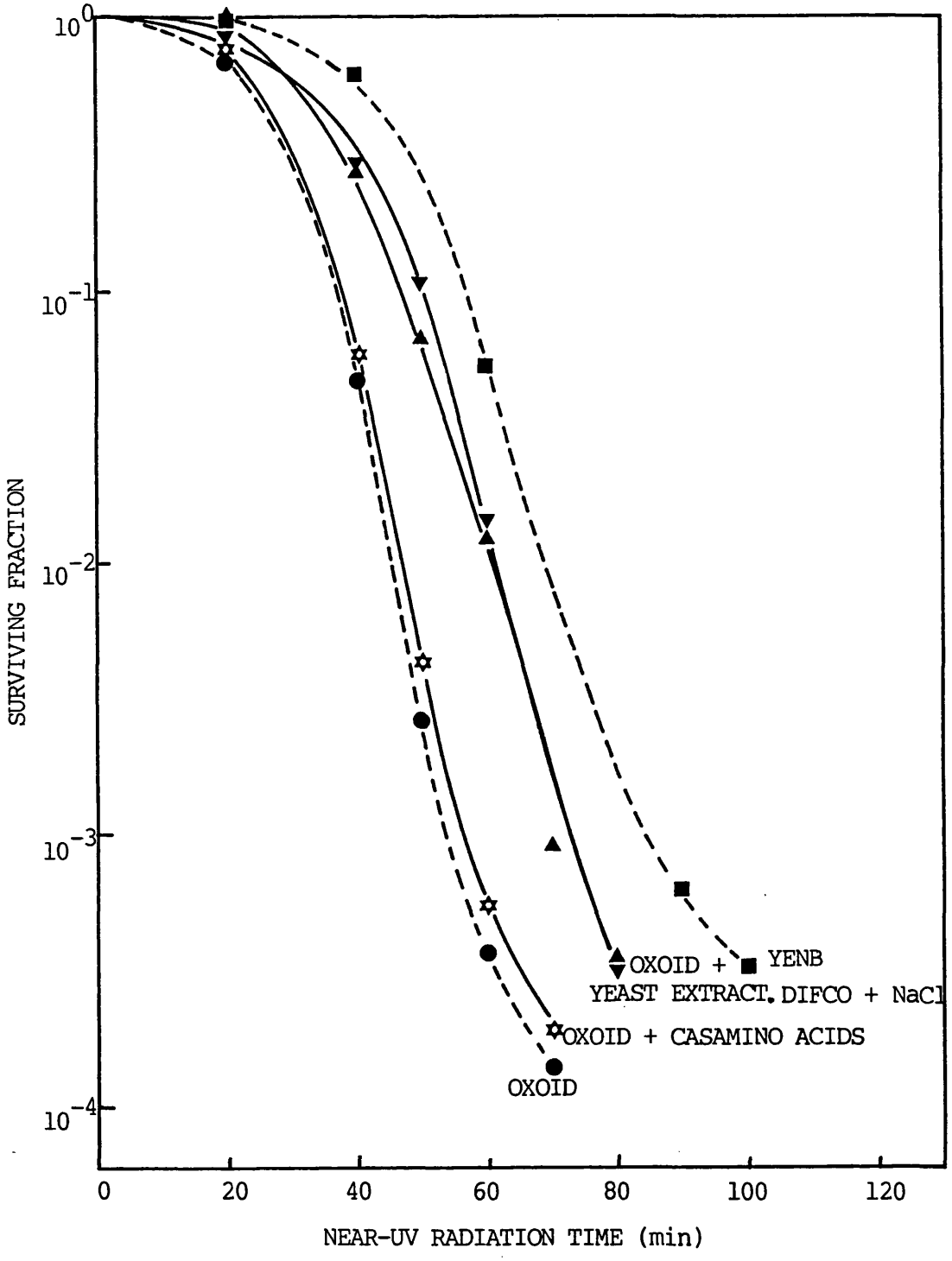

Figure 29 Survival curves for E. coli K-12 (SR 385) after broad-band near-UV radiation, with viability assessed on Oxoid nutrient agar (●), YENB (■), Oxoid nutrient agar plus Casamino Acids at 2mg/ml (✡), Oxoid nutrient agar plus yeast extract at 7.5g/l (▲) and Difco nutrient agar plus Sodium chloride at 100mM (▼).

for various times, the viability of each cell sample was assessed by plating on either complex YENB or minimal high salt (i.e. one-tenth diluted inorganic salts plus sodium chloride added at 200 mM) media.

The results of such an experiment, where strain K-12 SR 385 was irradiated with broad-band near-UV radiation for 50 minutes, are shown in Figure 30. The unirradiated cells show a lag phase of about 2 hours, expected as the cells were in stationary phase, before growth occurred. There was no significant difference in cell survival shown between assessment on the YENB plates and the high salt minimal medium plates. For the near-UV irradiated cells assessed for viability on the YENB plates, in addition to the lag phase, a growth delay was observed; a near-UV radiation-induced phenomenon previously reported (see introduction for a discussion). Thus, the increase in cell numbers between 2 and 6 hours post-irradiation holding was very small compared to that for unirradiated cells. For near-UV irradiated cells assessed for viability on high salt minimal medium, there is, at time zero, a striking difference in the surviving fraction, when compared to the YENB plates, indicating the presence of salt sensitivity (as shown in Fig. 26). However, a recovery from the initial salt sensitivity then occurs, especially throughout the initial 2 hour post-irradiation holding period, where the unirradiated cells were still in lag phase of growth.

As with the studies of Iandolo and Ordal (1966) involving the return to salt tolerance in mild-heat treated cells, in an attempt to establish the nature of the observed recovery process, the effect of various inhibitory agents on the recovery was then investigated. Agents were chosen which inhibited bacterial protein synthesis (chloramphenicol) and, because the salt sensitivity was thought to be due to a membrane damaging effect (Moss and Smith, 1981), cell wall synthesis (penicillin)

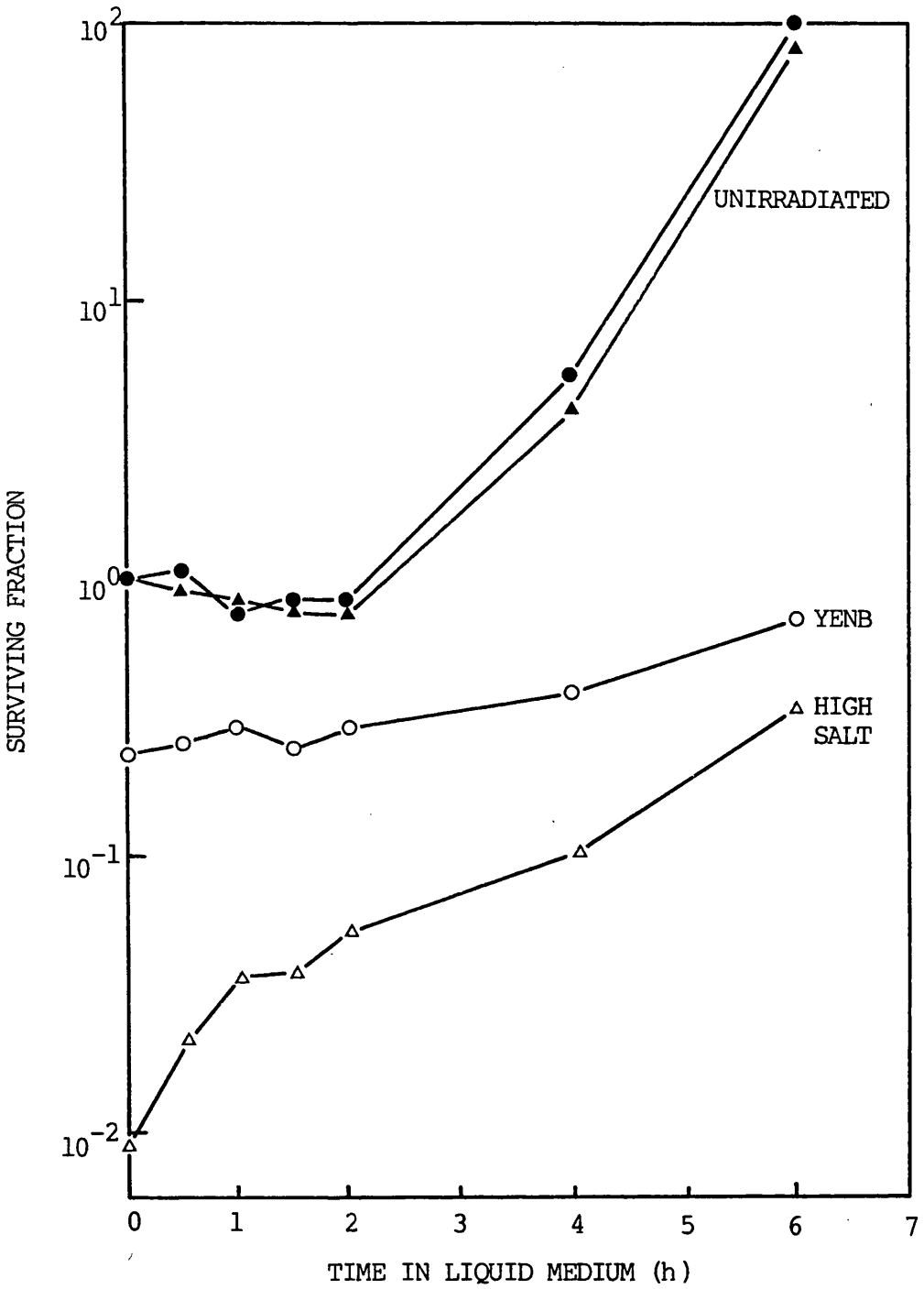

Figure 30 The surviving fraction of E. coli K-12 (SR 385) unirradiated (closed symbols) or irradiated for 50 minutes with broad-band near-UV radiation (open symbols). Samples were held at 37°C in recovery medium for the times indicated on the abscissa before assessing viability on YENB plates (●,O) or 'high salt' minimal medium (▲,△)

and membrane synthesis (bacitracin). By performing preliminary experiments, a concentration of inhibitory agent was chosen such that, throughout the 6 hour post-irradiation holding period, there was little or no lethal effect on unirradiated cells, while a minimum of cell multiplication was allowed. In order to eliminate any inhibitory agent from the final 0.2ml aliquot used for the assessment of viability, a 10^2 or 10^3 serial dilution of the recovery medium sample, using M9 salts solution, was performed.

(a) The effect of chloramphenicol.

The first inhibitory agent used was chloramphenicol, at a concentration of 40 μg/ml. This concentration was chosen from papers where a range of concentrations from 20 to 100 μg/ml has been used to inhibit bacterial protein synthesis (e.g. Youngs et al., 1974; Bridges and Mottershead, 1978, Iandolo and Ordal, 1966). Chloramphenicol provides an effective inhibition of protein synthesis by combining with the 50-S subsection of the ribosomes and thereby preventing the transfer from the P to the A site involved in peptide bond formation and subsequent protein assembly (see Davis et al., 1980 for a general review). The results of such an experiment are shown in Figure 31, with the previous result from Figure 30 included to aid comparison.

As chloramphenicol acts on E. coli by preventing growth, there is little effect observed during the lag phase for the unirradiated cells, whereas the chosen concentration of 40 μg/ml was sufficient to prevent subsequent growth of the cells into log phase. In neither phase of growth is there any significant difference observed by plating unirradiated cells on the two types of medium. The irradiated cells plated on YENB also show no significant change in the surviving fraction over the 6 hour holding period. For near-UV irradiated cells

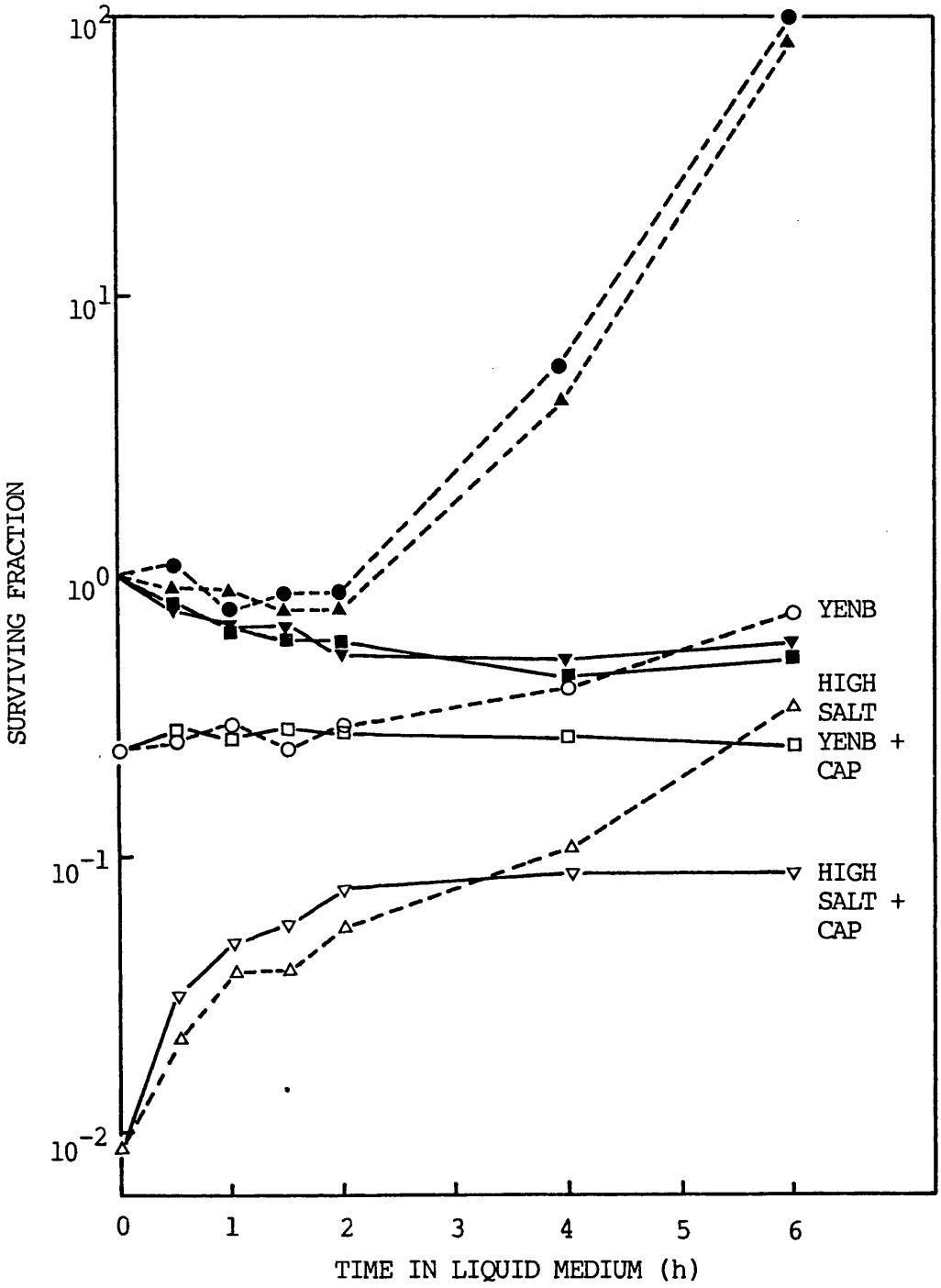

Figure 31 The surviving fraction of E. coli K-12 (SR 385) unirradiated (closed symbols) or irradiated for 50 minutes with broad-band near-UV radiation (open symbols).

Samples were held at 37°C in recovery media, either alone (O,Δ) or supplemented with chloramphenicol (40μg/ml) (∇,□) for the times indicated on the abscissa, before assessing for viability on YENB plates (O,□) or 'high salt' minimal medium (Δ,∇).

assessed on the high salt minimal medium there is, however, even in the presence of chloramphenicol, an observed recovery from the salt sensitivity. Again this is particularly apparent over the initial 2 hour post-irradiation recovery period resulting in a very similar shaped curve over this period to that observed in the absence of chloramphenicol. However, the increase in cell numbers from 2 to 6 hours post-irradiation holding, observed in the absence of the agent, was not apparent in the presence of chloramphenicol.

(b) The effect of penicillin G.

The results of a preliminary experiment, where E. coli SR 385 was incubated for 6 hours in recovery media containing different concentrations of penicillin G, are shown in Figure 32. This figure shows that the ideal conditions for a subsequent recovery experiment, where little significant inactivation or division of bacteria occurred over the 6 hour holding period, was provided by a concentration of approximately 12 U/ml. The figure shows that lower concentrations than this (9,6 and 3 U/ml) did not prevent cell division and higher concentrations (15,18,21,24,27 and 30 U/ml) inactivated the bacteria. A concentration of 11 U/ml was used to determine the effect of penicillin G on the recovery from near-UV radiation-induced salt sensitivity. The result of such an experiment is shown in Figure 33a.

As with the chloramphenicol experiment (Fig. 31), to aid comparison, control curves for the unirradiated and irradiated cell samples in the absence of any agent were determined in the same experiment. For this experiment an irradiation time of 70 minutes was used which caused inactivation through about 1.5 log cycles on the YENB plates and inactivation through about 3 log cycles on the high salt plates.

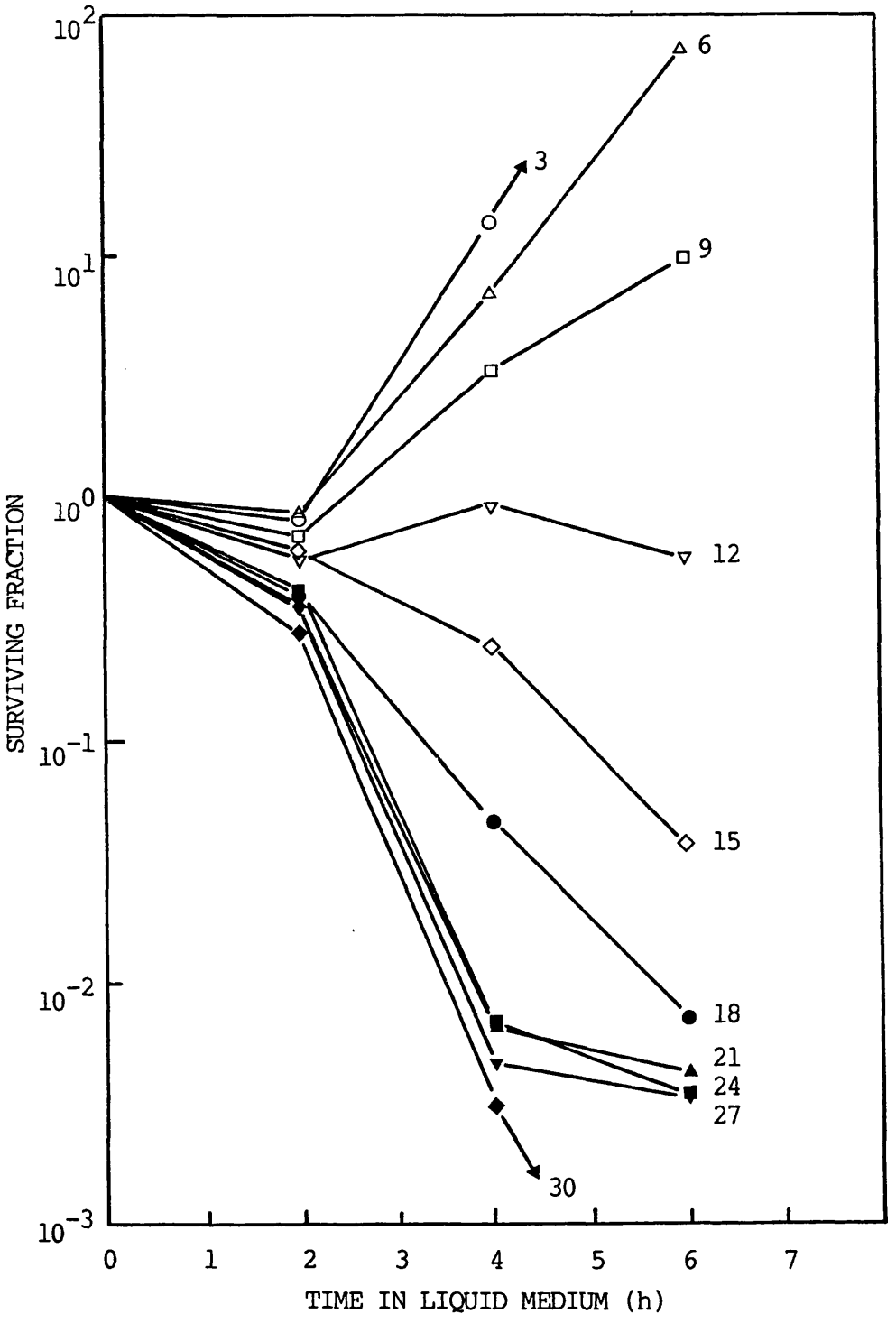

Figure 32 Survival of E. coli K-12 (SR 385) held at 37°C in recovery media containing varying concentrations of penicillin G (numbered as U/ml), before plating on YENB.

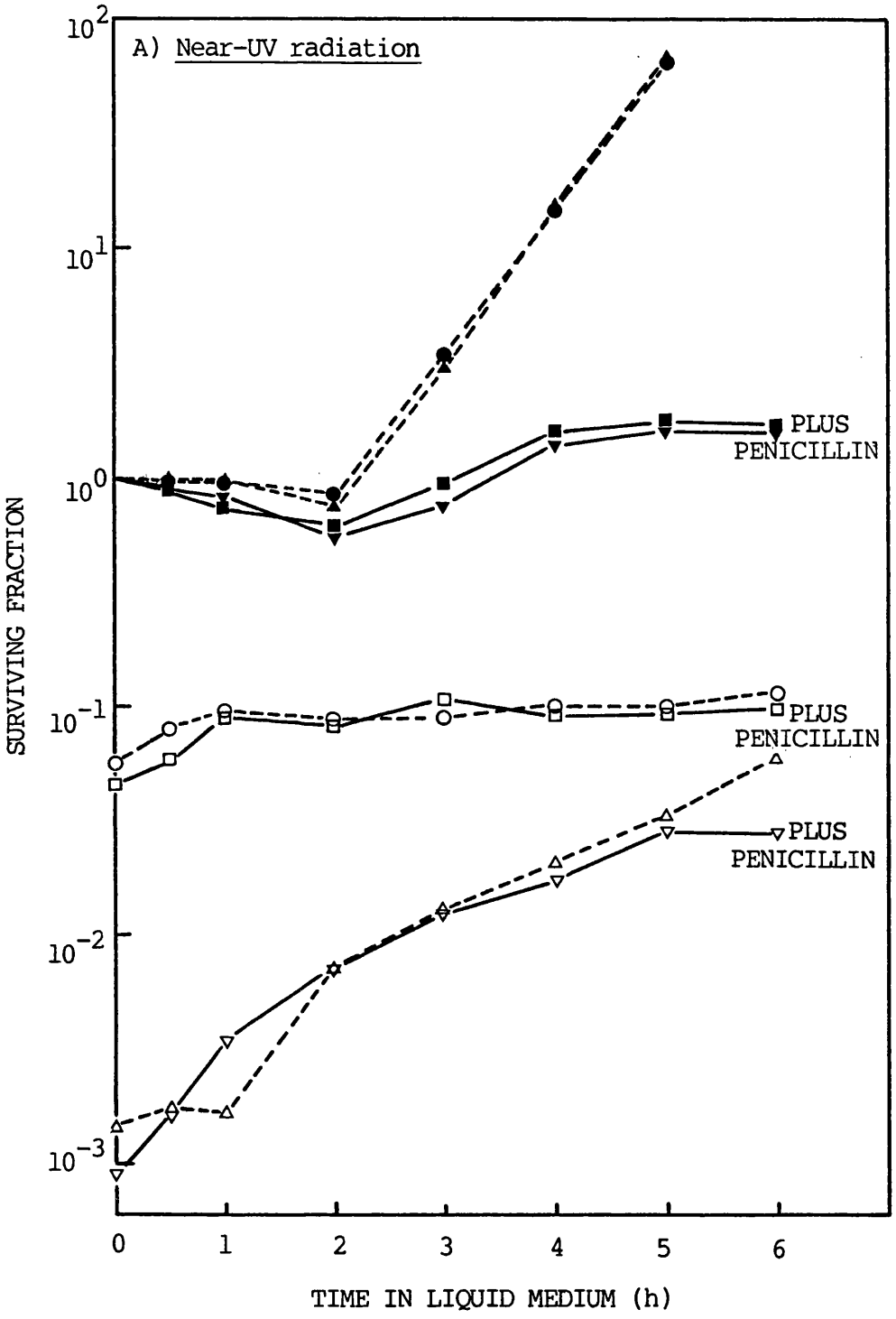

Figure 33 The surviving fraction of E. coli K-12 (SR 385) unirradiated (closed symbols) or A) irradiated for 70 minutes with broad-band near-UV radiation (open symbols); or B) irradiated with 70Jm^{-2} of 254 nm radiation (open symbols). Samples were held at 37°C in recovery media, either alone (○,△ - dotted lines), or supplemented with penicillin G (11 units/ml) (□,▽ - solid lines) for the times indicated on the abscissa, before assessing for viability on YENB plates (○,□) or 'high salt' minimal medium (△,▽).

Although the mechanism by which penicillin inactivates bacteria is not understood completely, it is generally agreed that it specifically blocks cell wall synthesis (Blumberg and Strominger, 1974). It is known to bind to enzymes involved in the formation of pentapeptide cross-links in the rigid peptidoglycan layer of the cell envelope and is believed to inactivate bacteria by inhibiting the synthesis of these cross-links between glycine and D-alanine. A review of these effects is available by Garrod et al., 1981.

Figure 33a shows that the concentration of penicillin chosen caused little or no inactivation of the unirradiated cells during lag phase or subsequently during the period which would, in the absence of penicillin, be a period of exponential growth, 11 U/ml was sufficient to prevent an overall increase in numbers of unirradiated cells. Again, there was no significant difference observed in survival of unirradiated cells on the two types of plates, nor, in the case of near-UV irradiated cells, did the presence of penicillin G in the recovery medium, significantly affect the recovery from salt sensitivity.

As part of the same experiment, the effect of far-UV radiation (254 nm) on cells was determined with respect to salt sensitivity and recovery effects, and in the presence of absence of penicillin G. A fluence of 70 Jm^{-2}, sufficient to produce a surviving fraction of about 10% (i.e. 1 log cycle's inactivation) for K-12 SR 385, was used. The result obtained is shown in Figure 33b.

The figure, which also includes the control, unirradiated cell data as described in Fig. 33a, shows that no salt sensitivity is observed with far- UV irradiated cells. Indeed, the number of survivors at zero holding time is slightly higher on the high salt plates compared

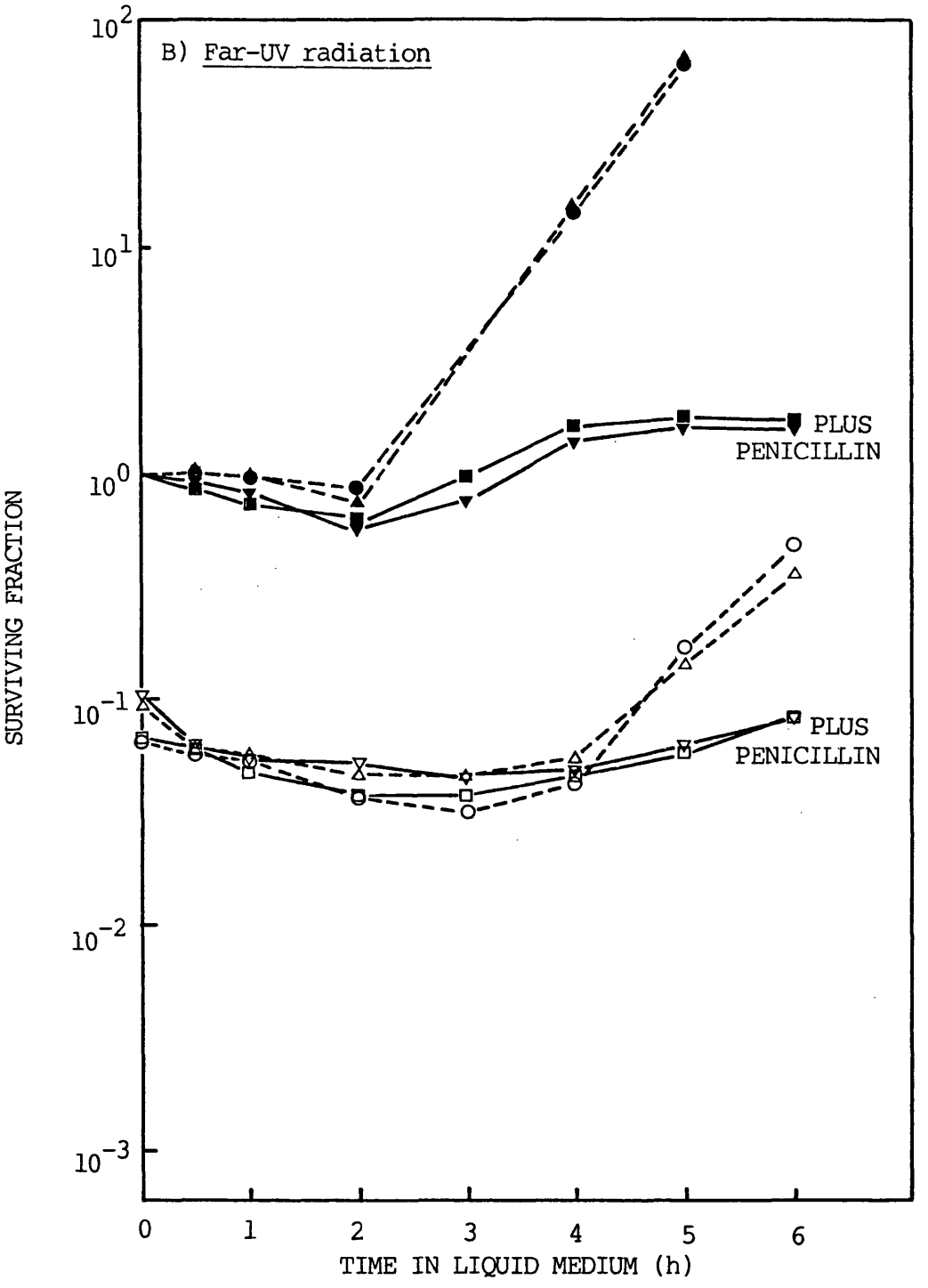

Figure 33 The surviving fraction of E. coli K-12 (SR 385) unirradiated (closed symbols) or A) irradiated for 70 minutes with broad-band near-UV radiation (open symbols) ; or B) irradiated with 70 Jm^{-2} of 254 nm radiation (open symbols). Samples were held at 37°C in recovery media either alone (O,Δ - dotted lines), or supplemented with penicillin G (11 units/ml), (□,▽ - solid lines) for the times indicated on the abscissa, before assessing for viability on YENB plates (O,□) or 'high salt' minimal medium (Δ,▽).

to the YENB plates. Again, the far-UV irradiated cells exhibit a growth delay, but of shorter duration than for the near-UV irradiated cells (4 hours compared to about 7 hours for near-UV irradiation of K-12 SR 385). The presence of penicillin G (again 11 U/ml) does not induce any significant effect on the far-UV irradiated cells when plated on either type of medium, except in partially preventing the rapid multiplication of cells shown after 4 hours holding with the cells held in the absence of the agent.

(c) The effect of bacitracin.

The mechanism of action of bacitracin is known to be complex but it is recognised to exert an effect on both bacterial cell walls and membranes (see Rogers et al., 1980; Storm and Toscano, 1979; Gale et al., 1981 for reviews). It exerts its principal activity by means of combining with the pyrophosphate derivative of the C_{55} carrier lipid, undecaprenol alcohol, contained within the cytoplasmic membrane, which has an essential involvement in the synthesis of cell wall peptidoglycan and of the 'O' antigen chain of membrane lipopolysaccharides. However, unlike penicillin, it also has a lethal action on protoplasts, due to its membrane - acting effects. This has been observed as an efflux of K^+ ions from protoplasts, and has been explained by a disruption of the protoplast membrane resulting from complex formation between the antibiotic and undecaprenol-pyrophosphate in the membrane (Storm and Strominger, 1974).

As membrane synthesis occurs during the lag phase of bacterial growth, bacitracin, with its membrane - acting effects, induces a lethal action on lag-phase cells as well as on growing cells. As the agent acts essentially by means of a competitive inhibition of cell wall and membrane synthesis, a much higher concentration (approximately 20 U/ml)

is required to inhibit the rapid increase in wall and membrane synthesis occurring during the subsequent exponential growth of the cells. This effect is shown in Figure 34 where, as a preliminary experiment, E. coli K-12 SR 385 was incubated for 4 hours in recovery media containing different concentrations of bacitracin. The figure shows that a concentration range from 0.1 to 7 U/ml caused a progressive increase in the lethality of lag phase cells from about 20% inactivation, in the presence of 0.1 U/ml, to about 70% inactivation, in the presence of 7 U/ml of bacitracin. However, after 2 hours holding, none of the concentrations of agent prevented the rapid multiplication of cells associated with the exponential growth phase.

Therefore, in order not to complicate this study by the addition of more agent after 2 hours holding, it was decided to choose a concentration of agent to prevent lethality during the lag-phase of the growth cycle and to allow subsequent growth to proceed, as the majority of the near-UV radiation-induced recovery from salt sensitivity occurred during the initial 2 hour post-irradiation holding period, which is within the lag phase for the unirradiated control cells (as shown in Figs. 30, 31 and 33a). The result of such an experiment, where the cells were irradiated with near-UV radiation for 60 minutes and held in recovery media containing either no agent, or containing bacitracin added at 0.6 or 0.2 U/ml, before plating on either low salt or high salt minimal media, is shown in Figure 35.

The figure shows that, for the unirradiated cells (only plated on low salt plates since previous experiments had shown there was no difference in surviving fractions obtained between low and high salt minimal media), the presence of 0.2 U/ml bacitracin caused no detectable cell death during the lag phase. The presence of the higher concentration

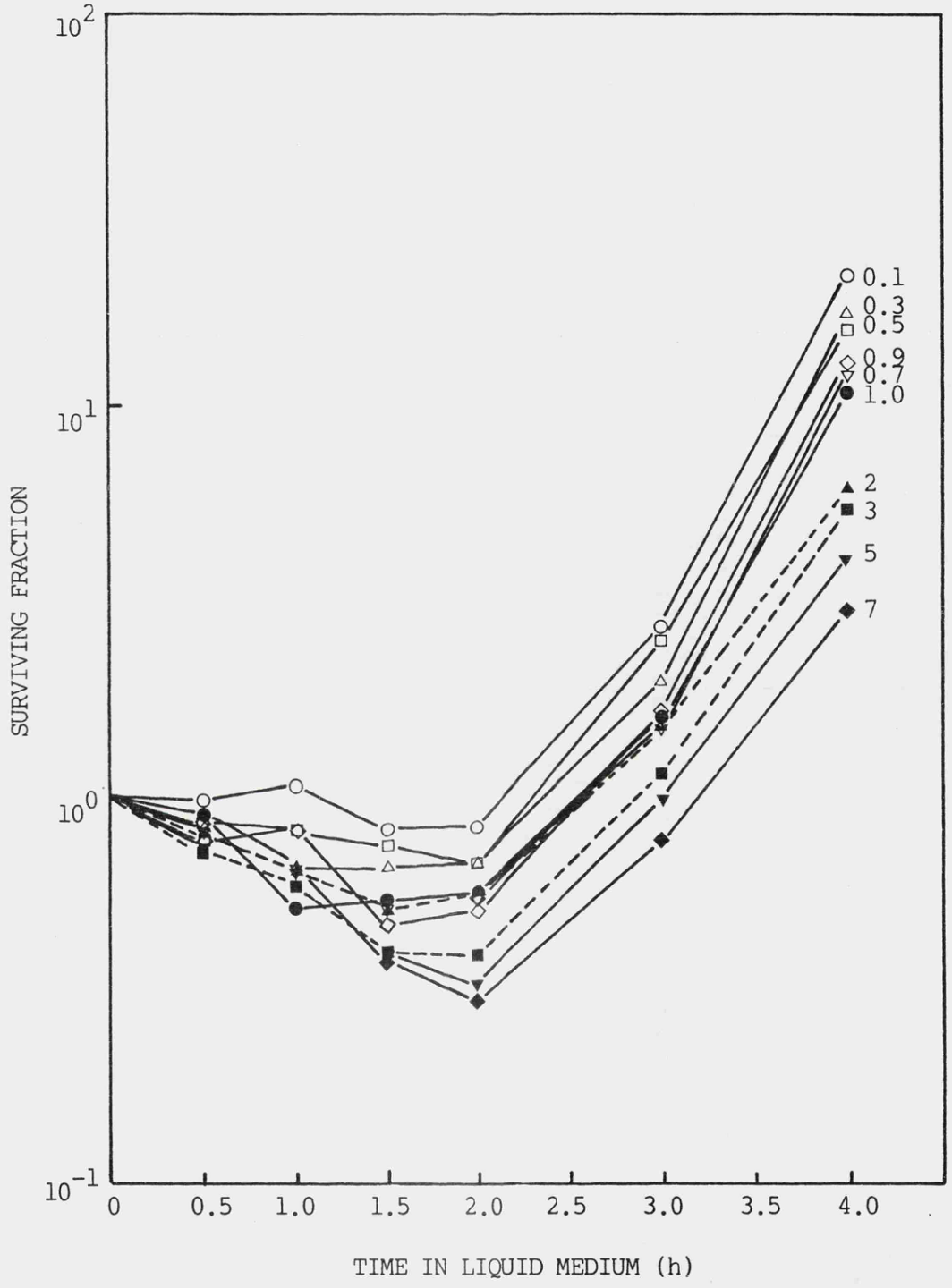

Figure 34 Survival of E. coli K-12 (SR 385) held at 37°C in recovery media containing varying concentrations of bacitracin (numbered as U/ml), before plating on YENB.

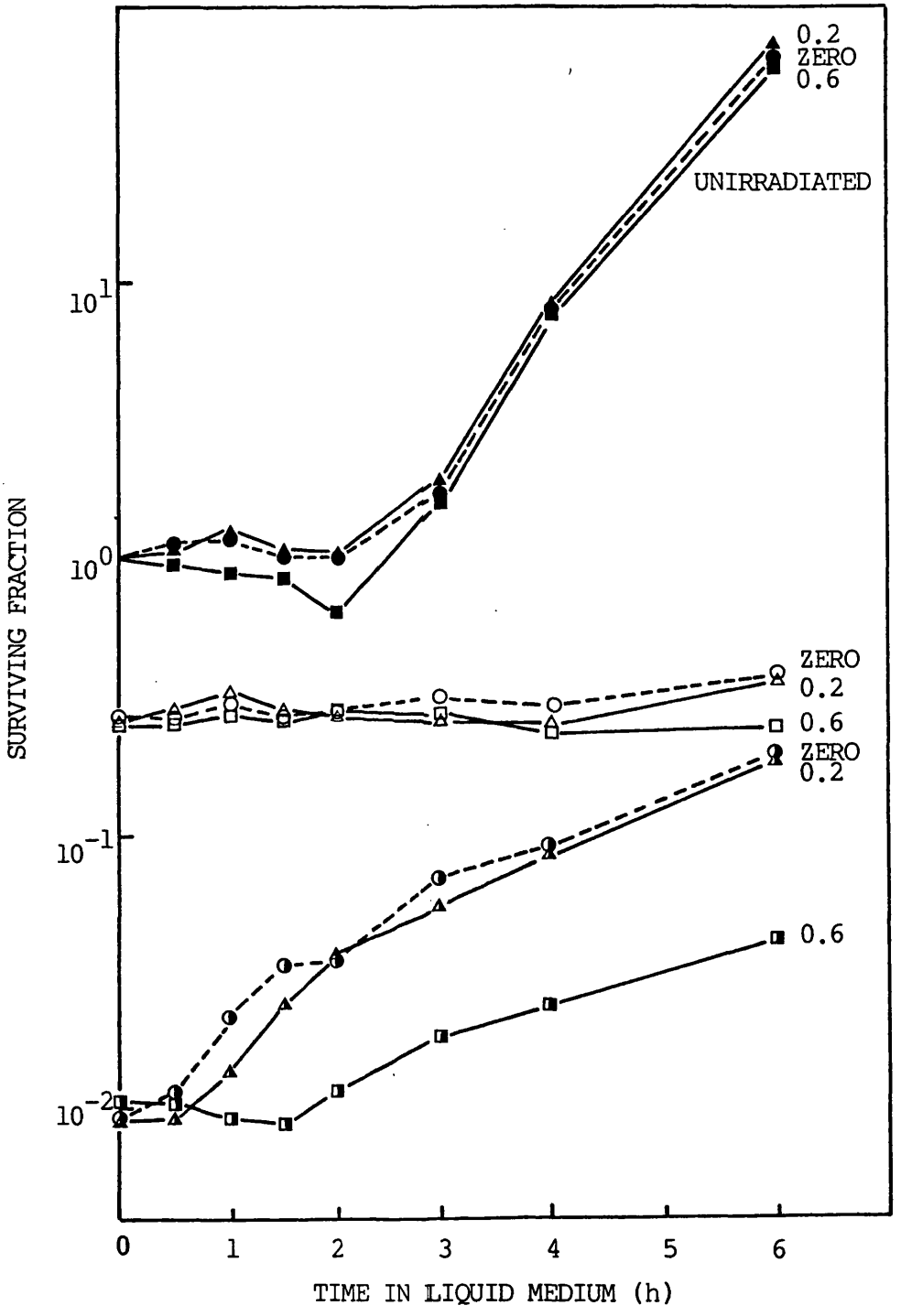

Figure 35 The surviving fraction of E. coli K-12 (SR 385) unirradiated (closed symbols) or irradiated for 60 minutes with broad-band near-UV radiation (open and half-open symbols). Samples were held at 37°C in recovery media alone (○,●,◑) or supplemented with bacitracin at 0.6 (□,■,◨) or 0.2 (△,▲,▲) units/ml, for the times indicated on the abscissa, before assessing for viability on 'low salt' (closed and open symbols) or 'high salt' minimal medium (half-open symbols).

of 0.6 U/ml did cause some cell death (about an average 15% reduction from the corresponding number of cells held in medium containing no inhibitory agent). However, both concentrations of bacitracin allowed subsequent growth of the unirradiated cells after 2 hours holding.

For the irradiated cells, Figure 35 shows that whereas, for the low salt plates, the bacitracin had no significant effect on survival throughout the 6 hour holding period (with again, as shown in Figs. 30, 31 and 33a, the surviving fractions remaining relatively constant) its presence, when plating on high salt medium, did reduce the recovery from near-UV radiation-induced salt sensitivity. This was particularly apparent when using a concentration of 0.6 U/ml, which significantly inhibited the recovery process, especially over the initial 2 hour post-irradiation holding period (where most of the recovery is observed - see Fig. 30). Even in the presence of 0.2 U/ml bacitracin, a small reduction in the recovery from salt sensitivity, shown in the absence of any inhibitory agent, was apparent, again particularly over the initial 2 hour post-irradiation holding period.

DISCUSSION

The initial results presented in this chapter confirm the general findings of Moss and Smith (1981) who showed, using the same *E. coli* K-12 strain SR 385, a sensitivity to inorganic salt after irradiation with broad-spectrum near-UV radiation. This has been demonstrated using low, normal and high salt minimal media (8.5, 85 and 208.5mM, respectively) in two DNA repair-competent *E. coli* K-12 strains; SR 385 (Fig. 25) and AB 1157 (Fig. 28). In addition, the absence of

sensitivity to inorganic salt was demonstrated for unirradiated cells (Table 1) Appendix B and far-UV (254 nm) irradiated cells (Fig. 33b) confirming this effect to be due to the near-UV radiation itself.

In addition to the Moss and Smith observations, it was observed that differences in near-UV radiation sensitivity may also be exhibited between commonly used complex nutrient agars; some of these differences being large (Figs. 26 and 27). These figures show that, when using Oxoid and Tryptone Soya agar (TSA) plates for the assessment of viability, the cell sensitivity is much greater than when viability is assessed on YENB medium (the only complex medium used in the Moss and Smith studies). For example, the time of irradiation required to reduce the surviving fraction to 1% on the TSA and on the Oxoid plates, is 53 and 50 minutes, respectively, whereas it is 75 minutes on the YENB plates (from Fig.27). As noted in the results section, thymine at a concentration of 10 μg/ml was required to be added to the TSA, in order for any colonies of SR 385, either unirradiated or irradiated, to appear. This is presumably due to a lack of this growth requirement in the agar medium. No such addition was needed for the Oxoid and YENB media. This addition, therefore, needs to be considered for all experiments, involving thymine-requiring E. coli strains, where viability is to be assessed on TSA.

In agreement with the inorganic salt hypothesis being the reason for the increase in sensitivity of near-UV irradiated cells on minimal media, the differences in sensitivity between nutrient agar plates appears to be due largely to the much higher concentrations of sodium chloride in Oxoid and TSA media (see Fig. 27 and Table 7). Figure 27 shows that, on omitting the sodium chloride content from Oxoid nutrient agar, the survival of near-UV irradiated cells show

approximately the same sensitivity as when plated on YENB medium. However, on adding sodium chloride, in the same concentration as present in the Oxoid and TSA plates, to YENB medium, an increase in sensitivity is observed, but this is not as great an increase as would be predicted if the sodium chloride content in the plates was the sole reason for the differences in sensitivity. An explanation for this may be evident from Fig. 29 where it is apparent that small amounts of Casamino Acids (a protein hydrolysate) and yeast extract protect irradiated cells from the sensitivity to inorganic salt. As the YENB medium contains more yeast extract than the Oxoid medium (7.5g to 2g respectively) this may protect the cells on YENB medium from sensitivity to inorganic salt. However, on adding sodium chloride (at 100mM) to Difco nutrient agar, and omitting the 7.5g of yeast extract, the sensitivity is still not as great as that shown on Oxoid plates (Fig. 29). This is probably due to Difco nutrient agar itself possessing more protective properties, i.e. containing more nutrients responsible for protection from salt sensitivity, than the corresponding Oxoid nutrient agar.

A protection from the salt sensitivity effects observed after the mild-heat treatment of cells has also been seen, by the addition of numerous agents to the plating media. For example, Hurst et al. (1976), using sublethally heat-injured Staphylococcus aureus, (52°C treatment) showed a restoration of salt tolerance, by the addition of Difco yeast extract (1.5%), sodium pyruvate (0.2%), L-histidine (0.5%), Difco casitone (1.5%), acetyl phosphate (0.5%) and adenosine 5'-triphosphate (1.0%) to the plating medium. Rayman et al. (1978), using heat-stressed cells of Salmonella senftenberg, showed that the addition of compounds capable of degrading hydrogen peroxide allowed growth of heat-injured cells (e.g. sodium pyruvate, 0.25%; catalase, 50 units of activity per millilitre; $FeCl_3$, 0.05%; and $FeSO_4 . 7H_2O$,

0.05%). Furthermore, these compounds did not stimulate growth of heated cells of Streptococcus faecium, an organism which does not possess catalase.

Further evidence of the catalase system being involved in the protection of cells from salt sensitivity has been provided by Kapuscinski and Mitchell (1981). They showed that a higher surviving fraction occurred on lactose nutrient agar than on glucose minimal agar, for E. coli held in coastal seawater (salinity 26%) and irradiated with sunlight, the difference being reduced by the addition of catalase (275 units per plate) or sodium pyruvate (0.1%) to the glucose plates. Also, Martin et al. (1976), studying the effect of catalase on microbial enumeration, found that its addition to plates permitted increased enumeration of physically or chemically injured (stressed) microorganisms; the catalase acting by preventing the accumulation of hydrogen peroxide in or around injured cells.

It would, therefore, appear that the protection offered by Casamino Acids and yeast extract, in near-UV irradiated cells plated on high salt media (Fig. 29), may be due to a scavenging of peroxide radicals produced, either indirectly, or directly, by near-UV radiation. In addition, a protective effect by large numbers of 'dead' cells, releasing or providing nutrients required for protection from salt sensitivity, may explain the shape of the survivor curves often obtained when using high salt media; where often, at fluences resulting in low surviving fractions (i.e. below 10^{-4}) viable counts were higher than would be predicted from an extrapolation of the exponential inactivation part of the survival curve (Moss and Smith, unpublished; and Fig. 26 Oxoid nutrient agar survival curve).

Indirect evidence for a possible protective effect by large numbers of 'dead' cells has been provided by Tuveson and Violante (1982), who described the effect of liquid holding (LH), in 0.85% saline or M9 salts solution, on near-UV irradiated (300-400 nm) E. coli, and attempted to determine the reasons for published differences in liquid holding effects on viability. They showed that, using relatively high cell densities (10^8 - 10^9 cells ml^{-1}), LH caused cell viability to increase, whereas previously, Eisenstark (1971), using intermediate cell densities (10^4 - 10^5 cells ml^{-1}), showed that viability remained constant and, using low cell densities (10^2 - 10^3 cells ml^{-1}), Hollaender (1943) showed that viability decreased. They have interpreted these differences to be due to cell lysis with a corresponding release of nutrients at high cell densities, which may allow growth of undamaged survivors in non-nutritive medium. At intermediate cell densities, cell death might be balanced with multiplication of undamaged cells resulting in no apparent effect of LH on viability, whereas at low cell densities, insufficient nutrients are released from lysed cells to support multiplication of undamaged survivors.

Further work involving the relative protective effects of catalase, pyruvate and the individual amino acids and vitamins contained in Casamino Acids and yeast extract, would help elucidate the nature of this process in near-UV irradiated cells. Also, the addition of 'overkilled' cells to plating media may help determine the reason for the typical shape of the survival curves obtained.

Results presented in this chapter also show that a recovery from near-UV radiation-induced salt sensitivity occurs when cells are held, at 37°C, in a rich growth medium; the recovery occurring particularly over the initial 2 hours of holding (Fig. 30). Therefore, recovery was not due to a growth of the organism as it occurs within the lag phase for the unirradiated cells, but rather possibly reflects enzymatic activity directed towards a repair of damaged components.

The recovery from mild-heat-induced salt sensitivity also occurred largely within the initial 2 hour post-treatment period (Iandolo and Ordal, 1966). However, whereas their studies showed that a complete recovery was achieved after about 3 hours post-treatment holding, such a complete recovery was not observed from near-UV radiation-induced salt sensitivity (Fig. 30). Iandolo and Ordal (1966) showed that the time required for complete recovery to occur depended upon the nature of the holding medium. In tryptone soya broth the process was complete in 3-4 hours, whereas, in limiting media, not all the cells regained the ability to grow in the presence of sodium chloride. Further work by Clark and Ordal (1969) showed complete recovery after 4 hours holding to be possible in nutrient broth, lactose broth and lauryl tryptose broth. However, if the recovery process involved after near-UV radiation-induced salt sensitivity was identical in nature to the mild-heat effect, then YENB medium should provide sufficient nutrients to enable a complete recovery.

Figure 30 shows that, after 6 hours holding in medium and with conditions allowing recovery, only approximately 70% of the salt sensitive damage is repaired. This indicates that there may be a sector of non-repairable salt-sensitive damage (about 30%) which may represent cells whose membranes have been disrupted so severely as to

cause lysis and leakage of vital cell components. It should also be considered that some cells may have sustained salt-sensitive damage to a degree such that they will be inactivated even when plated on 'low salt' YENB plates.

These results show that the recovery process, particularly over the initial 2 hour post-irradiation holding period, where the majority occurred, was not affected by the presence of chloramphenicol (Fig.31) or penicillin G (Fig. 33a). This indicates that neither protein synthesis nor cell wall synthesis, respectively, were required for recovery. However, the increased recovery from 2 to 6 hours post-irradiation holding, observed in Fig. 30, was not apparent in the presence of chloramphenicol and occurred to a lesser extent in the presence of penicillin G. This probably indicates that this latter portion of the 'recovery' curve is due to some cell division and growth of the irradiated cells and further suggests that the large increase in recovery observed over the initial 2 hour holding period is not due to a growth of the irradiated cells.

The implication that cell-wall synthesis is not required for the recovery process provides a difference between near-UV and X-radiation effects, where Gillies et al. (1979), with a similar type of experiment, showed that penicillin caused an increase in lethality of aerobically X-irradiated cells of E. coli B/r, indicating that the peptidoglycan layer is damaged by X-radiation.

The presence of bacitracin in the post-irradiation holding medium is shown to reduce the amount of recovery from salt sensitivity (Fig. 35), whereas the purely cell-wall acting penicillin G did not (Fig. 33a). This implies that the recovery process has some cell

membrane involvement, but since bacitracin exerts several different effects on the membranes of cells, the precise nature of this membrane involvement cannot be deduced. As no agent available specifically inhibits membrane synthesis without affecting other cellular processes, it is difficult to prove with certainty that the recovery process does involve a repair of damaged membrane components. However, the effect of bacitracin in reducing the recovery does suggest that at least part of the process is occurring by means of a repair of damaged membrane components.

Attempts by several studies to elucidate the mechanisms involved in the return to salt tolerance after mild-heat treatment have thus far not produced any clear-cut answers. Using Staph. aureus, Iandolo and Ordal (1966) showed that a return to salt tolerance was not inhibited by the presence of penicillin (100 μg/ml), chloramphenicol (100 μg/ml), or cycloserine (100 μg/ml), indicating that neither cell wall nor protein synthesis was intimately involved. However, inhibition was achieved by the presence of the RNA synthesis inhibitor, actinomycin D (5 μg/ml). Therefore, the mild-heat studies of Iandolo and Ordal concluded that recovery is primarily due to a resynthesis of RNA, thus requiring the presence of amino acids. However, they also showed that damage to the membrane occurred, which they observed as a leakage of intracellular material (potassium, free amino acids and RNA derivatives). Thus a repair of the membrane must also occur during recovery.

Some other studies have also shown RNA synthesis to be important for recovery (Tomlins and Ordal, 1971), while others have shown other requirements. Hurst et al. (1973) attempted to relate the recovery of salt tolerance in Staph. aureus with the return of membrane functions.

They found that although membrane lipid was lost during injury (about 33%) and an oversynthesis of C_{16} and C_{18} fatty acids occurred during recovery, penicillin (100 μg/ml) blocked this reaction without affecting recovery. Furthermore, chloramphenicol did not affect fatty acid oversynthesis but did interfere with recovery, indicating that the process was possible even when a number of membrane functions were still impaired. They concluded that salt tolerance may not be a membrane function and could return before complete membrane repair. However, they expressed reservations concerning this conclusion, and suggested that further work was required to elucidate the mechanism.

Subsequently, Hurst et al. (1974) described a good correlation between loss of salt tolerance and loss of cellular magnesium. Magnesium ions are well known to be necessary for the activity of many enzymes and for the integrity of ribosomes, and they may link membrane phospholipids with the carboxyl groups of membrane proteins (Diamond and Rose, 1970). Furthermore, membrane porosity appears to be affected by Mg^{2+} (Scherrer and Gerhardt, 1973).

Also, the recovery process has been linked to lipid biosynthesis, thus producing a competent membrane for the concentration of essential intracellular pools (Tomlins et al., 1972; Pierson et al., 1971). However, Grau (1978) pointed out that there may not always be a relationship between cause and effect, as cells made nonviable by heating were still seen to have significant membrane integrity. In general though, the evidence is that recovery to salt tolerance involves the repair of damaged membranes with RNA synthesis also being a requirement. A review of the recovery of mild-heat treated cells is available (Tomlins and Ordal, 1976).

The salt sensitivity effects described in this chapter may help explain the difficulty in obtaining reproducibility with near-UV radiation experiments often reported (e.g. Peak, 1970), no such difficulties arising with far-UV radiation experiments where no salt sensitivity effects are apparent (Moss and Smith, 1981; Fig. 33b).

The results show that the type of nutrient agar used to assess viability can affect the sensitivity of near-UV irradiated cells. Moreover, of the frequently used minimal media, differing total molarities of inorganic salts may be present and thus also contribute to sensitivity differences to near-UV radiation. For instance, Neidhardt et al. (1974) have shown the following total inorganic salt molarities in commonly used minimal media : MOPS, 106mM; Tris, 243mM; Davis-Mingioli, 83.4mM; Vogel-Bonner, 101mM; M9, 93mM; modified Werkman, 166mM; and M63, 116mM. This may have particular consequence in the 'classical' scoring of mutations, by reversion to prototrophy, after near-UV radiation, where minimal media plates are used. This consequence of near-UV radiation-induced sensitivity to inorganic salts is discussed in Chapter 5. Also, salt sensitivity effects may be important where near-UV radiation and mild-heat interaction experiments are performed.

In addition, the age, temperature of storage, the temperature at the time of pouring, and the time and temperature of autoclaving of agar plates may lead to differing final compositions of agar with regard to inorganic salt and, more especially, the amount of protective agents present. Further work needs to be carried out to determine whether any of these parameters are important in contributing to near-UV radiation survival. Also, it was particulary noticeable during the

series of recovery experiments that the method of mixing, diluting and spreading of near-UV irradiated cells affected their survival characteristics (data not shown). Vigorous and prolonged mixing using a Whirlimix resulted in fewer colonies on the final plating medium compared to gently mixing by hand. This presumably reflects the weakened cell membranes of the irradiated cells being disrupted by vigorous mixing techniques.

Perhaps the most important finding in this chapter is that a recovery from near-UV radiation-induced salt sensitivity is possible when irradiated cells are held in a rich growth medium. This finding has helped to elucidate the nature of the near-UV radiation-induced salt sensitivity effects in E. coli.

CHAPTER 2

AN ACTION SPECTRUM FOR UV RADIATION - INDUCED SALT SENSITIVITY IN *E. coli* K-12 SR 385.

The results presented in Chapter 1 showed that a sensitivity to inorganic salts was apparent after irradiation of strain K-12 SR 385 with broad-band near-UV radiation, but not after far-UV (254nm) radiation. By comparison with mild- heat studies and by the use of metabolic inhibitors, evidence was presented indicating that the observed salt sensitivity was associated with damage to the cytoplasmic membrane.

The purpose of performing the series of experiments described in this chapter was to elucidate the wavelength dependence for inorganic salt sensitivity, and thus determine an action spectrum for that UV radiation-induced damage, which is presumed to be membrane damage. From such an action spectrum it may then be possible to identify any chromophore (or chromophores) involved in producing radiation-induced cell sensitivity to inorganic salt.

All the experiments described in this chapter involved the irradiation of a secondary, 24 hour culture of strain SR 385, grown and prepared for irradiation at an initial concentration of about $1x10^7$ CFU/ml, as described in the general methodology section. A 3ml volume of suspension was irradiated at 0°C; radiation being provided by one of the three monochromatic sources detailed in the general methodology section. These were the Penray lamp for 254nm radiation, the Bausch and Lomb super pressure Hg lamp for wavelengths from 260 to 365nm and the Oriel Hg-Xe arc lamp for 365 and 405nm radiations. The appropriate stray light filter used at each wavelength is described in the general methodology section. Assessment of viability was then carried out using either 'low salt' media, which were of two types YENB complex media or minimal media with one-tenth-diluted inorganic salt , or 'high salt' medium, which was minimal media with one-tenth-

diluted inorganic salt and sodium chloride added at 200mM.

Results

The inactivation by 254nm radiation of E.coli SR 385, when assessed for viability on YENB and low and high salt minimal media, is shown in Figure 36a. There was no significant difference observed by assessing for viability on the two types of low salt plates, i.e. YENB and low salt minimal media, and there was also no difference in survival between the low and high salt plates. Therefore, no salt sensitivity is apparent after irradiation with 254nm radiation. Inactivation of E. coli SR 385 by 260, 270, 280, 290, 300 and 305nm radiations with viability again assessed on one or both types of low salt media and high salt media are shown in Figures 36b, 37a and b, 38a and b and 39 respectively. As with the 254nm radiation response (Fig. 36a) there is no significant increase in lethality observed at these wavelengths when viability is assessed on the high salt plates.

The survival curves obtained with E. coli SR 385 after 310nm irradiation are shown in Figure 40a. This shows a sensitivity to inorganic salts, but only with cells irradiated at high fluences ($>7\times10^{4}Jm^{-2}$), when the surviving fraction is approx. 0.25. The salt sensitivity then increases with increasing fluence up to $1.2\times10^{5}Jm^{-2}$; thereafter the difference in cell survival on low and high salt plates remains approximately the same (a fluence enhancement factor at the 1% survival level of approx. 1.2).

The survival curves obtained after 313nm irradiation are shown in Figure 40b. As with the 310nm radiation response (Fig. 40a), a sensitivity to inorganic salts is apparent at high fluences, with the

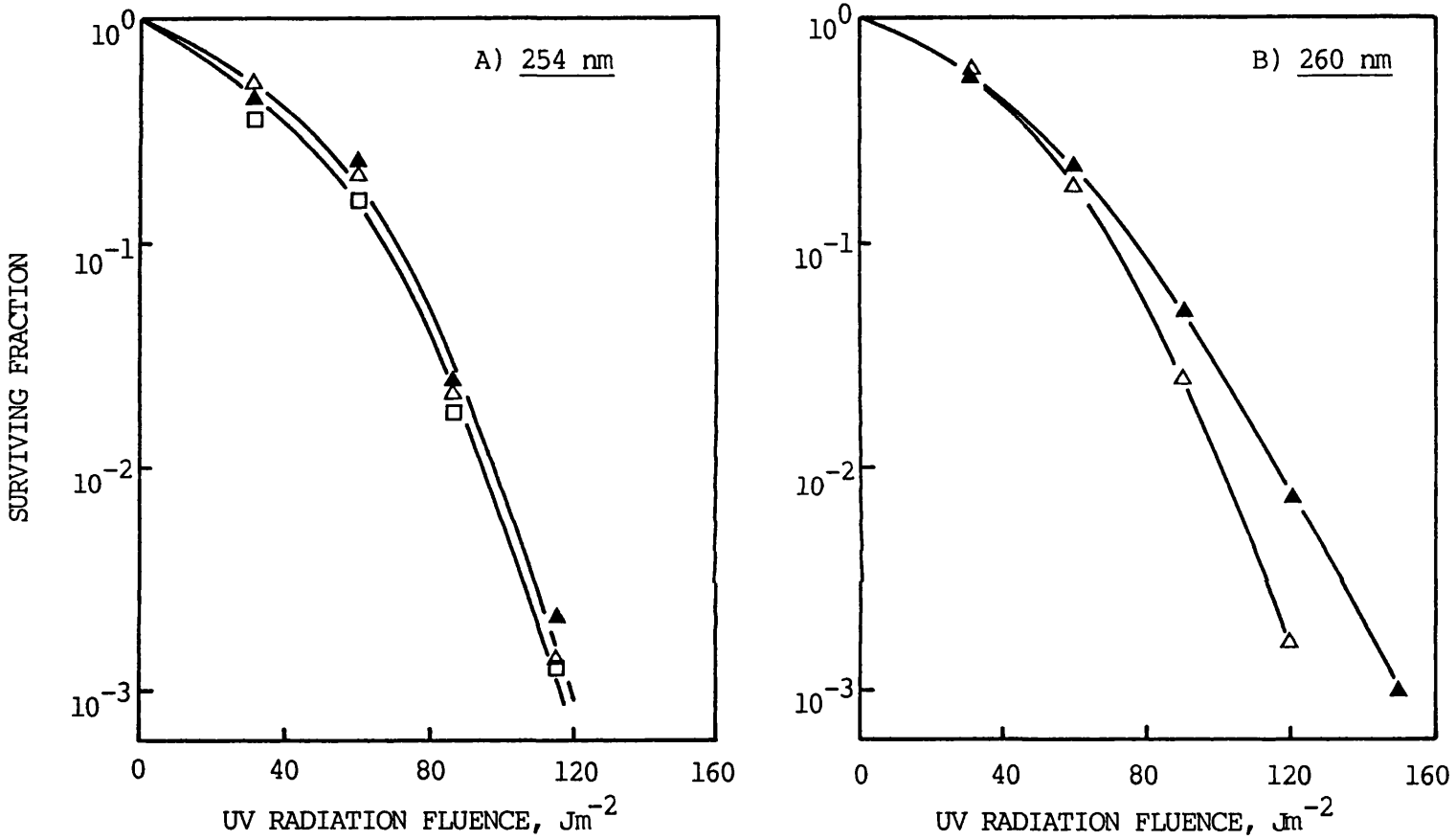

Figure 36

The fluence survival response at0°C of E. coli K-12 (SR 385) in stationary phase to A) 254 nm and B) 260 nm radiations. Viability was assessed on YENB (□), and low salt (△) or high salt (▲) minimal media.

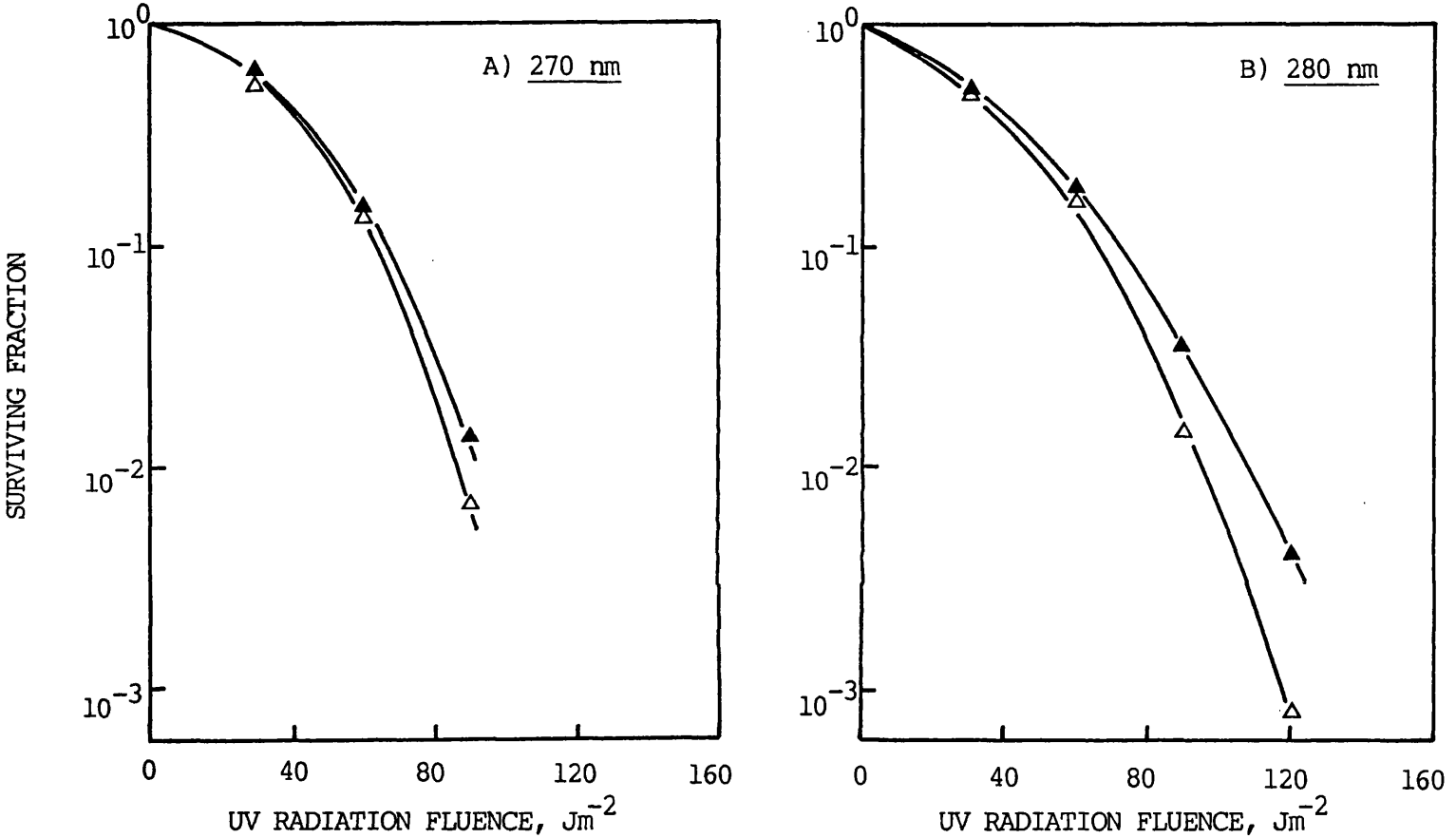

Figure 37

The fluence survival response at 0°C of E. coli K-12 (SR 385) in stationary phase to A) 270 nm and B) 280 nm radiations. Viability was assessed on either low salt (△) or high salt (▲) minimal media.

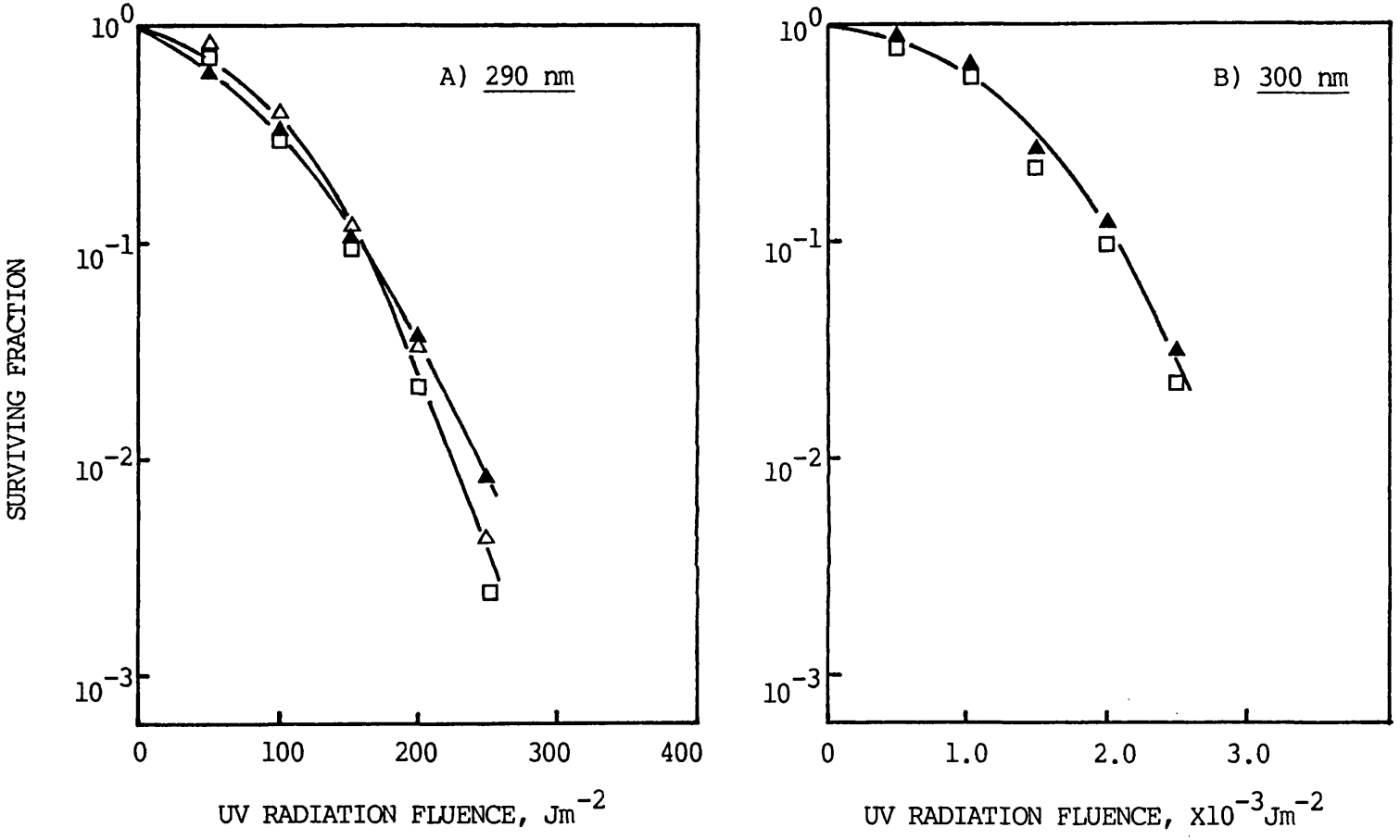

Figure 38

The fluence survival response at 0°C of E. coli K-12 (SR 385) in stationary phase to A) 290 nm and B) 300 nm radiations. Viability was assessed on YENB (□), and low salt (△) or high salt (▲) minimal media.

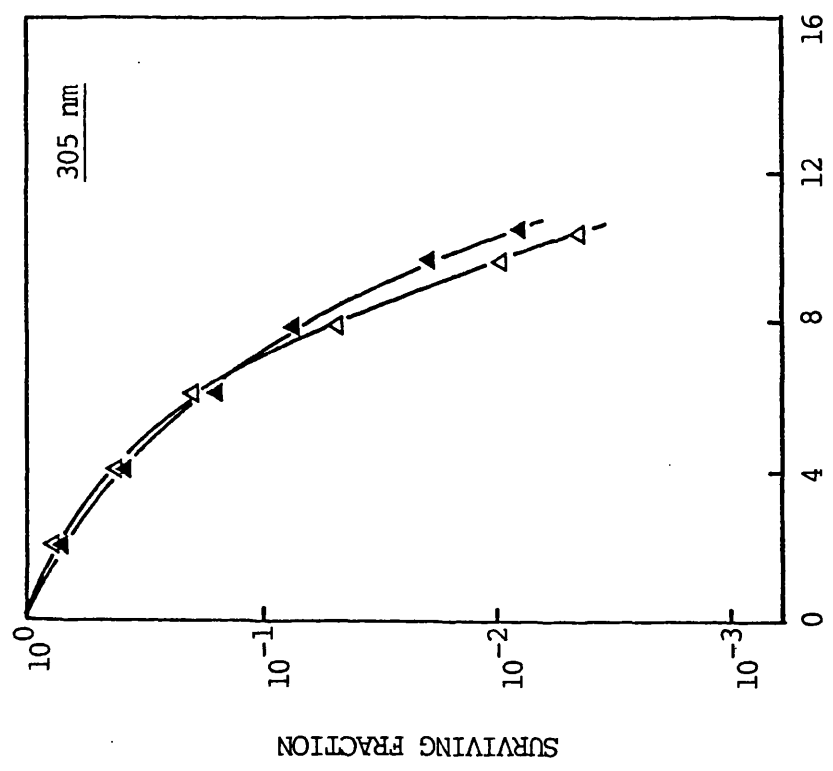

Figure 39

The fluence survival response at 0°C of E. coli K-12 (SR 385) in stationary phase to 305 nm radiation with viability assessed on either low salt (Δ) or high salt (▲) minimal media.

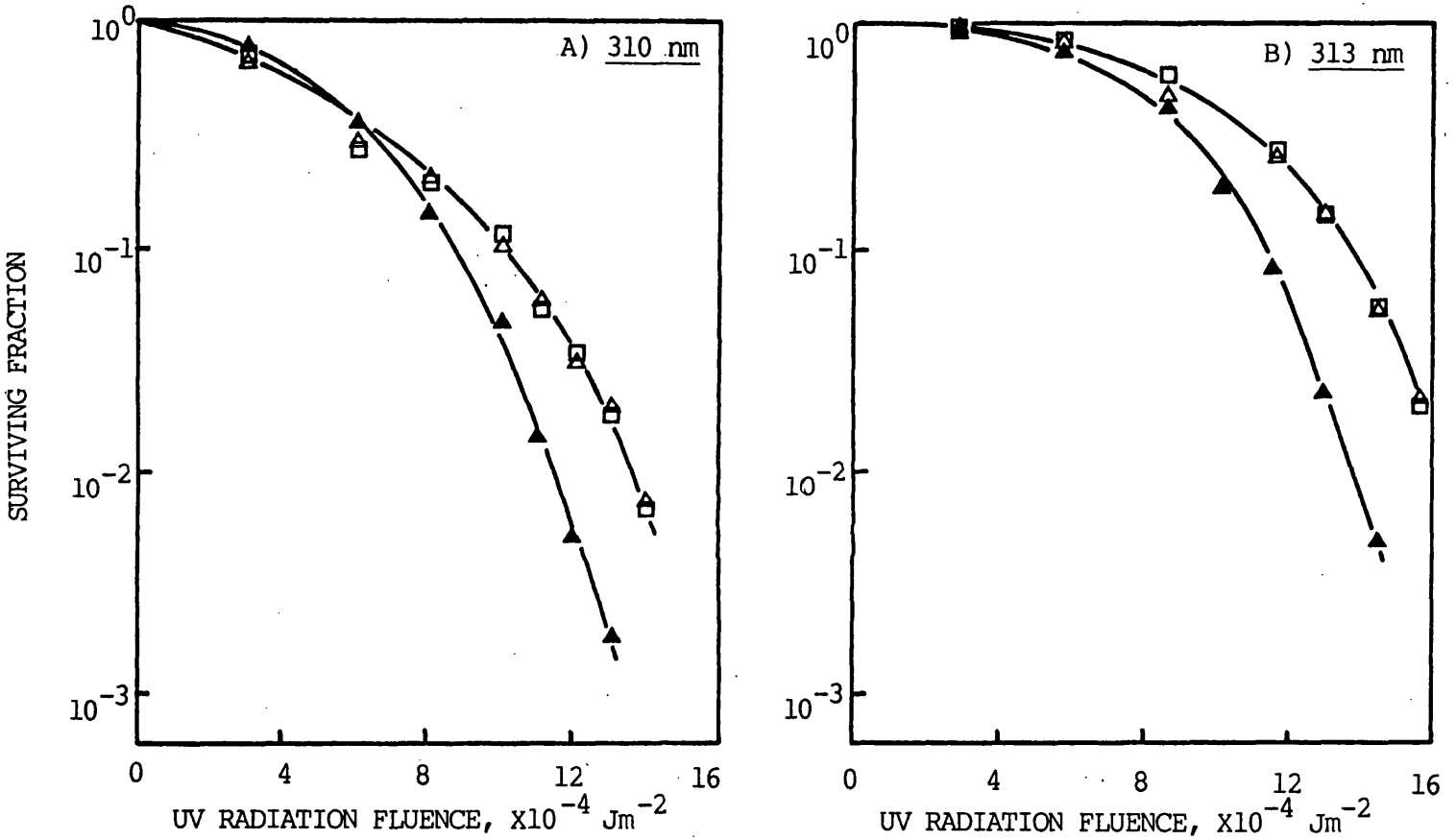

Figure 40

The fluence survival response at 0°C of E. coli K-12 (S.R 385) in stationary phase to A) 310 nm and b) 313 nm radiations. Viability was assessed on YENB (□), and low salt (△) or high salt (▲) minimal media.

onset again occurring at a fluence of about $7x10^4$ Jm^{-2}, where at this wavelength, the surviving fraction is approx. 0.7. Also, in common with the 310nm response, there is an increase in salt sensitivity with increasing fluence over the shoulder region of the survival curve before the curve becomes approximately parallel with the response on the low salt plates at higher fluences, again with a fluence enhancement factor at the 1% survival level of about 1.2.

The responses of E. coli SR 385 to 325, 334, 365 and 405nm radiations are shown in Figures 41a and b and 42a and b, respectively. At these wavelengths the irradiated cells' sensitivity to inorganic salt is apparent even at the low fluences that do not significantly affect cell viability on the low salt plates. Although the overall shape of the survival curves at 325 and 334nm is different from those observed at all the other wavelengths tested, as shown at 310 and 313nm, the salt sensitivity appears to increase over the shoulder region of the lethality curves before becoming approximately parallel with the low salt plate lethality curves at high fluences for 325, 334, 365 and 405nm irradiations.

Discussion.

The results presented in this chapter show that there is a clear division in the effectiveness of the different wavelengths in inducing sensitivity to inorganic salts in E. coli SR 385. Irradiation with wavelengths from 254nm to 305nm (Figs. 36 to 39) results in no significant increase in sensitivity of cells being observed by assessing for viability on high salt plates, over the entire fluence range required to cause about 3 log cycles inactivation. In fact, as Moss and Smith

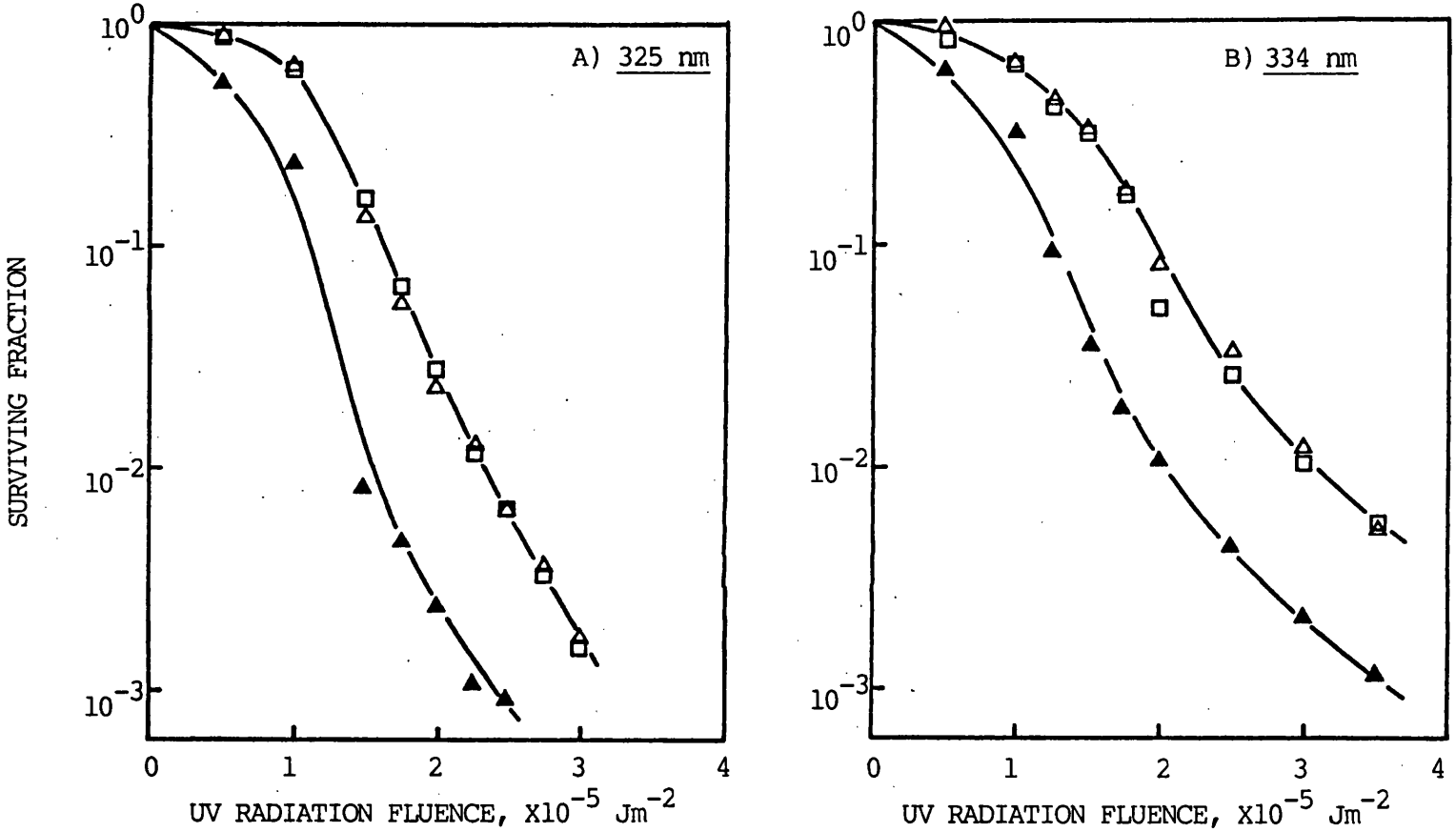

Figure 41

The fluence survival response at 0°C of E. coli K-12 (SR 385) in stationary phase to A) 325 nm and B) 334 nm radiations. Viability was assessed on YENB (□), and low salt (△) or high salt (▲) minimal media.

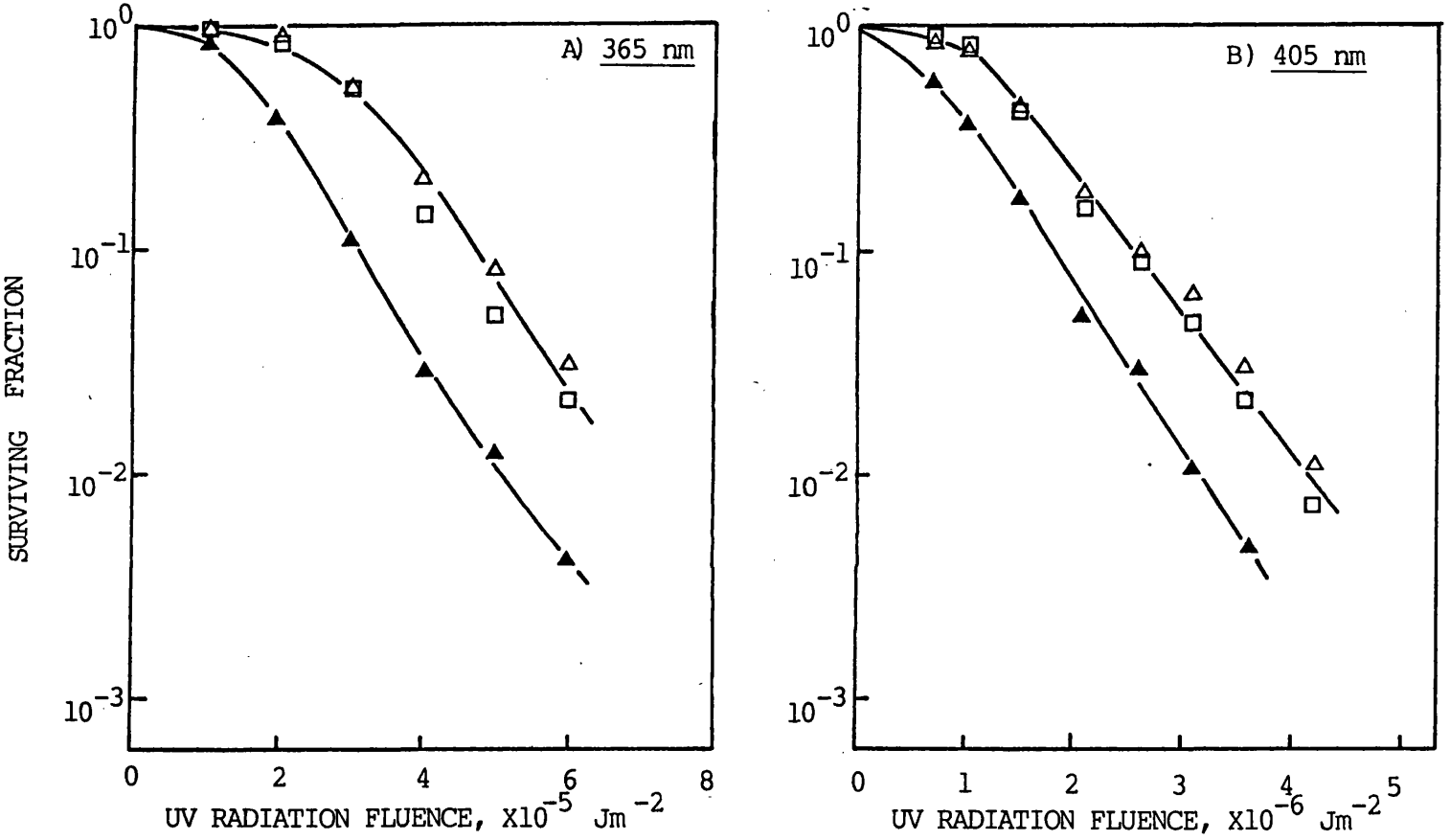

Figure 42

The fluence survival response at 0°C of E. coli K-12 (SR 385) in stationary phase to A) 365 nm and B) 405 nm radiations. Viability was assessed on YENB (□) and low salt (△) or high salt (▲) minimal media.

(1981) observed, using 254nm, Figures 36 to 39 show a 'minimal medium recovery' phenomenon where higher surviving fractions are shown on minimal media. This phenomenon is characteristically shown to a small extent by repair-competent strains, and to a greater extent by excision repair-deficient strains. The sensitivity of strain SR 385 at 254nm is similar to that reported for other DNA repair-competent strains. For example, Webb and Brown (1976), using similar experimental conditions, showed that, for E. coli B/r, a fluence of about 75 Jm^{-2} was required to reduce the surviving fraction to 10%, whereas Fig. 36a shows that about 70 Jm^{-2} is required to effect an equal amount of inactivation in E. coli SR 385.

The responses after 310 and 313nm irradiation (Fig. 40a and b) show that a sensitivity to inorganic salt is apparent but only at fluences greater than about $7x10^4$ Jm^{-2}, a fluence that results in, in the case of 310nm irradiation, a surviving fraction of about 0.25 and, in the case of 313nm irradiation, a surviving fraction of 0.7. However, at the longer wavelengths of 325, 334, 365 and 405nm (Figs. 41a and b, and 42a and b respectively), a sensitivity to inorganic salt is apparent throughout the fluence range used, even at low fluences where there is little inactivation on low salt media. Therefore, it may be concluded that it is only wavelengths above 305nm, that is those within the mid- and near-UV radiation regions, that induce a sensitivity to inorganic salt and thus may be causing a damaging effect on cell membranes at fluences important to cell survival.

However, it is not readily apparent from the survival curves as to the relative wavelength effectiveness in producing salt sensitivity effects. An appropriate method for determining the wavelengths that are

most effective at producing any observed effect is by the derivation of an action spectrum; a plot of the reciprocal of the fluence required to produce a given effect, versus wavelength. However, in order to plot an action spectrum certain criteria have to be met.

First, because the times of irradiation were vastly different for the shorter wavelengths of 254 to 300nm compared to the longer wavelengths of 334, 365 and 405nm (where much greater fluences were required) it is necessary to demonstrate reciprocity of time and fluence rate over the range of exposure times used in the study. Reciprocity of time and fluence rate means that the effect obtained is a function only of total fluence, and not of the time during which the irradiation occurs.

Ideally, the approach to investigate reciprocity would be to test at each wavelength using differing combinations of fluence rate and time of irradiation. However, at longer wavelengths, fluence rates were the maximum that the radiation source could deliver so could not be increased, and conversely could not be reduced due to the practicality of performing such experiments. Therefore, the reciprocity studies were restricted at this stage to 254nm. Ten-fold and one hundred-fold reductions in fluence rate at 254nm were achieved by using one of two rotating discs with sectors of 36° and 3.6° removed, respectively. The appropriate disc was then placed between the 254nm light source and the cuvette, and rotated at constant velocity throughout the time of exposure to reduce the incident fluence rate by a factor of 10 or 100. Thereby the typical time of exposure for a fluence of 100 Jm^{-2} was increased from 144 seconds to 24 minutes and to 4 hours.

The results of irradiating with fluences of 50, 100 and 150 Jm^{-2} of 254nm radiation, using a suspension of E. coli SR 385 at an initial concentration of $1x10^{8}$CFU/ml, and with viability assessed on either low or high salt minimal media, are shown in Figure 43. If the damage to membranes is a function of fluence rate, i.e. it accumulates over a long period of time and is not a function of wavelength, then one would have expected salt sensitivity to 254nm irradiation with long periods of illumination. The time of 4 hours irradiation is relevant to the experiments performed with longer wavelengths, i.e. 334 and 365nm, where salt sensitivity effects are apparent (Figs. 41 and 42). Figure 43 shows that, over one tenth and one hundred-fold differences in the fluence rate of 254nm radiation, no salt sensitivity is induced. This suggests that the salt sensitivity effects observed during the series of experiments described in this chapter do not appear to be due to a function of the time of irradiation.

In addition, an action spectrum is strictly valid only if the fluence-effect curves are of a similar shape at all the wavelengths tested, implying that the mechanism of action is the same at all wavelengths. Examination of the survival curves obtained from 254 to 405nm show that this is not the case, indicating that differing processes may be taking place at different wavelengths. Moreover, the different shape in survival curves makes the choice of parameter from the survival curves, to be used in the plotting of an action spectrum, a difficult one.

The use of the inactivation constant (or k value) for plotting an action spectrum for salt sensitivity is clearly not ideal as, firstly, at the wavelengths where salt sensitivity is apparent, the final

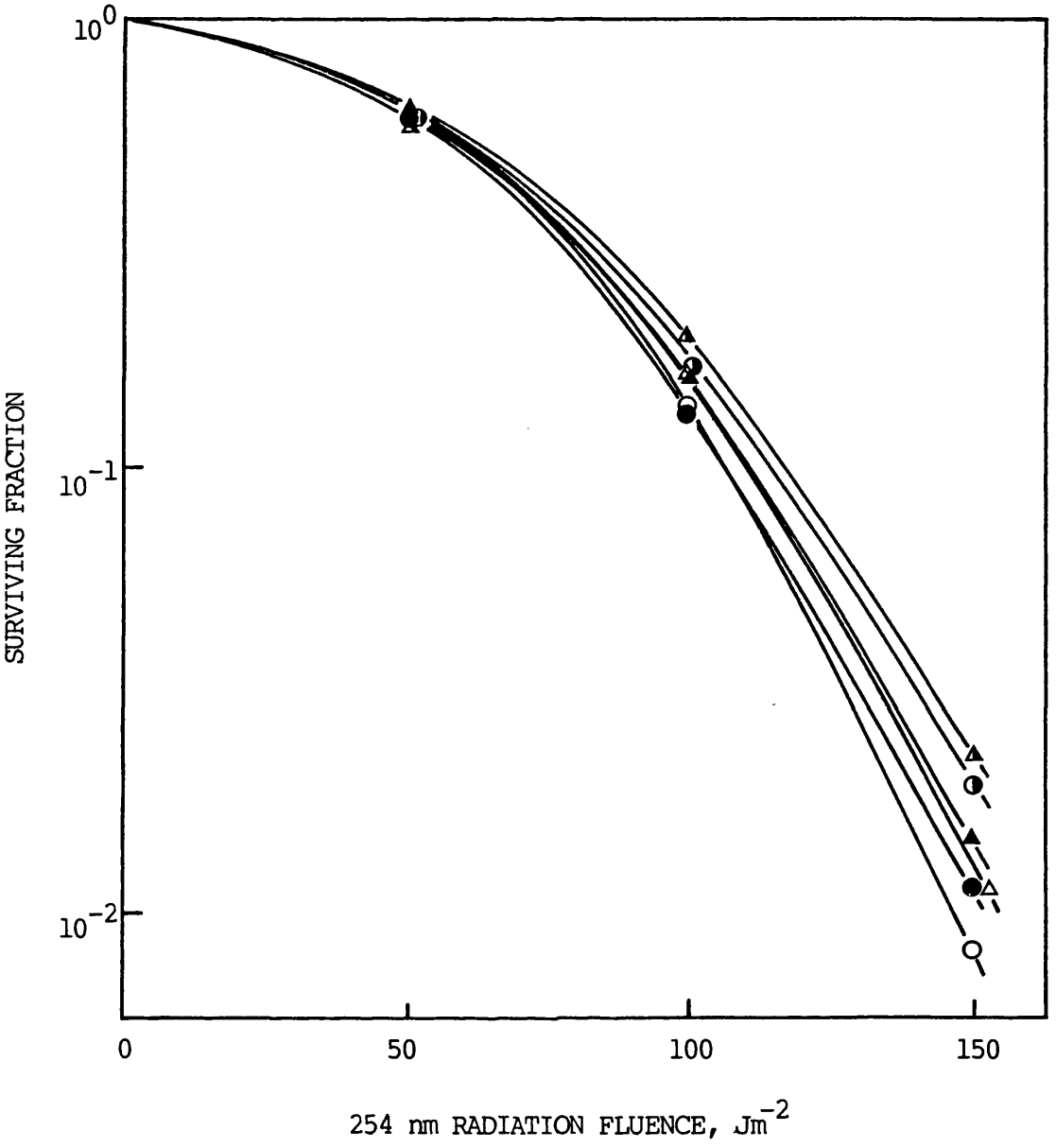

Figure 43

The effect of fluence rate on the inactivation of E. coli K-12 (SR 385) by far-UV (254 nm) radiation, with viability assessed on low salt (O,●,◑) or high salt (△,▲,▲) minimal media. Open symbols, 6.954×10^{-1} Wm^{-2}; closed symbols, 6.954×10^{-2} Wm^{-2}; half-open symbols, 6.954×10^{-3} Wm^{-2}.

slopes on low and high salt media are generally similar, the salt sensitivity being largely due to a reduction in the shoulder of the survival curve, and secondly, at 325 and 334 nm the shape of the curves is such that an accurate determination of the straight-line portion of the curves is not possible.

The observation that the k values are similar on high and low salt plates after irradiation with 365 nm is different from the result obtained on low and high salt media by irradiation with a broad-band near-UV radiation source (see Fig. 25 and Moss and Smith, 1981). After broad-band near-UV irradiation, the salt sensitivity appears to increase with increasing fluence, resulting in an increased inactivation constant for cells assessed on high salt medium. This may implicate some synergistic wavelength interactions occurring within the near-UV wavelength region, resulting in the increased cell sensitivity to inorganic salt shown at high fluences with broad-band radiation.

Other parameters which have been used for the determination of action spectra include the empirical use of $^{1}/F_{37}$ values and $^{1}/F_{10}$ values, that is the reciprocal of the fluences required to reduce the surviving fraction to 37% and 10% respectively. These parameters do incorporate some measure of the shoulders of survival curves and thus the $^{1}/F_{10}$ values for low and high salt plating media were used to determine an action spectrum for UV radiation-induced sensitivity to inorganic salt. $^{1}/F_{10}$ was used in preference to $^{1}/F_{37}$ as, particularly at 310 nm, the observed salt sensitivity was not apparent until the surviving fraction was less than 37%. Although obviously a compromise due to the differing shapes of the observed survival curves, the $^{1}/F_{10}$ value was considered an appropriate parameter to use.

Finally, for the plotting of an action spectrum, the $^{1}/F_{10}$ values need to be corrected for quantum efficiency by calculation in terms of the reciprocal of the incident quanta/m^2, where the energy of a single quantum is derived by application of the Planck equation, $E = hc/\lambda$ as described in the introduction.

An action spectrum for lethality of E. coli SR 385, when assessed for viability on low and high salt media, is shown in Figure 44. Sensitivity is expressed as $^{1}/F_{10}$ in quantum units and is plotted against the wavelength studied. From this figure it may be concluded that, over the wavelength range 254-313nm, the lethal action spectrum closely corresponds to the absorption spectrum of DNA (as shown in Fig. 3 in the introduction). Thus, the ratio of sensitivity based on quantum units at 254 versus 313nm of 2.63×10^{3} for this strain is very close to the ratio of absorbance of DNA at these wavelengths. Moreover, over the 254-310nm wavelength range, there was no significant difference observed by assessing for cell viability on low or high salt plates.

However at 310nm and above, throughout the near-UV wavelength region of the spectrum, the direct absorption of radiation by DNA cannot account for the sensitivity observed. Also, above 310nm and throughout the near-UV wavelength region of the spectrum, there is a significant increase in lethality observed for irradiated cells in the presence of inorganic salts in the plating medium, which is not apparent at the shorter wavelengths tested. The increases in near-UV radiation-induced sensitivity in the presence of inorganic salt do not appear to be large when plotted on a log scale, but the differences are significant, e.g. at 334nm there is a 1.6 fold decrease in the F_{10} value when assessed on high salt compared to low salt medium (at 365nm the ratio is 1.45).

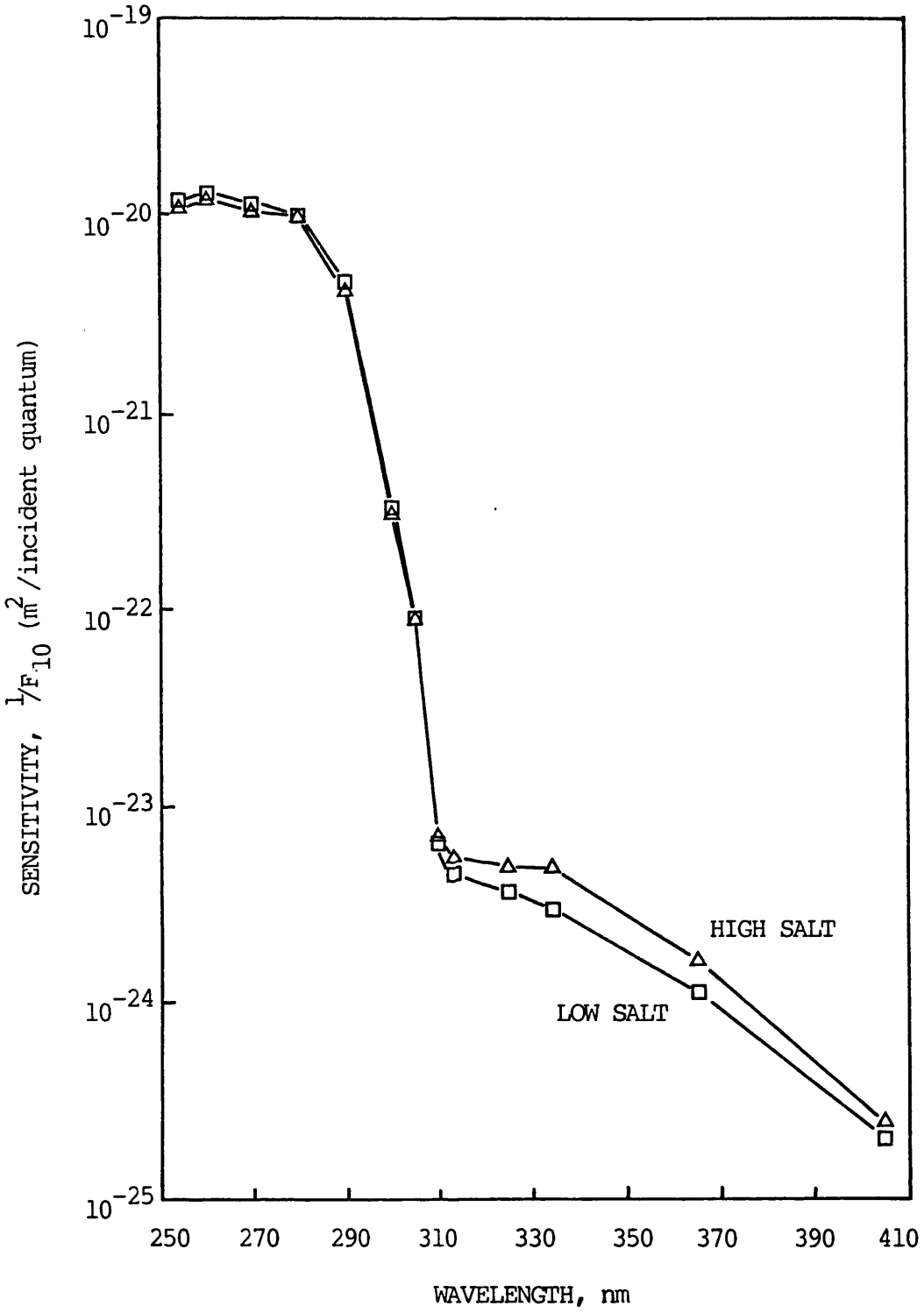

Figure 44

An action spectrum for lethality of stationary phase cells of E. coli K-12 (SR 385) with sensitivity expressed as $^{1}/F_{10}$ in quantum units, and viability assessed either on 'Low salt' (□),or 'high salt' (△) minimal media.

A measure of the salt sensitivity present at each wavelength was calculated by determining the difference in $^{1}/F_{10}$ values for high and low salt plates i.e. $^{1}/F_{10}$ HIGH SALT - $^{1}/F_{10}$ LOW SALT. In this way, zero or negative values represent no increased cell sensitivity on high salt plates, whereas positive values represent a measure of the increase in salt sensitivity of cells after irradiation. An action spectrum for salt sensitivity, expressed in this manner, over the wavelength range 254 - 405nm is shown in Figure 45. The figure shows that no salt sensitivity is induced by wavelengths of 305nm and below. However, in the near-UV wavelength range the salt sensitivity increases with increasing wavelength, up to a peak at 334nm. The sensitivity to inorganic salts at the longer wavelengths of 365nm and 405nm is then less than at 334nm.

Therefore from the discussion of Chapter 1, where the salt sensitivity effects were correlated with a damaging effect on cell membranes, Fig. 45 suggests that a peak of cell membrane damage is induced around the region of 334nm. Furthermore, the action spectrum shown in Fig. 45 suggests that, in a DNA repair- proficient strain, membrane damage can contribute to near-UV (but not far-UV) radiation-induced cell lethality. For the repair - deficient strains E. coli K-12 AB 1886 uvrA6 or AB 2480 uvrA, recA, however, sensitivity to inorganic salt after treatment with near-UV radiation was not apparent (Moss and Smith, unpublished data). These results are interpreted as reflecting the overriding importance of damage to DNA in the strains deficient in DNA repair mechanisms.

Published action spectra for lethality of various cells, both bacterial and mammalian, typically show a break and shoulder around 320 to 330nm, and a departure from the absorption curve for thymidine.

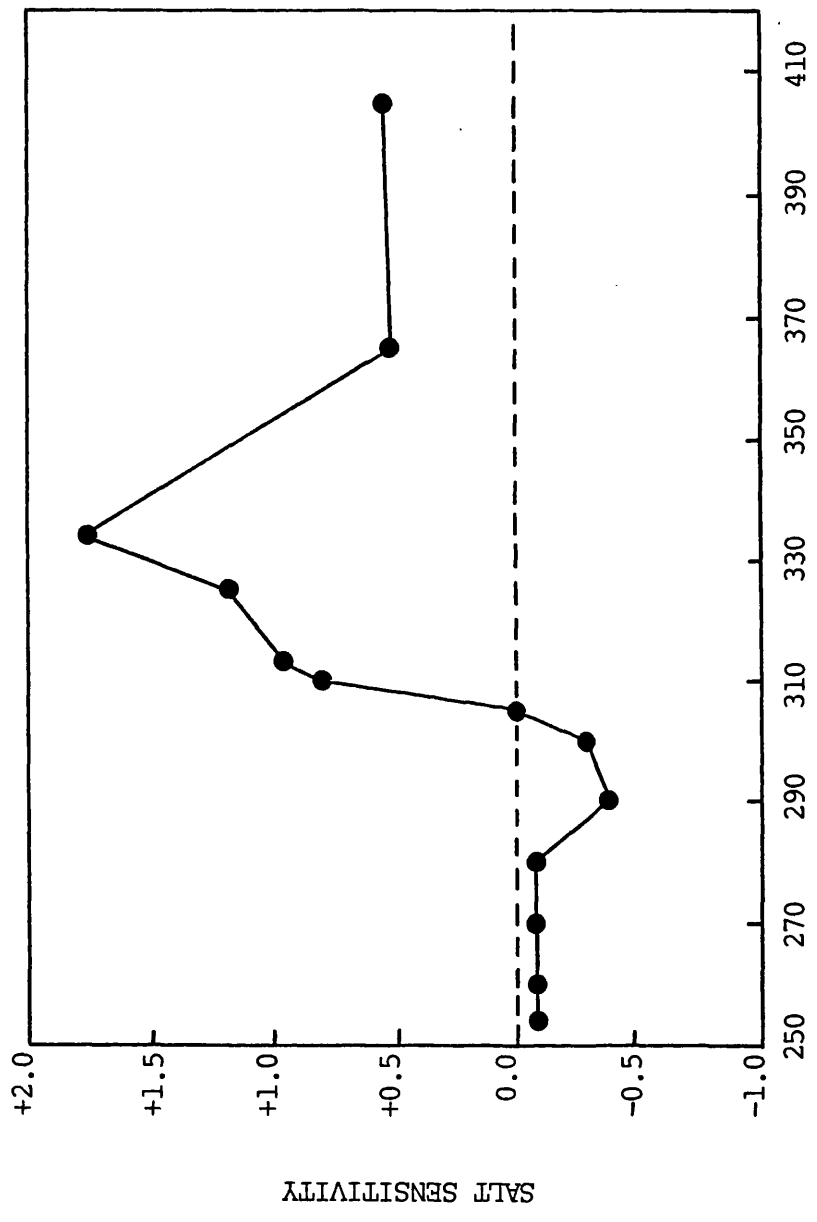

Figure 45

An action spectrum for salt sensitivity of stationary phase cells of E. coli K-12 (SR 385). Salt sensitivity is expressed as $^{1}/_{F10}$ High Salt - $^{1}/_{F10}$ Low Salt plates for each wavelength studied.

A summary of the knowledge concerning the location of the 'break' in slope in near-UV action spectra for inactivation and mutation is shown, for a variety of organisms, in Table 8. It would appear that a radical change in the mechanism of inactivation and mutation always occurs at a wavelength of about 325nm. A shoulder around 330nm has also been reported for an action spectrum for the production of single-strand breaks in DNA in B. subtilis (Peak and Peak, 1982). The increase in lethality at wavelengths about 320nm is strongly oxygen-dependent (Webb and Brown, 1979a), and consequently has been attributed to an involvement of photodynamic processes mediated by endogenous sensitizers, the identity of which are largely unknown at present (Webb, 1977). The action spectrum in Fig. 45 shows a 'break' at a wavelength of about 310nm, compared to 320-330nm reported by other workers (see Table 8). This is associated with the sensitivity of cells as reported in this chapter, which is about an order of magnitude greater in the near-UV radiation region. For example, at 365nm, Fig. 42a shows that a fluence of 4.7×10^5 Jm^{-2} is required to reduce the surviving fraction to the 10% survival level on nutrient agar, whereas Webb and Brown (1976), using E. coli B/r, found that about 6×10^6 Jm^{-2} were needed to cause an equal amount of lethality, and Webb et al. (1976), using E. coli AB 1157, found the required fluence to be about 2.2×10^6 Jm^{-2}.

It is also noticeable that an action spectrum for growth delay induced by near-UV radiation shows a peak around 334nm (Kubitschek and Peak, 1980) and may be considered similar to the action spectrum for inorganic salt sensitivity (Fig. 45). The main chromophore for the induction of near-UV radiation-induced growth delay has been identified as 4 - thiouridine (^{4}Srd), (Ramabhadran and Jagger, 1975; Thomas and

Table 8. Wavelength where a 'break' occurs in the slope of near-UV radiation action spectra for inactivation and mutation.

Biological end point.	Organism.	'Break' wavelength (nm).	Reference.
a) Lethality	*E. coli* WP2s	320	Webb and Brown (1979b)
	E. coli B/r & B/r (Hcr)	325	Webb and Brown (1976)
	S. typhimurium, rec	330	Mackay *et al.* (1976)
	Coliphage T7	315	Peak and Peak (1978)
	Coliphage T7	330	Ananthaswamy *et al.* (1979)
	B. subtilis spores	334	Tyrrell (1978a)
	normal human skin fibroblasts (1BR)	313	Keyse *et al.* (1983)
b) Inactivation, transforming DNA	*B. subtilis*	320	Peak *et al.* (1973)
	H. influenzae	330	Cabrera-Juárez *et al.* (1976)
c) Mutation	*E. coli*	334	Tyrrell (1980)

Favre, 1975). In addition, Tsai and Jagger (1981) have shown that $^{4}Srd^{-}$ mutants are about twice as resistant to 334nm as DNA repair-proficient cells, thus suggesting that 4-thiouridine may be a chromophore for near-UV radiation-induced cell lethality as well as for growth delay. Peak et al. (1983a) have correlated the increase in resistance of $^{4}Srd^{-}$ mutants with a slower induction of single-strand breaks. However, it would appear that ^{4}Srd is not the principal chromophore for near-UV radiation-induced salt sensitivity, as $^{4}Srd^{-}$ mutants show the same degree of near-UV radiation-induced salt sensitivity as $^{4}Srd^{+}$ strains (Moss and Smith, 1981).

One possibility as to the cause of the radiation-induced salt sensitivity effects, as discussed in Chapter 1, is the radiation-induced destruction of catalase, an enzyme responsible for the catalytic decomposition of intracellular hydrogen peroxide. An action spectrum for the in vitro photoinactivation of catalase by near-UV radiation of 350nm and extending into the visible radiation spectrum, has been reported by Cheng et al. (1981). They showed that maximum photo-inactivation occurs at a wavelength of 405nm with a greatly reduced effect at 350nm (about half the degree of inactivation). The action spectrum for salt sensitivity induced in E. coli SR 385, described in Fig. 45, shows that there is a slightly greater degree of salt sensitivity to inorganic salt shown at 405nm compared to that shown at 365nm. However, as the action spectrum described in Fig. 45 is based upon the empirical use of $^{1}/F_{10}$ values, it is not appropriate at present to draw any conclusions regarding the role of catalase destruction in producing near-UV radiation-induced sensitivity to inorganic salt.

CHAPTER 3

LEAKAGE STUDIES AFTER NEAR-UV IRRADIATION OF *E. COLI* K-12 SR 385 : DIRECT EVIDENCE FOR DAMAGE TO MEMBRANES.

Results presented in Chapters 1 and 2 have shown that, for near-UV (but not far-UV) irradiated cells of E. coli SR 385, a sensitivity to inorganic salts is induced, a peak effect occurring at a wavelength of 334nm. From studies involving the effects of mild-heat (52°C) on cells, the salt sensitivity effects have been presumed to be associated with a damaging effect on cell membranes. Therefore, the evidence for membrane damage being a factor in near-UV radiation-induced lethal effects is, thus far, only indirect. The purpose of the experiments presented in this chapter was to extend the investigation of near-UV radiation effects leading to a sensitivity to inorganic salts, and thus possible effects on the cell membrane, and in particular, provide a more direct means of assessing this damage.

Studies with mild-heat have shown that a leakage of 260nm absorbing material, which is probably amino acids or nucleotides, occurs from treated cells, and have therefore provided some direct evidence of a disruption of the permeability barrier being involved after mild-heat treatment (Iandolo and Ordal, 1966; Russell and Harries, 1967; Allwood and Russell, 1967). Therefore, experiments were performed to test whether UV irradiation of E. coli K-12 SR 385 cells caused an increase in the leakage of 260nm absorbing substances. In addition, experiments were carried out that were designed to investigate the leakage of radioactively-labelled compounds from cells after near- (both broad-band and monochromatic wavelength sources) and far-UV irradiation.

Additional methodology.

(a) Media.

(i) K^+ free M9 salts solution

This was M9 salts solution (see general methodology section)

but with the K^+ content replaced mole for mole with Na^+ as NaH_2PO_4. Therefore M9 A concentrate was prepared as before and M9 B concentrate was prepared with NaH_2PO_4 at 49.2g/l replacing KH_2PO_4 at 37.5g/l. The two concentrates were then sterilized, mixed with distilled water in the same proportions and sterilized, as described previously. These media were used for all dilutions involving cells labelled with rubidium-86.

(ii) KCl solution.

A 0.4 M solution was prepared by dissolving 2.982g KCl (B.D.H. Ltd.) in 90ml distilled water and making up to 100ml with distilled water before sterilizing in an autoclave at 121°C for 15 minutes.

(iii) $CaCl_2$ solution.

This was prepared as a 10^{-2} M solution by dissolving 111mg $CaCl_2$ fused, granular (B.D.H. Ltd) in 90ml distilled water and making up to 100ml with distilled water, before sterilizing in an autoclave at 121°C for 15 minutes.

(b) Radioactive labelling of strain SR 385.

Where indicated, cells were labelled with either [methyl-^{3}H] thymidine or rubidium-86 (^{86}RbCl). In both cases, primary cultures were grown to stationary phase in 250ml flasks containing 100ml of minimal growth medium at 37°C in a shaking water bath. Then, a 0.1ml or 0.05ml sample of the stationary phase primary culture was inoculated into 9.90ml of minimal growth medium for labelling with [methyl-^{3}H] thymidine, or 4.95ml of minimal growth medium for labelling

with $^{86}RbCl$, respectively. The compositions of the minimal growth media used for labelling with [methyl-^{3}H] thymidine and $^{86}RbCl$ are shown in Table 9. The cells, contained in 50ml conical flasks, were then grown for 24 hours (to stationary phase) at 37°C in a shaking water bath.

As described in Table 9, 0.37 MBq (10μCi)ml^{-1} of [methyl-^{3}H] thymidine was present in the minimal growth medium for the labelling of cells with tritiated thymidine. This concentration was obtained by adding 0.1ml of a sterile aqueous solution of [methyl-^{3}H] thymidine of radioactive concentration 37.0MBq ml^{-1} (1.0mCi.ml^{-1}) purchased from Amersham International plc code TRA 310, specific activity 74 GBq $mmol^{-1}$ (2.0Ci$mmol^{-1}$). A value of 0.37 MBq ml^{-1} (10μCiml^{-1}) was chosen by comparison with published data involving the labelling of E. coli cells in logarithmic phase up to a concentration of $1x10^{8}$ CFU/ml, with tritiated thymidine. For example, Setlow and Carrier (1964), for the labelling of various E. coli B strains, used 2μgml^{-1} of [methyl-^{3}H] thymidine of activity 6.7Ci.$mmol^{-1}$, that is a concentration of 0.5μCi.ml^{-1} ($1.85x10^{4}$ Bq ml^{-1}). Therefore, as labelling of cells into the stationary phase of growth, that is approximately $2x10^{9}$ CFU/ml, was required for this study, a concentration of about twenty times, i.e. 0.37MBq ml^{-1} (10μCiml^{-1}) was employed.

The concentration and procedure adopted for the labelling of cells with $^{86}RbCl$ was taken from previously described work involving the labelling of E. coli cells with $^{86}Rb^{+}$ (Oldmixon and Braun, 1978). As described in Table 9, a 0.05 ml sample of the stationary phase primary culture was inoculated into 4.95 ml of modified low K^{+} growth medium (containing 4mM K^{+}) plus 0.111 MBq (3μCi) ml^{-1} $^{86}RbCl$. The $^{86}RbCl$ was obtained as a sterile aqueous solution of radioactive

Table 9 Composition of growth media for labelling of strain SR 385 with [methyl-^{3}H] thymidine (A) or ^{86}RbCl (B).

Ingredient	[methyl-^{3}H] thymidine (ml) (A).	^{86}RbCl (ml) (B).
glucose 40%	0.1	0.05
thymine 1mg/ml	0.1	0.05
thiamine 0.1mg/ml	0.05	0.025
$CaCl_2$ 10^{-2} M	-	0.05
KCl 0.4 M	-	0.05
[methyl-^{3}H] thymidine TRA 310 = 0.37 MBq (10μCi) ml^{-1}	0.1	-
^{86}RbCl 0.111MBq (3μCi) ml^{-1}	-	0.015
M9 salts	9.55	-
K^+ free M9 salts	-	4.71

concentration 37.0 MBq.ml^{-1} (1mCi.ml^{-1}) from Amersham International plc, specific activity 37-296 MBq.mg^{-1} rubidium (1-8 mCi.mg^{-1}). As ^{86}RbCl has a radioactivity half-life of 18.66 days, the volume of ^{86}RbCl added was adjusted by calculating the amount of decay from the date when the activity was determined, so that approximately 0.111 MBq.ml^{-1} (3μCiml^{-1}) was always added. A corresponding adjustment to the volume of K^+ free M9 salts solution contained in the minimal growth medium was made so that the total volume was always 5.0ml. No such adjustment for decay of radioactivity was necessary for the tritiated thymidine, which only decomposes at a rate of 1-3% per month. However, tritiated thymidine stored for longer than 3 months was discarded.

(c) Treatments of cells.

For all treatments, that is mild-heat, near-UV and far-UV irradiation, the secondary, stationary phase cultures were prepared by three centrifugations using a MSE minor centrifuge (MSE Scientific Instruments). The centrifuge was operated for 30 minutes at 1500xg, and after each centrifugation the cells were resuspended in M9 salts solution or, for the $^{86}Rb^+$ labelled cells, in K^+ free M9 salts solution, to produce a concentration of approximately 10^9CFU/ml. This suspension was then diluted in M9 or K^+ free M9 salts solution.to give the final appropriate concentration required, as indicated for each experiment described.

(i) Mild-heat.

18ml volumes of M9 or K^+ free M9 salts solution in 24mm diameter test-tubes were pre-heated to 52°C in a water bath and, at time zero, 2ml of cell suspension was added to give the required

concentration of cells, as indicated. Stirring was achieved by means of a magnetic stirrer. At the time intervals specified, samples were removed for the assessment of viability on either low or high salt minimal media as described in the general methodology section. Samples were also removed for the assessment of membrane damage by one of the two methods described below.

(ii) UV irradiation.

The full experimental details for both the broad-band and monochromatic wavelength irradiation of cells has been described previously in the general methodology section.

For each treatment, untreated control samples were stirred at the same rate and, for the UV-irradiation determinations, kept at the same temperature, and assessments made as for the test samples.

(d) Assessments of membrane damage.

(i) Leakage of 260nm absorbing substances.

Mild-heat or UV-irradiated treated samples were centrifuged at 1500xg for 30 minutes in a MSE minor centrifuge. The supernatant fluids were then carefully removed using a Pasteur pipette and, the absorption was measured at 260nm and over the range 220 to 400nm, (to check that the absorption peak was at 260nm), using a SP1800 ultraviolet spectrophotometer (Pye-Unicam) in conjunction with a linear recorder (Unicam AR 25), using a blank consisting of the suspending medium without bacteria. The absorption of control samples was taken for each treatment determination.

(ii) Leakage of radioactive isotopes.

The method chosen for the measurement of the leakage of

radioactive material from cells was liquid scintillation counting, a method which, since its introduction for biological measurements by Hayes and Gould (1952), has become extensively used. Briefly, liquid scintillation counting involves placing the radioactive sample in an appropriate medium which converts radioactive energy into a pulse of light energy. This pulse of light energy is detected by means of a synchronized photocathode and is converted to an electrical pulse by a photomultiplier. During liquid scintillation counting the following energy steps occur between the radioactive sample (Rs) and the constituents of the scintillation cocktail:

$$\text{Rs} \xrightarrow{1} \text{Solvent} \xrightarrow{2} \text{solute} \xrightarrow{3} \text{photocathode.}$$

At each of the three energy transfer steps there is a probability that an incomplete energy transfer will occur due to the nature of the scintillation cocktail. Interference may arise from photon quenching, chemical quenching and colour quenching. Therefore, the quantification of any radioactive sample depends upon the extent of this interference, termed 'quenching', and the ability of the photocathode to detect the light pulses. The resultant quantification is expressed in counts per minute (cpm) which is a characteristic of a particular liquid scintillation counter and scintillation cocktail. Identical quantities of radioactive material may produce different cpms in the same liquid scintillation counter and scintillation cocktail due to the presence of quenching agents. To convert cpm to an absolute quantity of radioactivity, a quench curve must be constructed so that the efficiency of the counting process may be estimated, hence taking into account interferences in energy transfer. From the efficiency measurement the absolute value of disintegrations per minute (dpm) may be determined. Therefore, dpm = cpm x efficiency.

Four methods exist for quench curve construction, those being

internal standard, external standard, channels ratio and external standard channels ratio. The liquid scintillation counter used for these studies was a 1215 Rackbeta, LKB wallac (Turku, Finland) and the scintillant was a xylene-based commercial product, aqua luma (Lumac Systems A.G., Basle, Switzerland). Quench curves had previously been constructed for both the tritium and rubidium systems by the external standard channels ratio method, due to the ease with which they may be constructed by this method on the LKB 1215 counter. Briefly, this involved adding 4ml of aqua luma to a series of 7 plastic mini-vials each containing a capsule of known radioactivity. To each sample, 0.2ml of distilled water was added to simulate the emulsion system found in the experimental conditions. Increasing amounts from 0 to 40μl of carbon tetrachloride were then added to provide quenching. The samples were then loaded into the counter, which had been programmed to count the samples and automatically construct a quench curve. The resultant quench curves used for ^{3}H and ^{86}Rb are included in Appendices A5 and A6 respectively. These curves were then stored in the counter's memory so that dpms for all subsequent samples were calculated automatically. Despite the ease of construction of quench curves by the external standard channels ratio method, an important shortcoming was borne in mind.

The determination of the external standard channels ratio is critically dependent on the geometry of the scintillation vial, particularly its thickness. Moreover, in this study polyethylene vials were used which tended to absorb the xylene in the scintillant so over the course of time the effective volume of scintillant changed, so producing a continuous drift in the external standard ratio. In order to minimize this effect, upon adding scintillant, samples were immediately

placed at 4°C in the counting chamber before counting was begun.

Measurement of leakage.

Both mild-heat and UV-irradiated treated samples were filtered via 0.2 μm membrane filters (Millipore Corp.) contained in swinnex holders, and 0.25ml of the filtrate added to 4.75ml aqua luma scintillant in plastic scintillation vials. The amount of radioactive isotope in the filtrate was then determined using the 1215 Rackbeta liquid scintillation counter. The counter is able to count beta emissions and some gamma emissions over the energy range of 1keV to 2.8 MeV. From the specifications given for the Rackbeta 1215 counter, counting window settings of 008-110 and 110-212 were used for [methyl-^{3}H] thymidine and $^{86}Rb^{+}$ respectively. Counting of samples was for either 10 minutes or 10,000 counts, depending on which was reached first. A radioactive count of 0.25ml of the untreated bacterial cell suspension was also taken at the beginning of each experiment, to determine the total amount of radioactive label present. For each treated sample, a control without radiation or mild-heat treatment was also taken and assessed for radioactive isotope leakage in exactly the same manner.

RESULTS.

The initial method which was used for assessing whether any damage to the cell membrane is produced by UV radiation was to attempt to detect the leakage of soluble pool components from irradiated cells. A leakage of soluble pool components after mild-heat treatment has been detected by an increase in 260nm absorption (Iandolo and Ordal, 1966). Figure 46a shows the release of 260nm absorbing substances from E. coli K-12 SR 385 after near- (broad-band Black-Light Blue source) and far-(254nm) UV radiation and mild-heat (52°C). The mild-

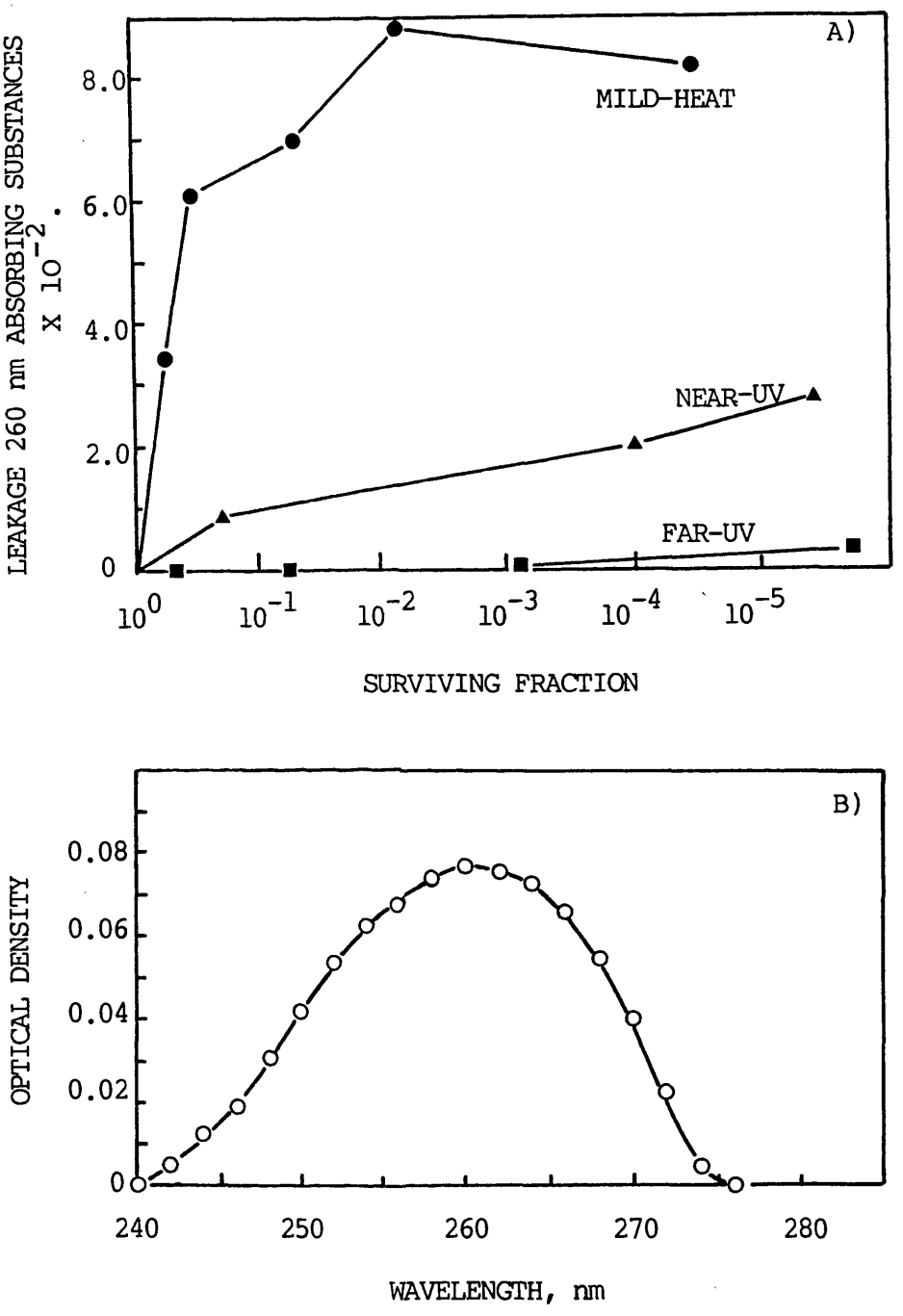

Figure 46 a) The effect of far-UV radiation (254 nm, initial cell concentration $5x10^8$ CFU/ml), (■): broad-band near-UV radiation, (initial cell concentration $5x10^8$ CFU/ml), (▲); and mild-heat (52°C, initial cell concentration $1x10^8$ CFU/ml), (●), on the release of 260 nm absorbing substances from E. coli K-12 (SR 385). Leakage is expressed as the absorbance at 260 nm for the treated samples minus that for a corresponding untreated sample and is expressed in relation to surviving fractions assessed on minimal medium low salt plates.

b) Absorption scan of the supernatant from a suspension of E. coli K-12 (SR 385), of initial concentration $1x10^9$ CFU/ml after 4 hours broad-band near-UV irradiation (surviving fraction approx. 10^{-5}).

heat experimental data is included as a control as it is known to cause membrane damage to cells, and the release of 260nm absorbing substances after such treatment has been reported (Russell and Harries, 1967). Leakage is expressed in terms of surviving fractions, where viability was assessed on 'low salt' minimal medium, i.e. minimal growth medium with one-tenth diluted inorganic salt content. The figure shows that, in agreement with published mild-heat data, a release of 260nm absorbing substances is observed after mild-heat treatment of E. coli cells. In addition, the results indicate a release of 260nm absorbing substances after broad-band near-UV radiation but not after far-UV radiation. In each case where 260nm absorbing substances were detected, absorption was measured over a range of wavelengths to ensure that a peak of absorption occurred at 260nm. A typical absorption scan of the supernatant from a suspension of E. coli SR 385, of initial concentration $1x10^9$CFU/ml, after 4 hours of Black-Light Blue near-UV irradiation is shown in Fig. 46b. This shows a peak absorption at 260nm.

Although Figure 46a shows that near-UV (but not far-UV) radiation causes a release of cell components that absorb at 260nm, this effect is difficult to quantify as high concentrationsof cells are required, and 'shielding' effects may interfere with the calculation of the fluence received by each cell. In addition, even when using high cell concentrations, the amount of 260nm absorption observed is very small (0-0.03 for the near-UV radiation data) and is near the limits at which accurate determinations of absorption can be made.

Therefore, it was decided to assess thispossible membrane damaging effect of near-UV radiation by means of a more sensitive method. Cells of E. coli SR 385 were radioactively labelled with [methyl-^{3}H]

thymidine and at various near-UV radiation time intervals, irradiated and unirradiated samples were filtered and the filtrates tested for a leakage of labelled material from the cells. Figure 47 shows the leakage of [methyl-^{3}H] thymidine, expressed in dpm, from E. coli SR 385 at an initial cell concentration of $5x10^8$CFU/ml, either irradiated with broad-band near-UV radiation or from a corresponding unirradiated sample. The figure shows that an increase in the leakage of [methyl-^{3}H] thymidine occurs with increasing time for both the irradiated and unirradiated samples. However, it is clearly apparent that the increase in leakage with time is much greater for the near-UV irradiated cell samples than for the unirradiated cell samples. The figure shows the importance of determining the leakage from control samples for each test sample in subsequent experiments, due to the gradual leakage of radioisotope (presumably by passive diffusion) from the untreated samples over several hours.

As with the 260 nm absorption studies, experiments were then performed to investigate the leakage of [methyl-^{3}H] thymidine from mild-heat and near- and far-UV irradiated cells, and to relate any observed leakage in terms of surviving fractions. Figure 48 shows the results of such experiments with leakage expressed as the ratio of decompositions per minute (dpm) for the treated samples compared to its corresponding control, untreated sample, thus taking into account the gradual leakage of radioisotope from untreated samples, as shown in Figure 47. Again the mild-heat data is included as a control for a treatment known to cause damage to cell membranes, and survival was assessed on 'low salt' minimal medium.

Figure 48 shows that a leakage of [methyl-^{3}H] thymidine from cells is observed after mild-heat treatment, and after near-UV irradiation, while there is little detectable leakage after far-UV irradiation,

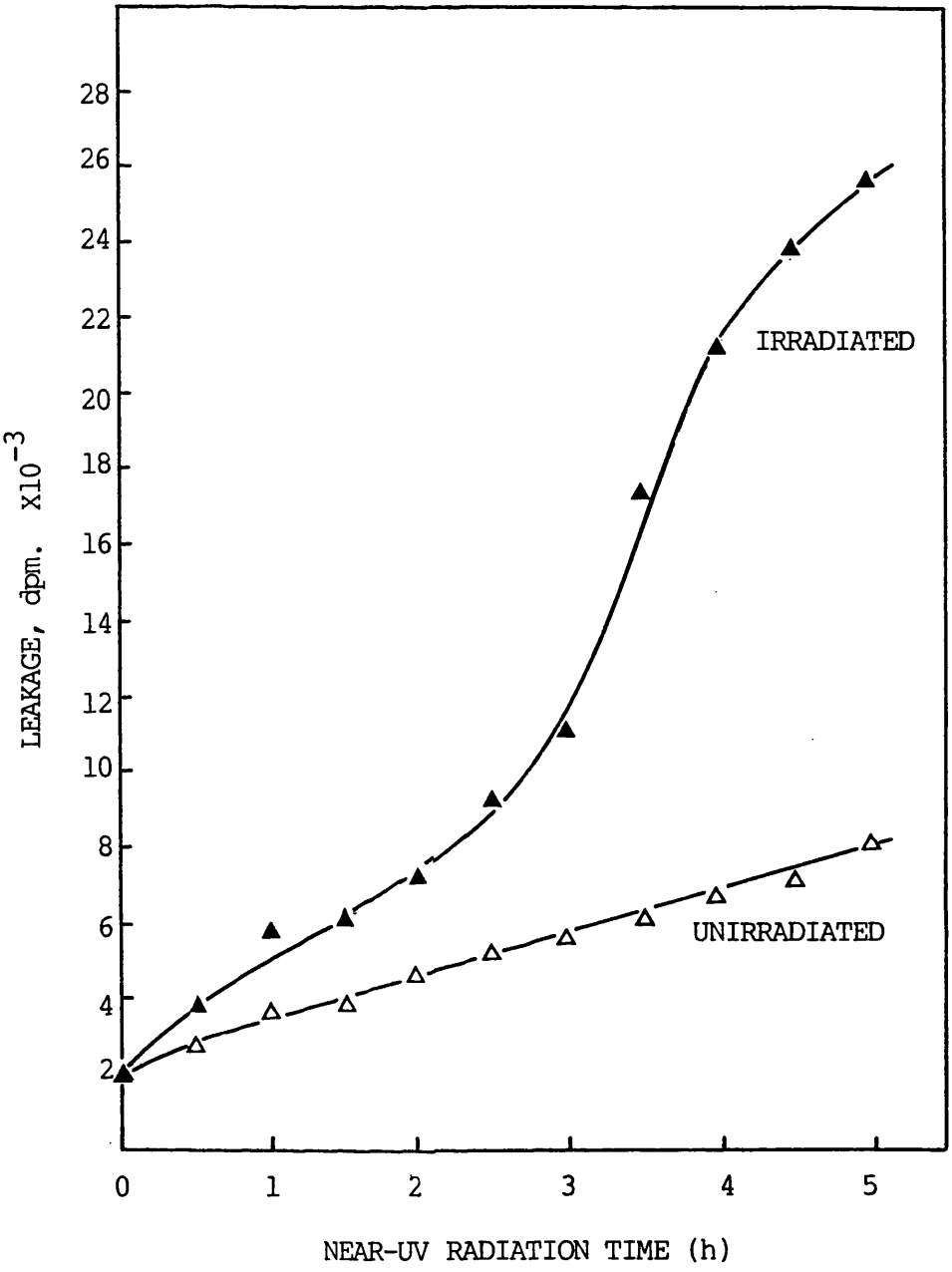

Figure 47

The leakage of [methyl-^{3}H] thymidine expressed in dpm, from E. coli K-12 (SR 385), initial cell concentration 5x10^{8}CFU/ml, either irradiated with broad-band near-UV radiation (▲) or unirradiated corresponding control sample (△).

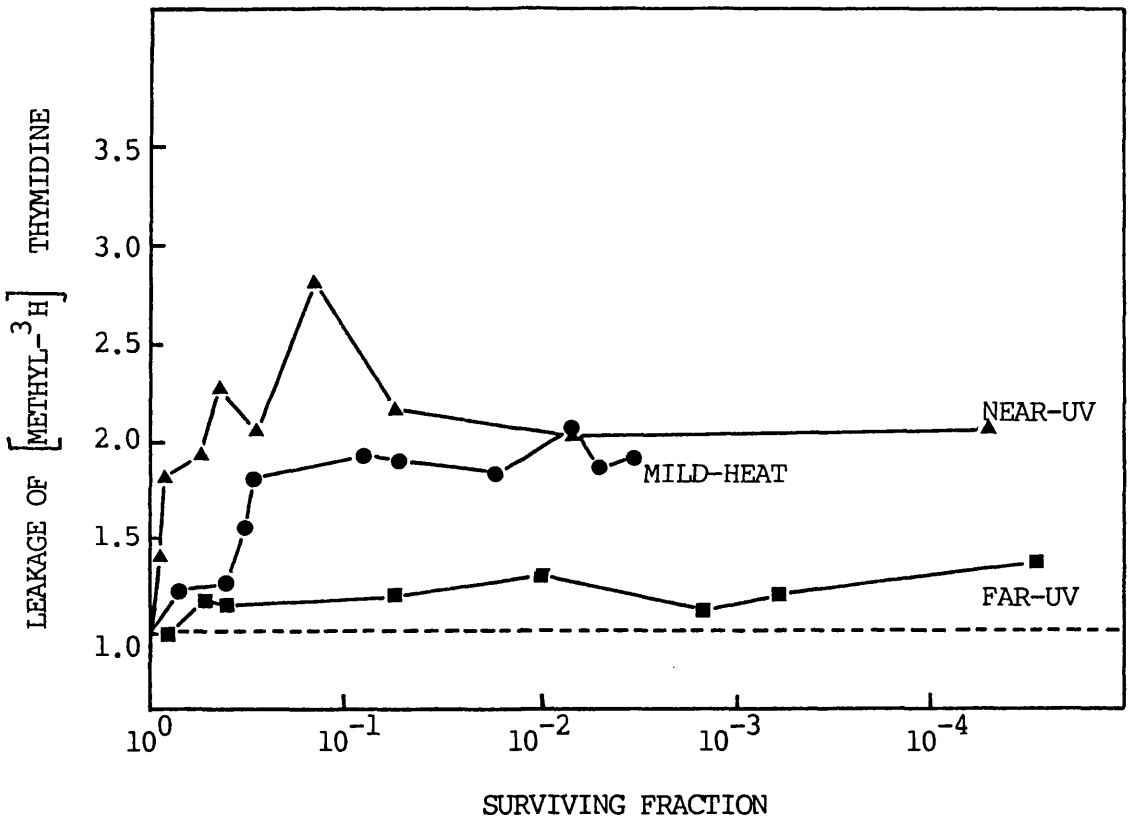

Figure 48

The effect of far-UV radiation (254 nm; initial cell concentration $4x10^8$ CFU/ml), (■); near-UV radiation (broad-band; initial cell concentration $5x10^8$ CFU/ml), (▲); and mild-heat (52°C; initial cell concentration $1x10^8$ CFU/ml), (●) on the leakage of [methyl-^{3}H] thymidine from E. coli K-12 (SR 385). Leakage is expressed as the ratio of dpm for the treated samples compared to a corresponding control, untreated sample. Survival was determined using minimal medium 'low salt' plates.

even at fluences causing 99.9% cell death. However, while a clear indication of near-UV radiation-induced damage to the cell's permeability barrier is shown by the results in Figs. 47 and 48, for a number of reasons another assay for membrane damage was developed in order to determine eventually the wavelength dependence of this damage, and so produce an action spectrum. Firstly, as with the 260nm absorption studies, for the UV-irradiation determinations, high concentrations of cells (about $5x10^8$CFU/ml) were necessary in order to achieve a workable leakage of [methyl-^{3}H] thymidine. By using such high concentrations of cells, 'shielding' effects make fluence calculations difficult, and, in addition, this may explain the difficulty realised in achieving good reproducibility with this method (although the general observation of leakage after near-UV but not far-UV irradiation was always apparent).

Secondly, by using [methyl-^{3}H] thymidine as the radioactive label, a proportion of the label may be incorporated into cellular DNA, and as far-UV and, to some extent, near-UV radiation are known to induce damage to cellular DNA, including strand breaks and pyrimidine dimer formation (see introduction), this makes the interpretation of the importance of membrane damage in relation to cell lethality, difficult. Thirdly, [methyl-^{3}H] thymidine is a relatively large molecule, when compared to a simple ion, to pass through any damage induced in the cell membrane, so additional near-UV radiation-induced damage may be present which remains undetectable by this method.

Therefore, the use of $^{86}Rb^+$ as a K^+ analog was employed to extend this investigation of near-UV radiation-induced membrane damage. This use of $^{86}Rb^+$ as a K^+ analog has been described previously in work involving rabbit erythrocytes (Olcerst et al., 1980), rose cells

(Murphy and Wilson, 1982) and E. coli cells (Oldmixon and Braun, 1978). As the procedure adopted from the work of Oldmixon and Braun for the labelling of E. coli with $^{86}Rb^{+}$ involved the use of low K^{+} M9 growth medium (concentration of K^{+} adjusted to 4mM) and potassium has been shown to be important for the growth of bacteria and for the activation of some cell enzymes (Epstein and Davies, 1970), it was felt necessary to perform survival and growth curves to show that the low K^{+} concentration had no effect on the growth of the organism or its survival after near-UV irradiation.

Figure 49 shows the effect of different concentrations of KCl in the minimal growth medium (0, 4, 8 and 16mM) on the growth of E. coli SR 385. The result indicates that no significant effect on the growth of the organism is observed with the different concentrations of K^{+} present, over a 24 hour growth period, i.e. through to the stationary phase of growth. Figure 50 shows the effect of growth in different concentrations of K^{+} (again, 0, 4, 8 and 16mM) on the sensitivity of E. coli SR 385 exposed to broad-band near-UV radiation, with viability assessed on low and high salt minimal media. It is apparent from Fig. 50 that similar survival curves result for irradiated cells grown in the presence of 4, 8 and 16mM K^{+} as, although a degree of salt sensitivity is observed, the respective survival curves on low and high salt plates for all three K^{+}concentrations fall roughly in the same region. For near-UV irradiated cells grown in the absence of K^{+}, an increase in sensitivity compared to the other concentrations of K^{+}, on both low and high salt media, is observed. However, from Figs. 49 and 50 it can be concluded that the presence of only 4mM K^{+} in the minimal growth medium for the labelling of cells with $^{86}Rb^{+}$ does not significantly affect the growth or near-UV radiation-induced survival of E. coli SR 385.

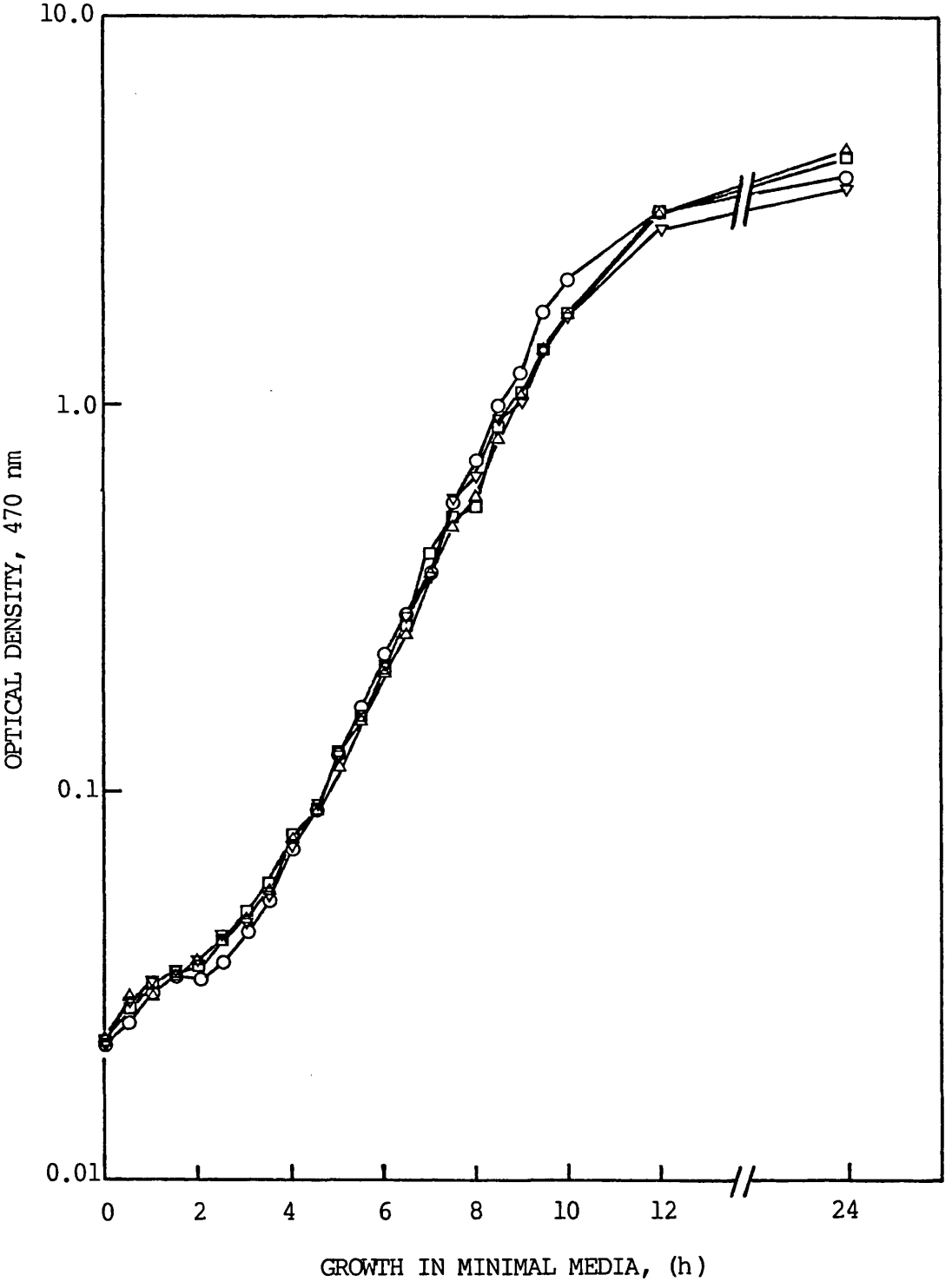

Figure 49

The effect of K^+ concentration on the growth of E. coli K-12 (SR 385) at 37°C in minimal media. KCl was added at 0mM (O), 4mM (□), 8mM (△) and 16mM (▽).

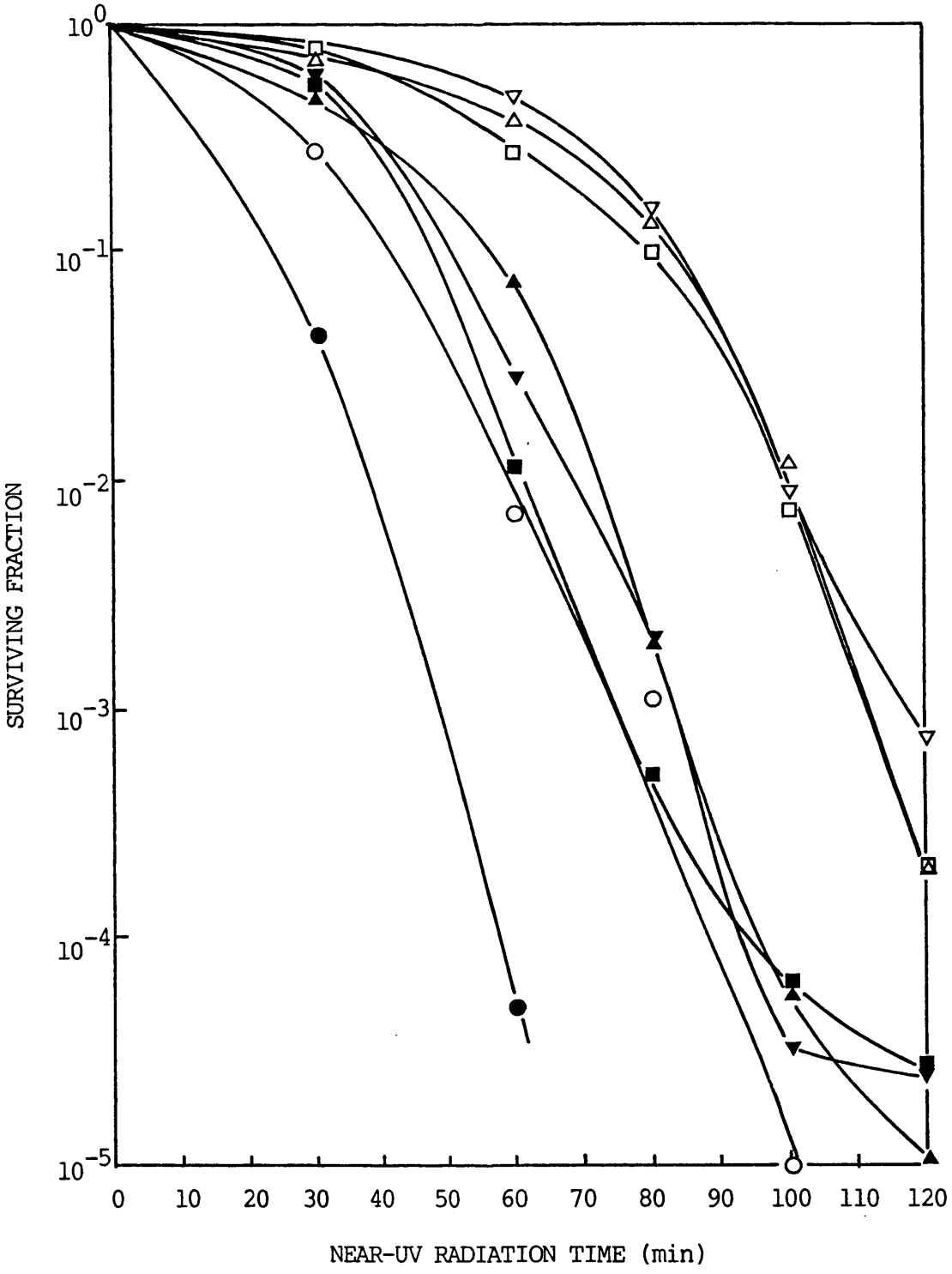

Figure 50

The effect of growth in varying concentrations of K^+ on the sensitivity of E. coli K-12 (SR 385) to broad-band near-UV radiation. KCl was present at 0mM (●,○), 4mM (■,□), 8mM (▲,△) and 16mM (▼,▽) in the minimal growth medium and viability was assessed on either low salt (open symbols) or high salt (closed symbols) minimal media.

Figure 51 shows the release of $^{86}Rb^{+}$, expressed in dpm, from E. coli SR 385, at an initial cell concentration of $1x10^{8}$CFU/ml, either irradiated with far-UV (254nm) radiation or broad-band near-UV radiation. Leakage from corresponding unirradiated samples for both the far and near-UV radiation experiments is included. As with the leakage of [methyl-^{3}H] thymidine data, for both the far and near-UV radiation experiments, there is an increase in leakage of radioisotope observed with increasing time for both the unirradiated and irradiated cell samples. However, there is a striking difference in the relative amounts of leakage observed from test and control samples between the far and near-UV radiation cell samples. Irradiation with far-UV radiation (Fig. 51a) results in little difference in observed leakage between irradiated and unirradiated cell samples, indicating that far-UV radiation does not induce additional leakage of $^{86}Rb^{+}$ over control values. In contrast, irradiation with near-UV radiation (Fig. 51b) results in a large increase in observed leakage from irradiated cell samples with increasing time of radiation, compared to the unirradiated samples, providing further evidence that near-UV radiation induces a disruption of the cell's permeability barrier. As for the [methyl-^{3}H] thymidine data (Fig. 47), Fig. 51 shows the importance of determining leakage from control samples for each test sample in subsequent experiments.

As with the 260nm absorption and [methyl-^{3}H] thymidine leakage studies, leakage of $^{86}Rb^{+}$ from E. coli SR 385 after mild-heat and near-and far-UV radiation treatments was then assessed and related in terms of surviving fractions. Figure 52 shows the results of such experiments, again with leakage expressed as the ratio of dpm for the treated samples compared to its corresponding untreated control sample.

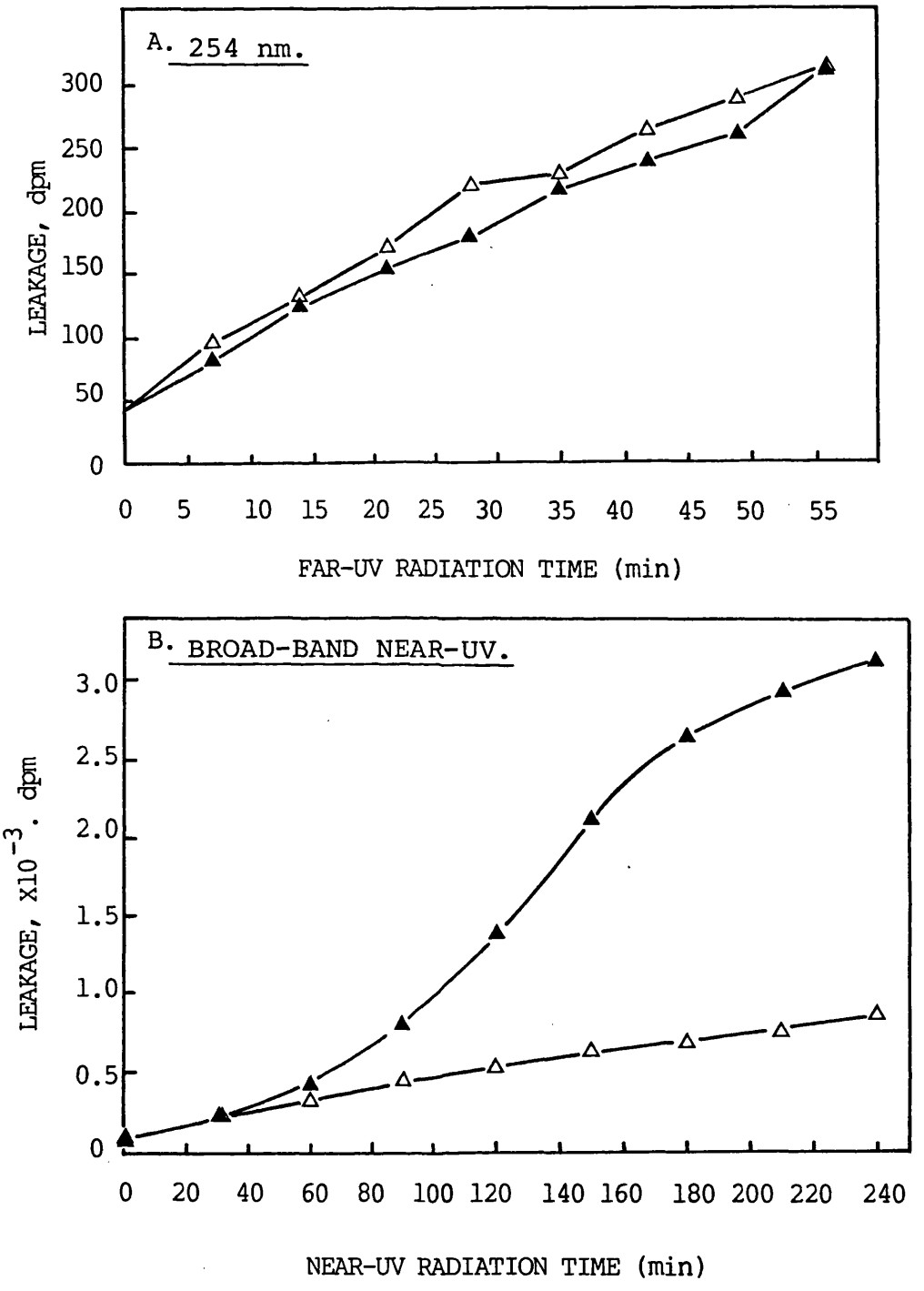

Figure 51

The leakage of $^{86}Rb^{+}$ from E. coli K-12 (SR 385) (initial cell concentration $1x10^{8}$CFU/ml). A) irradiated with 254 nm radiation or B) irradiated with broad-band near-UV radiation; samples either irradiated (▲) or control, unirradiated (△).

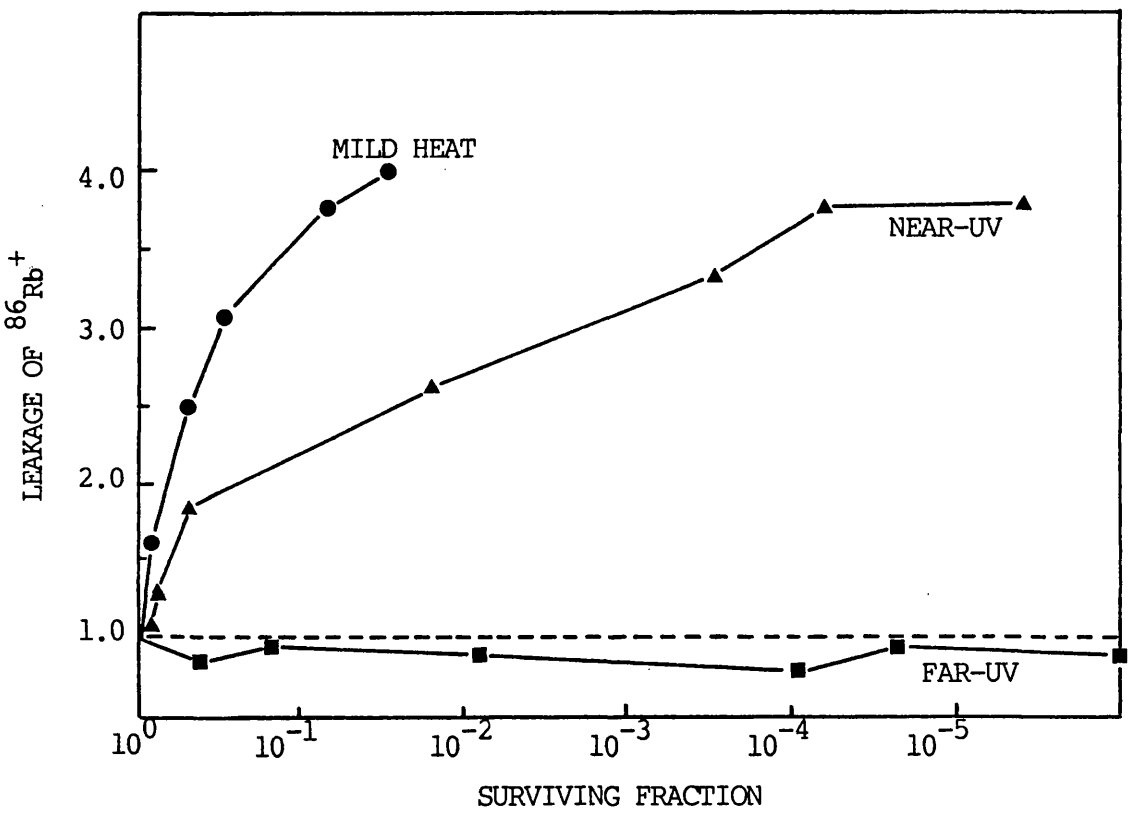

Figure 52

The effect of far-UV radiation (254 nm), (■); near-UV radiation (broad-band), (▲): and mild-heat (52°C), (●) on the leakage of $^{86}Rb^+$ from E. coli K-12 (SR 385) expressed in relation to surviving fractions assessed on low salt minimal medium plates. Leakage is expressed as the ratio of dpm for the treated samples compared to a corresponding control sample. Initial cell concentrations were all $1x10^8$ CFU/ml.

The figure shows that a leakage of $^{86}Rb^{+}$ from cells occurs, as expected, after treatment with mild-heat. In addition, at fluences causing similar cell lethality and using initial cell concentrations of $1x10^{8}$ CFU/ml similar to the mild-heat studies, $^{86}Rb^{+}$ leakage from cells occurs after near-UV irradiation but not after far-UV irradiation.

Using $^{86}Rb^{+}$, leakage could be measured with good reproducibility and, by using a lower cell concentration of $1x10^{8}$CFU/ml compared to the 260nm absorption and [methyl-^{3}H] thymidine studies, accurate fluence determinations could be achieved in order to ascertain the wavelength specificity for leakage from cells. Therefore, in an attempt to relate UV- induced leakage to lethality in E. coli SR 385, fluence-$^{86}Rb^{+}$ leakage curves were determined using monochromatic wavelength UV radiation from 254-405nm.

As the broad-band near-UV radiation studies described previously (Figs. 46-52) involved irradiation at about 28°C and the monochromatic wavelength studies were to be performed at 0°C (in order to compare with the lethality and salt sensitivity action spectra studies described in Chapter 2), it was necessary to investigate the effect of temperature on the leakage of $^{86}Rb^{+}$ from unirradiated control samples. Immediately after the final centrifugation in the preparation of the labelled cell suspension and resuspending in K^{+} free M9 salts solution, leakage of $^{86}Rb^{+}$ was measured at 30 minute intervals for 3 hours. Figure 53 shows the leakage of $^{86}Rb^{+}$ from unirradiated cells of SR 385 held at four different temperatures, 0, 20, 28 and 37°C. The figure shows that an increase in leakage with time is observed at all four temperatures but with differing degrees of effectiveness; 37°C being most effective then 0°C, then 28°C, and 20°C being least effective. From Fig. 53 it is

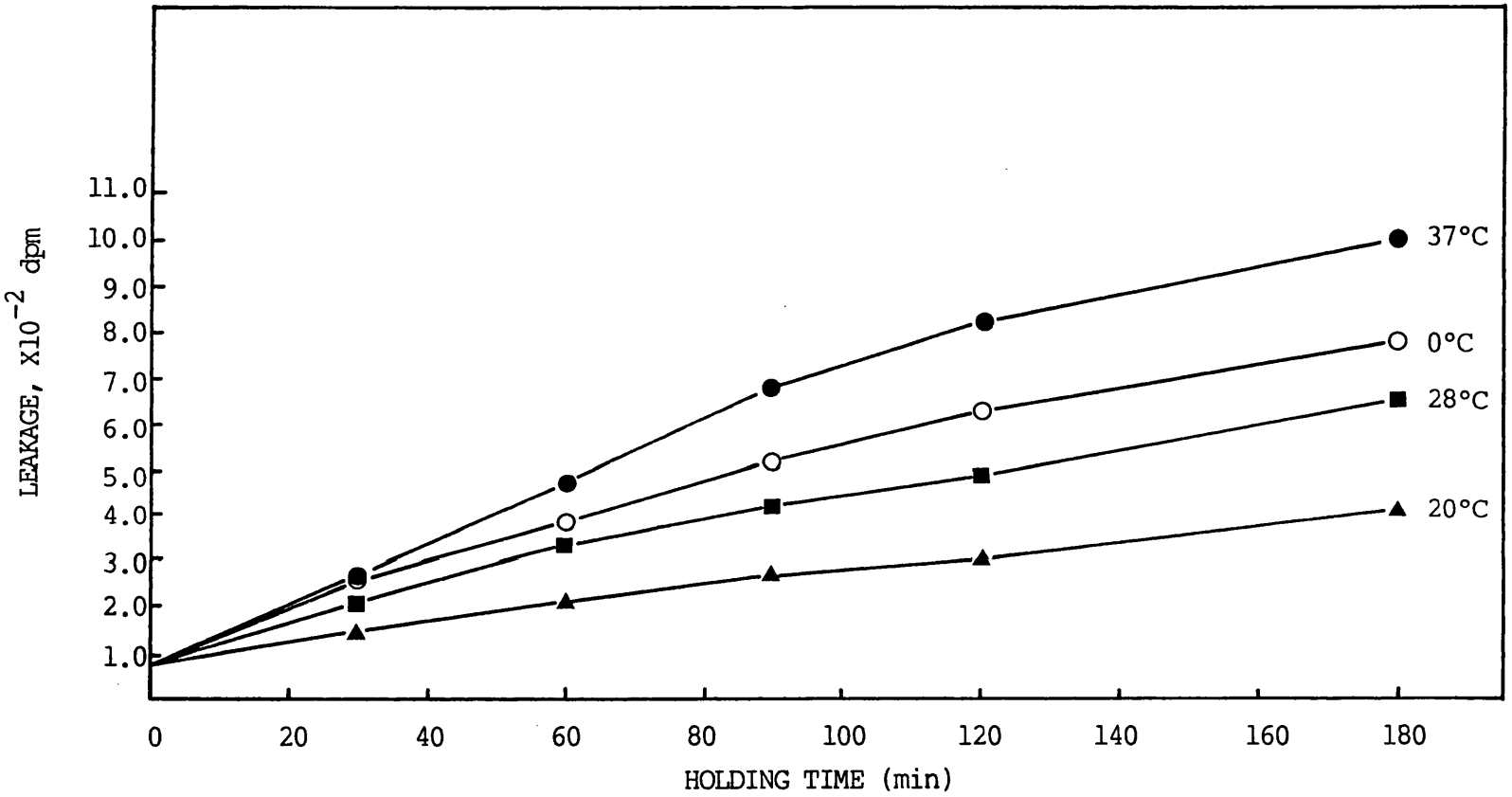

Figure 53

The effect of temperature on the leakage of $^{86}Rb^{+}$ from untreated control samples of E. coli K-12 (S.R 385): 37°C, (●); 28°C, (■); 20°C, (▲); 0°C, (O).

apparent that during the subsequent studies with monochromatic wavelength UV radiations, where irradiation at 0°C is required, the control samples must also be held at 0°C. Therefore, in order to provide ideal control data for the monochromatic UV wavelength fluence - leakage determinations, individual control leakage determinations were performed using the same volume and concentration of cell suspension as that used for the irradiations. In addition, the cells were held at 0°C, and stirring was achieved using a quartz paddle operated at the same speed as that used for the test suspensions.

Figures 54 (a,b,c, and d), 55 (a,b,c and d) and 56 (a,b,c and d) show the fluence- $^{86}Rb^{+}$ leakage profiles at 0°C of E. coli SR 385, at an initial concentration of $1x10^{8}$CFU/ml, obtained with monochromatic UV radiations of 254, 270, 280, 290, 300, 305, 310, 313, 325, 334, 365 and 405nm, respectively. Again, leakage is expressed as the ratio of dpm for the irradiated samples compared to an individual unirradiated control sample. Figs. 54, 55 and 56 show that a leakage of $^{86}Rb^{+}$ from E. coli SR 385 was observed after irradiation, with all the wavelengths tested. Therefore, a leakage of $^{86}Rb^{+}$ may be observed after far-UV irradiation as well as after near-UV irradiation. All the fluence-leakage curves show that an increase in leakage is observed with increasing fluence; all the curves being generally sigmoidal in shape. In addition to the fluence-leakage curves described, similar curves were obtained at 260, 317 and 328nm, but these were only of a preliminary nature.

In order to relate the fluence-leakage curves obtained at each wavelength studied with lethality, survival curves were obtained at each wavelength using $^{86}Rb^{+}$ labelled cells. However, these survival curves are not presented since, as expected, cell sensitivity at each

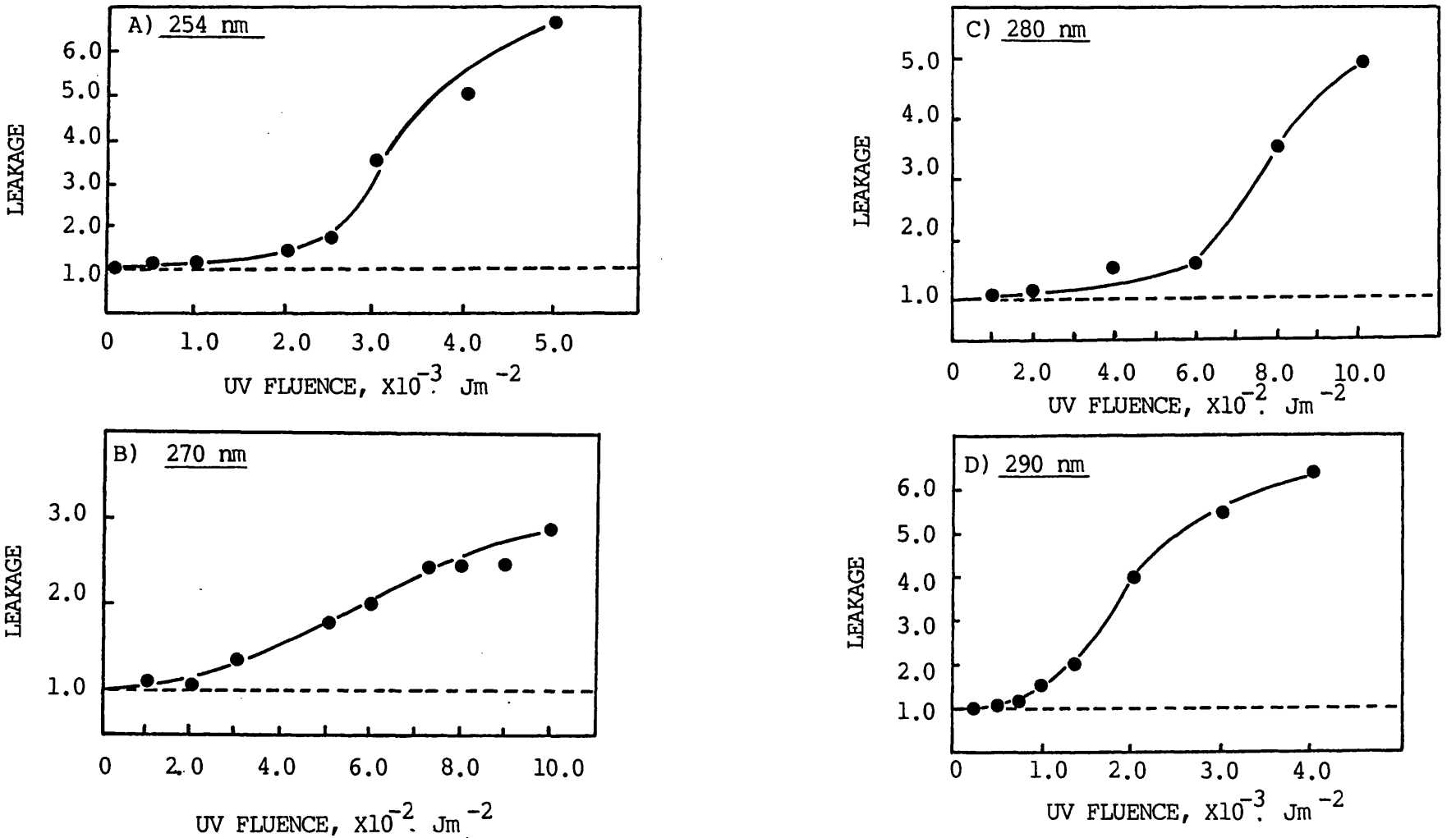

Figure 54

The fluence- $^{86}Rb^{+}$ leakage response at 0°C of E. coli K-12 (SR 385) to A) 254 nm, B) 270 nm, C) 280 nm and D) 290 nm radiations, with leakage expressed as dpm Test/Control.

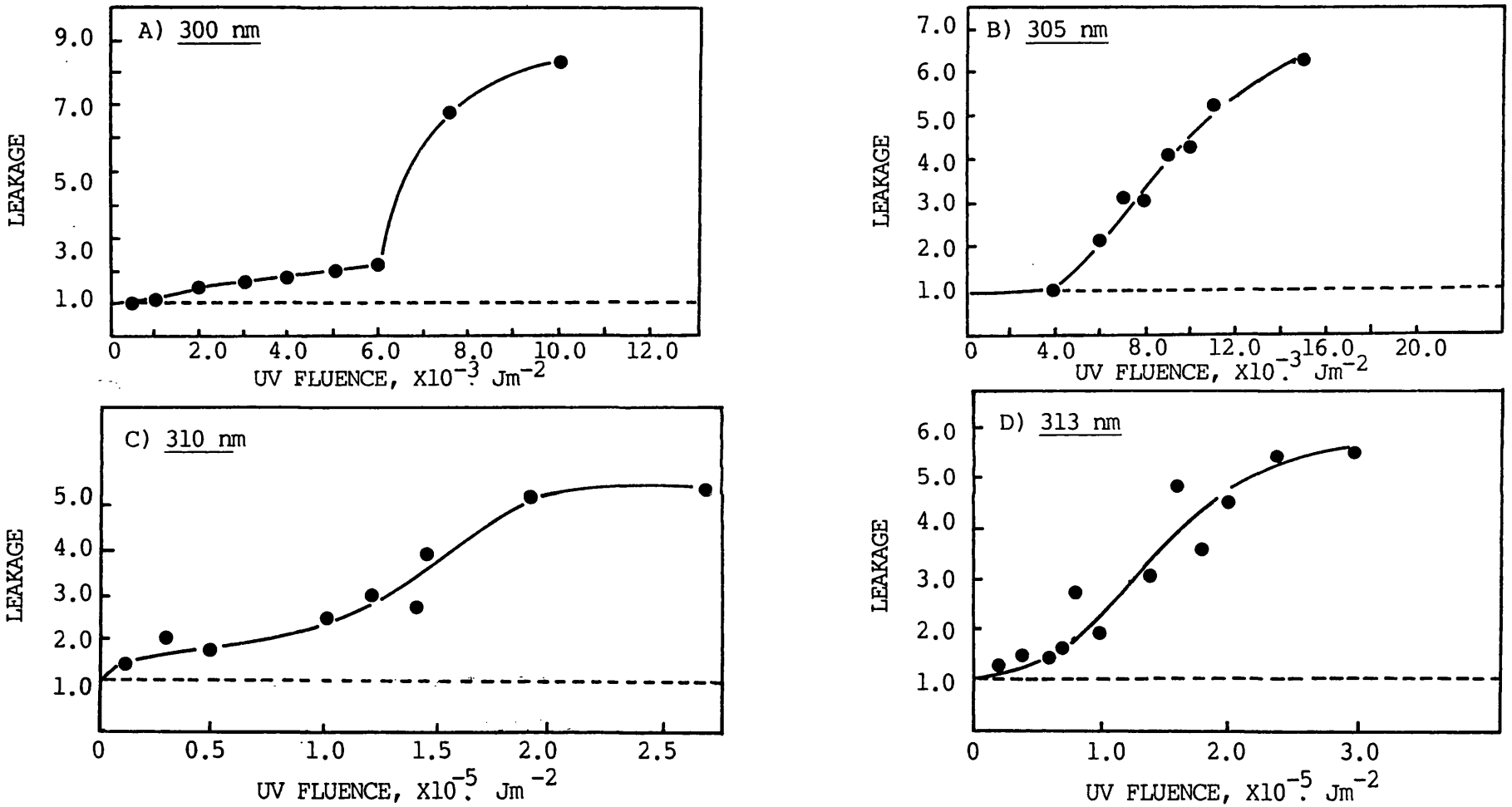

Figure 55

The fluence - $^{86}Rb^{+}$ leakage response at 0°C of E. coli K-12 (SR 385) to A) 300 nm, B) 305 nm, C) 310 nm and D) 313 nm radiations, with leakage expressed as dpm Test/Control.

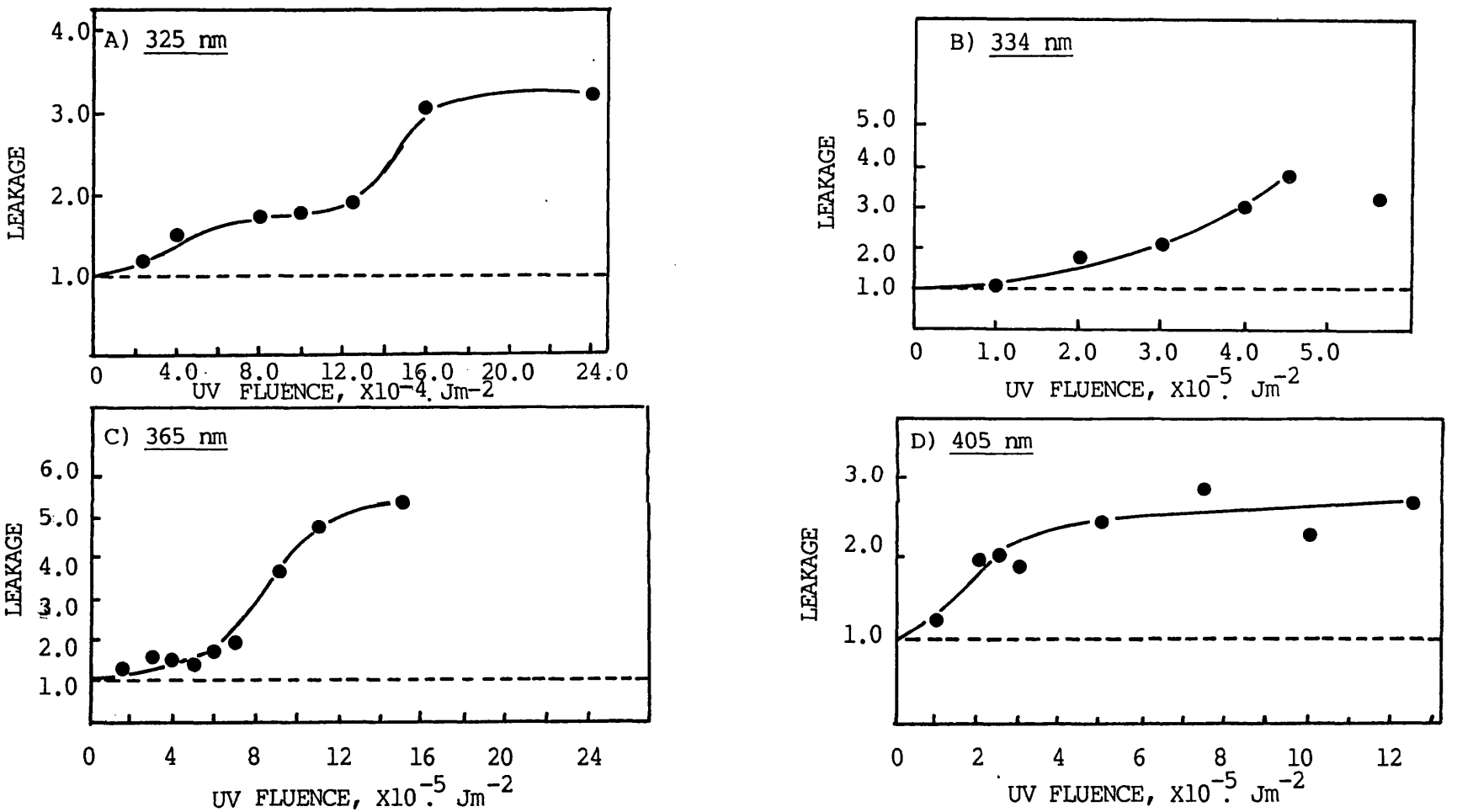

Figure 56

The fluence - $^{86}Rb^{+}$ leakage response at 0°C of E. coli K-12 (SR 385) to A) 325 nm, B) 334 nm, C) 365 nm and D) 405 nm radiations, with leakage expressed as dpm Test/Control.

wavelength was very similar to that observed for unlabelled cells, the survival curves of which are shown in Chapter 2.

As the use of monochromatic radiation of differing wavelengths involved using various fluence rates and quite different times of irradiation to achieve the fluences required to produce a complete 'leakage curve', experiments were performed to attempt to test reciprocity of time and fluence rate. However, as for the salt sensitivity effects observed at different monochromatic wavelengths (as shown in Chapter 2), at the longer wavelengths fluence rates were the maximum that the radiation source could deliver; hence irradiation times could not be reduced due to the practicality of performing such experiments. Therefore, limited reciprocity studies, pertaining to the induction of leakage, were carried out at the shorter UV wavelengths of 254nm and 290nm. Then, if the leakage observed after near-UV irradiation of cells, is a function of fluence rate, i.e. it accumulates over a long period of time and is not a function of wavelength, then one would expect leakage to 254 or 290nm irradiation with long periods of illumination.

Ten-fold and one hundred-fold reductions in fluence rate were achieved using sectored discs, as described in Chapter 2, and cells were irradiated at 254 or 290nm. The results of a series of such experiments are presented in tabular form, in Table 10. The table shows that there was no significant pattern of leakage observed by varying the fluence rate over a one hundred-fold range, thus suggesting that the leakage effects observed during the series of experiments described in this chapter do not appear to be due to a function of the time of irradiation.

Table 10. The effect of fluence rate on the leakage of $^{86}Rb^{+}$ from E. coli SR 385.

Wavelength (nm)	Fluence rate Wm^{-2}	Fluence Jm^{-2}	$^{86}Rb^{+}$ leakage (dpm test : control)
254	$9.483x10^{-1}$	150	1.069
	$9.483x10^{-2}$	150	1.322
	$9.483x10^{-3}$	150	1.111
	$9.483x10^{-1}$	150	1.131
	$9.483x10^{-2}$	150	1.179
	$9.483x10^{-3}$	150	1.230
	$6.954x10^{-1}$	100	1.370
	$6.954x10^{-2}$	100	1.177
	$6.954x10^{-3}$	100	1.132
290	$1.075x10^{0}$	130	1.047
	$1.075x10^{-1}$	130	1.143
	$1.075x10^{-2}$	130	1.160
	$1.075x10^{0}$	220	1.013
	$1.075x10^{-1}$	220	1.128
	$1.075x10^{-2}$	220	1.122

Irradiation was carried out at 0° C using suspensions of initial concentration $1x10^{8}$ CFU/ml.

Finally, having observed that near-UV radiation induces a leakage of material from cells over a fluence range that may be correlated with lethality (Fig. 52), experiments were performed to test whether variations in near-UV radiation sensitivity, shown between some DNA repair-proficient E. coli strains, are due to differences in the extent of UV radiation-induced leakage effects. Using broad-band near-UV radiation, survival and $^{86}Rb^{+}$ fluence-leakage curves were determined within the same experiment for four E. coli strains; K-12 AB 1157, K-12 SR 385, and B/r (all DNA repair-proficient) and K-12 SR 246 (pol B 100), the latter showing an approximately three-fold increase in sensitivity to near-UV radiation compared to the DNA repair-proficient strains (Webb, 1977). Viability was assessed on low salt minimal media and leakage expressed as dpm test : control. E. coli K-12 SR 246 was included in this study as previously it had been shown that, after near-UV irradiation, as well as being more sensitive than DNA repair-proficient strains, it was particularly sensitive to the presence of inorganic salt in the plating media (Moss and Smith, unpublished data). Therefore, it was tested whether this sensitivity to inorganic salt shown by SR 246 could be related to an initial increase in UV radiation-induced leakage of $^{86}Rb^{+}$. Figures 57a and b show the survival curves and the corresponding leakage of $^{86}Rb^{+}$ curves, after broad-band near-UV irradiation of these four strains. As expected, the survival curves show strain SR 246 to be much more sensitive to near-UV radiation than the three DNA repair-proficient strains. The survival curves for the three DNA repair-proficient strains show that SR 385 is more sensitive than AB 1157 and B/r, which show approximately equal sensitivity to near-UV radiation. However, Fig. 57b shows that the $^{86}Rb^{+}$ leakage - time profiles for all four strains show an increase in leakage with increasing time of irradiation; but, moreover, there is little difference

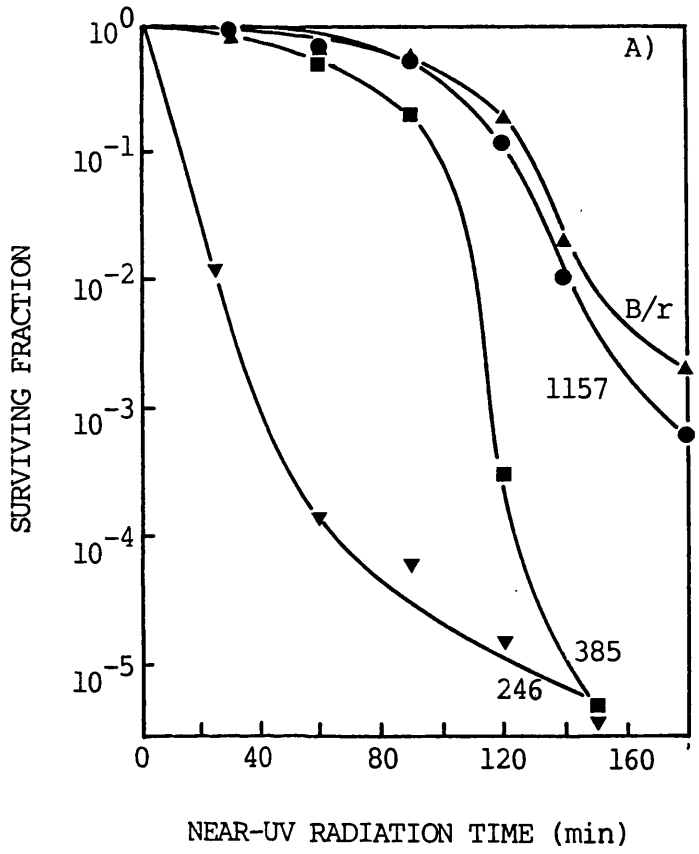

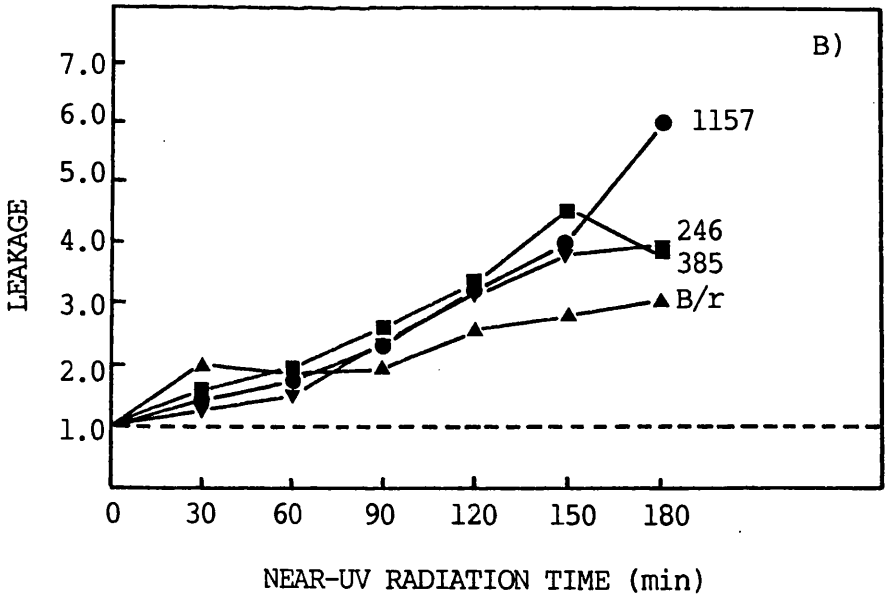

Figure 57

The effect of broad-band near-UV radiation on A) survival (assessed on low salt minimal medium) and B) $^{86}Rb^+$ leakage (expressed as dpm Test/Control) of E. coli K-12 AB 1157 (●), K-12 SR 385 (■), B/r (▲) and K-12 SR 246 pol B (▼).

in the amount of leakage of $^{86}Rb^{+}$ observed between all four strains.

DISCUSSION.

The results presented in this chapter show that, for a DNA repair-proficient stationary phase culture of E. coli K-12 (SR 385), a damaging effect on the cell's permeability barrier is induced by mild-heat and near-UV irradiation, with treatment times equivalent to or less than those required for cell inactivation. However, at fluences causing significant cell lethality, no such damage was detected for far-UV irradiated cells (Figs. 46a, 48 and 52). The results involving mild-heat treatments support the findings of Iandolo and Ordal (1966) and Russell and Harries (1967) who both showed a leakage of 260nm absorbing substances (and thus a membrane damaging effect) after such treatment, and provide a control response for membrane damage in relation to the UV-radiation findings.

Near-UV radiation-induced damage to the cell membrane has been shown by three different methods of assay : the release of 260nm absorbing substances (Fig. 46a); the leakage of [methyl-^{3}H] thymidine (Fig. 48); and the leakage of $^{86}Rb^{+}$ (Fig. 52). For the radioactive labelling methods, the importance of determining the leakage from individual, unirradiated, control samples has been shown by Fig. 47 for [methyl-^{3}H] thymidine and Fig. 51 for $^{86}Rb^{+}$. Also, for the $^{86}Rb^{+}$ leakage assay, it has been shown that leakage from unirradiated cells is temperature dependent (Fig. 53); the figure showing that the order of temperature effectiveness in inducing leakage of $^{86}Rb^{+}$ from control cells was 37>0>28>20°C. The unexpected degree of leakage from cells held at 0°C may be due to an increased instability of the bacterial

membrane at 0°C.

In addition, for the $^{86}Rb^{+}$ leakage assay, results have shown that the growth of cells in 4mM K^{+}, a requirement for the assay, did not significantly affect the growth rate of the cells (Fig. 49) or their sensitivity to broad-band near-UV radiation (Fig. 50). From Figs. 49 and 50 it is interesting to observe that the complete removal of K^{+} from the growth medium of E. coli SR 385 did not appear to affect the growth rate, but did increase the cell's sensitivity to broad-band near-UV radiation. An explanation for this effect is, as yet, unknown.

From Figures 46a, 48 and 52, describing the three methods of assay used for assessing near-UV radiation-induced membrane damage, it is apparent that mild-heat seems more effective, at treatments causing equivalent inactivation, than near-UV radiation in causing leakage of 260nm absorbing substances (Fig. 46a) and $^{86}Rb^{+}$ (Fig. 52), while the two treatments seem almost equally effective when assessed by thymidine leakage (Fig. 48). This may indicate that the nature of the damage induced by the two methods qualitatively differs.

From the three assays used for assessing membrane damage, $^{86}Rb^{+}$ leakage was chosen to determine the wavelength dependence of radiation-induced leakage, due to the good reproducibility and the use of lower initial cell concentrations with this assay method. On determining fluence-$^{86}Rb^{+}$ - leakage curves, expressed as leakage relative to that of unirradiated cells, with monochromatic wavelengths from 254 - 405nm , and with a broad-band near-UV radiation source, curves sigmoidal in shape were apparent (Figs. 54, 55, 56 and 51 respectively). As a

measure of leakage, the fluence required to increase the leakage by a factor of 2 was chosen on the basis that it generally fell on the straight line portion of the sigmoidal fluence- leakage curve. The reciprocal of this fluence value was then taken for each monochromatic wavelength studied and plotted in quantum units, as explained in Chapter 2.

Figure 58 shows an action spectrum for $^{86}Rb^{+}$ leakage, with an action spectrum for lethality for stationary phase cells of E. coli K-12 SR 385, also included to aid a comparison of leakage and lethality. The action spectrum for lethality is expressed in terms of $^{1}/F_{37}$ values, in quantum units. The $^{1}/F_{37}$ values were obtained from the survival curves, at each wavelength tested, for a suspension of $^{86}Rb^{+}$ labelled E. coli SR 385 at an initial concentration of $1x10^{8}$CFU/ml. The figure shows that, at wavelengths below 305nm, $^{86}Rb^{+}$ leakage occurs only at fluences much greater than is required to induce kill to the 37% level, and so membrane damage does not appear to be a significant cause of cell death at the wavelengths from 254 to 305nm. However, at wavelengths above 305nm, a leakage of $^{86}Rb^{+}$ occurs at fluences approximately equivalent to, or lower than, that necessary to induce a surviving fraction of 0.37. The wavelength of 305nm is also the wavelength above which UV-radiation-induced inorganic salt sensitivity is observed (Fig. 45). This correlation provides further evidence that the near-UV radiation-induced sensitivity to inorganic salt described previously (see Chapters 1 and 2) is indicative of near-UV radiation-induced cell membrane damage.

A further illustration of the relative importance of inactivation and leakage after far-and near-UV irradiation, is shown in Figures 59 a and b, which show two typical fluence (or time)- $^{86}Rb^{+}$ leakage curves

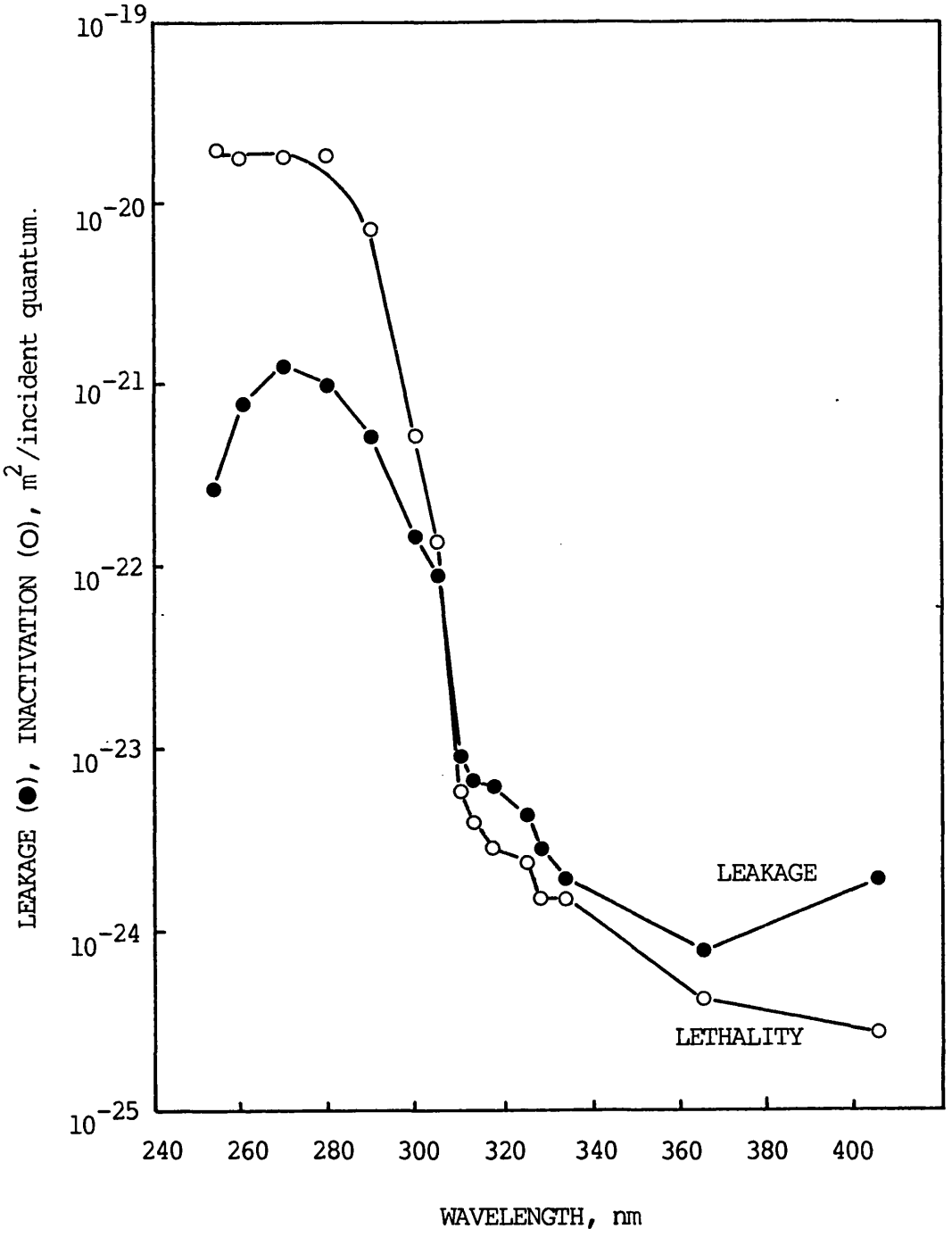

Figure 58

Action spectra for a) $^{86}Rb^{+}$ leakage (expressed in terms of the reciprocal of the fluence required to increase the dpm of the test sample compared to its unirradiated control by a factor of 2.0, in quantum units), (●) and b) lethality (expressed as $^{1}/F_{37}$ on low salt minimal medium plates in quantum units), (O), for E. coli K-12 (SR 385) labelled with $^{86}Rb^{+}$.

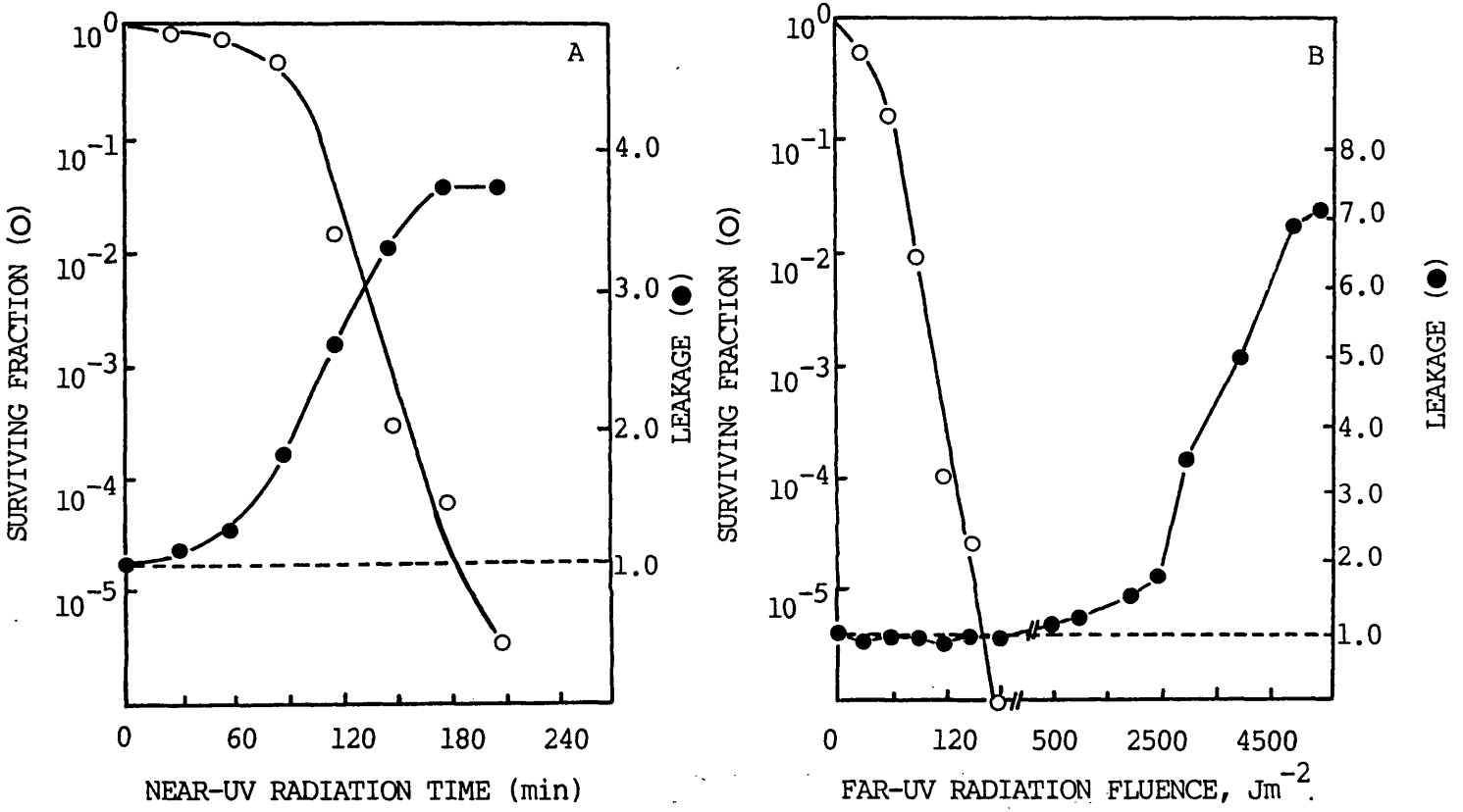

Figure 59

Survival curves at 25°C for $^{86}Rb^{+}$ - labelled cells of E. coli K-12 (SR 385), (initial cell concentration 1x10^{8}CFU/ml after A) broad-band near-UV radiation and B) far-UV radiation (254 nm) with viability assessed on low salt minimal medium (O), with a comparison of the leakage of $^{86}Rb^{+}$ expressed as dpm Test/ Control (●).

obtained for stationary phase E. coli cells after a) broad-band near-UV irradiation and b) far-UV (254nm) irradiation, superimposed on their respective survival curves obtained on low salt medium. The data for this figure is derived from Figs. 52 and 54, and shows that, for near-UV irradiated cells, a leakage of $^{86}Rb^{+}$ occurs within the same time of irradiation range as cell inactivation. Moreover, the large increase in lethality observed beyond the shoulder region of the survival curve (over the time of irradiation range 60-180 minutes) may be correlated with a large increase in leakage of $^{86}Rb^{+}$ observed over the same time of irradiation range. Also, by measuring the total amount of $^{86}Rb^{+}$ label present in a 0.25ml volume of the initial unirradiated bacterial suspension, it is apparent that, at the plateau region of the $^{86}Rb^{+}$ leakage curve, above a time of irradiation of 200 minutes (where over 99.99% of the cells are dead), in the region of 95% of the label had leaked through the membrane.

In contrast, Figure 59b shows that, for far-UV irradiated cells, there was no observed leakage of $^{86}Rb^{+}$ over the fluence range causing cell inactivation to a surviving fraction of 10^{-5}. However, at much higher fluences, that is, about ten times that required to induce 2 log cycles inactivation in a DNA repair-proficient E. coli strain, a leakage of $^{86}Rb^{+}$ was observed.

The action spectrum for $^{86}Rb^{+}$ leakage described in Figure 58 exhibits several interesting features. First, within the far-UV radiation region of the action spectrum, where leakage only occurs at fluences much greater than is required to inactivate 99.9% of the cell population, there appears to be a peak in leakage produced at 270nm. At this wavelength, a fluence of only 550 Jm^{-2} (about 10 times that required to produce a surviving fraction of 0.37) is required to induce

significant leakage of $^{86}Rb^{+}$, whereas, at 254nm, a fluence of 2.75 x 10^{3} Jm^{-2} is required (about 50 times that required to produce a surviving fraction of 0.37). Explanation of this may involve the absorption of 270nm radiation by a chromophore, as yet unknown, either within the cell membrane, leading to direct damage, or outside the cell membrane, producing an indirect damaging effect on the membrane.

A possible insight into the chromophore involved for this leakage effect by far-UV radiation may be gained from similar results obtained by Cook and co-workers (see 1975 for a review). They have presented an action spectrum for the haemolysis of erythrocytes by far-UV radiation, which showed a peak in effectiveness near 280nm and a minimum near 265nm. They have suggested that this action spectrum resembles that of a typical protein containing aromatic amino acids. In addition, they have suggested that the haemolysis results from an increase in the passive permeability of the membrane to cations (mainly K^{+} and Na^{+}) leading to swelling and subsequent lysis.

Various workers have shown a leakage of material after high fluences of far-UV radiation (254nm). Murphy and Wilson (1982), using $^{86}Rb^{+}$ as a K^{+} analog, have shown a leakage from rose (Rosa damascena var. Gloire de Guilan) cells after irradiation with 1.68×10^{3} Jm^{-2} of 254nm radiation (compared with about 2.0×10^{3} Jm^{-2} for the initial detection of leakage in this study). Doughty and Hope (1973) have shown an efflux of Na^{+}, K^{+}, and Cl^{-} from cells of Chara corallina after 2.82×10^{3} Jm^{-2} of 253.7nm radiation and Siegel and Corn (1974) using beet roots, have shown, after irradiation with $3 \times 10^{4} Jm^{-2}$ of 254nm radiation, sufficient disruption for betacyanin to leak out of the cells.

A mechanism for the efflux effects observed after high fluences of far-UV radiation has been forwarded by other workers. Roshchupkin et al. (1975) have reported that membrane lipid peroxidation is one of the causative factors of 254nm - (above 1.5×10^3 Jm^{-2}) induced haemolysis of rat erythrocytes. In support of a lipid peroxidation mechanism, Wright et al. (1981), using wheat root vesicles, showed a production of malondialdehyde, a product of lipid peroxidation, after far-UV (254nm) radiation fluences of greater than 1.8×10^3 Jm^{-2}.

Concerning the mid-and near-UV radiation regions, from Fig. 58 it may be estimated, by comparing the difference in fluence required to induce a surviving fraction of 0.37 and to induce the chosen measure of $^{86}Rb^+$ leakage from cells, that, firstly, only wavelengths above 310nm induce leakage, and, secondly, there is an apparent large peak in effectiveness shown at 405nm. However, due to the large fluences required, and the UV radiation sources available for these studies, it was not practical to perform experiments at wavelengths above 405nm in order to determine whether the wavelength of 405nm does indeed provide the peak in leakage from cells. Therefore, no suggestion of a chromophore for near-UV radiation-induced leakage, absorbing at a maximum around 405nm can justifiably be made from Fig. 58, although this may be the case.

Also, from Fig. 58, it is apparent that a break or shoulder for the $^{86}Rb^+$ leakage and the lethality curves is apparent around 310-320nm. This break or shoulder in the UV radiation wavelength region was also observed for the action spectra for UV radiation-induced lethality of E. coli SR 385 on low and high salt media (Fig. 44), and has been observed in many other action spectra for UV radiation-induced effects in E. coli. A full description of the present knowledge

concerning this shoulder around 320nm is included in Chapter 2.

Finally, from the results presented in Fig. 57, it is apparent that the differences in sensitivity to near-UV radiation observed between three DNA repair-proficient E. coli strains, K-12 AB 1157, K-12 SR 385 and B/r, are not due to differing initial degrees of membrane damage, as the amount of induced $^{86}Rb^{+}$ leakage was approximately equal for all three strains. In addition, the results suggest that the additional sensitivity of strain K-12 SR 246 (pol B) to near-UV radiation, observed when plated on high salt minimal medium, (as observed by Moss and Smith) is also not due to an initial increase in damage to membranes in this strain. However, the differences observed within the DNA repair-proficient strains, and between them and strain SR 246, may still be associated with the cytoplasmic membrane. One approach, which may be useful, would be to determine the ability of the membranes in these strains to recover after near-UV radiation, as, although initial damage may be the same, there may be differences in their ability to recover. In particular, a deficiency in strain SR 246 may be evident.

Another approach may be to perform similar leakage experiments to those described by the results of Fig. 57, at 365nm, or preferably at 405nm, where direct absorption of radiation by DNA would be much lower than with a broad-band near-UV radiation source. Consequently, if the sensitivity differences are due to genetic damage induced by the shorter wavelengths, i.e. 320-350nm present in the radiation source, then this effect would be much reduced. Further work, possibly involving mapping procedures to determine whether the sensitivity of

strain SR 246 is due to a particular gene product, may also help elucidate the reason for the results obtained using SR 246. Another approach to explain near-UV radiation sensitivity differences observed between DNA repair-proficient strains, may be to investigate the differences associated with phase of growth. Studies involving the effect of the phase of growth of four DNA repair-proficient strains on their sensitivity to near-UV radiation, are described in Chapter 4.

In summary, the results presented in this chapter show direct evidence of a near-UV radiation induction of membrane damage, which may be important in terms of lethality. However, it should be noted that these results do not provide any evidence as to the relative importance of membrane damage, compared to damage to DNA, in near-UV radiation-induced cell inactivation.

CHAPTER 4

THE EFFECT OF THE PHASE OF GROWTH ON THE SENSITIVITY OF FOUR *E. coli* DNA REPAIR - COMPETENT STRAINS TO NEAR-UV RADIATION.

The results presented in Chapters 1, 2 and 3 involving the near-UV irradiation of various E. coli strains were all obtained using cells in the stationary phase of growth. However, it is well established that cells in the logarithmic (or exponential) phase of growth are generally more sensitive to near-UV radiation than are cells in the stationary phase of growth (e.g. Peak, 1970). A review of the effect of phase of growth on sensitivity to near-UV radiation, for eucaryotic as well as procaryotic cells, is included in the introduction. Klamen and Tuveson (1982) have shown that, with increasing degrees of unsaturation of membrane fatty acids, sensitivity to near-UV radiation increases, this effect being more pronounced for logarithmic-phase cells than stationary-phase cells, thus implicating membrane damage after near-UV irradiation to be more important in logarithmic-phase cells. Ito and Ito (1983) have observed a membrane damaging effect for yeast cells in logarithmic phase that was not observed for stationary phase cells under the same experimental conditions. However, during preliminary investigations with E. coli K-12 SR 385, Moss and Smith (unpublished data) observed that this strain was more resistant to near-UV radiation in the logarithmic phase of growth than in the stationary phase of growth, thus observing the opposite to published results with other DNA repair-competent strains of E. coli.

Therefore, a series of experiments were performed to; first, determine the sensitivity of K-12 SR 385 to near-UV radiation throughout its growth cycle; second, to investigate the degree of membrane damage (measured as the difference in sensitivity on low and high salt plating media) observed throughout the growth cycle of K-12 SR 385; and third, to compare the sensitivity obtained with strain K-12 SR 385 at various phases of growth with other DNA repair-proficient E. coli strains, e.g. NCTC 86 (a wild-type strain), B/r and K-12

AB 1157, and with published work on growth phase effects on cell sensitivity to near-UV radiation. The published work used as comparison with the effects observed for K-12 SR 385 was from Peak (1970), who used B/r, and Tuveson and Jonas (1979), who used K-12 AB 1157 and K-12 AB 2463 (rec A).

Specialized Methodology.

For experiments involving sensitivity determinations throughout the complete growth cycle of the organisms, cells at an initial concentration of approximately 10^7CFU/ml were irradiated with an appropriate constant fluence of broad-band Black-Light Blue near-UV radiation. This fluence was chosen from previous investigations using stationary phase cultures of each organism tested (e.g. Fig. 57a) and was such that approximately one log cycle's inactivation was observed when plating on low salt medium. To achieve approximately the same initial concentration of cells for each irradiation, an appropriate amount of the growth suspension was filtered via a 0.45μm pore size membrane filter contained in a Sartorius apparatus and the cells washed with M9, as described in the general methodology section. The cells were then resuspended by gentle agitation of the filter in 9ml M9 and the optical density of the resulting suspension was determined at 470 nm using a Unicam SP600 spectrophotometer. By reference to an optical density viable count calibration curve constructed for each organism (e.g. Appendix A3 for K-12 SR 385), an appropriate dilution in M9 was made to produce the initial concentration of cells for irradiation of $1x10^7$CFU/ml.

For experiments involving near-UV radiation sensitivity determinations at every hour throughout a 24 hour growth period, all irradiations were performed on the same day by inoculation of 1ml from a primary

saturated culture at 9.00 pm on the previous day of the experiment (Flask A) and at 9.00 am on the day of the experiment (Flask B). Thereby, the 12 to 24 hour sensitivity determinations were performed using Flask A and, simultaneously, the 1 to 11 hour determinations were performed using Flask B. During irradiation, which was either in position 6 or 7 of the lamp box, where it had been shown previously that equal fluence rates were apparent (Fig. 22), the 5ml bacterial samples were stirred by bubbling with filtered, humidified air. In addition, at the time of sampling, optical density determinations at 470 nm were taken and plotted to check the phase of growth the cells had reached.

Viability was assessed on low salt medium (i.e. minimal medium with tenfold-diluted inorganic salts) and high salt medium (i.e. minimal medium with tenfold-diluted inorganic salts and sodium chloride added at 200mM). The surviving fractions of cells were calculated after each irradiation in terms of the viable count, determined on high and low salt minimal media, made for a corresponding unirradiated cell sample.

Irradiation at different temperatures with the BLB source.

During these studies, irradiation procedures were carried out at 35°C and 0°C in addition to the normal fan-cooled irradiation at 28 $\pm$ 1°C. For irradiation at 0 and 35°C, a jacketed test-tube with an inlet at the base and an outlet at the top, was constructed and fitted into position 7 of the lamp box. By use of a peristaltic pump (Watson Marlow Ltd.) and lagged rubber tubing, circulating fluid from water baths at 0 or 35°C was then forced through the test-tube. For irradiation at 0°C, a 15% ethanol in water solution, cooled to -2°C using a U-cool

refrigeration unit, (Neslab Instruments Inc.), was used. For irradiation at 35°C, M9 salts solution, warmed to 35°C in a water bath using a heating coil pump (Grant Instruments Ltd.), was used. An absorption scan over the wavelength range 300 - 450 nm was run for both of the circulating fluids to ensure that no absorption, which would interfere with the fluence received by the cell suspension, was apparent. By use of a probe thermometer (Comark Ltd.) it was found that, during experiments, the sample within the jacketed test-tube remained at ±0.5°C of the desired temperature.

RESULTS.

Initially, experiments were performed to assess the sensitivity of E. coli K-12 SR 385, the strain routinely used throughout this study, to broad-band near-UV radiation in various phases of growth. From a growth curve determined for K-12 SR 385 grown in minimal medium at 37°C in a shaking water bath (as shown in Appendix A2), it is apparent that, after an initial lag period of about 2 hours, exponential growth occurs up to about 13 hours growth, after which the cells remain in stationary phase for up to at least 25 hours growth. Therefore, the sensitivity to near-UV radiation, using low and high salt minimal media for the assessment of viability, of cultures of K-12 SR 385 grown for 24 (i.e. stationary phase), 3 (i.e. early log phase) and 6 (i.e. mid log phase) hours, was determined. The survival curves obtained from such an experiment are shown in Figure 60. The figure shows that there is an order of sensitivity to near-UV radiation; the 24 hour culture being most sensitive; then the 3 hour culture, and the 6 hour culture being most resistant. These initial results add support to Moss and Smith's preliminary findings, as it is apparent that SR 385 is more sensitive to near-UV radiation in the stationary phase of growth than in the log phase. This is different to the majority of published

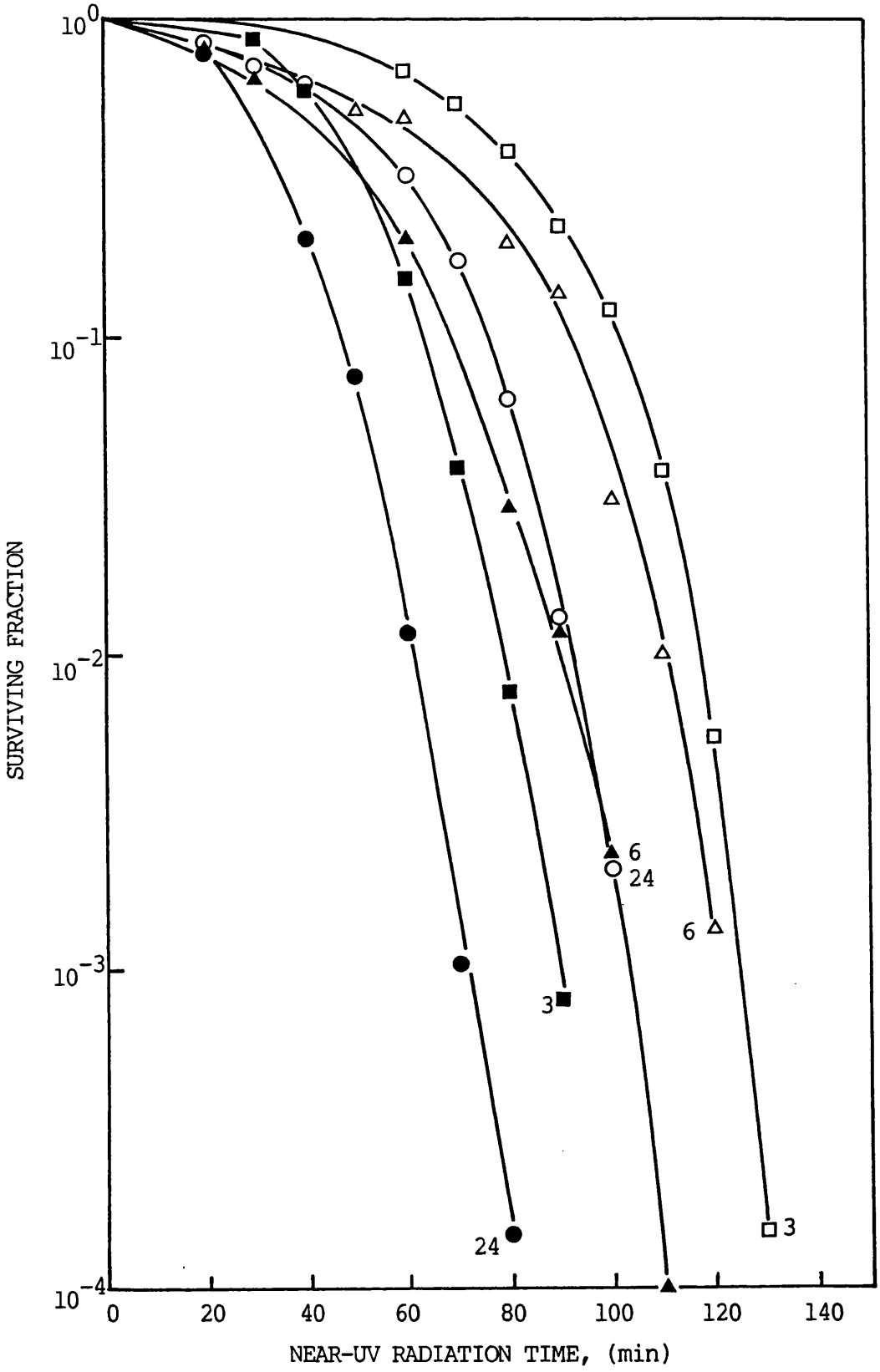

Figure 60

Survival curves after broad-band near-UV irradiation of E. coli K-12 (SR 385) grown for 24 (●,○), 3 (■,□) and 6 (▲,△) hours, with viability assessed on low salt (open symbols) and high salt (closed symbols) minimal media.

data regarding growth phase effects on the sensitivity of E. coli to near-UV radiation. In addition, it appears that the degree of salt sensitivity observed for the strain, is similar in all three phases of growth tested.

In order to add support to these preliminary findings, the sensitivity of K-12 SR 385 to a constant fluence of broad-band near-UV radiation was determined at half-hourly intervals during the first 6 hours of growth. The results of a typical experiment, where cells were irradiated with 60 minutes of broad-band near-UV radiation, are shown in Figure 61. This figure shows that, as cells are in late lag phase and about to enter the log phase of growth, there is a large decrease in sensitivity to near-UV radiation, which is apparent when viability is assessed on low and high salt minimal media. Also, the figure exhibits an interesting feature in that there appears to be some regular fluctuation in the observed sensitivity, on both low and high salt media, for cells over the early log phase of growth (i.e. from 0.5 to 5 hours). One possible reason for these fluctuations in response is that it is associated with some degree of synchronous cell division. That is, in the log phase of growth, bacterial culture cells are not distributed randomly among all stages in their division cycle, and hence give rise to discontinuous rather than continuous cell formation.

In an attempt to ascertain whether some degree of synchronous growth was responsible for the regular fluctuations in sensitivity observed in Fig. 61, using the same culture and done simultaneously with the experiment described in Fig. 61, optical density (at 470 nm) and viable count (on Oxoid nutrient agar) determinations were carried

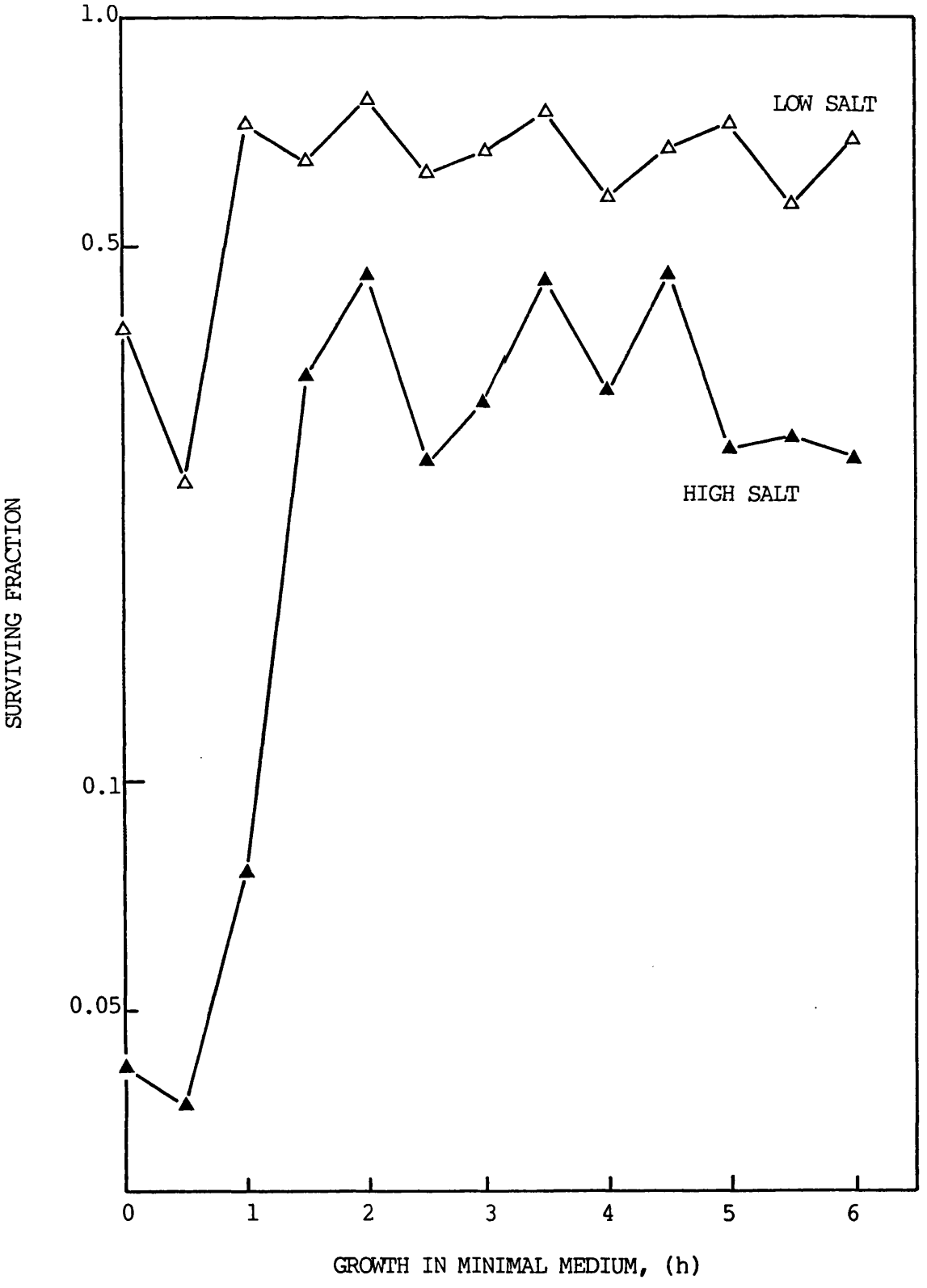

Figure 61

Survival curves for E. coli K-12 (SR 385) assessed on either low salt (△) or high salt (▲) minimal media, after irradiation with 60 minutes of broad-band near-UV radiation at 28°C, after growth in minimal medium for the times indicated on the abscissa.

out at 15 minute intervals over the initial 6 hours of growth in minimal medium. The results obtained are shown in Figure 62. While this figure does not give evidence of synchronous growth, other experiments in this laboratory (unpublished) have shown that inoculation from stationary phase cells can lead to 2 or 3 generations of partially synchronous growth.

Sensitivity was then determined for strain K-12 SR 385 throughout a 24 hour growth period, to include cells in late log and early stationary phase. Figure 63 shows the surviving fractions obtained on low and high salt media for strain SR 385 at various stages throughout its growth cycle, after irradiation with 85 minutes of near-UV radiation. Also included are the optical density readings at 470 nm, for the same suspension over the 24 hour period. The figure shows that, in agreement with Figs. 60 and 61, log phase cells of K-12 SR 385 are more resistant to near-UV radiation than are stationary phase cells.

Although the results presented in Figs. 60, 61 and 63 show the opposite effect to most published results (e.g. Peak, 1970; Tuveson and Jonas, 1979), their data was obtained under somewhat different experimental conditions and with different DNA repair-proficient strains. One of the main differences between the data obtained by Peak and Tuveson and Jonas, and that presented in Figs. 60, 61 and 63, is the temperature of irradiation. While the irradiations of K-12 SR 385, described previously in this chapter, were performed at 28 $\pm$ 1°C, Peak's irradiation procedures were carried out at 35°C, and Tuveson and Jonas performed theirs at approximately 10°C. Therefore, a series of experiments was carried out, using K-12 SR 385 in various phases of growth, to test the effect of irradiation at different temperatures on near-UV radiation sensitivity. First, to enable a closer comparison

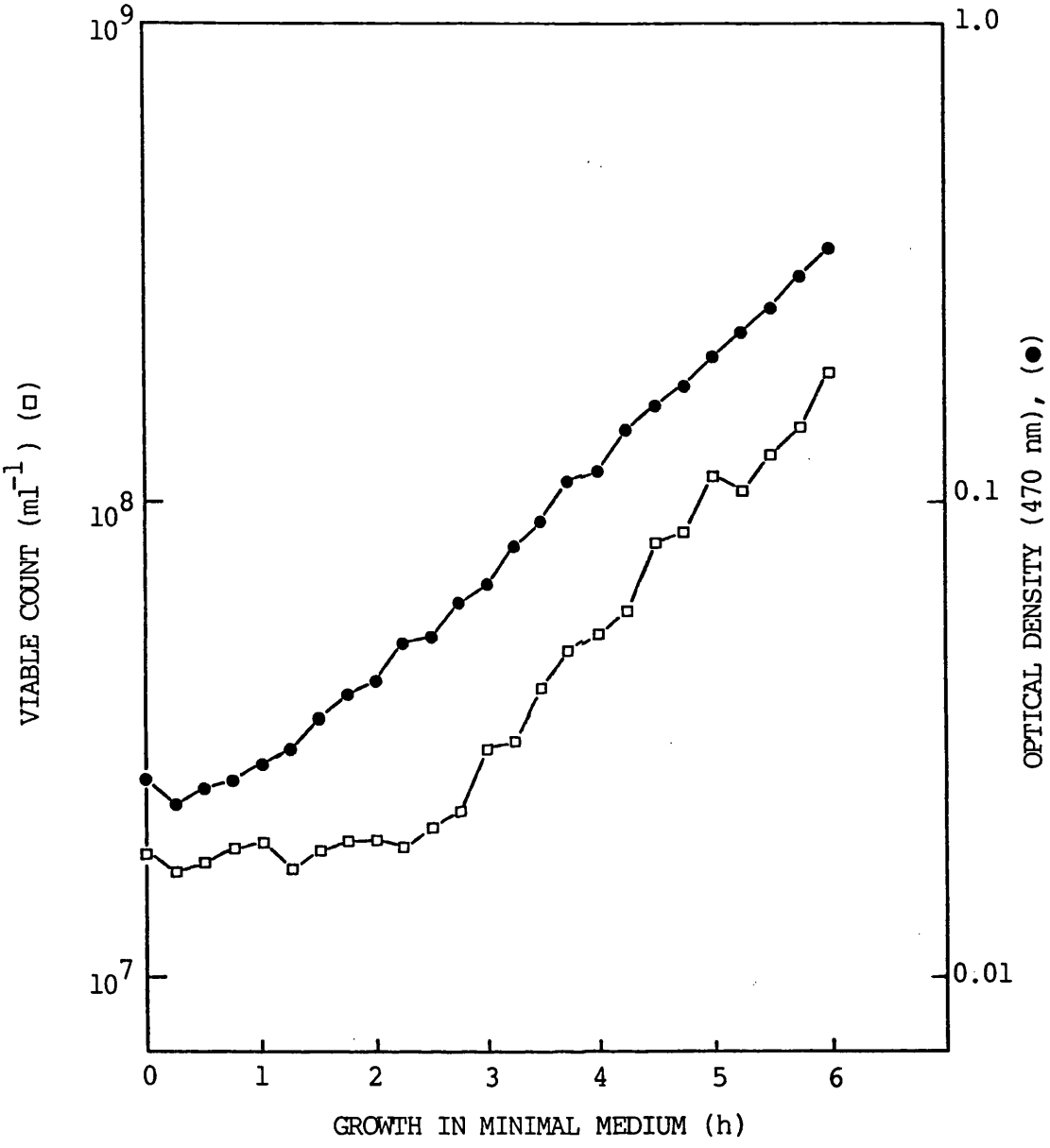

Figure 62

Viable counts (assessed on Oxoid nutrient agar), (□) and optical densities (470 nm), (●) during the growth of *E. coli* K-12 (SR 385) in minimal medium.

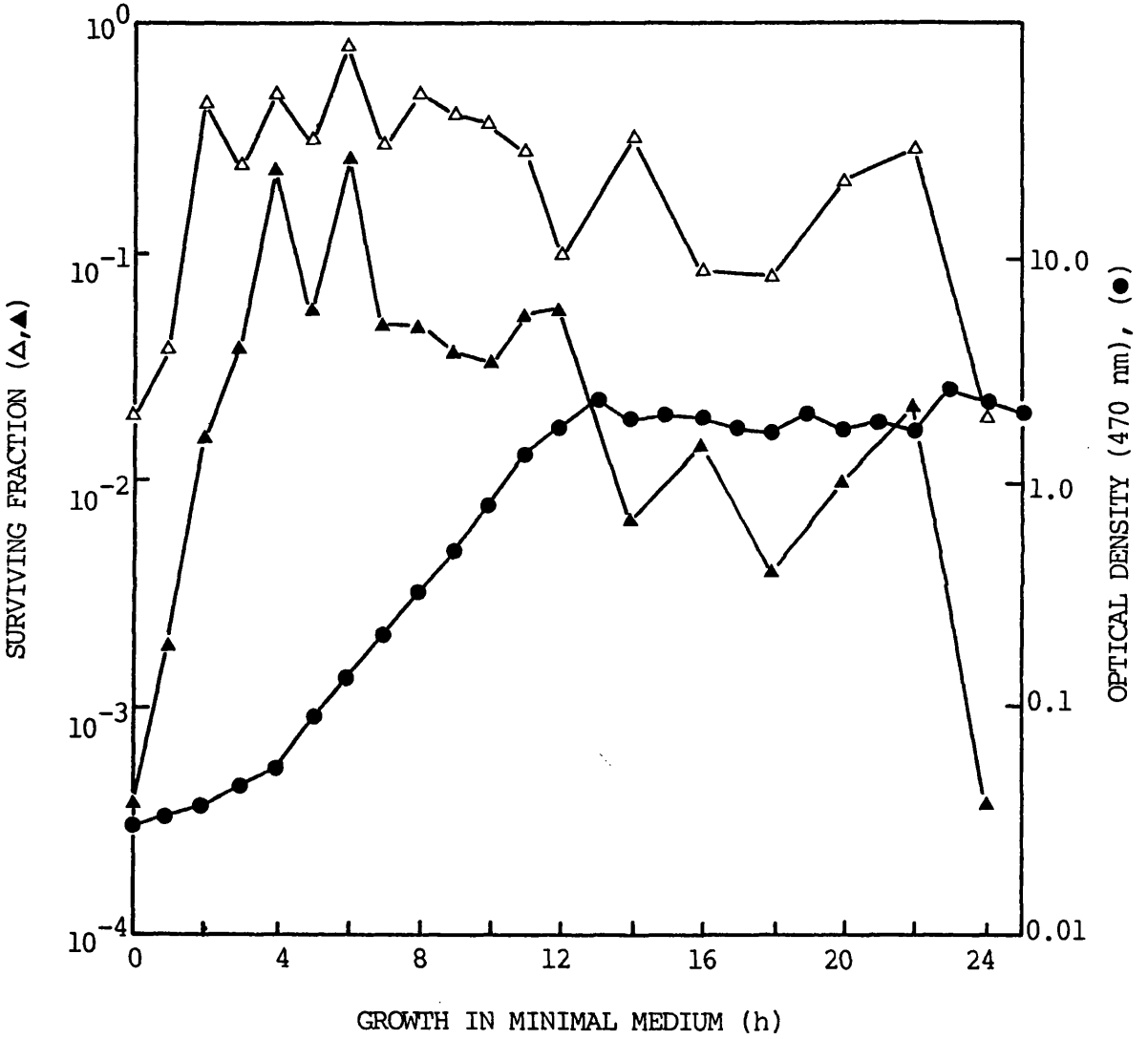

Figure 63

Surviving fractions for E.coli K-12 (SR 385) assessed on either low salt (△) or high salt (▲) minimal media after irradiation with 85 minutes of broad-band near-UV radiation at 28°C; and optical densities at 470 nm (●) after growth in minimal medium for the number of hours indicated on the abscissa.

with Peak's 1970 observations, Figure 64 shows the effect of irradiating, with broad-band near-UV radiation at 35°C, stationary - (24 hours growth) and log - (6 hours growth) phase cultures of K-12 SR 385, and assessing for viability on low and high salt minimal media. The figure shows that, when irradiated at the higher temperature of 35°C, stationary phase cells of K-12 SR 385 are again more sensitive than are log phase cells. Also, a sensitivity to inorganic salts is observed for both log and stationary phase irradiated cells,with the log phase cells exhibiting less salt sensitivity than the 24 hour stationary phase cultures.

Tuveson and Jonas carried out their experiments at 10°C, in order to limit metabolism during the exposure period. Therefore, as a comparison, irradiation of K-12 SR 385 was performed at 0°C, where metabolism is minimized. As a preliminary experiment, the sensitivity on low and high salt minimal media for K-12 SR 385 was compared at irradiation temperatures of 28 and 0°C. The survival curves obtained are shown in Fig. 65 and were obtained using the same stationary phase (24 hour) culture of SR 385 and by irradiating simultaneously in position 6 of the lamp box at 28°C and position 7 at 0°C. From Fig. 65 it is apparent that cells irradiated at 0°C show an increased sensitivity to near-UV radiation compared to cells irradiated at 28°C. Also, the figure shows that approximately equal degrees of sensitivity to inorganic salts are induced by irradiating at 0°C or 28°C. Figure 66 shows the effect of irradiating, with broad-band near-UV radiation at 0°C, stationary - (24 hours growth) and log - (6 hours growth) phase cells of K-12 SR 385. As seen after irradiation at 28 and 35°C, the cells in stationary phase show the greater sensitivity to near-UV radiation. In order to provide a comparison with the results presented in Fig. 61 after irradiating at 28°C, the sensitivity of K-12 SR 385 to a constant

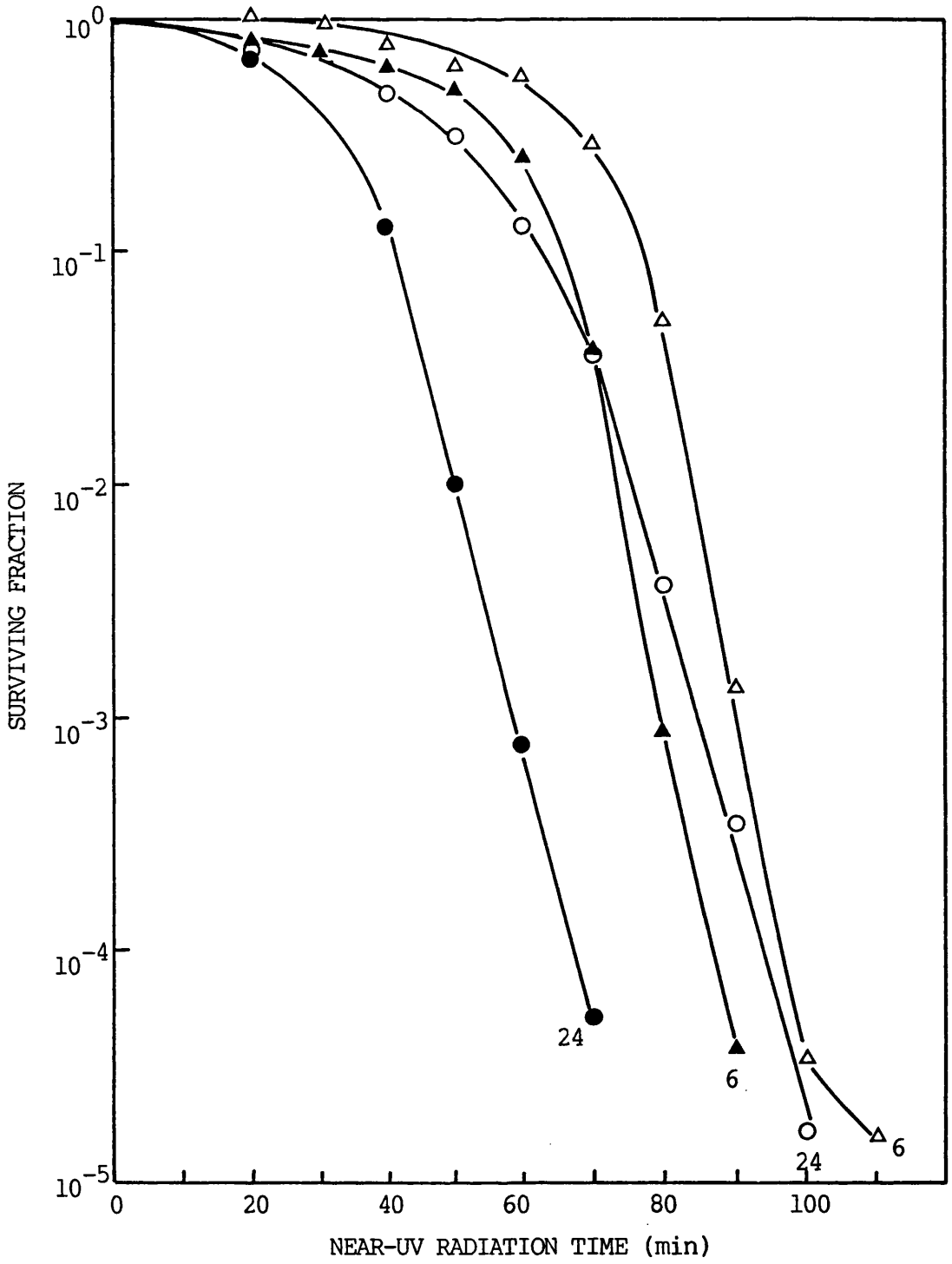

Figure 64

The effect of irradiation at 35°C with broad-band near-UV radiation on the sensitivity of log- (6 hours growth), (△,▲) and stationary- (24 hours growth), (○,●) phase cells of E. coli K-12 (SR 385) with viability assessed on low salt (△,○) or high salt (▲,●) minimal media.

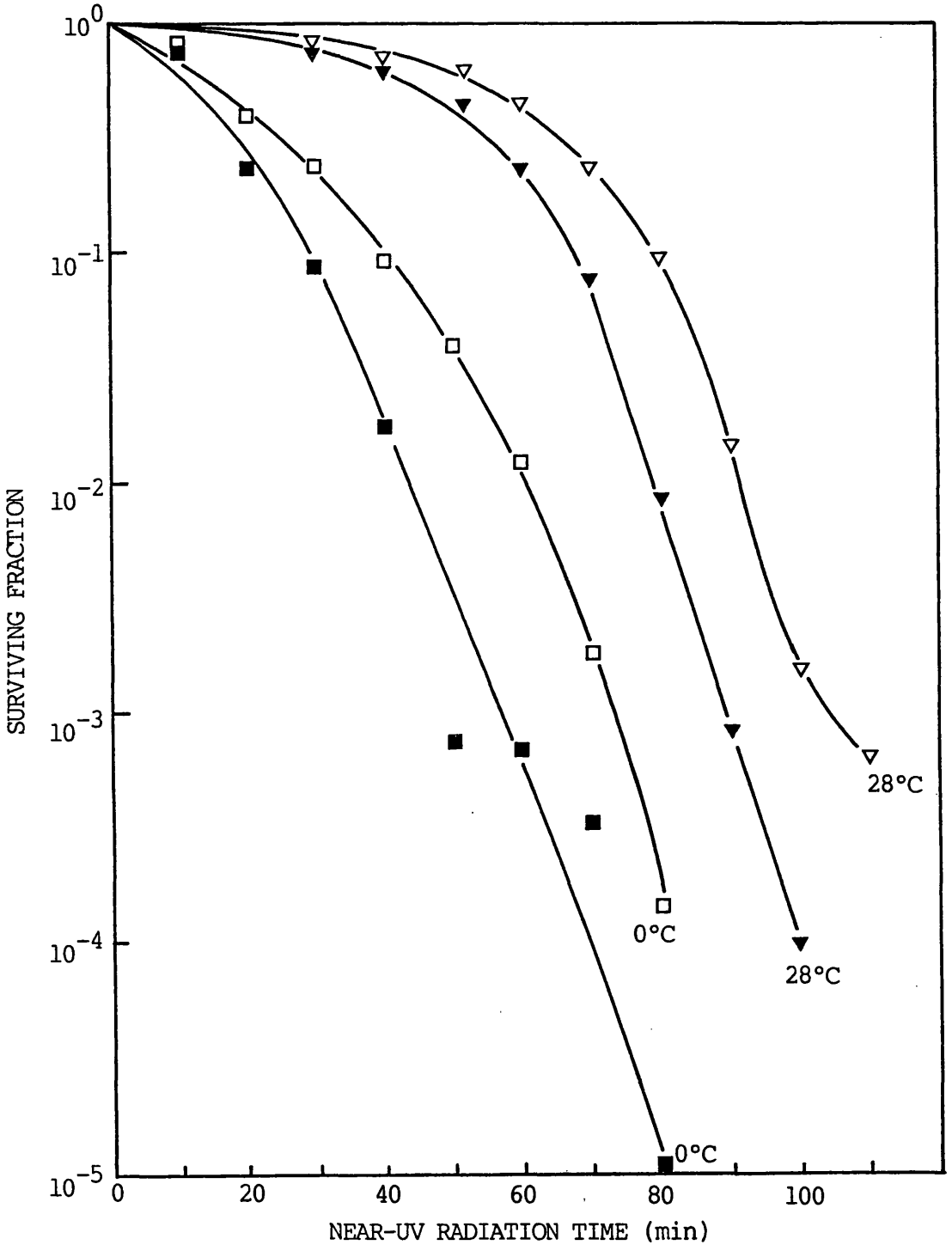

Figure 65

The effect of irradiation at 28°C (▽,▼) or 0°C (□,■) with broad-band near-UV radiation on the sensitivity of 24 hour cultures (stationary phase) of E. coli K-12 (SR 385). Viability was assessed on either low salt (▽,□) or high salt (▼,■) minimal media.

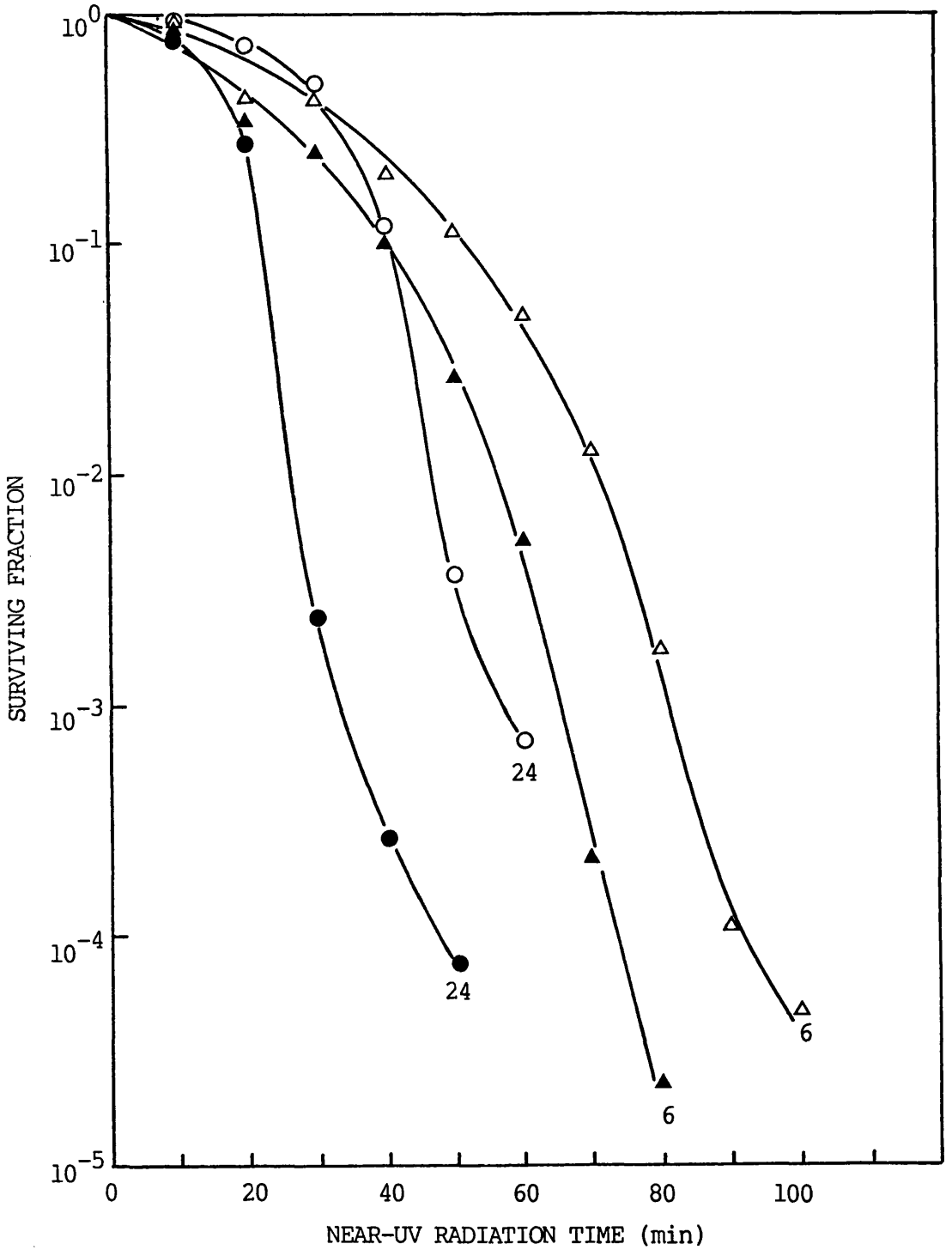

Figure 66

The effect of irradiation at 0°C with broad-band near-UV radiation on the sensitivity of log- (6 hours growth), (△,▲) and stationary- (24 hours growth), (O,●) phase cells of E. coli K-12 (SR 385). Viability was assessed on either low salt (△,O) or high salt (▲,●) minimal media.

fluence of broad-band near-UV radiation, was tested at hourly intervals during growth to the stationary phase. The result from an experiment, where cells from 0 to 12 hours growth in minimal medium were irradiated for 35 minutes at 0°C and assessed for viability on low and high salt minimal media, is shown in Figure 67. As with the results presented in Fig. 61 for cells irradiated at 28°C, the figure indicates that there is a decrease in sensitivity to near-UV radiation as cells enter the log phase of growth which is maintained throughout the log phase of growth.

It is apparent, from the experiments involving irradiation at different temperatures, that E. coli K-12 SR 385 is more sensitive to near-UV radiation in stationary phase than in log phase when irradiated at 0, 28 or 35°C. Experiments were then performed to determine whether this effect was peculiar to strain K-12 SR 385 or was observed for other DNA repair-proficient E. coli strains. The first additional strain chosen for study was E. coli B/r, the strain used by Peak (1970), who reported that it was more sensitive to near-UV radiation in the log phase of growth.

Figure 68 shows the survival curves obtained on low and high salt minimal media after near-UV irradiation of E. coli B/r grown in minimal medium for 4 hours or 24 hours. From a growth curve constructed for this strain (as shown in Fig. 69), it is apparent that the 4 hour culture represents mid-log phase cells and the 24 hour culture represents stationary phase cells. In contrast to the previous results observed for K-12 SR 385, Fig. 68 shows that E. coli B/r is more sensitive to near-UV radiation during the log phase of growth, particularly when assessed for viability on high salt minimal medium. Figure 69 shows the surviving fractions obtained on low and high salt

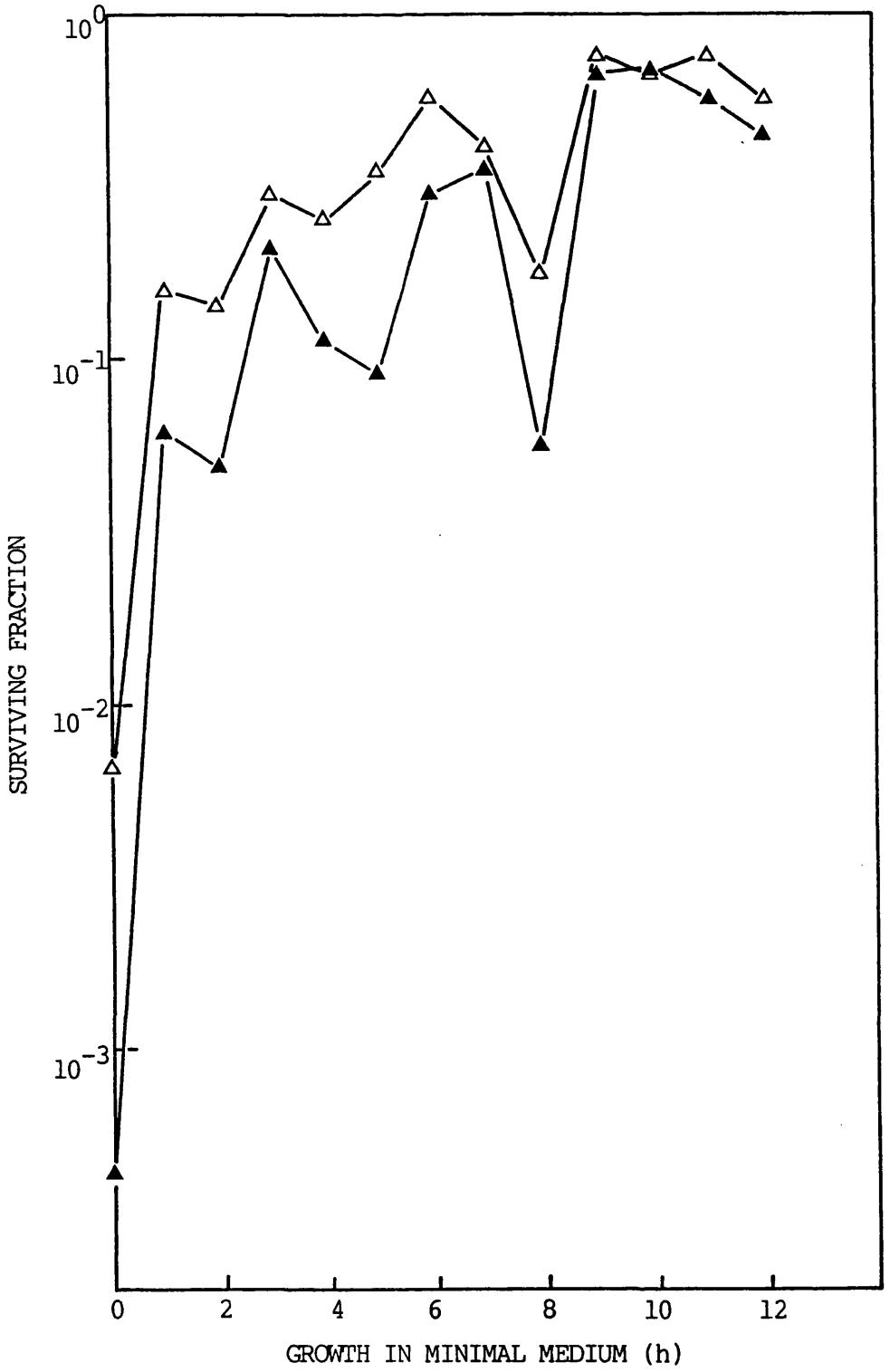

Figure 67

Surviving fractions for E. coli K-12 (SR 385) assessed on either low salt (△) or high salt (▲) minimal media, after irradiation with 35 minutes of broad-band near-UV radiation at 0°C.

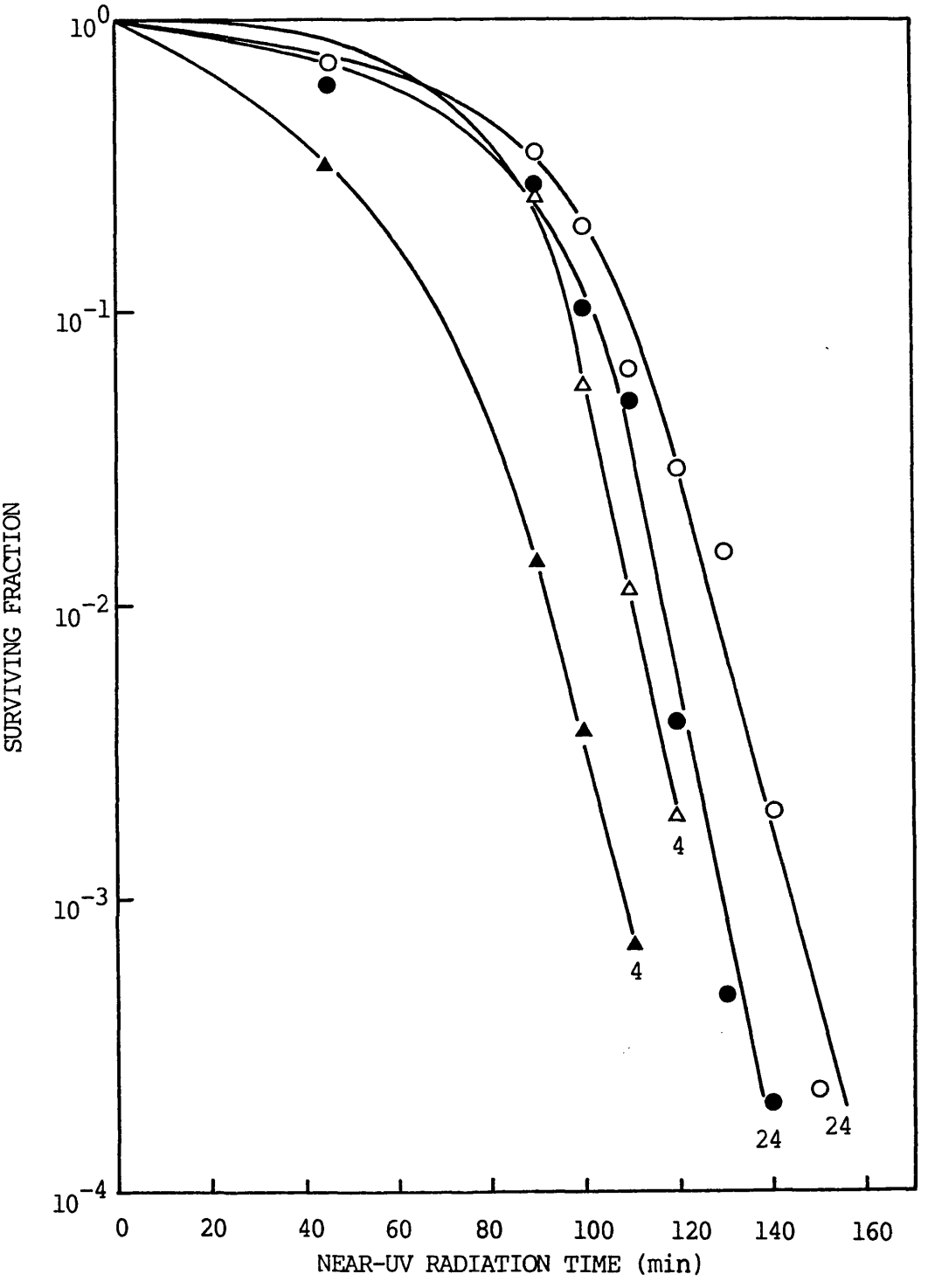

Figure 68

Survival curves after broad-band near-UV irradiation of E. coli B/r grown for 4 (△,▲) or 24 (○,●) hours with viability assessed on low salt (△,○) and high salt (▲,●) minimal media.

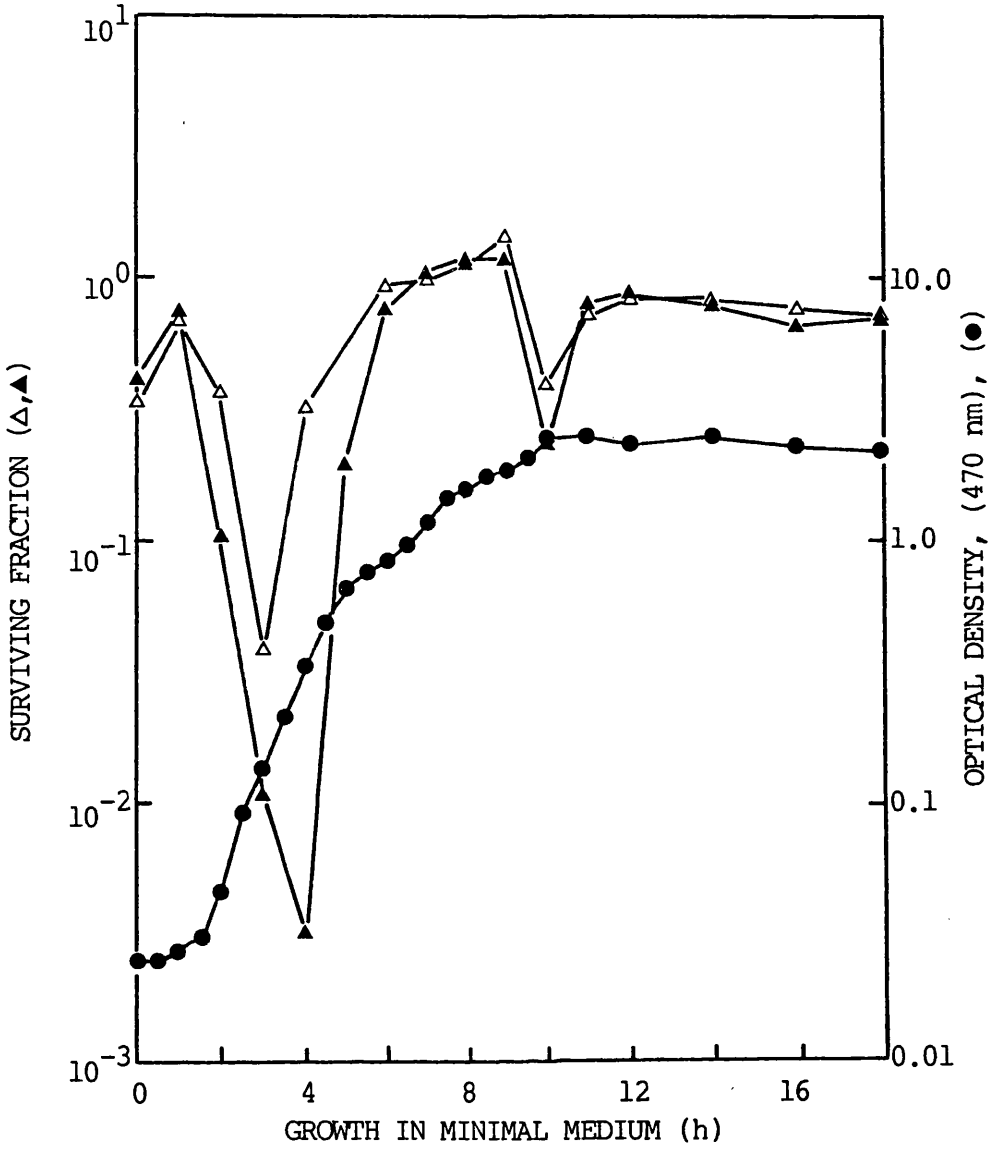

Figure 69

Surviving fractions for E. coli B/r assessed on either low salt (△) or high salt (▲) minimal media, after irradiation with 100 minutes of broad-band near-UV radiation; and optical densities at 470 nm (●), after growth in minimal medium for the number of hours indicated on the abscissa.

minimal media for E. coli B/r at intervals of growth throughout a 24 hour growth period, after irradiation with a constant fluence of 100 minutes, chosen from Fig. 68, of near-UV radiation. Superimposed on this figure is a growth curve for E. coli B/r in minimal medium in terms of optical density measurements at 470 nm. The figure clearly shows that a dramatic increase in near-UV radiation-induced lethality is observed for cells in the mid-log phase of growth.

To gain another comparison with published work (e.g. Tuveson and Jonas, 1979), the sensitivity of another DNA repair-proficient K-12 strain, K-12 AB 1157, to near-UV radiation was determined for log and stationary phase cells. Figure 70 shows the survival curves obtained on low and high salt minimal media after near-UV irradiation of K-12 AB 1157, grown for 6 or 24 hours. From a growth curve in minimal medium constructed for this strain (as shown in Figure 71) it can be seen that the 6 hour culture represents mid-log phase cells and the 24 hour culture represents stationary phase cells. Figure 70 shows that, as with E. coli B/r (Fig. 68), the cells in log phase show the greater sensitivity to near-UV radiation. This is particularly apparent for cells assessed for viability on high salt minimal medium. Therefore this result supports those of Tuveson and Jonas involving the same strain.

Figure 71 shows the surviving fractions obtained on low and high salt minimal media for K-12 AB 1157, at hourly intervals of growth from 0 to 11 hours, after irradiation with a constant fluence of near-UV radiation. The fluence chosen, from Fig. 70, was 80 minutes. Also included in Fig. 71 is a growth curve for AB 1157, plotted in terms of optical density at 470 nm. In contrast to Fig. 70, the figure indicates that lag and early log phase cells show a decreased sensitivity

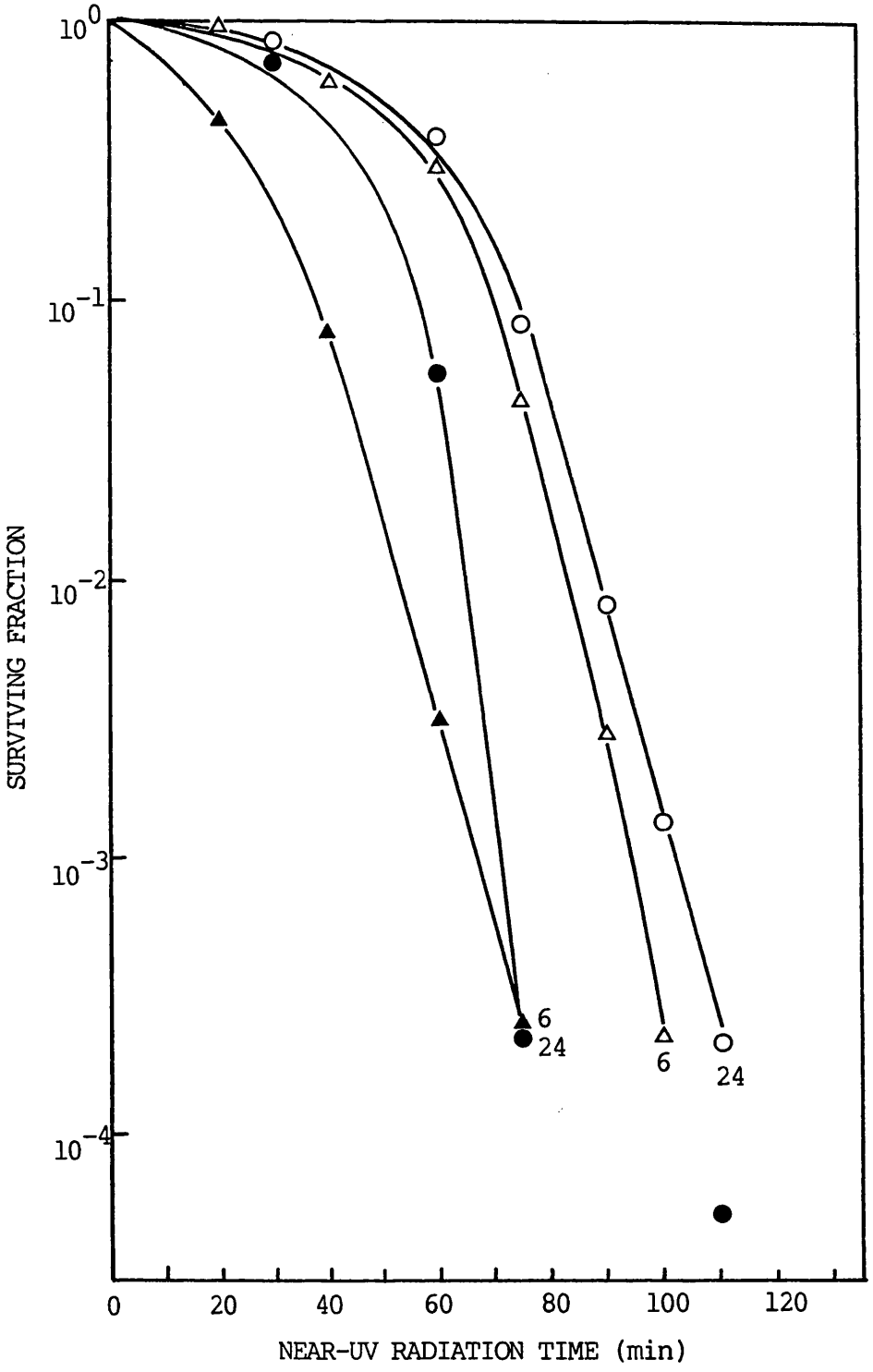

Figure 70

Survival curves after broad-band near-UV irradiation of E. coli K-12 AB 1157 grown for 6 (△,▲) or 24 (○,●) hours, with viability assessed on either low salt (△,○) or high salt (▲,●) minimal media.

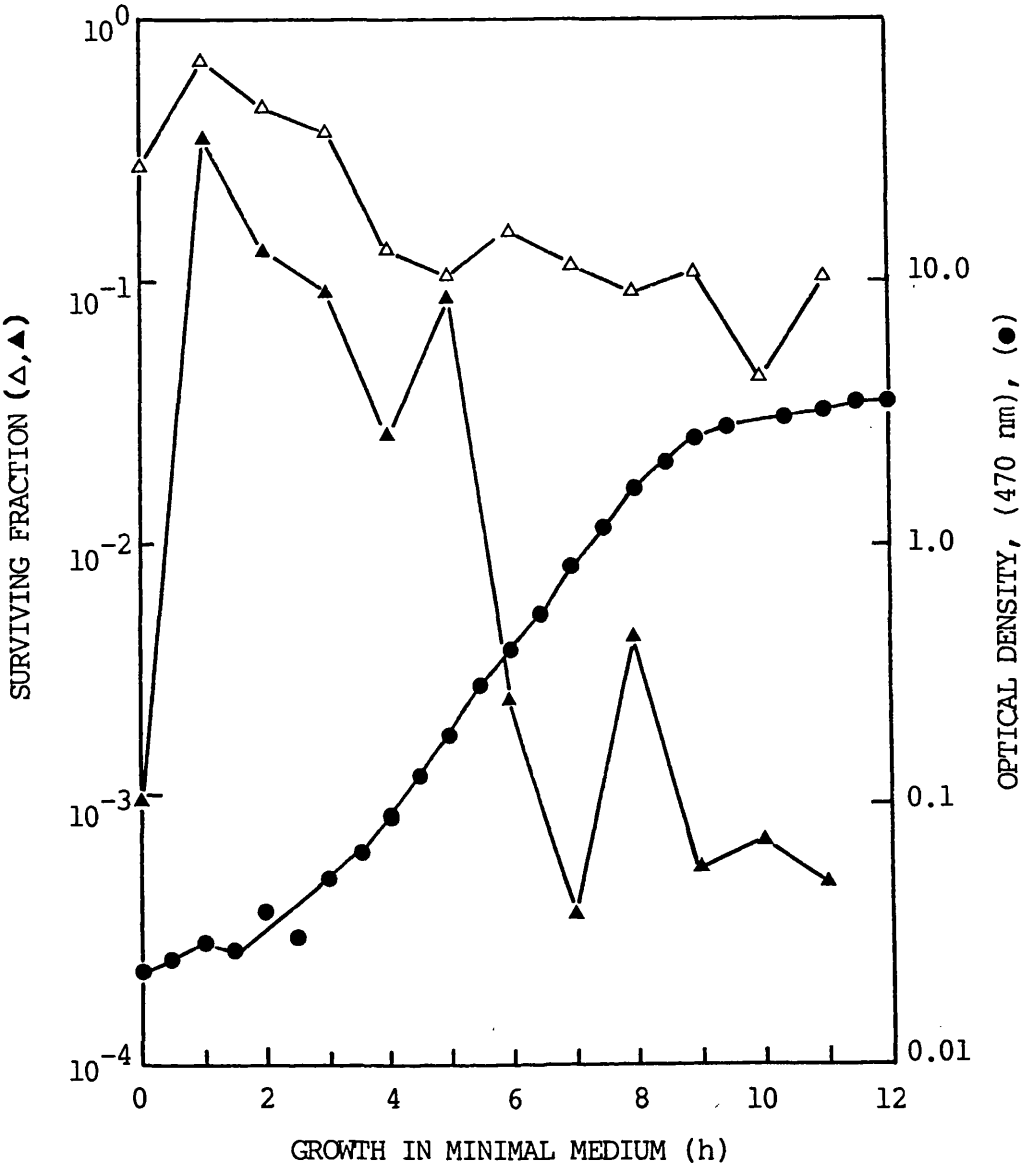

Figure 71

Surviving fractions for E. coli K-12 AB 1157 assessed on either low salt (△) or high salt (▲) minimal media after irradiation with 80 minutes of broad-band near-UV radiation; and optical densities at 470 nm (●), after growth in minimal medium for the number of hours indicated on the abscissa.

to near-UV radiation compared to 24 hour stationary phase cells. However, cells in late log phase which are about to enter the stationary phase of growth show a sensitivity comparable to that observed for 24 hour cultures, and hence increased sensitivity compared to early log phase cells. This effect is particularly apparent when assessing for viability on high salt minimal medium.

As a final comparison of the effects observed using K-12 SR 385, with other DNA repair-proficient E. coli strains, the sensitivity to near-UV radiation was tested for log and stationary phase cultures of E. coli NCTC 86, a wild-type strain. Figure 72 shows the survival curves obtained after near-UV irradiation of 3.5 hour and 24 hour cultures of E. coli NCTC 86. From a growth curve determined for this strain (as shown in Figure 73), it is evident that cells grown for 3.5 hours represent mid log-phase cells and cells grown for 24 hours represent stationary-phase cells. Figure 72 indicates that, whether viability is assessed on low or high salt minimal media, log phase cells of this wild-type strain are more sensitive to near-UV radiation than are stationary phase cells. It is also evident that a similar degree of salt sensitivity appears to be induced in log and stationary phase cells of NCTC 86.

Figure 73 shows the surviving fractions obtained on high and low salt minimal media for NCTC 86 at intervals of growth over a 24 hour period, after irradiation with a constant fluence (90 minutes as chosen from Fig. 72) of near-UV radiation. In addition, the figure includes a growth curve in minimal medium in terms of optical density measurements at 470 nm. The figure shows that cells in the early log phase of growth exhibit an increase in sensitivity to near-UV radiation

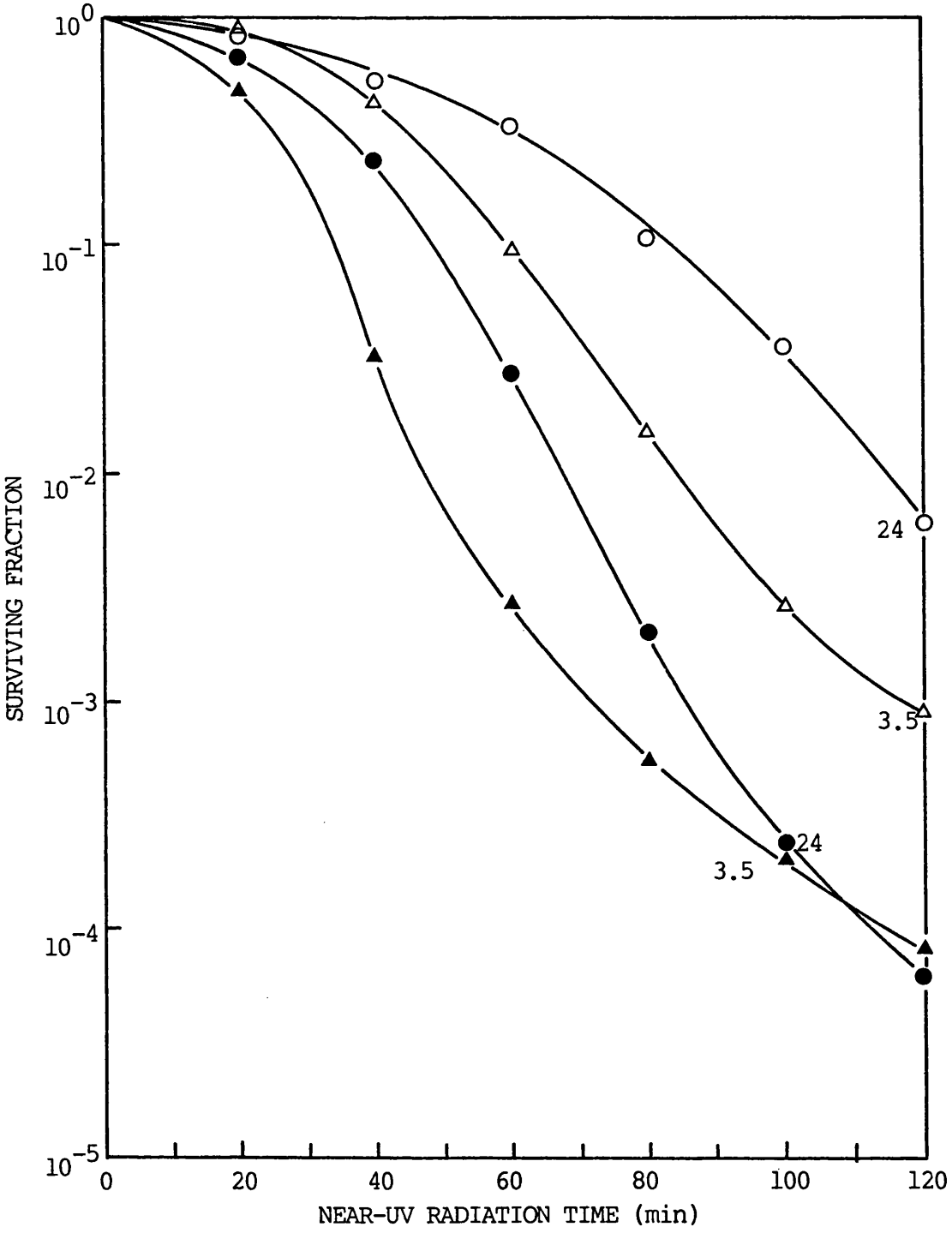

Figure 72

Survival curves after broad-band near-UV irradiation of *E. coli* NCTC 86 grown for 3.5 (△,▲) or 24 (○,●) hours, with viability assessed on either low salt (△,○) or high salt (▲,●) minimal media.

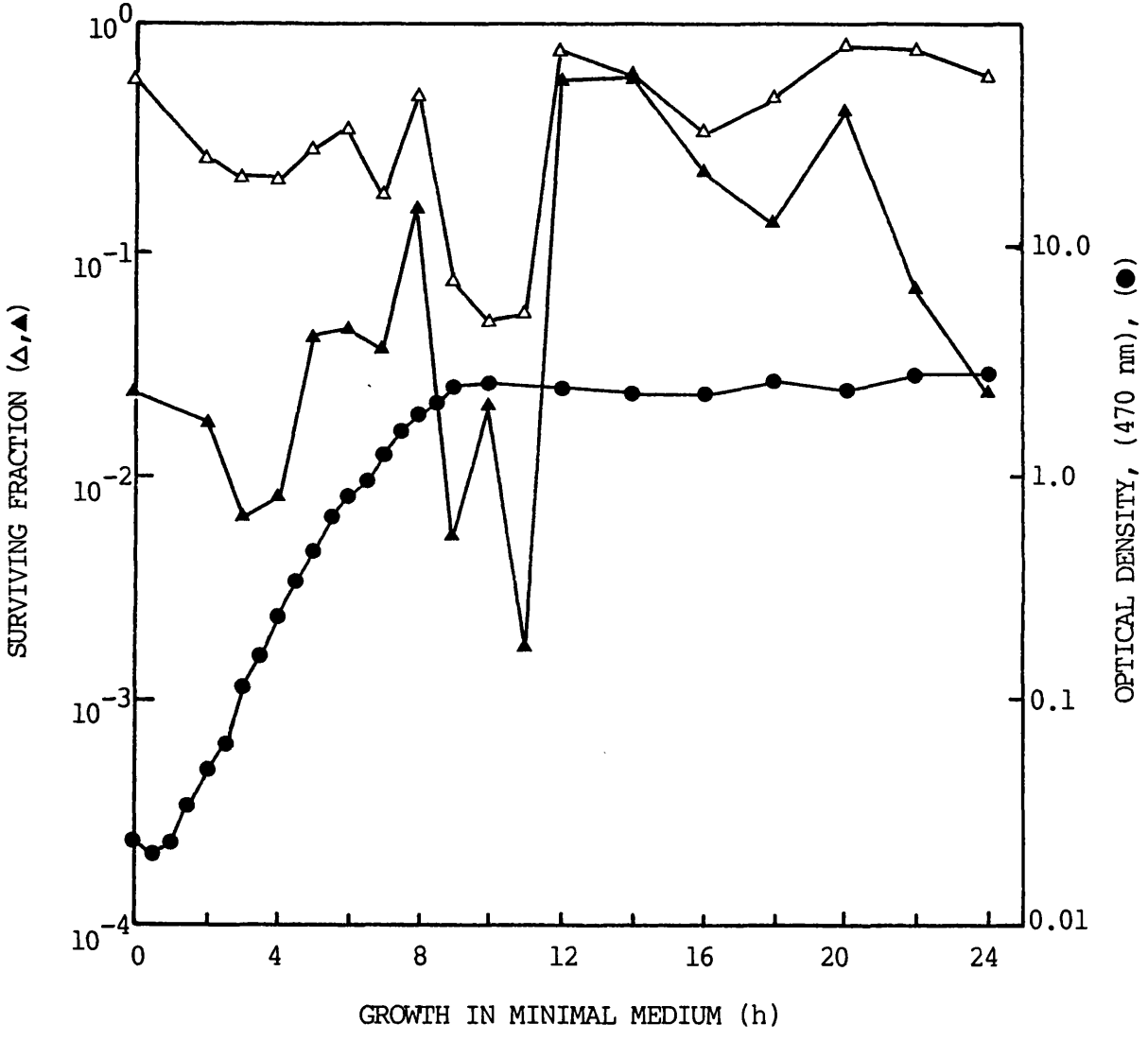

Figure 73

Surviving fractions for E. coli NCTC 86 assessed on either low salt (Δ) or high salt (▲) minimal media after irradiation with 90 minutes of broad-band near-UV radiation; and optical densities at 470 nm (●), after growth in minimal medium for the number of hours indicated on the abscissa.

compared to that observed for stationary phase cells, and cells in the late log phase of growth exhibit an even greater sensitivity.

DISCUSSION.

The results presented in this chapter illustrate the importance of carrying out experiments, involving the near-UV irradiation of E. coli, with cells that are in a particular phase of growth. Moreover, the results show that, for some DNA repair-proficient E. coli strains, e.g. B/r (Figs. 68 and 69) and NCTC 86 (Figs. 72 and 73), log phase cells show a greater sensitivity to near-UV radiation than do stationary phase cells, whereas for others, e.g. K-12 SR 385 (Figs. 60 and 63) and, to a lesser extent, K-12 AB 1157 (Figs. 70 and 71), the opposite effect is observed. The effects observed for B/r add support to the published findings of Peak (1970), and with NCTC 86 add support to the view that log phase cells show a greater sensitivity to near-UV radiation than do stationary phase cells (see Webb, 1977 for a review).

However, it is apparent that log phase cells of E. coli K-12 SR 385 show a decreased sensitivity to near-UV radiation compared to that observed for stationary phase cells, whether the cells are irradiated at 0°C (Figs. 66 and 67), 28°C (Figs. 60, 61 and 63), or 35°C (Fig. 64). Therefore, it may be concluded that the differences in the temperature of irradiation used by Peak (1970), who irradiated cells at 35°C, Tuveson and Jonas (1979), who irradiated at 10°C, and the irradiation temperature of 28°C used in these studies, does not significantly affect the relative sensitivity of log and stationary phase cells of K-12 SR 385.

The results obtained using K-12 AB 1157 (Figs. 70 and 71) indicate that the phase of growth is particularly important when determining this strain's sensitivity to near-UV radiation. Figure 71 shows that, compared to the sensitivity observed for 24 hour stationary phase cells, early log phase cells show a decreased sensitivity, whereas late log phase cells show an increased sensitivity. This observation helps to clarify the results observed with 6 and 24 hour cultures of this strain (as shown in Fig. 70), which indicate that 6 hour cells are slightly more sensitive to near-UV radiation than are 24 hour cells, thus leading to the general assumption that the log phase cells are more sensitive.

The results shown in Fig. 71 may also help explain the published findings of Tuveson and Jonas (1979), who observed that log phase cells of K-12 AB 1157 show a greater sensitivity to broad-band near-UV radiation (300-425 nm) than do stationary phase cells. However, it is not apparent from their paper whether these cells were in the early or late phase of the logarithmic part of the growth cycle; this being of importance, as the results described in Fig. 71 show that small changes in the phase of growth of K-12 AB 1157 dramatically affect its sensitivity to near-UV radiation. Tuveson and Jonas did, however, examine the kinetics of altered near-UV radiation sensitivity during growth, using a single cell population of K-12 AB 2463, a rec A derivative of K-12 AB 1157. They observed that near-UV irradiated cells of K-12 AB 2463 show a decrease in sensitivity as cells approach stationary phase. Furthermore, they observed that resistance to near-UV radiation continued to increase up to 24 hours growth. Therefore, these results do not show much similarity with those obtained for K-12 AB 1157 described in Fig. 71. However, these data do not provide

a good comparison with Fig. 71 as, firstly, a rec A derivative of K-12 AB 1157 was used and, secondly, the emission spectrum for the broad-band near-UV radiation source they used, which was from 300-425 nm, is different from the 320-400 nm range used in the present work.

Peak and Webb (unpublished but cited by Webb, 1977) have tested the 365 nm sensitivity of four strains of E. coli K-12 differing in repair capability (including AB 1157) at differing stages of the growth cycle. They described the pattern of sensitivity for 365 nm radiation as being similar to that reported by Tyrrell et al. (1972) for 254 nm radiation in that strains capable of excision repair, AB 1157 and AB 2463 (rec A), showed much greater sensitivity to near-UV radiation in log phase. On examination of the 254 nm radiation data of Tyrrell et al. (1972), it is apparent that the observed variation of sensitivity with stage of growth for K-12 AB 1157 is similar to that shown in Fig. 71 after broad-band near-UV irradiation of this strain; i.e. a sharp decrease in sensitivity was observed in early log phase and then a large increase in sensitivity was observed in late log phase.

From the results presented in this chapter, it is difficult, for a number of reasons, to provide an adequate explanation for the variations in sensitivity to near-UV radiation in different phases of growth shown by the four DNA repair proficient E. coli strains tested. In particular, it is difficult to explain, at present, why two of the strains tested, K-12 SR 385 and K-12 AB 1157, show that log phase cells are more resistant to near-UV radiation than are stationary phase cells, whereas B/r and NCTC 86 show the opposite effect. This difficulty arises firstly, as a consequence of using batch cultures

since, unless very low numbers of cells for inoculation are used, the log phase of growth in minimal medium for these strains is relatively short compared to the stationary phase of growth. As a result of this relatively short period of time when cells are in the log phase, the effects observed with cells described as being in log phase may be complicated by the population initially retaining some of the characteristics of the lag phase during the early part of the log phase, and conversely showing a progressive change towards the stationary phase during the latter part of log phase. A clearer indication of the reasons for the near-UV radiation sensitivity differences shown between log and stationary phase cells might be gained by studies involving the use of continuous cultures, in which a stable cell population showing the characteristics of log phase cells might be obtained.

Another factor which complicates the interpretation of results with batch phase cultures concerns the stage of the cell cycle of the individual cells which make up the population. There is some indication from the regular fluctuations in sensitivity to near-UV radiation, shown by SR 385 during its early log phase of growth (Figs. 61, 63 and 67), that some degree of synchronous growth of the cell population might be occurring. The use of synchronous cultures might help to explain this result and determine the importance of the stages of the cell cycle on near-UV radiation sensitivity of individual cells. Although this approach has not been attempted after near-UV radiation, some studies have been carried out after far-UV radiation. Two of the main studies using far-UV radiation give different answers. Helmstetter and Uretz (1963) used synchronously dividing populations of E. coli B and found a sharp drop in sensitivity in the middle and at

the end of the division cycle, whereas Kubitschek et al. (1973) separated E. coli B/r and Bs-1 by size (and thus cell age) on sucrose gradients and found no differences in sensitivity throughout the cell cycles for either strain.

Another difficulty in making predictions as to the reasons for the near-UV radiation sensitivity differences, shown by these data for log and stationary phase cells, is that so far very few attempts have been made to understand the molecular basis of such differences. In particular, few studies, involving the identification and measurement throughout the growth stages of strains of possible chromophores involved in producing cell sensitivity to near-UV radiation, have been carried out.

A possible insight into the basis of the variability in sensitivity to near-UV radiation, shown by the four DNA repair proficient strains under investigation in this study, may be obtained from data involving 254 nm irradiation of these strains. It is well established that E. coli cells are more sensitive to 254 nm radiation (where damage to DNA is known to be the principal cause of lethality) during the log phase than during the stationary phase of growth (e.g. Durham and Wyss, 1956). However, Ginsberg and Jagger (1965) have shown that, with a given fluence of 254 nm radiation, the induced amount of initial damage to DNA is independent of growth phase, despite differences observed in survival. Hanawalt (1966) then suggested that the cause of 254 nm sensitivity of repair proficient strains in log phase of growth is the onset of DNA replication after the occurrence of excision, but before the completion

of the polymerization and rejoining steps. Thereafter, attempted replication of the resultant single-strand regions of DNA would result in lethal configurations.

More recently, Morton and Haynes (1969) have tested the far-UV radiation sensitivity of E. coli B/r during growth in batch cultures and found that a period of increased sensitivity is shown by cells in late log phase, the increased sensitivity being associated with a decreased shoulder of UV survival curves. They attributed the increased sensitivity of late log phase cells to a depletion of the intracellular activity or concentration of one or more of the enzymes responsible for the repair of DNA. A similar type of experiment was then performed by Tyrrell et al. (1972), who used four strains of E. coli K-12 differing in DNA repair capability, including K-12 AB 1157. The response pattern for K-12 AB 1157 was similar to that observed by Morton and Haynes for E. coli B/r, except that a more pronounced decrease in sensitivity was observed for early log phase cells, before a similar large increase in sensitivity was observed for late log phase cells.

This pattern of response after 254 nm irradiation is very similar to the data shown in Fig. 71, obtained after broad-band near-UV irradiation of K-12 AB 1157. In addition, as with the far-UV radiation data of Morton and Haynes and Tyrrell et al., the survival curves obtained after near-UV irradiation of log and stationary phase cells of AB 1157 (Fig. 70) and of the other strains tested (Fig. 60 for SR 385 ; Fig. 68 for B/r ; and Fig. 72 for NCIC 86), indicate that the observed sensitivity differences are largely associated with a decrease in the shoulder of the survival curves. From data involving K-12 mutants

deficient in excision and/or post-replication repair of damaged DNA, Tyrrell et al. concluded that the pattern of response observed with AB 1157 was due to a decrease in excision efficiency, which, during early log phase, was small enough to be compensated for by the post-replication repair mechanism. However, as the efficiency of excision decreased throughout the log phase, for late log phase cells, they concluded that this reduction in efficiency was such that the post-replication system could no longer cope, resulting in an increased sensitivity to far-UV radiation. During stationary phase, the efficiency of excision repair increased, resulting in the increased recovery of AB 1157 cells.

While there are empirical similarities between the changes in sensitivity throughout the growth phase after far and near-UV radiation, the reasons for these changes may not necessarily be the same. After far-UV radiation, it may be assumed that the changes reflect differences in the efficiency of DNA damage. However, there is evidence, including that presented in Chapters 1 to 3, that near-UV radiation induces damage to other cell components, in particular to membranes, which may be important. For example, the additional sensitivity to 365 nm radiation shown by cells of B/r in the log phase of growth may be partially due to membrane-damaging effects. Some indirect evidence to support this may be gained from the well established observation that, as cells enter the stationary phase of growth, the unsaturated fatty acids of the membranes are converted to less chemically reactive saturated fatty acids (Cronan, 1968).

However, if the higher unsaturated fatty acid content of membranes, and hence the provision of more targets for singlet oxygen to form peroxides and hydroperoxides, is the reason for log phase cells of B/r

(and NCTC 86, and to some extent K-12 AB 1157) showing a greater sensitivity to near-UV radiation than do stationary phase cells, this does not explain the data regarding K-12 SR 385, where the opposite occurs. This interpretation is further complicated by the work of Klamen and Tuveson (1982), using E. coli K1060, who observed that, although this strain does not efficiently convert the double bonds in its membrane fatty acids to saturated cyclopropane analogues (13% versus the expected 25-30%), log phase cells are again more sensitive to near-UV radiation than are stationary phase cells. They have concluded that, for K1060, the unsaturated sites are not such important near-UV radiation targets in stationary phase cells as they are in log phase cells.

A possible explanation, regarding the growth phase effects on the sensitivity to near-UV radiation for K-12 SR 385, may be proposed from preliminary investigations by K. C. Smith (personal communication) regarding the determination of catalase levels in log and stationary phase cells of this strain. They have found that stationary phase cells contain less catalase (a scavenger of peroxide radicals) than do log phase cells. Furthermore, Cheng et al. (1981) have shown the in vitro photoinactivation of catalase by near-UV radiation at wavelengths above 350 nm. Therefore, if catalase levels are important in affecting near-UV radiation-induced cell sensitivity, and, during the stationary phase of growth, there is less catalase to prevent the build-up of peroxide (which is produced as a natural consequence of the cells' metabolism), potential damage to membranes is therefore increased for cells in the stationary phase of growth.

Some support for this may be gained by comparing the data obtained

for SR 385 on low and high salt minimal media, which, from the discussions of Chapters 1 to 3, may be used as a measure of membrane damage. Although the data, involving determinations of sensitivity to a constant fluence of radiation throughout the growth cycle, do not lend themselves to such a comparison, due to different survival levels being apparent, some conclusions may be drawn from the survival curves shown in Figs. 60,64 and 66. These data indicate that, for SR 385, membrane damage is more important in near-UV radiation-induced cell lethality of stationary phase cells than of log phase cells.

A detailed discussion of the evidence to support the role of catalase in near-UV radiation-induced cell lethality was presented in Chapter 1. However, more recently, some additional indirect evidence to support such a mechanism has been reported by Demple et al. (1983) who have shown that E. coli xth A mutants (strains lacking exonuclease III) are hypersensitive to hydrogen peroxide. Moreover, Sammartano and Tuveson (1983) have shown that xth A mutants are particularly sensitive to broad-band (300-400 nm) near-UV radiation, whereas they are no more sensitive to far-UV radiation than are DNA repair-proficient strains. Therefore, the accumulation of peroxide radicals, as a result of near-UV radiation-induced catalase destruction, might be important in the effects observed with K-12 SR 385. Further work involving the determination of catalase levels in other DNA repair proficient strains, including K-12 AB 1157, B/r and NCTC 86, may help elucidate the explanation for the growth phase effects observed in this study for these strains, where generally membrane damage, as measured by the differing survival responses on low and high salt minimal media for complete survival curves (Figs. 68, 70 and 72 for B/r, AB 1157 and NCTC 86 respectively), appears to be more important in the inactivation of log phase cells than of stationary phase cells.

CHAPTER 5

THE EFFECT OF NEAR-UV RADIATION-INDUCED SENSITIVITY TO INORGANIC SALT ON THE ASSESSMENT OF MUTAGENESIS BY REVERSION TO PROTOTROPHY.

One of the possible consequences of near-UV radiation-induced cell sensitivity to inorganic salts, as shown in Chapters 1 and 2, may be in the interpretation of experiments where minimal medium plates are used. One important example of such experiments is the 'classical' scoring of mutations by reversion to prototrophy. The usual experimental protocol adopted for the assessment of mutagenesis by reversion to prototrophy is based on the method of Green et al. (1972) and is shown diagrammatically (in this case for histidine) in Figure 74. The data shown in Figure 74 are not experimentally obtained, but presented only to aid explanation of the calculation of the induced mutation frequency. The figure shows that firstly, for a series of UV radiation fluences, a survival curve is determined by an appropriate serial dilution of the irradiation suspension, followed by assessment for viability on minimal medium plates. Secondly, at each fluence interval, using the same irradiation suspension, the number of induced mutants is determined by plating an appropriate volume of undiluted irradiation suspension onto the same type of minimal medium as used in the assessment of viability.

The minimal medium plates used contain a low level supplement of the required amino acid (i.e. histidine) in order to allow sufficient growth, following irradiation, for any induced mutation to be expressed. The low level supplement of amino acid may be supplied in the form of the amino acid itself, e.g. histidine, that is histidine supplemented media (HSM), or in the form of 2 to 3% nutrient broth, that is semi-enriched media (SEM). The usual concentration of histidine in HSM is 0.8μg/ml. Using these two media, mutations appear as single discernible colonies against a background lawn of residual auxotrophic growth, the background lawn being due to growth of non-mutants, which ceases when the low level of histidine supplement is exhausted.

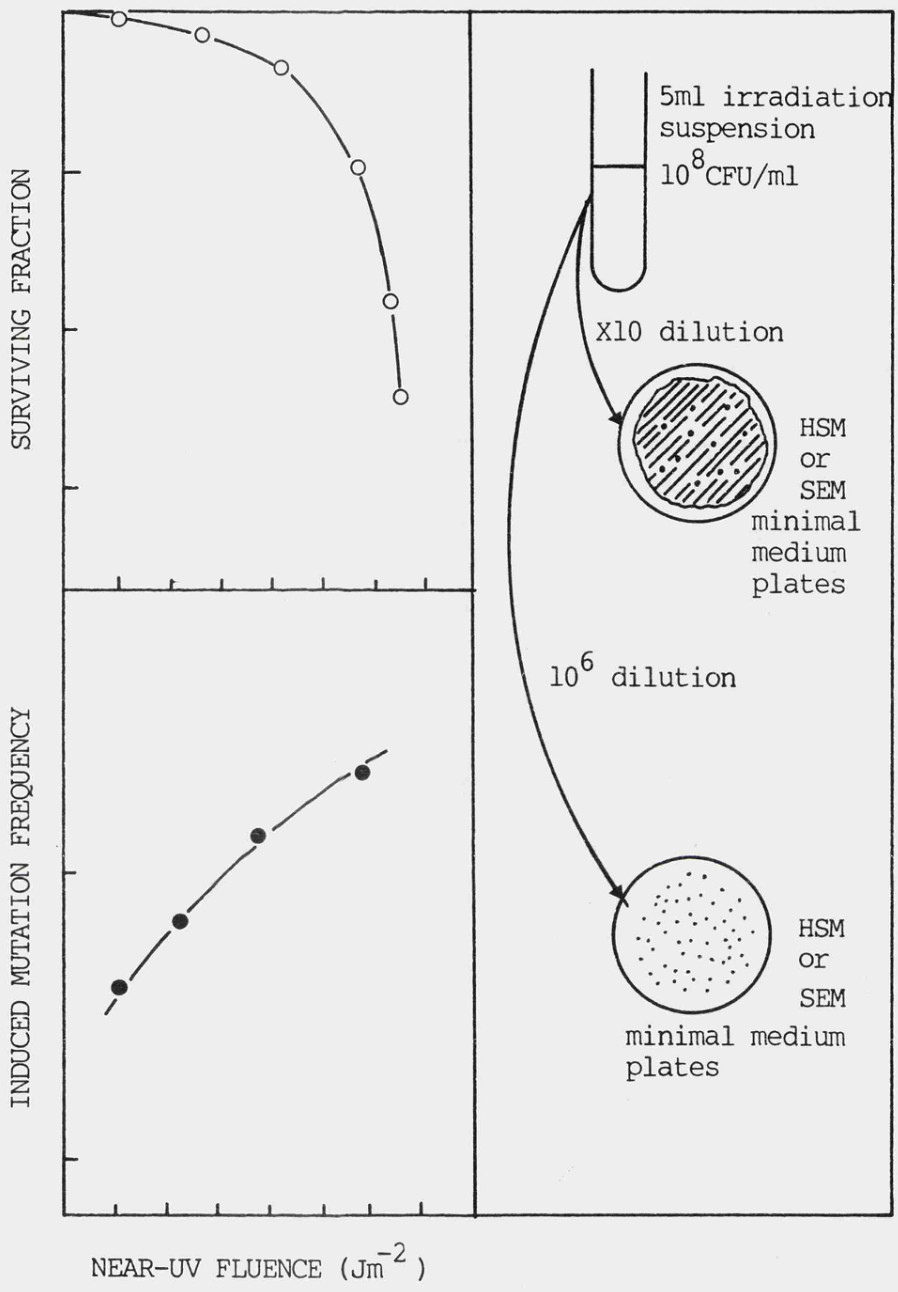

Figure 74

Usual method for the assessment of mutagenesis by reversion to prototrophy after near-UV irradiation of *E. coli*.

At each fluence interval, the fraction of mutations per survivor, termed the induced mutation frequency (M), is calculated from the number of mutants observed and the corresponding viable count. On calculating the induced mutation frequency, it is necessary to correct for any 'spontaneous' mutants, as failure to do so will lead to over-estimation of the mutation frequency. Spontaneous mutants may be of two types; namely 'pre-existing mutations', which are present in the bacterial suspension prior to irradiation and will be expressed in the absence of any amino acid supplement, and 'plate mutations', which arise during the period of growth on the selective media and are consequently dependent upon the level of amino acid supplementation for their expression. The number of pre-existing mutants is estimated by plating unirradiated samples onto minimal agar plates containing no histidine, while the number of plate mutants is estimated by plating unirradiated samples onto HSM and SEM plates and then correcting for pre-existing mutants. The induced mutation frequency (M), at each fluence interval, is then calculated using the following formula:

$$M = \frac{(a-b)-cA}{A} \qquad (5i)$$

where a is the number of mutant colonies observed
b is the number of plate mutants
c is the pre-existing mutation frequency
and A is the number of viable cells plated

In using this formula, it is assumed that the number of plate mutants is not affected by the radiation treatment, and that the pre-existing mutants are inactivated during irradiation to the same extent as the non-mutants. Webb (1978) has suggested another method of calculating the induced mutation frequency which does take into account the possibility that the number of plate mutants may alter during

irradiation. However previous work in this laboratory (Hodges, 1979) has shown that the two methods give very similar results ; therefore, the induced mutation frequency was calculated, in this study, by application of equation (5i).

The majority of UV radiation-induced mutagenesis studies have been carried out using 254 nm radiation, where damage to DNA is known to be the principal cause of lethality. After irradiation of cells with wavelengths above 320 nm, where damage to DNA has clearly been demonstrated, and with the existence of error-prone repair systems involved in the repair of such damage, it is perhaps surprising that most early efforts to induce mutations at these wavelengths were either unsuccessful or of doubtful validity (see Eisenstark, 1971 for a review). Although more recently, near-UV radiation-induced mutagenesis has been demonstrated, it has been consistently difficult to observe in DNA repair-proficient E. coli strains. In particular, mutagenesis has been difficult to observe when using broad-band near-UV radiation sources. For example, Webb (1977) reported that monochromatic radiation, at 254, 313, 334 and 365 nm, induced mutation to tryptophan independence in E. coli B/r trp, but no mutations were observed in this strain when it was exposed to broad-band near-UV radiation (Black-Light Blue lamp ; 313-405 nm), although cell killing was observed.

In addition, Turner and Webb (1981) using a series of E. coli strains differing in repair capability, reported that, after 254 nm irradiation, mutants were observed in all strains except the lex A and rec A mutants, whereas after broad-band near-UV radiation, in addition to the lex A and rec A mutants, no significant mutation

induction was apparent for the pol A and wild-type, for DNA repair, strains. Webb and Turner (1981) then used monochromatic 365 nm radiation instead of the broad-band source and observed some degree of mutation induction in the pol A and repair-proficient strains but only at fluences where more than 90% of the population had been inactivated. A review of these effects and a discussion of the proposed reasons for them has been presented in the introduction.

As a consequence of near-UV radiation inducing a sensitivity to inorganic salts in DNA repair-proficient E. coli cells (as shown by Moss and Smith, 1981 ; and in Chapter 1), the absence of observable mutants, after broad-band near-UV irradiation of such cells, may be due to membrane damage being the dominant lethal factor under the conditions of the experiment. For example, cells receiving sub-lethal damage to their DNA, which might be expected to be scored as mutations, may be inactivated by damage to their membranes when assessed for viability on minimal media plates.

In addition, where mutants have been observed after near-UV irradiation of cells, the induced mutation frequency may also be affected by the use of minimal medium plates leading to membrane damage. From results presented in Chapter 1, near-UV radiation-induced sensitivity to inorganic salts (and hence membrane damage) may be expected to be more important in the plates used to assess viability than in the plates used to observe mutants. This is because, with the plates used to assess the number of induced mutants, there is a much higher number of cells present which may act, as with the

Casamino Acids (Fig. 29), to provide a protective effect against the radiation-induced membrane damage. Further evidence to support this protective role on the plates used for the assessment of induced mutants, was discussed in Chapter 1, where it was observed that near-UV radiation survival curves, for cells plated on minimal media, often showed greater surviving fractions, at high fluences and hence a large amount of inactivation, than would be predicted from an extrapolation of the straight line portion of the survival curves. This effect was attributed to large numbers of 'dead' cells providing nutrients to promote protection from membrane damage.

Furthermore, the assessment of mutagenesis may be dependent upon the type of minimal medium plates used in the experiments, as the SEM plates, containing 2 to 3% nutrient broth, may be expected to offer more protection from membrane damage than the entirely minimal HSM plates. Some evidence to support this has been reported by Webb (1978), who showed, using E. coli WP2s (uvrA, trp) irradiated at 365 nm, that cell survival was lower on trp M plates than on SEM plates. In addition, on the trp M plates when compared to the SEM plates, mutagenesis was reduced by an even greater extent than was survival. Moreover, at 254 nm, survival and mutagenesis were slightly higher on the trp M plates than on the SEM plates. Therefore, if the cell surviving fractions for near-UV irradiated cells are dependent upon the concentration of inorganic salt in the plating medium, then the induced mutation frequency, which is calculated in terms of the number of viable cells, must also be affected.

The purpose of this study was to attempt to protect cells against the lethal effects of membrane damage during near-UV radiation-induced assessment of mutagenesis by reversion to prototrophy. The method chosen to achieve protection was to use minimal medium plates containing a lower inorganic salt concentration than normally present in minimal media. Then, if membrane damage was the reason for the lack of observed mutants, the use of lower salt concentrations in the minimal media would result in the detection of 'normal' numbers of mutants after near-UV irradiation of DNA repair-proficient E. coli cells.

Methodology.

In addition to the media described in the general methodology section, the following media were employed during the studies presented in this chapter.

(a) 'Amino acid mixture'.

This was prepared by dissolving 4.0g L-threonine, L-proline, L-leucine and L-arginine (all obtained from Sigma Chemical Company) in about 1500ml of glass distilled water. Then 10ml of a 1mg/ml solution of thiamine HCl (prepared as described in the general methodology section) was added, and the solution made up to 2 litres with glass distilled water. This final solution, termed the 'amino acid mixture' was then sterilized by filtration, using a 0.2 μm pore-size membrane filter, and stored in 40ml aliquots. For each 800ml volume of agar, 40ml of the amino acid mixture was then added.

(b) L-histidine solution.

This was prepared as a 640 μg/ml solution by dissolving 640mg

L-histidine (obtained from Sigma Chemical Company) in, and making up to 100ml with, glass distilled water. Ten ml of this solution was then diluted to 100ml with glass distilled water and this final solution sterilized by filtration as above. To give a final concentration of 0.8 μg/ml in the plating medium, this stock solution requires a 1 in 800 dilution.

(c) Plating media.

The plating media used in this chapter were of two main types; those being semi-enriched media (SEM) and histidine supplemented media (HSM). The compositions of these media are shown in Table 11. The media were prepared in the same manner as described in the general methodology section for minimal media plates, i.e. the agar and appropriate amount of water was sterilized by autoclaving at 121°C for 15 minutes and the appropriate sterile supplements added after allowing the agar to cool to approximately 60°C. Where indicated, the inorganic salt contents of these media were diluted ten-fold or two-fold. In addition, where indicated, sodium chloride at varying molarities was added to the minimal media.

(d) MOPS buffer.

In one particular experiment the M9 salts solution, the buffer normally present in the minimal media plates, was replaced with MOPS buffer. This was prepared from its individual ingredients according to the general method of Neidhardt et al. (1974). Firstly, 250ml of a 10X concentrate was prepared by mixing the following solutions in the given order, to prevent precipitation of various salts : potassium morpholinopropane sulphonate (MOPS), freshly prepared, 1.0 M i.e. 23.13g/100ml adjusted to pH 7.4 with potassium hydroxide (100ml); N-Tris (hydroxymethyl) methyl glycine (Tricine), freshly prepared,

Table 11.

Composition of main plating media used in Chapter 5.

All volumes are in millilitres for 1x800ml batch.

Ingredient	PLATE TYPE				
	SEM	1/10th SEM	HSM	1/10th SEM	Histidine
Agar No 3	9.6g	9.6g	9.6g	9.6g	9.6g
M9 A concentrate	16	1.6	16	1.6	16
M9 B concentrate	16	1.6	16	1.6	16
Glucose 40%	8	8	8	8	8
'Amino Acid' Mixture	40	40	40	40	40
L- Histidine 640 µg/ml	-	-	1.0	1.0	-
Nutrient Broth	24	24	-	-	-
Distilled water	648	720	671	743	672

1.0M i.e. 17.92g/100ml adjusted topH 7.4 with potassium hydroxide (10ml); $FeSO_4.7H_2O$, freshly prepared, 0.01M i.e. 0.278g/100ml (2.5ml); NH_4Cl, 1.90M i.e. 10.163g/100ml (12.5ml); K_2SO_4,0.276M, i.e. 4.81g/100ml (2.5ml); $CaCl_2.2H_2O$, 5×10^{-4}M i.e. 73.5mg/l (2.5ml); $MgCl_2.6H_2O$, 0.528M i.e. 10.735g/100ml (2.5ml) and glass distilled water (117.5ml). Total volume is 250ml. This concentrate was then sterilized by filtration using a 0.2 μm pore size membrane filter. Note, this MOPS concentrate differs from that described by Neidhardt et al. (1974) in that it does not contain any NaCl or any 'micronutrients' solution.

For use in minimal medium plates as a replacement for the M9 salts solution buffer, 80ml of the MOPS concentrate and 8ml of 0.132 M K_2HPO_4 (termed 'MOPS buffer') were added, and the volume of water adjusted accordingly. 0.132M K_2HPO_4 solution was prepared by dissolving 2.299g K_2HPO_4 in, and making up to 100ml with glass distilled water, and sterilizing by autoclaving at 121°C for 15 minutes. Where indicated, the MOPS buffer was diluted ten-fold and also, where indicated, the NaCl content of MOPS buffer as described by Neidhardt et al., was included by adding 2.5ml of a 5.0M solution (prepared by dissolving 29.22g in, and making up to 100ml with, glass distilled water and sterilizing as for the K_2HPO_4 solution).

The strain chosen for this investigation was E. coli K-12 AB 1157, a DNA repair-proficient strain, which requires the amino acids threonine, arginine, leucine, proline and histidine for growth. Reversion to histidine independence in this strain has been used previously in this laboratory to study UV radiation-induced mutagenesis (Hodges, 1979; Ahmed, 1983). In addition, due to the low number of near-UV radiation-

induced mutants obtained with this strain, its excision-repair deficient derivative, AB 1886, was also used in some experiments.

The general method of assessment of mutagenesis was that based on the protocol of Green et al. (1972), described previously. 24 hour stationary phase cultures of the test organism were grown in Oxoid nutrient broth and prepared as a suspension for irradiation by centrifugation or filtration, as described in the general methodology section. Cells were then irradiated with broad-band near-UV radiation and viability assessed on various minimal media, as indicated for each experiment, as described in the general methodology section. The number of induced mutations was assessed by plating 0.05ml of the irradiated suspension, at each fluence interval, onto the surface of minimal media plates, three of each of the types used for the assessment of viability. All plates were incubated at 37°C; plates for the determination of surviving fractions for 3 days and plates for the determination of induced mutants for 4 days.

Results

Initially, survival and mutation induction after broad-band near-UV irradiation of E. coli K-12 AB 1157, at an initial concentration of 5×10^7 CFU/ml, was assessed using both SEM and HSM plates but either with tenfold-diluted inorganic salt content, i.e. low salt medium, or with tenfold-diluted inorganic salt content plus sodium chloride added at 200mM, i.e. high salt medium. The data obtained are shown in Figure 75. From the data shown in this figure, it is clear that an enhanced sensitivity to near-UV radiation is observed for cells plated on the high salt SEM or HSM compared to that observed for cells plated

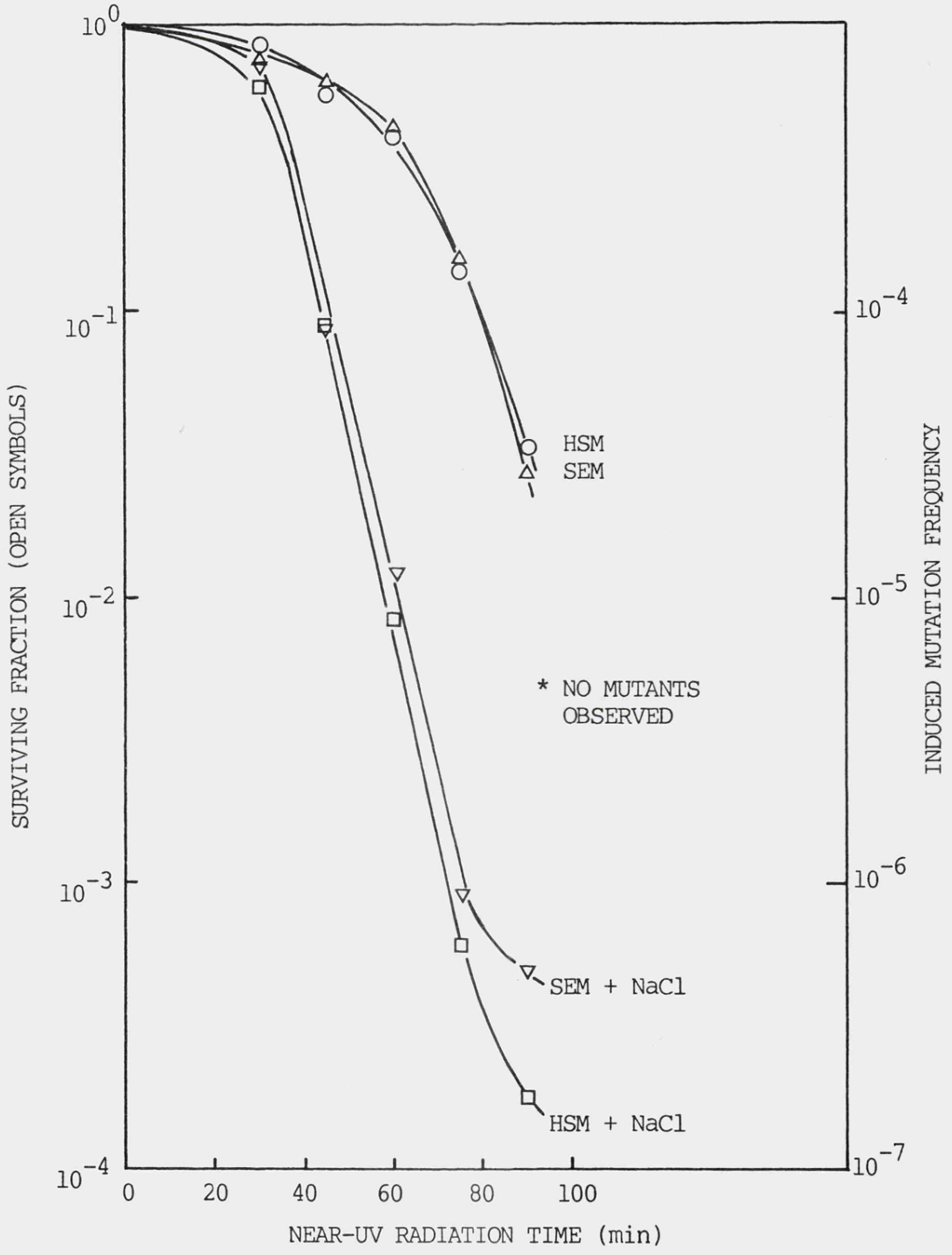

Figure 75

Surviving fractions obtained following broad-band near-UV irradiation of K-12 AB 1157 assessed on either SEM (Δ) or HSM (O) with tenfold-diluted inorganic salt content; or SEM (▽) or HSM (□) with tenfold-diluted inorganic salt supplemented with sodium chloride at 200mM.

Note: No mutants were detected on any of the media.

on low salt SEM or HSM. However, there is no significant difference in sensitivity observed between plating on the respective high and low salt SEM and HSM, and moreover, no mutants were observed for irradiated or unirradiated cells on any of the different plate types, although a background 'lawn' of growth was apparent.

A number of reasons may be proposed for this lack of induced mutants shown in Fig. 75. Firstly, the initial concentration for irradiation of $5x10^7$CFU/ml may be too low to detect the induced mutation frequencies obtainable with this strain under the experimental conditions employed. Secondly, the broad-band near-UV radiation source may indeed be non-mutagenic for this DNA repair proficient strain; and thirdly, the low concentration of phosphates in the plating media, which may result in a reduced buffering capacity, may be too low for the expression of mutations.

In an attempt to elucidate the reasons for the lack of mutants observed in Fig. 75, firstly a uvrA derivative of K-12 AB 1157, namely AB 1886, was employed. Previous workers have shown that this strain produces workable induced mutation frequencies after broad-band near-UV irradiation (e.g. Tyrrell, 1978b). Secondly, survival and mutation induction were assessed on plates of HSM and SEM containing low, normal and high inorganic salt concentrations (i.e. one-tenth diluted inorganic salt content, normal inorganic salt content, and one-tenth diluted inorganic salt content plus sodium chloride added at 200mM). The data obtained from such an experiment, where AB 1886, at an initial concentration of $6x10^8$CFU/ml, was irradiated with broad-band near-UV radiation, are shown in Figure 76. The figure indicates that, firstly, mutations are only detectable on the SEM and HSM plates

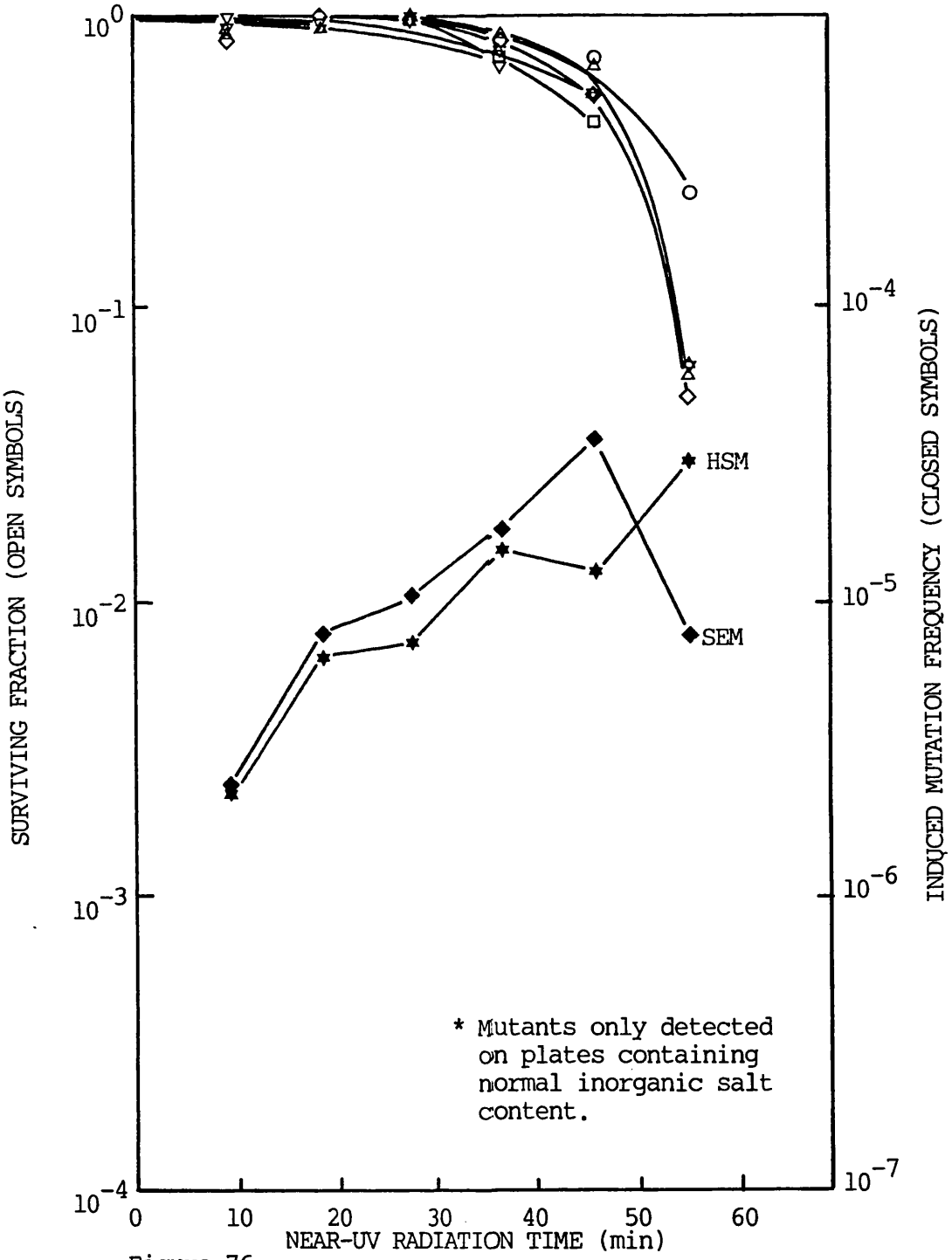

Figure 76

Induced mutation frequencies (closed symbols) and surviving fractions (open symbols) obtained following broad-band near-UV irradiation of K-12 AB 1886 (uvr A) assessed on either SEM [with low (Δ), normal (◆,◇) and high (▽) inorganic salt content] or HSM [with low (O), normal (✱,✲) and high (□) inorganic salt content] . Irradiation times have been corrected to allow for absorption.

containing the 'normal' inorganic salt concentration, with little difference in the induced mutation frequencies being observed between the SEM and HSM plates. Secondly, for this strain, little difference in survival was observed by plating on the low, normal and high salt media. It should be noted that, at this high initial cell concentration ($6x10^8$CFU/ml), the absorbed fluence was significantly reduced, relative to the incident fluence, and the time scale has been corrected using the method of Morowitz (1950) as modified by Jagger et al. (1975). The results of a series of absorption measurements, taken by placing a thermopile directly behind a cuvette containing a range of concentrations of the cell suspension (K-12 AB 1886) illuminated with Black-Light Blue radiation, are given in Appendix A7. The data indicate that no fluence correction was required when using initial cell concentrations up to approximately $5x10^7$CFU/ml while, when using $6x10^8$CFU/ml as in the experiment described in Fig. 76, a fluence correction factor of 0.9 was necessary.

Therefore, from the data described in Fig. 76, the concentration of inorganic salts in the plating media appears to be important for the expression of mutations. In order to determine the exact requirements within the M9 buffer solution for mutation expression, an experiment, again involving broad-band near-UV irradiation of AB 1886, was performed, and viability and mutation induction assessed on a number of histidine supplemented media containing varying fractions of the constituents of the M9 buffer solution. The following histidine supplemented media were used : HSM; HSM with tenfold-diluted inorganic salts containing either NH_4Cl or $MgSO_4.7H_2O$ in the same concentrations as present in normal strength M9 salts solution i.e. 18.7 and 0.81mM, respectively; HSM with a twofold-dilution of inorganic salt content; and HSM containing additional sodium chloride at 100 and 200mM. The

results obtained are shown in Figure 77, again with the fluence corrected to take into account the absorption of radiation due to the high initial cell concentration used. The figure indicates that mutants are only detected on HSM containing the full inorganic salt content of M9 salts solution ; a two-fold reduction in inorganic salts, or a ten-fold reduction in inorganic salts but in the presence of normal concentrations of NH_4Cl or $MgSO_4.7H_2O$, not being sufficient for the expression of mutations. In addition, the figure indicates that, for AB 1886, an enhanced sensitivity to near-UV radiation is observed for cells plated on HSM containing additional sodium chloride at 100 or 200mM, a still higher concentration than used with AB 1157 or SR 385 in previous studies, but mutation induction did not appear to be significantly affected by the presence of these very high concentrations of inorganic salt in the plating media.

From the data described in Fig. 77, it is probably the phosphate content of the M9 salts buffer which is required for the expression of mutations in K-12 AB 1886. Consequently, this is also probably apparent for the expression of mutations in K-12 AB 1157. This requirement for phosphates was then verified by the use of HSM plates containing M9 B concentrate only, i.e. the phosphate part of the salts solution at the normal concentration of 57.7mM but no $MgSO_4.7H_20$ or NH_4Cl present, where, after broad-band near-UV irradiation of K-12 AB 1157, at an initial concentration of $2x10^8$CFU/ml, mutants were detected on these plates. However, the numbers of mutants obtained were very low (average of 1 to 6 per plate) and so were not represented in a figure.

In an attempt to obtain workable numbers of mutants using K-12 AB 1157, the inital cell concentration for irradiation was increased to $2x10^9$CFU/ml. However, even initial concentrations as high as this

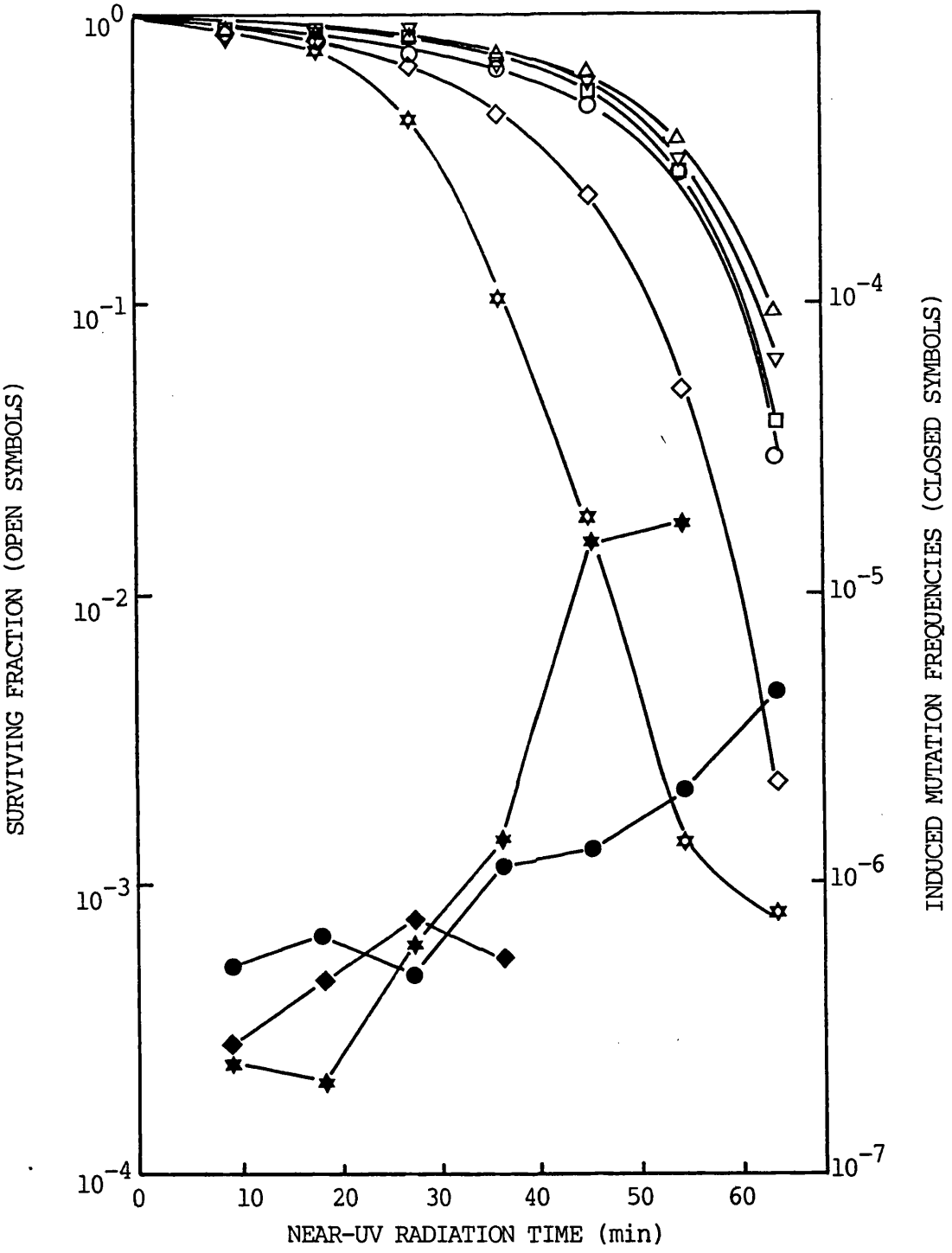

Figure 77

Induced mutation frequencies (closed symbols) and surviving fractions (open symbols) obtained following broad-band near-UV irradiation of K-12 AB 1886 (uvr A) assessed on HSM (●,○); HSM with tenfold-diluted inorganic salts containing either NH_4Cl (□) at 18.7mM or $MgSO_4.7H_2O$ (△) at 0.81mM; HSM with twofold-diluted inorganic salts (▽); and HSM containing additional NaCl at 100mM (◆,◇) or 200mM (★,☆). Irradiation times have been corrected to allow for absorption.

did not permit the detection of more than 5 to 10 mutants per plate and so was still unusable in calculating meaningful induced mutation frequencies.

In a further attempt to elucidate the role of near-UV radiation-induced membrane damage in affecting the determination of induced mutation frequencies, strain AB 1886 (which had previously shown some degree of sensitivity to very high concentrations of inorganic salts after near-UV irradiation,as in Fig. 77) was used, and assessed for viability and mutation induction on HSM plating media (containing MOPS buffer instead of the M9 salts buffer). As described in the methodology section, MOPS buffer was prepared according to the procedure of Neidhardt et al. (1974) except that the sodium chloride content of the buffer (50mM) was omitted. This produced a buffer of a total molarity of 55.6mM which may be compared with a total molarity of 84mM in M9 salts solution. In addition to the HSM plates used, containing MOPS buffer itself, other HSM plates were prepared containing MOPS buffer plus sodium chloride added at 50mM (producing a total molarity of 105.6mM), and containing tenfold-diluted MOPS buffer (producing a total molarity of 5.56mM), or tenfold-diluted MOPS buffer plus sodium chloride added at 50mM (producing a total molarity of 55.6mM). Therefore, provided mutants are detectable on these media of differing total molarities of inorganic salt, the influence of membrane damage on near-UV radiation-induced mutagenesis assessment may be elucidated.

The results of a preliminary experiment, where AB 1886, at an initial concentration of 6×10^8 CFU/ml, was irradiated with broad-band near-UV radiation and assessed for viability and mutation induction on these various plating media, are shown in Figure 78. The figure shows that, as expected, no mutants were observed on the plates containing

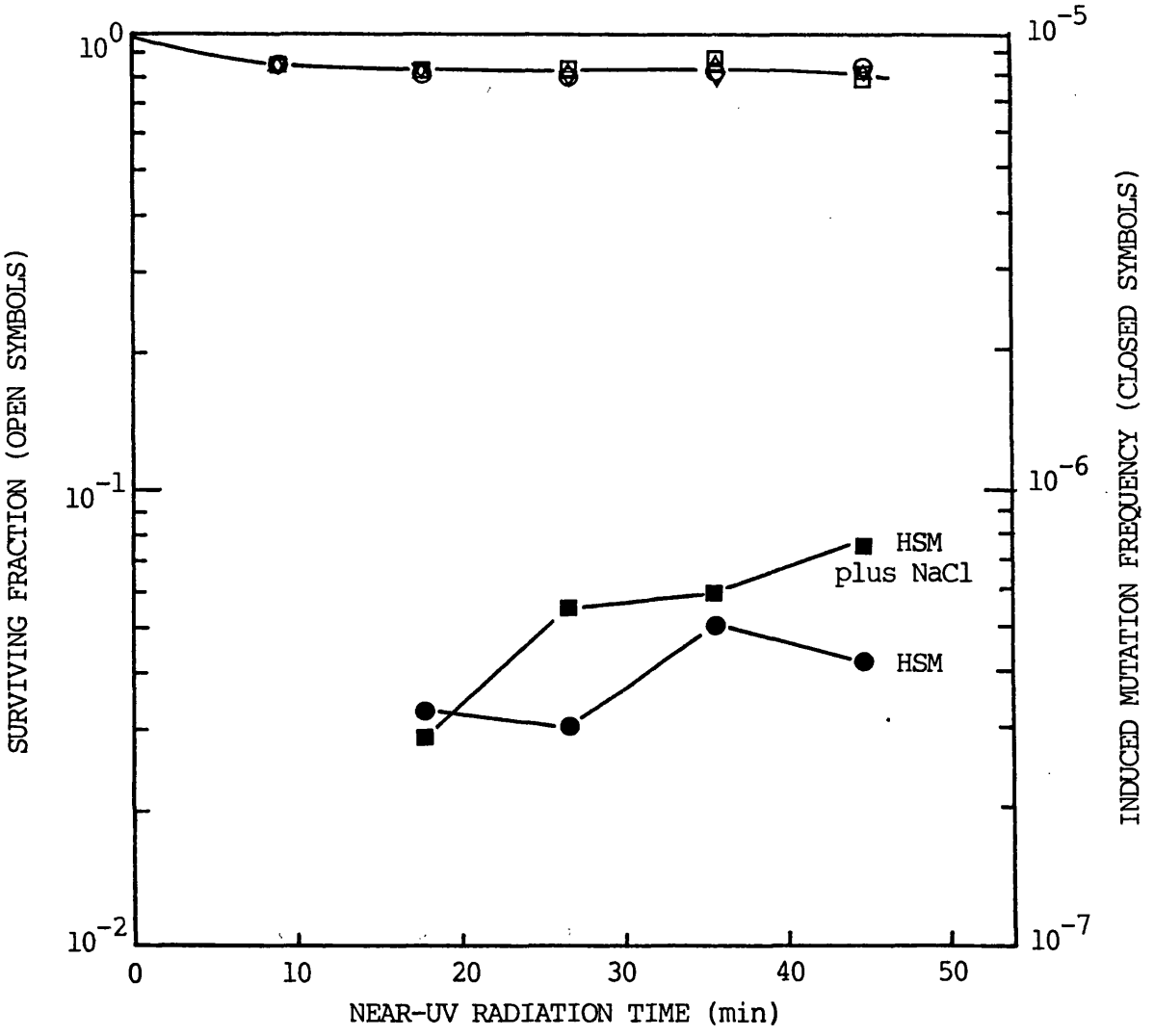

Figure 78

Induced mutation frequencies (closed symbols) and surviving fractions (open symbols) obtained following broad-band near-UV irradiation of K-12 AB 1886 (uvr A) assessed on HSM containing MOPS buffer (●,○), MOPS buffer plus NaCl at 50mM (■,□), tenfold-diluted MOPS buffer (△) and ten fold-diluted MOPS buffer plus NaCl at 50mM (▽). Irradiation times have been corrected to allow for absorption.

diluted MOPS solution. In addition, no significant difference in mutation induction was observed by plating on MOPS plus or minus sodium chloride (50mM) HSM. However, the degree of inactivation observed in this experiment was too low to provide any valid conclusions as to the effect of these differing molarities of inorganic salt in the plating media on the assessment of near-UV radiation-induced mutagenesis. It may be noted that the degree of inactivation observed in this experiment using MOPS buffer in the plating media, is less than that observed in Figs. 77 and 78 for the broad-band near-UV irradiation of the same strain. At present, no explanation may be offered for this as the experiment shown in Fig. 78 was only performed once. Repeat experiments involving longer irradiation times may elucidate the reason and may improve the comparison of mutation induction on the differing plating media.

Finally, in an attempt to relate the role of membrane damage in determining induced mutation frequencies, AB 1886 (uvrA) was irradiated with broad-band near-UV radiation and assessed for viability and mutation induction on HSM plates and on HSM plates containing additional sodium chloride added at 25, 50 or 75mM. The data obtained are shown in Figure 79. The figure indicates that, although differences in cell survival between the plates are observed, with a general pattern of increased salt concentration leading to an increase in sensitivity to near-UV radiation, there is no such pattern observed for the induced mutation frequency curves.

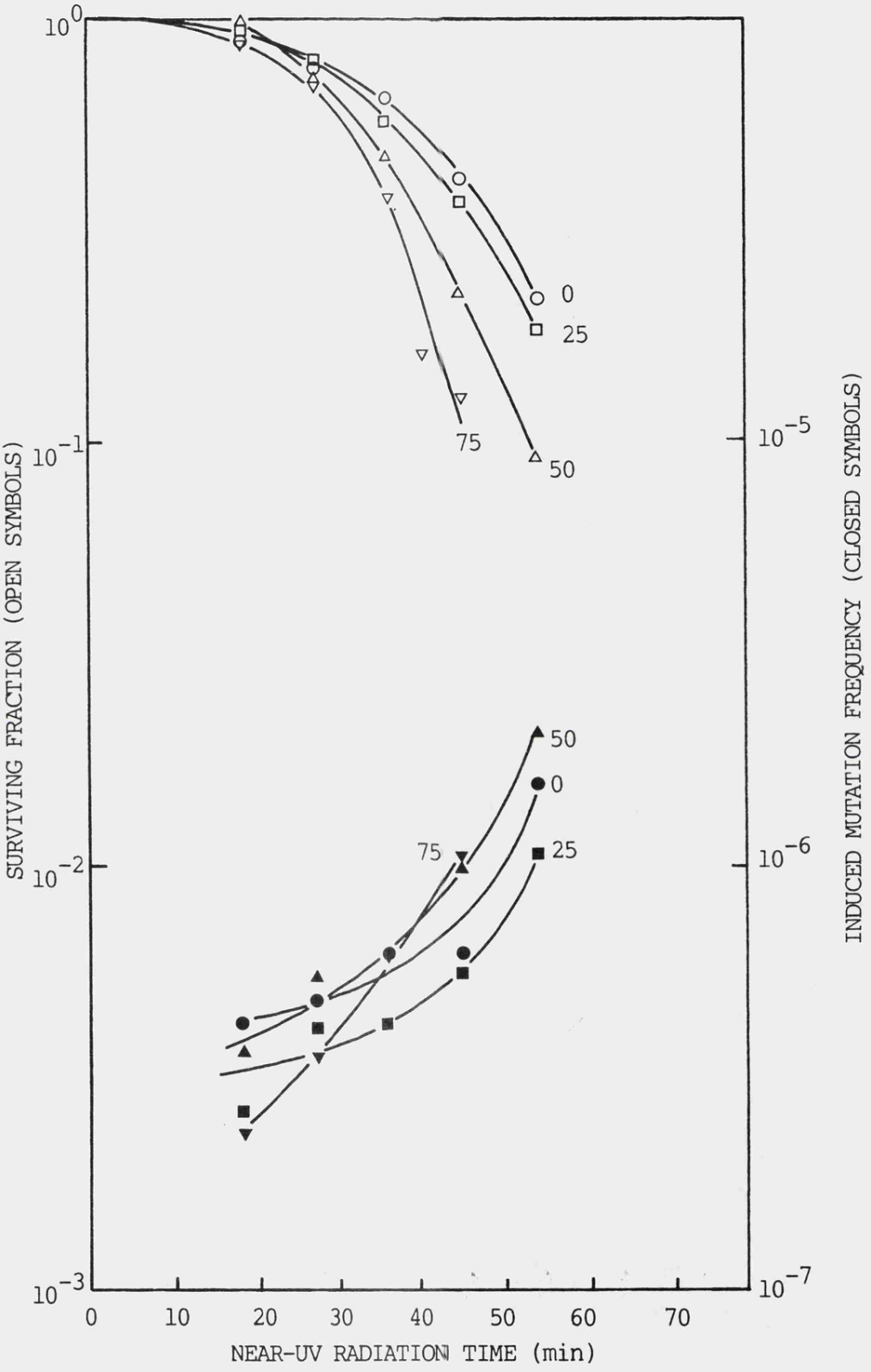

Figure 79

Induced mutation frequencies (closed symbols) and surviving fractions (open symbols) obtained following broad-band near-UV irradiation of K-12 AB 1886 (uvr A) assessed on HSM (●,O) or HSM containing NaCl added at 25mM (■,□), 50mM (▲,△) or 75mM (▼,▽). Irradiation times have been corrected to allow for absorption.

DISCUSSION

The experimental data described in this chapter have attempted to show that, by protecting broad-band near-UV irradiated cells of the DNA repair proficient E. coli K-12 strain AB 1157, or its excision repair deficient derivative AB 1886, from membrane damage, 'normal' numbers of induced mutants are obtained. However, it is clear from these preliminary data (e.g. Figs. 75 and 76) that the main chosen method of protection from membrane damage, i.e. a lowering of the inorganic salt content of the minimal plating media, does not allow the expression of any induced mutants. One possible means of providing alternative differing degrees of protection from membrane damage was attempted, where MOPS buffer (total molarity of 55.6mM) was used in the minimal plating media instead of M9 buffer (total molarity of 84mM). However, this experiment (Fig 78), which was only attempted once, did not show any significant difference in the number of induced mutants obtained between assessing on plates containing MOPS buffer alone, MOPS buffer plus NaCl added at 50mM, and results obtained using M9 buffer, although the extent of inactivation observed was very small.

Therefore, it is apparent that these preliminary studies do not provide much evidence for a role of membrane damage in the assessment of near-UV radiation-induced mutagenesis by reversion to prototrophy. Consequently, further work, possibly involving another means of providing protection from near-UV radiation-induced membrane damage, is required to determine this role.

Another such means of providing protection from membrane damage may be by the use of amino acid supplemented plates, i.e. minimal medium plates containing added amino acids, except of course the amino acid involved in the mutation scoring system. Then the presence of the amino acids may act in a similar way as the presence of Casamino Acids in

the plating medium, and provide protection from near-UV radiation-induced salt sensitivity (as shown in Fig. 29), and thus lead to the detection of 'normal' numbers of near-UV radiation-induced mutants.

However, despite the preliminary nature of the results described in this chapter, and the need to use high concentrations of cells for irradiation ($>5x10^8$CFU/ml) in order to obtain workable numbers of mutants, some important conclusions may be drawn. Firstly, it is apparent that the inorganic salt content of the minimal plating medium, used in the assessment of mutation experiments, plays an important role in the expression of mutants (Figs. 76 and 77). The data indicate that a ten-fold or a two-fold reduction in inorganic salt content of the M9 buffer used in the plating medium does not permit the expression of mutants, although the 'background' lawn is observed. Subsequent experiments have indicated that, in particular, it is the phosphate content of the buffer which is essential for the expression of mutants.

Secondly, on comparison of the survival curves obtained for the broad-band near-UV irradiation of AB 1157 (Fig. 75) and its excision-repair deficient derivative AB 1886 (Figs. 76, 77 and 79), and taking into account the appropriate fluence correction due to the different initial cell concentrations used, it is apparent that, dependent upon conditions, they show differing relative sensitivities. For example, when viability is assessed on low salt minimal media plates, AB 1886 shows the greater sensitivity. However, when viability is assessed on high salt minimal media plates, AB 1157 appears to be the more sensitive of the two. These data thus appear to reflect the importance of membrane damage in near-UV radiation-induced lethality of DNA repair-

proficient strains in the presence of high salt levels. Conversely with the excision repair-deficient strain AB 1886, membrane damage is observable only in the presence of very high concentrations of inorganic salt in the plating media (Figs. 77 and 79), and thus inactivation appears to be due to the overriding importance of DNA damage. In addition, the data obtained with AB 1886, involving differing amounts of sodium chloride in the plating media, indicate that, although survival was affected, no difference in the number of induced mutants was observed (Figs. 77 and 79).

It should be noted that some other studies have shown that strains differing in DNA repair capability may show an equal sensitivity to near-UV radiation. Harrison (1967) reported that B/r (repair-proficient) and B_{S-1} (uvrB, lexA), showed equal sensitivity to broad-band near-UV radiation (330-380nm); and Peak (1970) observed that these two strains had equal sensitivities to 365 nm radiation.

Perhaps the most important observation described by the data of this chapter is that, after broad-band near-UV irradiation of the DNA repair-proficient strain AB 1157, even when using initial cell concentrations as high as $1x10^9$CFU/ml, the number of mutants induced is very low (around 5 per plate), and not sufficient to provide meaningful data. This observation is in general agreement with other reports that have failed to detect mutants after broad-band near-UV irradiation of DNA repair-competent E. coli cells (e.g. Webb, 1977 ; Turner and Webb, 1981). Turner and Webb (1981) proposed that the lack of observed mutants in DNA repair-competent strains, after broad-band near-UV irradiation, was due to a relative enhancement of error-free repair that results from an inhibition of error-prone $recA^+$, lex^+ - mediated pathways by the broad-band radiation. However, Tyrrell (1980) interpreted the lack of

mutants observed, after monochromatic 365 nm irradiation of K-12 AB 1157, and B/r, to be due to a near-UV radiation-induced growth delay, allowing more time for constitutive, primarily error-free, repair to occur. Further work, involving protection of near-UV irradiated cells from lethal membrane damage, as outlined above, may determine whether growth delay effects or inhibition of error-prone pathways are important, or whether membrane damage is indeed the reason for the lack of mutants observed in these experiments.

C O N C L U D I N G D I S C U S S I O N

The data presented in this thesis indicate that damage to cell membranes should be considered in the interpretation of data involving inactivation by near-UV irradiation (both broad-band and monochromatic wavelengths) of DNA repair-proficient E. coli cells, under some experimental conditions. Evidence for damage to membranes in near-UV irradiated cells has been obtained by two distinct methods; firstly, by observing a cell sensitivity to the presence of inorganic salts in various plating media, and secondly, by observing a leakage of material from cells.

The studies involving sensitivity to inorganic salts have shown that near-UV irradiated DNA repair-proficient E. coli strains exhibit an increasing sensitivity to the presence of inorganic salt in the minimal plating media used for assessing viability, with increasing concentrations of inorganic salt. An important practical aspect of these observations has been related to the physiological conditions of the cells used for irradiation. In one section of the experimental work it has been shown that near-UV radiation sensitivity is highly dependent on the phase of growth of the cells, and the nature of this dependence varies significantly between different strains of DNA repair-proficient E. coli. The salt sensitivity effects observed in this study have been related to similar effects that occur in mild-heat (52°C) treated cells, where the effects have been attributed to cell membrane damage.

Also, data has shown that, if near-UV irradiated cells are held in a complex growth medium at 37°C, a recovery from the sensitivity shown to inorganic salts occurs, particularly over the initial 2 hour holding period. By using various metabolic inhibitors, it is apparent

that neither protein nor cell wall synthesis is required for recovery from salt sensitivity to occur, as neither chloramphenicol nor penicillin G respectively, inhibited the process. Recovery from salt sensitivity may be related to a repair of membrane components, as the membrane-acting agent bacitracin partially inhibited the process.

A more direct means of assessing cell membrane damage has been provided by studies which have shown that a leakage of material occurs from near-UV irradiated cells of E. coli. Cell membrane damage has been observed by measuring the leakage of 260 nm absorbing substances, [methyl-^{3}H] thymidine and $^{86}Rb^{+}$, from cells.

Action spectra from 254 to 405 nm, using the two end-points, sensitivity to inorganic salts and leakage of $^{86}Rb^{+}$ label, are both in agreement in showing that membrane damage appears to be important only in lethality induced by wavelengths above 305 nm, i.e. by near-UV radiation and not far-UV radiation. It should be noted that the action spectrum determined for the leakage of $^{86}Rb^{+}$ indicates that leakage also occurs from far-UV irradiated cells, but only at fluences much greater than those required for the inactivation of the cell population to below detectable levels. The action spectra indicate that, with wavelengths from 254 - 305 nm, lethality closely follows the absorption spectrum of DNA, whereas at wavelengths above 305 nm, where DNA absorption is much reduced, lethality is much higher than would be predicted if the direct absorption of radiation by DNA, leading to damage, was the sole cause of lethality.

It would appear, therefore, that UV radiation of the environmentally relevant wavelengths from 305 to 405 nm, induces cell lethality by a combination of effects including DNA damage, damage to DNA repair enzymes

and, from these studies, cell membrane damage. However, it is not possible, from these studies, to proportion the importance of membrane damage in relation to the other types of potentially lethal damage known to occur in near-UV radiation-induced cell inactivation. In addition, it is not possible, from these studies, to make predictions as to the chromophore or chromophores involved in producing the damage to membranes induced by near-UV radiation.

The identification of chromophores absorbing in the near-UV radiation region which are involved in cell lethality, has thus far, with one notable exception, proved unsuccessful. The exception is the rare base 4-thiouridine (^{4}Srd) which occurs in the 8 position of many tRNA'S of E. coli. Absorption of near-UV radiation, in particular that of around 340 nm, by 4-thiouridine, has been shown to be responsible for near-UV radiation-induced growth delay (Ramabhadran et al., 1976), reduction of bacterial capacity for phage development (Wingo et al., 1980), inhibition of induced-enzyme (tryptophanase) synthesis (Sharma et al., 1981) and, possibly, some cell lethality (Tsai and Jagger, 1981). However, 4-thiouridine does not appear to be involved in the membrane damaging effects described in this study as ^{4}Srd$^-$ and ^{4}Srd$^+$ mutants show equal degrees of salt sensitivity after near-UV irradiation (Moss and Smith, unpublished data).

The possible chromophores involved in the near-UV radiation-induced membrane damage described in this study are either ones present within the cell membrane itself, leading to direct membrane damaging effects, orones present outside the membrane. Of the two possibilities, the latter seems more likely, as firstly, absorption of UV radiation by the majority of membrane components is important only at wavelengths lower than 300 nm (see Lamola, 1977 for a review).

Secondly, the salt sensitivity effects observed by Moss and Smith (1981), and extended in this study, show a degree of oxygen dependence, suggesting a photodynamic mechanism involving an endogenous sensitizer acting as the chromophore.

The absorption of near-UV radiation by chromophores present outside the membrane may lead to a damaging effect either by deposition of energy direct to the membrane or through a more indirect mechanism. Such an indirect mechanism may involve the enzyme, catalase, whose destruction may lead to membrane damage by an accumulation of peroxide ions. Further work involving the measurement of catalase levels using titanium oxysulphate (as described by Cheng et al., 1981) or the use of kat mutants of E. coli, which are mutants lacking the gene responsible for the control of catalase activity (Bachmann and Low, 1980), may help to elucidate whether catalase does have a role in near-UV radiation-induced membrane damage.

One type of damage to membranes which has been proposed, is the peroxidation of lipids. As described previously, studies using erythrocytes and liposomes have shown that near-UV radiation may induce lipid peroxidation, as measured by the formation of malondialdehyde by the thiobarbituric acid reaction (Roshchupkin et al., 1975; Mandal and Chatterjee, 1980). This method of assay, as well as measuring the increase in absorption at 233 nm due to increasing diene conjugation (Klein, 1970), may indicate whether lipid peroxidation or lipid oxidation is important.

A possible approach, which may be useful in extending the knowledge of the membrane damage described in this thesis, would be to use various E. coli mutants with altered membranes. Such mutants include env strains (Egan and Russell, 1972), which have an altered outer membrane leading to increased permeability properties, and plsB mutants (Wagner et al., 1982), which lack the ability to synthesize any phospholipids. These strains, such as E. coli BB26-36, have a defective glycerol-3-phosphate acyl transferase so that when this strain is not supplemented with glycerol, the membranes accumulate as much as 50% more membrane protein than is observed with normally growing cells. Further work using E. coli K1060 (fabB, fad), (as described by Overath et al., 1970), a strain lacking the ability to synthesize or degrade membrane unsaturated fatty acids, may also prove useful.

An important consequence of near-UV radiation-induced membrane damage, as investigated in this study, may be in the interpretation of mutagenesis assessment by near-UV radiation, by reversion to prototrophy, in that the design of mutagenesis experiments routinely involves assessment of viability and mutation on minimal media plates, which contain high concentrations of inorganic salts. Also, membrane damage may be particularly important in studies where near-UV radiation and mild-heat interaction experiments are performed.

In terms of the wider significance of these results, if near-UV radiation produces membrane damage in human skin cells, irradiated cells may become more susceptible to permeation of toxic environmental

agents (for example, carcinogens) than unirradiated cells. Therefore, excessive sunlight exposure in humans may increase the risk of chemical carcinogenesis. Some indirect support for this has been reported by Tyrrell (1978c), who observed that near-UV irradiated E. coli are much more sensitive to the lethal effects of methyl methane sulphonate (MMS) than are unirradiated cells. One interpretation that may be offered for this observation is that an increased uptake of MMS occurs after near-UV irradiation, through cells with damaged membranes.

Therefore, having established the nature and importance of near-UV radiation-induced membrane damage in E. coli, similar experiments to those described in this thesis should be conducted using mammalian cells. It should be pointed out that some indication of 365 nm radiation inducing a membrane damaging effect in normal human fibroblasts (1BR) was observed in the preliminary work of Keyse (1983). He showed that the presence of low concentrations of the cationic surfactant cetrimide (0.2μg/ml) in the plating media resulted in an increased sensitivity of 365 nm-irradiated cells. Furthermore, no increase in sensitivity in the presence of cetrimide was observed for 254 nm-irradiated cells.

A P P E N D I X A

FIGURE A1 : Derivation of strain K-12 SR 385 with a comparison of the derivation of K-12 AB 1157.

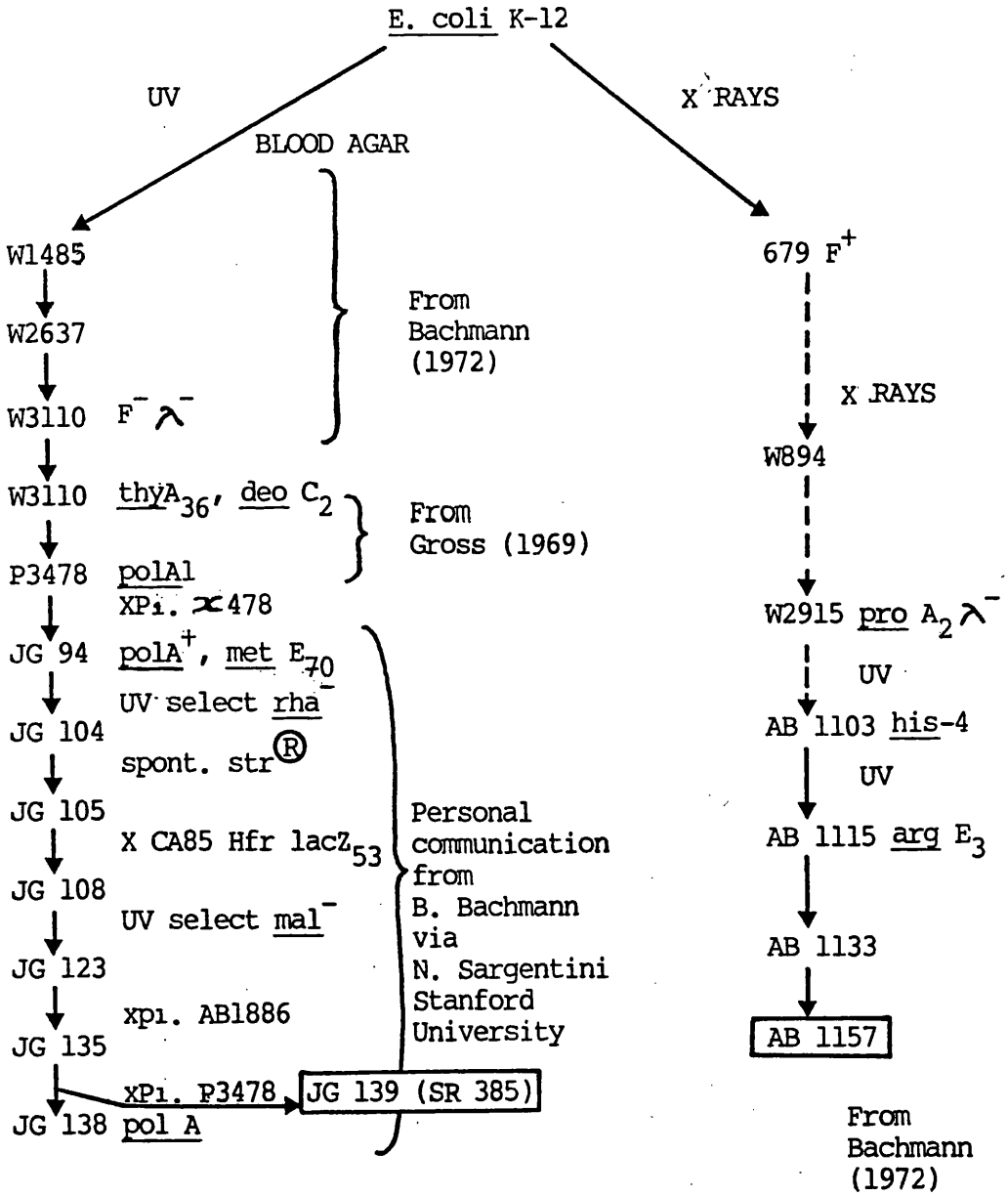

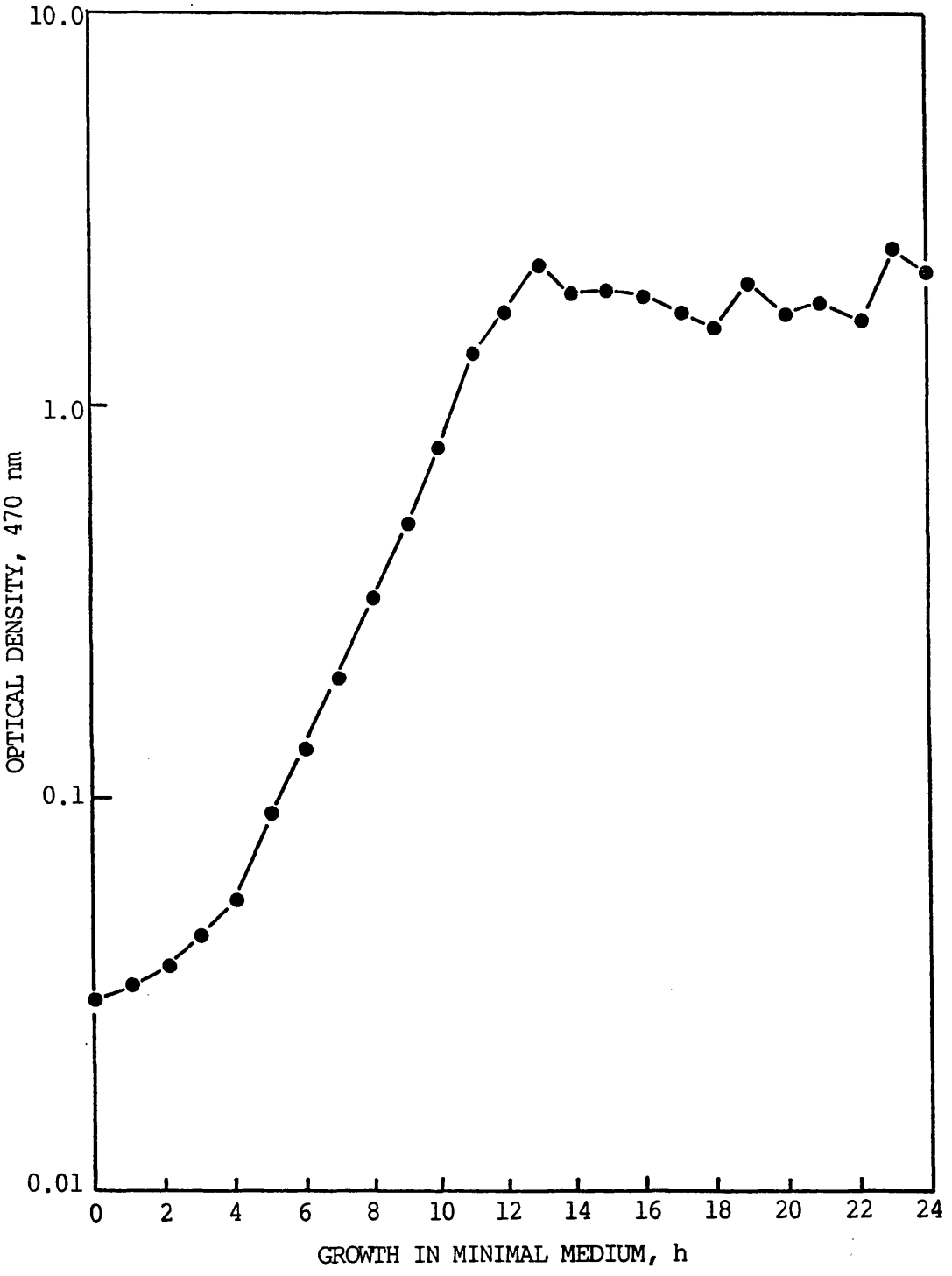

Figure A2

Growth curve of E. coli K-12 (SR 385) in minimal growth medium.

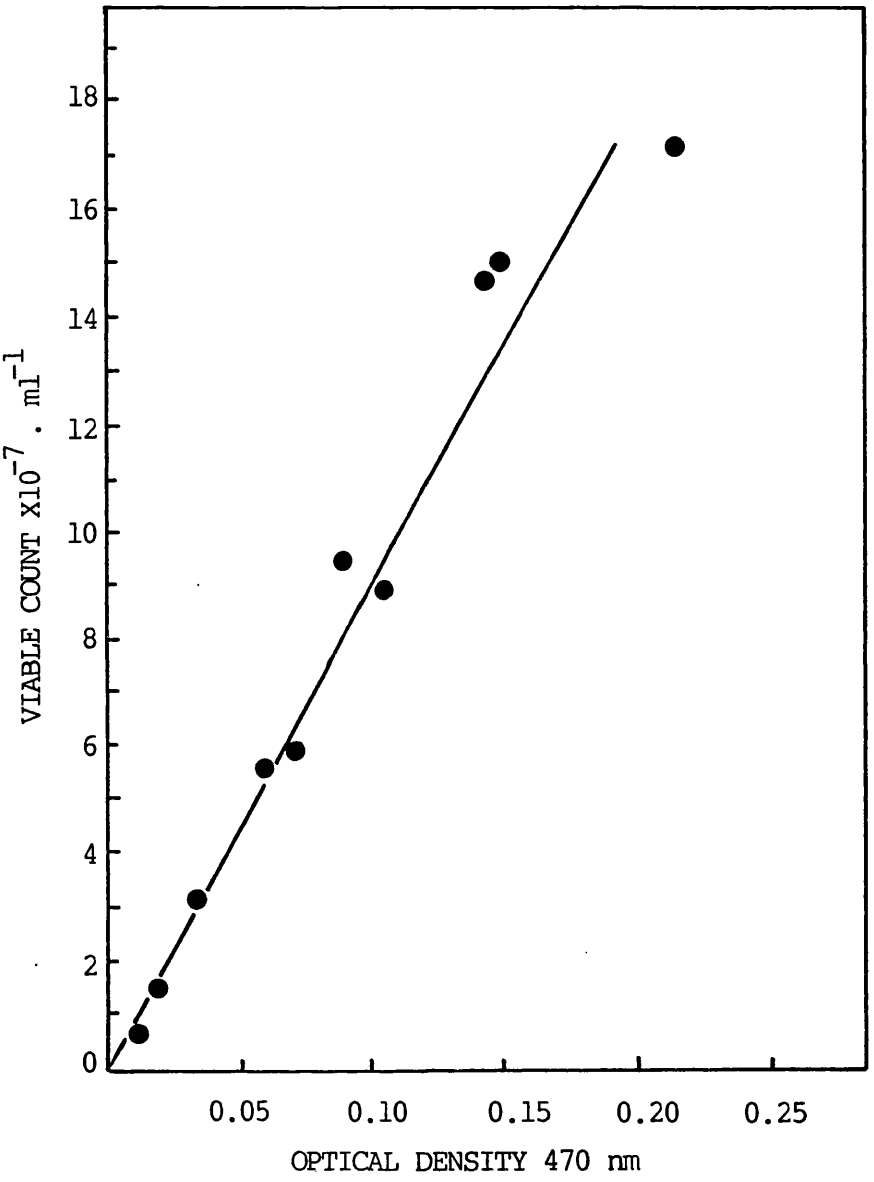

Figure A3

Optical density at 470 nm : viable count calibration graph for E. coli K-12 (S.R 385)

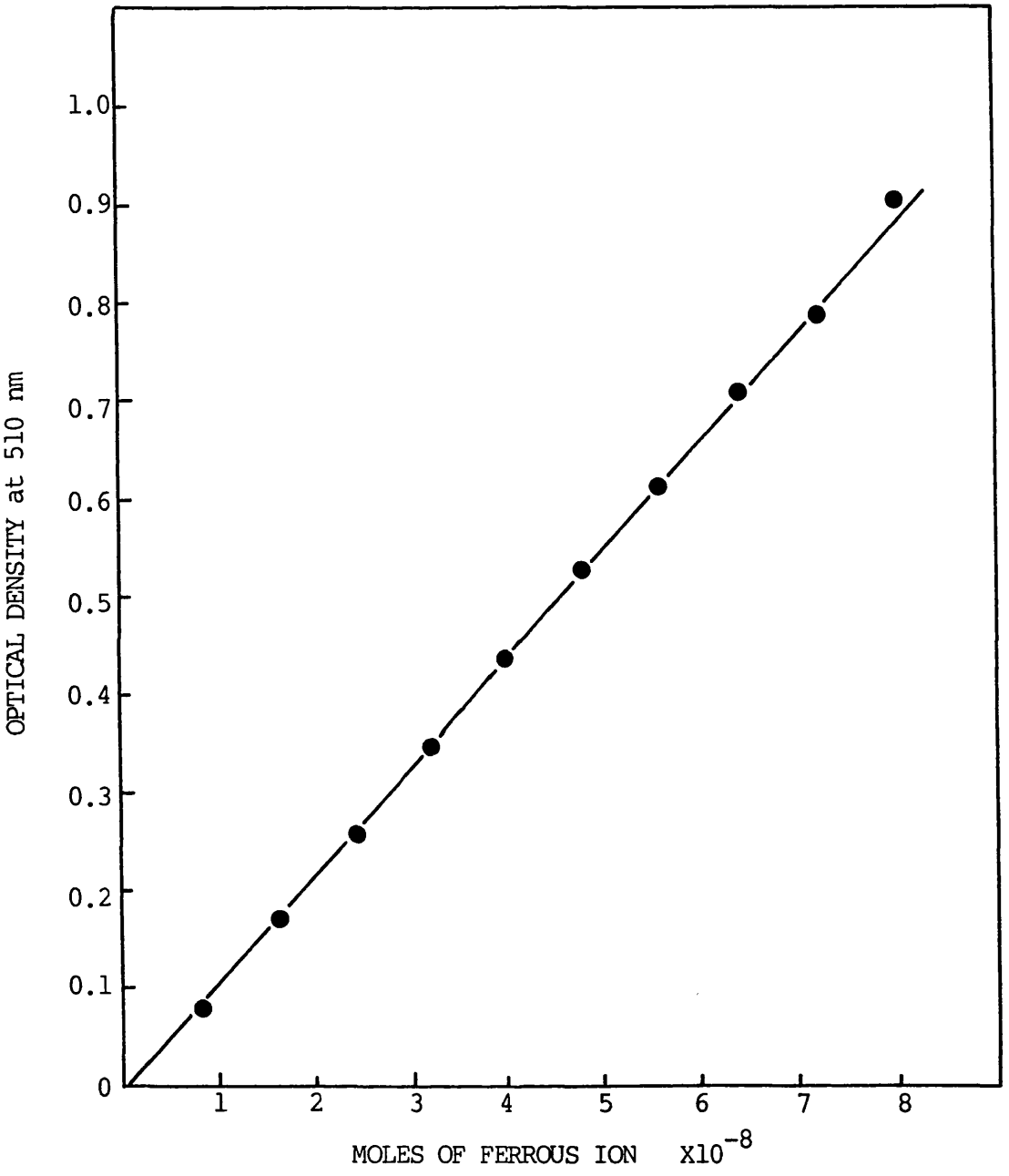

Figure A4

Calibration curve for the conversion of optical density to amount of ferrous ion.

```
   ID:  3H
   LINE ->15
15 EFF1%  RATIO
   46.64  1.699 ->
   38.28  1.385 ->
   32.84  1.196 ->
   20.87   .843 ->
   13.48   .623 ->
    1.64   .286 ->

PLOT QUENCH CURVES (R) ->R
```

```
ISOTOPE 1, WINDOW 1
```

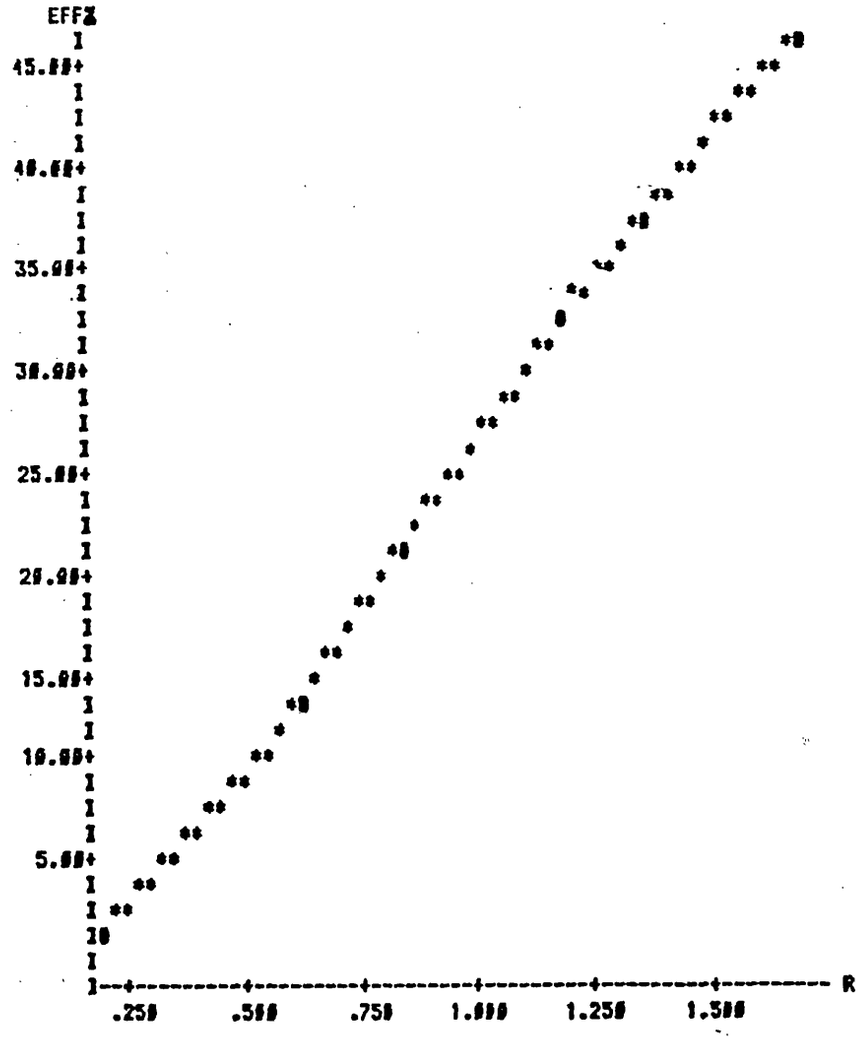

Figure A5

Quench curve for tritium determined by the LKB Rackbeta 1215 liquid scintillation counter.

```
   PARAMETER GROUP ->07
   ID:  RB 86  ->
   LINE ->15
15 EFF1%  RATIO
   90.36  1.879 ->
   89.20  1.598 ->
   88.19  1.420 ->
   87.55  1.143 ->
   80.48   .803 ->
   59.45   .443 ->
   21.66   .186 ->

PLOT QUENCH CURVES (R) ->R


BUSY CALCULATING


ISOTOPE 1, WINDOW 1
```

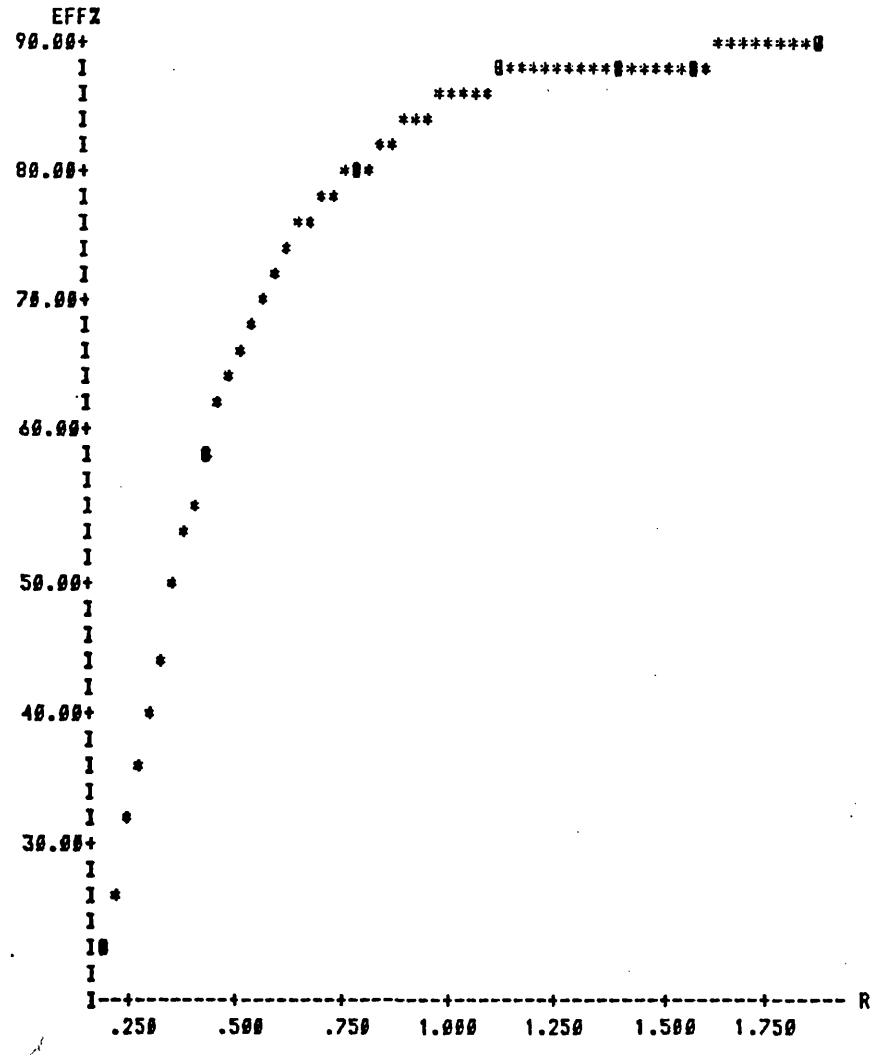

Figure A6

Quench curve for $^{86}Rb^{+}$ determined by the LKB Rackbeta 1215 liquid scintillation counter

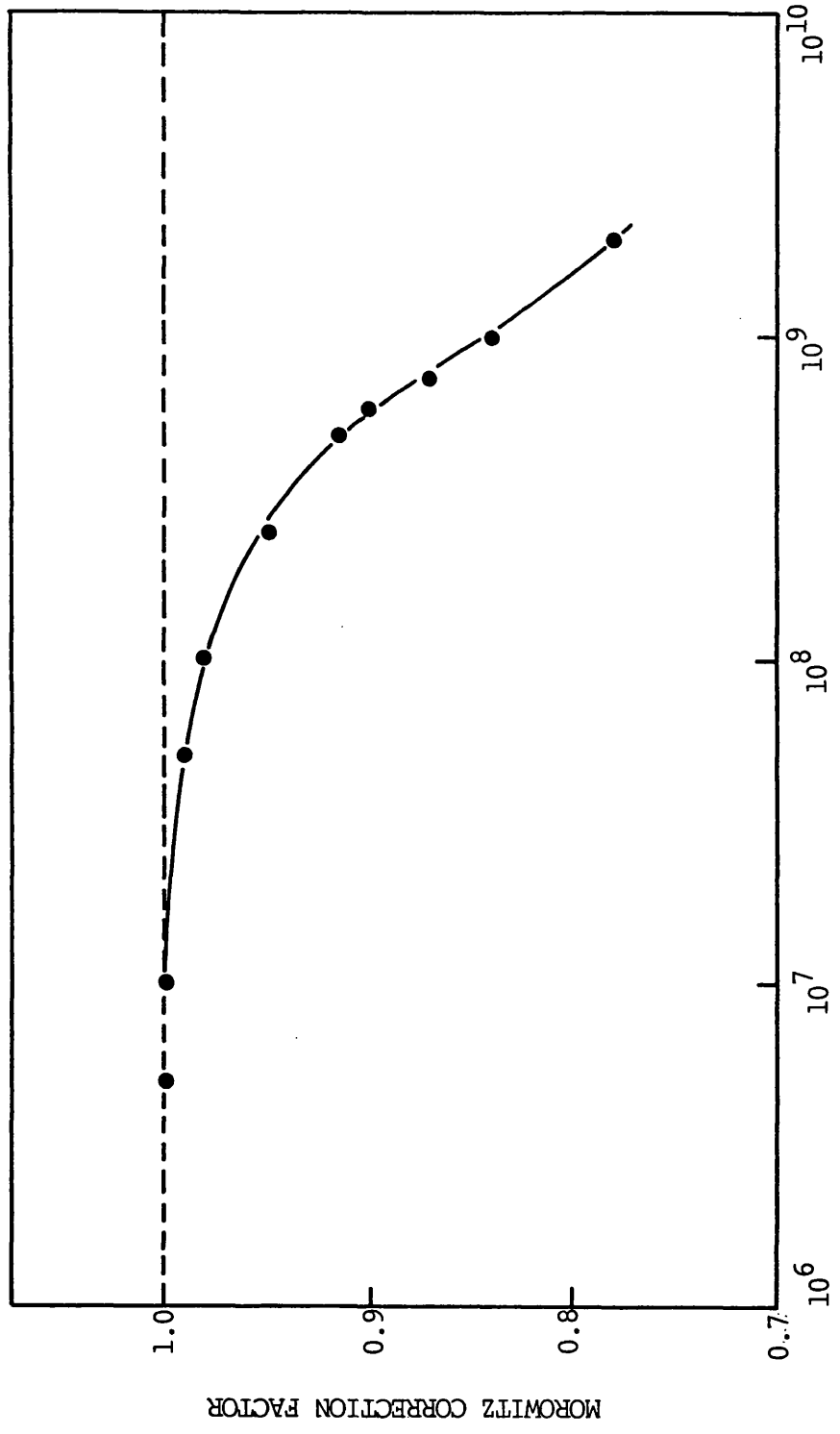

Figure A7

Fluence correction factors (from Morowitz, 1950) for Black-Light Blue radiation source.

A P P E N D I X B

TABLE 1.

Data pertaining to Figure 25.

PLATE TYPE	TIME OF IRRADIATION (min)	DILUTION	PLATE COUNT	MEAN PLATE COUNT	VIABLE COUNT (ml^{-1})	SURVIVING FRACTION
A=complex	0	10^5	127, 133, 134	131.3	1.31×10^7	1.0
B=Low salt	0	10^5	138, 159, 153	150.0	1.50×10^7	1.0
C=Normal salt	0	10^5	117, 126, 138	127.0	1.27×10^7	1.0
D= High salt	0	10^5	142, 131, 121	131.3	1.31×10^7	1.0
A	20	10^5	85, 89, 100	91.3	9.13×10^6	6.96×10^{-1}
B	20	10^5	121, 117, 112	116.7	1.17×10^7	7.78×10^{-1}
C	20	10^5	122, 124, 115	120.0	1.20×10^7	9.48×10^{-1}
D	20	10^5	97, 98, 125	106.7	1.07×10^7	8.12×10^{-1}
A	30	10^4	206, 224, 175	202.0	2.02×10^6	7.54×10^{-1}
D	30	10^5	47, 52, 52	50.3	5.03×10^6	3.83×10^{-1}
A	40	10^3	135, 122, 114	124.0	1.24×10^5	9.41×10^{-2}
B	40	10^5	107, 81, 92	93.3	9.33×10^6	6.22×10^{-1}
C	40	10^5	84, 88, 71	81.0	8.10×10^6	6.38×10^{-1}
D	40	10^4	263, 252, 249	255.0	2.55×10^6	1.94×10^{-1}
A	50	10^2	62, 77, 72	70.3	7.03×10^3	5.35×10^{-4}
D	50	10^4	43, 56, 51	50.0	5.00×10^5	3.81×10^{-2}
A	60	10^2	31, 39, 19	29.7	2.97×10^3	2.26×10^{-4}
B	60	10^5	37, 42, 37	38.7	3.87×10^6	2.58×10^{-1}
C	60	10^4	197, 277, 201	225.0	2.25×10^6	1.77×10^{-1}
D	60	10^3	121, 127, 118	122.0	1.22×10^5	9.29×10^{-3}
D	70	10^2	90, 94, 85	89.7	8.97×10^3	6.83×10^{-4}
B	80	10^4	50, 65, 53	56.0	5.60×10^5	3.73×10^{-2}
C	80	10^3	150, 118, 170	146.0	1.46×10^5	1.15×10^{-2}
D	80	10^2	35, 40, 46	40.3	4.03×10^4	3.05×10^{-4}
B	100	10^3	34, 49, 54	45.7	4.57×10^4	3.05×10^{-3}
C	100	10^3	18, 20, 14	17.3	1.73×10^4	1.36×10^{-3}
B	120	10^3	8, 12, 11	10.3	1.03×10^4	6.87×10^{-4}
C	120	10^2	73, 54, 82	69.7	6.97×10^3	5.49×10^{-4}

TABLE 2.

Data pertaining to Figure 26.

TIME OF IRRADIATION (min)	SURVIVING FRACTION				
	Oxoid complex medium	Difco YENB medium	MINIMAL MEDIA		
			Low salt	Normal salt	High salt
0	$\underline{1.30\times10^{7}}$	$\underline{1.46\times10^{7}}$	$\underline{1.57\times10^{7}}$	$\underline{1.69\times10^{7}}$	$\underline{1.20\times10^{7}}$
10	7.93×10^{-1}	-	-	-	6.97×10^{-1}
20	4.91×10^{-1}	8.65×10^{-1}	8.85×10^{-1}	6.63×10^{-1}	3.92×10^{-1}
30	7.40×10^{-2}	-	-	-	1.70×10^{-1}
40	1.24×10^{-2}	5.07×10^{-1}	4.39×10^{-1}	2.60×10^{-1}	7.64×10^{-2}
50	4.96×10^{-4}	-	-	-	2.69×10^{-2}
60	2.20×10^{-4}	1.74×10^{-1}	1.38×10^{-1}	6.62×10^{-2}	-
70	-	-	-	-	2.10×10^{-3}
80	-	6.20×10^{-2}	4.96×10^{-2}	1.82×10^{-2}	-
112	-	3.65×10^{-3}	4.12×10^{-3}	-	-
120	-	2.92×10^{-3}	-	1.39×10^{-3}	-

NOTE UNDERLINED VALUES AT TIME ZERO REFER TO INITIAL VIABLE COUNTS.

THE SAME FORMAT IS USED IN ALL SUBSEQUENT TABLES WHERE APPROPRIATE.

TABLE 3.

Data pertaining to Figure 27.

TIME OF IRRADIATION. (min)	SURVIVING FRACTION Oxoid nutrient agar	Tryptone soya agar (plus thymine 10µg/ml)	Difco YENB.	Oxoid minus sodium chloride	YENB plus sodium chloride (5g/l)
0	$\underline{2.33\times10^{7}}$	$\underline{2.02\times10^{7}}$	$\underline{2.18\times10^{7}}$	$\underline{1.45\times10^{7}}$	$\underline{2.22\times10^{7}}$
10	8.56×10^{-1}	-	-	-	-
20	7.01×10^{-1}	9.54×10^{-1}	8.11×10^{-1}	1.07×10^{0}	7.94×10^{-1}
30	2.80×10^{-1}	4.83×10^{-1}	-	7.64×10^{-1}	-
40	5.79×10^{-2}	1.35×10^{-1}	4.14×10^{-1}	3.96×10^{-1}	2.67×10^{-1}
50	1.08×10^{-2}	2.18×10^{-2}	-	-	-
60	-	3.76×10^{-3}	6.96×10^{-2}	6.26×10^{-2}	4.11×10^{-2}
70	1.27×10^{-4}	-	-	-	-
80	-	7.90×10^{-5}	4.09×10^{-3}	3.68×10^{-3}	1.94×10^{-3}
100	-	-	1.83×10^{-4}	2.44×10^{-4}	1.26×10^{-4}

UNDERLINED VALUES = VIABLE COUNTS.

TABLE 4.

Data pertaining to Figure 28.

TIME OF IRRADIATION (Min)	SURVIVING FRACTION		
	Low salt Minimal medium	Normal salt Minimal medium	High salt Minimal medium
0	$\underline{1.70\times10^{7}}$	$\underline{1.75\times10^{7}}$	$\underline{1.93\times10^{7}}$
20	1.07×10^{0}	9.69×10^{-1}	8.26×10^{-1}
30	-	-	7.43×10^{-1}
40	9.16×10^{-1}	7.70×10^{-1}	3.63×10^{-1}
50	-	-	1.20×10^{-1}
60	5.24×10^{-1}	3.04×10^{-1}	2.16×10^{-2}
70	-	-	1.33×10^{-3}
80	3.69×10^{-2}	1.29×10^{-2}	-
100	7.60×10^{-4}	5.70×10^{-4}	-

UNDERLINED VALUES = VIABLE COUNTS.

TABLE 5.

Data pertaining to Figure 29.

TIME OF IRRADIATION (min)	SURVIVING FRACTION Oxoid nutrient agar	Difco YENB	Oxoid plus yeast extract (7.5g/l)	Oxoid plus Casamino Acids (2mg/ml)	Difco nutrient agar plus sodium chloride (100mM)
0	$\underline{1.67\times10^{7}}$	$\underline{1.17\times10^{7}}$	$\underline{9.60\times10^{6}}$	$\underline{1.71\times10^{7}}$	$\underline{1.34\times10^{7}}$
20	6.94×10^{-1}	1.09×10^{0}	9.50×10^{-1}	7.52×10^{-1}	8.35×10^{-1}
40	4.67×10^{-2}	6.03×10^{-1}	2.70×10^{-1}	5.91×10^{-2}	2.90×10^{-1}
50	2.70×10^{-3}	-	6.67×10^{-2}	4.16×10^{-3}	1.04×10^{-1}
60	3.71×10^{-4}	5.37×10^{-2}	1.25×10^{-2}	5.40×10^{-4}	1.49×10^{-2}
70	1.45×10^{-4}	-	9.17×10^{-4}	1.90×10^{-4}	-
80	-	-	3.64×10^{-4}	-	4.34×10^{-4}
90	-	6.03×10^{-4}	-	-	-
100	-	3.47×10^{-4}	-	-	-

UNDERLINED VALUES = VIABLE COUNTS

TABLE 6.

Data pertaining to Figure 30.

HOLDING TIME (h)	SURVIVING FRACTION - UNIRRADIATED CELLS		SURVIVING FRACTION - IRRADIATED CELLS	
	Difco YENB	High salt minimal medium.	Difco YENB	High salt minimal medium.
0	$\underline{1.06 \times 10^{7}}$	$\underline{1.20 \times 10^{7}}$	2.46×10^{-1}	9.40×10^{-3}
0.5	1.07×10^{0}	9.19×10^{-1}	2.78×10^{-1}	2.25×10^{-2}
1.0	7.48×10^{-1}	7.52×10^{-1}	3.10×10^{-1}	3.67×10^{-2}
1.5	8.49×10^{-1}	7.99×10^{-1}	2.59×10^{-1}	3.79×10^{-2}
2.0	8.60×10^{-1}	7.52×10^{-1}	2.99×10^{-1}	5.46×10^{-2}
4.0	5.40×10^{0}	4.18×10^{0}	4.18×10^{-1}	1.08×10^{-1}
6.0	1.13×10^{2}	8.13×10^{1}	7.70×10^{-1}	3.51×10^{-1}

UNDERLINED VALUES = VIABLE COUNTS

TABLE 7.

Data pertaining to Figure 31.

HOLDING TIME (h)	SURVIVING FRACTION - UNIRRADIATED CELLS				SURVIVING FRACTION - IRRADIATED CELLS			
	YENB	YENB plus Chloramphenicol	High salt	High salt plus Chloramphenicol	YENB	YENB plus Chloramphenicol	High salt	High salt plus Chloramphenicol
0	$\underline{1.06\times10^{7}}$	$\underline{1.15\times10^{7}}$	$\underline{1.20\times10^{7}}$	$\underline{1.00\times10^{7}}$	2.30×10^{-1}	2.30×10^{-1}	9.10×10^{-3}	9.10×10^{-3}
0.5	1.07×10^{0}	7.94×10^{-1}	9.19×10^{-1}	9.30×10^{-1}	2.63×10^{-1}	2.55×10^{-1}	2.20×10^{-2}	3.10×10^{-2}
1.0	7.48×10^{-1}	6.55×10^{-1}	7.52×10^{-1}	6.50×10^{-1}	2.94×10^{-1}	2.64×10^{-1}	3.68×10^{-2}	4.90×10^{-2}
1.5	8.49×10^{-1}	6.38×10^{-1}	7.99×10^{-1}	6.87×10^{-1}	2.45×10^{-1}	2.88×10^{-1}	3.78×10^{-2}	5.76×10^{-2}
2.0	8.60×10^{-1}	5.91×10^{-1}	7.52×10^{-1}	5.50×10^{-1}	2.83×10^{-1}	2.91×10^{-1}	5.45×10^{-2}	7.69×10^{-2}
4.0	5.40×10^{0}	4.26×10^{-1}	4.18×10^{0}	5.10×10^{-1}	3.96×10^{-1}	2.66×10^{-1}	1.07×10^{-1}	8.90×10^{-2}
6.0	1.13×10^{2}	5.22×10^{-1}	8.13×10^{1}	5.73×10^{-1}	7.31×10^{-1}	2.50×10^{-1}	3.50×10^{-1}	8.50×10^{-2}

UNDERLINED VALUES = VIABLE COUNTS

TABLE 8.

Data pertaining to Figure 32.

HOLDING TIME (h)	SURVIVING FRACTION ON YENB medium after growth in different concentrations of penicillin G. Units/ml									
	3.0	6.0	9.0	12.0	15.0	18.0	21.0	24.0	27.0	30.0
0	$\underline{1.34\times10^{6}}$	$\underline{1.58\times10^{6}}$	$\underline{1.43\times10^{6}}$	$\underline{1.47\times10^{6}}$	$\underline{1.39\times10^{6}}$	$\underline{1.50\times10^{6}}$	$\underline{1.58\times10^{6}}$	$\underline{1.45\times10^{6}}$	$\underline{1.19\times10^{6}}$	$\underline{1.30\times10^{6}}$
2.0	8.20×10^{-1}	8.40×10^{-1}	6.90×10^{-1}	5.73×10^{-1}	6.15×10^{-1}	4.05×10^{-1}	4.40×10^{-1}	3.65×10^{-1}	3.57×10^{-1}	2.70×10^{-1}
4.0	1.36×10^{1}	6.90×10^{0}	3.36×10^{0}	9.05×10^{-1}	2.41×10^{-1}	4.65×10^{-2}	6.30×10^{-3}	4.50×10^{-3}	6.30×10^{-3}	3.10×10^{-3}
6.0	2.29×10^{2}	7.10×10^{1}	9.75×10^{0}	5.63×10^{-1}	3.60×10^{-2}	7.00×10^{-3}	4.10×10^{-3}	3.40×10^{-3}	3.40×10^{-3}	7.70×10^{-4}

UNDERLINED VALUES = VIABLE COUNTS

TABLE 9.

Data pertaining to Figure 33 a and b.

HOLDING TIME	SURVIVING FRACTION - UNIRRADIATED CELLS				SURVIVING FRACTION - IRRADIATED CELLS			
(h)	YENB	YENB plus Penicillin	High salt minimal medium	High salt minimal medium plus penicillin	YENB	YENB plus Penicillin	High salt minimal medium	High salt minimal medium plus Penicillin
FIGURE 33a	NEAR-UV RADIATION							
0	$\underline{1.37\times10^{7}}$	$\underline{1.47\times10^{7}}$	$\underline{1.37\times10^{7}}$	$\underline{1.41\times10^{7}}$	5.80×10^{-2}	4.56×10^{-2}	1.46×10^{-3}	9.00×10^{-4}
0.5	9.82×10^{-1}	8.80×10^{-1}	1.08×10^{0}	9.50×10^{-1}	8.10×10^{-2}	5.60×10^{-2}	1.78×10^{-3}	1.76×10^{-3}
1.0	9.50×10^{-1}	7.70×10^{-1}	9.64×10^{-1}	8.10×10^{-1}	9.90×10^{-2}	9.10×10^{-2}	1.71×10^{-3}	3.50×10^{-3}
2.0	8.80×10^{-1}	6.35×10^{-1}	7.30×10^{-1}	5.96×10^{-1}	8.90×10^{-2}	8.90×10^{-2}	7.37×10^{-3}	7.10×10^{-3}
3.0	3.34×10^{0}	9.72×10^{-1}	3.16×10^{0}	7.59×10^{-1}	9.10×10^{-2}	1.08×10^{-1}	1.30×10^{-2}	1.25×10^{-2}
4.0	1.54×10^{1}	1.64×10^{0}	1.65×10^{1}	1.46×10^{0}	1.08×10^{-1}	9.20×10^{-2}	2.16×10^{-2}	1.76×10^{-2}
5.0	6.50×10^{1}	1.81×10^{0}	6.90×10^{1}	1.74×10^{0}	1.04×10^{-1}	9.33×10^{-2}	3.40×10^{-2}	2.93×10^{-2}
6.0	3.24×10^{2}	1.78×10^{0}	3.64×10^{2}	1.68×10^{0}	1.17×10^{-1}	9.70×10^{-2}	6.00×10^{-2}	2.93×10^{-2}
FIGURE 33b	FAR-UV RADIATION (254 nm).							
0	DETAILS FOR UNIRRADIATED CELLS				7.00×10^{-2}	6.60×10^{-2}	9.26×10^{-2}	1.07×10^{-1}
0.5					5.70×10^{-2}	6.00×10^{-2}	5.80×10^{-2}	6.29×10^{-2}
1.0	AS ABOVE (Fig.33a)				5.30×10^{-2}	4.98×10^{-2}	5.63×10^{-2}	5.72×10^{-2}
2.0					3.74×10^{-2}	3.96×10^{-2}	4.60×10^{-2}	5.17×10^{-2}
3.0					3.22×10^{-2}	3.71×10^{-2}	4.70×10^{-2}	4.79×10^{-2}
4.0					4.39×10^{-2}	4.39×10^{-2}	5.44×10^{-2}	4.99×10^{-2}
5.0					1.72×10^{-1}	5.92×10^{-2}	1.57×10^{-1}	6.16×10^{-2}
6.0					4.95×10^{-1}	8.30×10^{-2}	3.78×10^{-1}	8.30×10^{-2}

UNDERLINED VALUES = VIABLE COUNTS

TABLE 10.

Data pertaining to Figure 34.

HOLDING TIME (h)	SURVIVING FRACTION ON YENB MEDIUM after growth in different concentrations of bacitracin. (units/ml)									
	7.0	5.0	3.0	2.0	1.0	0.9	0.7	0.5	0.3	0.1
0	$\underline{9.55\times10^{4}}$	$\underline{1.12\times10^{5}}$	$\underline{1.28\times10^{5}}$	$\underline{1.29\times10^{5}}$	$\underline{1.22\times10^{5}}$	$\underline{1.24\times10^{5}}$	$\underline{1.34\times10^{5}}$	$\underline{1.10\times10^{5}}$	$\underline{1.16\times10^{5}}$	$\underline{1.07\times10^{5}}$
0.5	9.32×10^{-1}	8.90×10^{-1}	7.23×10^{-1}	7.64×10^{-1}	8.81×10^{-1}	7.47×10^{-1}	7.10×10^{-1}	9.20×10^{-1}	8.30×10^{-1}	9.67×10^{-1}
1.0	6.86×10^{-1}	5.80×10^{-1}	5.86×10^{-1}	6.41×10^{-1}	5.00×10^{-1}	8.11×10^{-1}	6.79×10^{-1}	7.95×10^{-1}	6.42×10^{-1}	1.05×10^{0}
1.5	3.72×10^{-1}	3.91×10^{-1}	3.90×10^{-1}	5.09×10^{-1}	5.29×10^{-1}	4.62×10^{-1}	5.14×10^{-1}	7.40×10^{-1}	6.51×10^{-1}	8.00×10^{-1}
2.0	2.93×10^{-1}	3.29×10^{-1}	3.90×10^{-1}	5.44×10^{-1}	5.70×10^{-1}	5.10×10^{-1}	5.22×10^{-1}	6.64×10^{-1}	6.81×10^{-1}	8.30×10^{-1}
3.0	7.54×10^{-1}	9.73×10^{-1}	1.11×10^{0}	1.49×10^{0}	1.58×10^{0}	1.63×10^{0}	1.42×10^{0}	2.54×10^{0}	1.98×10^{0}	2.70×10^{0}
4.0	2.93×10^{0}	4.09×10^{0}	5.51×10^{0}	6.10×10^{0}	1.10×10^{1}	1.26×10^{1}	1.19×10^{1}	1.60×10^{1}	1.70×10^{1}	2.12×10^{1}

UNDERLINED VALUES = VIABLE COUNTS

TABLE 11.

Data pertaining to Figure 35.

HOLDING TIME (h)	SURVIVING FRACTION								
	UNIRRADIATED -plated on YENB			IRRADIATED - Low salt or minimal medium			High salt minimal medium		
	Bacitracin concentration (U/ml)			(U/ml)			(U/ml)		
	0	0.2	0.6	0	0.2	0.6	0	0.2	0.6
0	$\underline{1.52\times10^{7}}$	$\underline{1.46\times10^{7}}$	$\underline{1.41\times10^{7}}$	2.61×10^{-1}	2.56×10^{-1}	2.49×10^{-1}	9.20×10^{-3}	8.90×10^{-3}	1.07×10^{-2}
0.5	1.16×10^{0}	1.03×10^{0}	9.40×10^{-1}	2.62×10^{-1}	2.86×10^{-1}	2.48×10^{-1}	1.20×10^{-2}	9.10×10^{-3}	1.02×10^{-3}
1.0	1.14×10^{0}	1.27×10^{0}	8.84×10^{-1}	2.91×10^{-1}	3.26×10^{-1}	2.63×10^{-1}	2.20×10^{-2}	1.04×10^{-2}	9.31×10^{-3}
1.5	9.74×10^{-1}	1.07×10^{0}	8.35×10^{-1}	2.71×10^{-1}	2.78×10^{-1}	2.52×10^{-1}	3.40×10^{-2}	2.40×10^{-2}	8.80×10^{-3}
2.0	9.81×10^{-1}	1.01×10^{0}	6.34×10^{-1}	2.84×10^{-1}	2.58×10^{-1}	2.68×10^{-1}	3.56×10^{-2}	3.66×10^{-2}	1.15×10^{-2}
3.0	1.84×10^{0}	1.91×10^{0}	1.58×10^{0}	3.06×10^{-1}	2.50×10^{-1}	2.76×10^{-1}	7.10×10^{-2}	5.45×10^{-2}	1.78×10^{-2}
4.0	8.00×10^{0}	8.31×10^{0}	7.60×10^{0}	2.94×10^{-1}	2.51×10^{-1}	2.36×10^{-1}	9.05×10^{-2}	8.10×10^{-2}	2.39×10^{-2}
6.0	6.40×10^{1}	7.20×10^{1}	5.81×10^{1}	3.74×10^{-1}	3.58×10^{-1}	2.41×10^{-1}	1.90×10^{-1}	1.79×10^{-1}	4.10×10^{-2}

UNDERLINED VALUES = VIABLE COUNTS

TABLE 12.

Data pertaining to Figures 36 (a and b) and 37 (a and b).

Fluence. Jm^{-2}	SURVIVING FRACTION. Complex media YENB	Minimal media Low salt	Minimal media High salt
Figure 36a. 254 nm. Fluence rate: 4.78×10^{-2} $Jm^{-2}sec^{-1}$.			
0	$\underline{1.84 \times 10^{7}}$	$\underline{2.08 \times 10^{7}}$	$\underline{2.01 \times 10^{7}}$
28.68	4.64×10^{-1}	5.28×10^{-1}	4.91×10^{-1}
57.36	8.68×10^{-2}	9.90×10^{-2}	1.05×10^{-1}
86.04	1.84×10^{-2}	2.15×10^{-2}	2.65×10^{-2}
114.72	1.50×10^{-3}	1.47×10^{-3}	2.12×10^{-3}
Figure 36b. 260 nm. Fluence rate: 7.58×10^{-2} $Jm^{-2}sec^{-1}$.			
0	NOT	$\underline{7.53 \times 10^{6}}$	$\underline{7.33 \times 10^{6}}$
30	DONE	5.89×10^{-1}	5.50×10^{-1}
60		1.81×10^{-1}	2.29×10^{-1}
90		2.51×10^{-2}	5.00×10^{-2}
120		1.60×10^{-3}	7.09×10^{-3}
150		1.11×10^{-4}	9.78×10^{-4}
Figure 37a. 270 nm. Fluence rate: 8.218×10^{-2} $Jm^{-2}sec^{-1}$.			
0	NOT	$\underline{1.30 \times 10^{7}}$	$\underline{1.04 \times 10^{7}}$
30	DONE	5.49×10^{-1}	6.28×10^{-1}
60		1.32×10^{-1}	1.52×10^{-1}
90		6.60×10^{-3}	1.38×10^{-2}
120		2.30×10^{-4}	5.90×10^{-4}
Figure 37b. 280 nm. Fluence rate: 5.374×10^{-1} $Jm^{-2}sec^{-1}$.			
0	NOT	$\underline{9.97 \times 10^{6}}$	$\underline{9.43 \times 10^{6}}$
30	DONE	4.85×10^{-1}	5.19×10^{-1}
60		1.62×10^{-1}	1.77×10^{-1}
90		1.50×10^{-2}	3.62×10^{-2}
120		8.16×10^{-4}	4.10×10^{-3}
150		6.30×10^{-5}	2.29×10^{-4}

Note. Underlined values at zero fluence refer to initial viable counts.

TABLE 13.

Data pertaining to Figures 38(a and b) and 39.

FLUENCE (Jm^{-2})	SURVIVING FRACTION		
	Complex medium	Minimal media	
	YENB	Low salt	High salt
Figure 38a. 290 nm. Fluence rate: 2.18 $Jm^{-2}sec^{-1}$			
0	$\underline{1.12x10^{7}}$	$\underline{1.23x10^{7}}$	$\underline{8.73x10^{6}}$
50	$7.87x10^{-1}$	$8.35x10^{-1}$	$6.73x10^{-1}$
100	$2.96x10^{-1}$	$3.92x10^{-1}$	$2.95x10^{-1}$
150	$9.90x10^{-2}$	$1.36x10^{-1}$	$1.14x10^{-1}$
200	$2.30x10^{-2}$	$3.26x10^{-2}$	$3.66x10^{-2}$
250	$2.28x10^{-3}$	$4.16x10^{-3}$	$8.38x10^{-3}$
300	$3.20x10^{-4}$	$1.90x10^{-4}$	$1.40x10^{-3}$
Figure 38b. 300 nm. Fluence rate: 4.25 $Jm^{-2}sec^{-1}$			
0	$\underline{1.40x10^{7}}$	NOT	$\underline{1.38x10^{7}}$
$5.0x10^{2}$	$8.44x10^{-1}$	DONE	$8.53x10^{-1}$
$1.0x10^{3}$	$5.97x10^{-1}$		$6.40x10^{-1}$
$1.5x10^{3}$	$2.27x10^{-1}$		$2.71x10^{-1}$
$2.0x10^{3}$	$9.70x10^{-2}$		$1.37x10^{-1}$
$2.5x10^{3}$	$2.30x10^{-2}$		$5.80x10^{-2}$
Figure 39. 305 nm. Fluence rate: 7.88 $Jm^{-2}sec^{-1}$.			
0	NOT	$\underline{1.47x10^{7}}$	$\underline{1.11x10^{7}}$
$2.0x10^{3}$	DONE	$7.69x10^{-1}$	$7.12x10^{-1}$
$4.0x10^{3}$		$4.44x10^{-1}$	$4.11x10^{-1}$
$6.0x10^{3}$		$1.96x10^{-1}$	$1.56x10^{-1}$
$7.8x10^{3}$		$5.10x10^{-2}$	$7.57x10^{-2}$
$9.5x10^{3}$		$9.40x10^{-3}$	$1.92x10^{-2}$
$1.04x10^{4}$		$4.20x10^{-3}$	$7.80x10^{-3}$

Underlined values = Viable counts.

TABLE 14.

Data pertaining to Figures 40(a and b) and 41a.

FLUENCE (Jm^{-2})	SURVIVING FRACTION		
	Complex medium. YENB	Minimal media. Low salt	High salt
Figure 40a. 310 nm. Fluence rate: 6.20 $Jm^{-2}sec^{-1}$.			
0	$\underline{1.32\times10^{7}}$	$\underline{1.50\times10^{7}}$	$\underline{1.09\times10^{7}}$
3.0×10^{4}	6.90×10^{-1}	6.55×10^{-1}	7.15×10^{-1}
6.0×10^{4}	2.61×10^{-1}	3.11×10^{-1}	3.70×10^{-1}
8.0×10^{4}	1.81×10^{-1}	1.91×10^{-1}	1.53×10^{-1}
1.0×10^{5}	1.17×10^{-1}	1.05×10^{-1}	4.74×10^{-2}
1.1×10^{5}	5.30×10^{-2}	6.00×10^{-2}	1.50×10^{-2}
1.2×10^{5}	3.35×10^{-2}	3.22×10^{-2}	5.14×10^{-3}
1.3×10^{5}	1.97×10^{-2}	2.10×10^{-2}	1.83×10^{-3}
1.4×10^{5}	6.71×10^{-3}	6.98×10^{-3}	4.90×10^{-4}
Figure 40b. 313 nm. Fluence rate: 24.29 $Jm^{-2}sec^{-1}$.			
0	$\underline{1.44\times10^{7}}$	$\underline{1.38\times10^{7}}$	$\underline{1.43\times10^{7}}$
2.91×10^{4}	1.04×10^{0}	9.77×10^{-1}	9.41×10^{-1}
5.83×10^{4}	7.92×10^{-1}	8.00×10^{-1}	7.66×10^{-1}
8.75×10^{4}	5.98×10^{-1}	4.87×10^{-1}	4.25×10^{-1}
1.02×10^{5}	3.88×10^{-1}	3.89×10^{-1}	1.90×10^{-1}
1.17×10^{5}	2.85×10^{-1}	2.75×10^{-1}	8.31×10^{-2}
1.31×10^{5}	1.38×10^{-1}	1.37×10^{-1}	2.30×10^{-2}
1.46×10^{5}	5.76×10^{-2}	5.76×10^{-2}	4.90×10^{-3}
1.56×10^{5}	1.98×10^{-2}	2.33×10^{-2}	-
Figure 41a. 325 nm. Fluence rate: 15.34 $Jm^{-2}sec^{-1}$.			
0	$\underline{1.09\times10^{7}}$	$\underline{1.03\times10^{7}}$	$\underline{1.01\times10^{7}}$
5.00×10^{4}	9.20×10^{-1}	9.15×10^{-1}	5.76×10^{-1}
1.00×10^{5}	6.71×10^{-1}	6.54×10^{-1}	2.49×10^{-1}
1.50×10^{5}	1.44×10^{-1}	1.63×10^{-1}	8.10×10^{-3}
1.75×10^{5}	5.83×10^{-2}	6.80×10^{-2}	4.72×10^{-3}
2.00×10^{5}	2.42×10^{-2}	2.96×10^{-2}	2.43×10^{-3}
2.25×10^{5}	1.42×10^{-2}	1.21×10^{-2}	1.21×10^{-3}
2.50×10^{5}	6.94×10^{-3}	7.01×10^{-3}	9.80×10^{-4}
2.75×10^{5}	3.64×10^{-3}	3.45×10^{-3}	8.10×10^{-4}
3.00×10^{5}	1.68×10^{-3}	1.53×10^{-3}	6.10×10^{-4}

UNDERLINED VALUES = VIABLE COUNTS.

TABLE 15.

Data pertaining to Figures 41b and 42(a and b).

FLUENCE (Jm^{-2})	SURVIVING FRACTION		
	Complex medium	Minimal media	
	YENB	Low salt	High salt
Figure 41b. 334 nm. Fluence rate: 13.90 $Jm^{-2}sec^{-1}$.			
0	$\underline{1.22\times10^{7}}$	$\underline{1.64\times10^{7}}$	$\underline{1.13\times10^{7}}$
5.00×10^{4}	8.35×10^{-1}	9.90×10^{-1}	5.95×10^{-1}
1.00×10^{5}	6.27×10^{-1}	5.69×10^{-1}	3.34×10^{-1}
1.25×10^{5}	4.19×10^{-1}	4.29×10^{-1}	9.24×10^{-2}
1.50×10^{5}	3.26×10^{-1}	2.97×10^{-1}	3.66×10^{-2}
1.75×10^{5}	1.74×10^{-1}	1.66×10^{-1}	1.85×10^{-2}
2.00×10^{5}	5.10×10^{-2}	8.30×10^{-2}	1.20×10^{-2}
2.50×10^{5}	2.66×10^{-2}	3.53×10^{-2}	4.32×10^{-3}
3.00×10^{5}	1.07×10^{-2}	1.30×10^{-2}	2.05×10^{-3}
3.50×10^{5}	5.25×10^{-3}	5.87×10^{-3}	1.13×10^{-3}
Figure 42a. 365 nm. Fluence rate: 56.5 $Jm^{-2}sec^{-1}$.			
0	$\underline{1.35\times10^{7}}$	$\underline{1.60\times10^{7}}$	$\underline{1.31\times10^{7}}$
1.0×10^{5}	8.53×10^{-1}	1.02×10^{0}	8.29×10^{-1}
2.0×10^{5}	7.31×10^{-1}	8.55×10^{-1}	3.80×10^{-1}
3.0×10^{5}	5.12×10^{-1}	4.97×10^{-1}	1.09×10^{-1}
4.0×10^{5}	1.46×10^{-1}	2.19×10^{-1}	3.00×10^{-2}
5.0×10^{5}	4.90×10^{-2}	8.70×10^{-2}	1.30×10^{-2}
6.0×10^{5}	2.22×10^{-2}	3.40×10^{-2}	4.20×10^{-3}
Figure 42b. 405 nm. Fluence rate: 1.46×10^{2} $Jm^{-2}sec^{-1}$.			
0	$\underline{1.40\times10^{7}}$	$\underline{1.42\times10^{7}}$	$\underline{1.36\times10^{7}}$
7.90×10^{5}	8.97×10^{-1}	9.02×10^{-1}	5.70×10^{-1}
1.05×10^{6}	8.85×10^{-1}	8.20×10^{-1}	3.96×10^{-1}
1.58×10^{6}	4.36×10^{-1}	4.48×10^{-1}	1.70×10^{-1}
2.10×10^{6}	1.56×10^{-1}	1.85×10^{-1}	5.30×10^{-2}
2.63×10^{6}	8.80×10^{-2}	1.01×10^{-1}	3.26×10^{-2}
3.15×10^{6}	5.20×10^{-2}	6.80×10^{-2}	1.20×10^{-2}
3.68×10^{6}	2.30×10^{-2}	3.12×10^{-2}	4.80×10^{-3}
4.20×10^{6}	7.55×10^{-3}	1.15×10^{-2}	-

UNDERLINED VALUES = VIABLE COUNTS.

TABLE 16.

Data pertaining to Figure 43.

FLUENCE (Jm^{-2})	FLUENCE RATE ($Jm^{-2}sec^{-1}$)	SURVIVING FRACTION	
		Low salt minimal medium	High salt minimal medium
0	-	$\underline{2.39 \times 10^{8}}$	$\underline{2.28 \times 10^{8}}$
50	6.954×10^{-1}	5.71×10^{-1}	6.12×10^{-1}
50	6.954×10^{-2}	5.60×10^{-1}	6.06×10^{-1}
50	6.954×10^{-3}	5.98×10^{-1}	6.31×10^{-1}
100	6.954×10^{-1}	1.37×10^{-1}	1.62×10^{-1}
100	6.954×10^{-2}	1.32×10^{-1}	1.59×10^{-1}
100	6.954×10^{-3}	1.65×10^{-1}	1.96×10^{-1}
150	6.954×10^{-1}	8.20×10^{-3}	1.14×10^{-2}
150	6.954×10^{-2}	1.13×10^{-2}	1.47×10^{-2}
150	6.954×10^{-3}	1.92×10^{-2}	2.25×10^{-2}

UNDERLINED VALUES = VIABLE COUNTS.

TABLE 17.

Data pertaining to Figure 44.

WAVELENGTH (nm)	QUANTA/JOULE x 10^{18}	LOW SALT MEDIUM (or YENB)		HIGH SALT MEDIUM	
		F_{10} value (Jm^{-2})	$1/F_{10}$ (m^2/incident quantum)	F_{10} value (Jm^{-2})	$1/F_{10}$ (m^2/incident quantum)
254	1.279	65.0	1.203×10^{-20}	70.0	1.117×10^{-20}
260	1.309	58.0	1.317×10^{-20}	62.0	1.232×10^{-20}
270	1.359	63.0	1.168×10^{-20}	67.0	1.098×10^{-20}
280	1.409	69.0	1.028×10^{-20}	74.0	9.585×10^{-21}
290	1.460	1.49×10^{2}	4.597×10^{-21}	1.63×10^{2}	4.202×10^{-21}
300	1.510	1.92×10^{3}	3.449×10^{-22}	2.10×10^{3}	3.153×10^{-22}
305	1.536	7.10×10^{3}	9.169×10^{-23}	7.10×10^{3}	9.169×10^{-23}
310	1.560	9.90×10^{4}	6.475×10^{-24}	8.80×10^{4}	7.284×10^{-24}
313	1.580	1.38×10^{5}	4.586×10^{-24}	1.14×10^{5}	5.550×10^{-24}
325	1.636	1.65×10^{5}	3.704×10^{-24}	1.25×10^{5}	4.890×10^{-24}
334	1.682	1.98×10^{5}	3.000×10^{-24}	1.25×10^{5}	4.756×10^{-24}
365	1.838	4.70×10^{5}	1.157×10^{-24}	3.25×10^{5}	1.674×10^{-24}
405	2.039	2.90×10^{6}	2.025×10^{-25}	1.90×10^{6}	2.581×10^{-25}

TABLE 18.

Data pertaining to Figure 45.

WAVELENGTH. (nm)	$1/F_{10}$ HIGH SALT - $1/F_{10}$ LOW SALT
254	-0.086
260	-0.085
270	-0.070
280	-0.069
290	-0.395
300	-0.296
305	0.000
310	0.809
313	0.964
325	1.186
334	1.756
365	0.517
405	0.556

TABLE 19.

Data pertaining to Figure 46 a and b.

FIGURE 46a

TREATMENT TIME (Min)	SURVIVING FRACTION (Low salt minimal medium)	260 nm ABSORPTION (Test - Control)
(i) Mild-heat. Initial cell concentration : $1x10^8$ CFU/ml.		
10	$5.92x10^{-1}$	$3.40x10^{-2}$
20	$3.50x10^{-1}$	$6.10x10^{-2}$
30	$5.19x10^{-2}$	$7.00x10^{-2}$
40	$6.80x10^{-3}$	$8.80x10^{-2}$
50	$3.40x10^{-4}$	$8.20x10^{-2}$
(ii) Far-UV Radiation. Fluence rate: $4.78x10^{-2}$ $Jm^{-2}sec^{-1}$ Initial cell concentration : $5x10^8$ CFU/ml		
15	$4.78x10^{-1}$	$- 2.00x10^{-3}$
30	$5.50x10^{-2}$	$- 2.00x10^{-3}$
45	$8.00x10^{-4}$	$- 2.00x10^{-3}$
60	$2.00x10^{-6}$	$- 4.00x10^{-3}$
75	-	$5.00x10^{-3}$
(iii) Near-UV Radiation. Initial cell concentration : $5x10^8$ CFU/ml		
60	$2.00x10^{-1}$	$9.00x10^{-3}$
120	$1.00x10^{-4}$	$2.00x10^{-2}$
180	$3.90x10^{-6}$	$2.80x10^{-2}$
240	-	$2.90x10^{-2}$
300	-	$3.30x10^{-2}$

FIGURE 46b

Absorption scan after 4 hours near-UV irradiation.

WAVELENGTH (nm)	OPTICAL DENSITY	WAVELENGTH (nm)	OPTICAL DENSITY
240	0.000	262	0.076
242	0.005	264	0.073
244	0.012	266	0.066
246	0.019	268	0.055
248	0.031	270	0.040
250	0.042	272	0.023
252	0.054	274	0.005
254	0.063	276	0.000
256	0.068		
258	0.074		
260	0.077		

TABLE 20

Data pertaining to Figure 47.

NEAR-UV IRRADIATION TIME (h)	dpm TEST [methyl-^{3}H] thymidine	dpm CONTROL [methyl-^{3}H] thymidine
Initial cell concentration : 5×10^8 CFU/ml.		
0	2.0107×10^3	2.0140×10^3
0.5	3.9646×10^3	2.9489×10^3
1.0	5.9338×10^3	3.7757×10^3
1.5	6.1390×10^3	3.8961×10^3
2.0	7.2470×10^3	4.7311×10^3
2.5	9.3028×10^3	5.3519×10^3
3.0	1.1089×10^4	5.6167×10^3
3.5	1.7416×10^4	6.1932×10^3
4.0	2.1260×10^4	6.7835×10^3
4.5	2.3825×10^4	7.2431×10^3
5.0	2.5754×10^4	8.2620×10^3

TABLE 21.

Data pertaining to Figure 48.

TREATMENT TIME (min)	SURVIVING FRACTION Low salt minimal medium	[methyl -^{3}H] thymidine LEAKAGE (dpm Test / Control)
(i) Mild-heat (52 ^{o}C) Initial cell concentration 1x10^{8} CFU/ml		
5	7.00×10^{-1}	1.225
10	4.00×10^{-1}	1.252
15	3.33×10^{-1}	1.550
20	2.93×10^{-1}	1.825
25	8.87×10^{-2}	1.932
30	5.19×10^{-2}	1.901
35	1.67×10^{-2}	1.844
40	6.80×10^{-3}	2.084
45	5.04×10^{-3}	1.864
50	3.40×10^{-3}	1.902
(ii) Far- UV Radiation (254 nm) Fluence rate : 4.78×10^{-2} $Jm^{-2}sec^{-1}$. Initial cell concentration : 4x10^{8} CFU/ml.		
5	8.21×10^{-1}	0.984
10	5.28×10^{-1}	1.164
20	3.99×10^{-1}	1.131
30	5.50×10^{-2}	1.183
35	1.00×10^{-2}	1.311
40	1.47×10^{-3}	1.122
45	6.00×10^{-4}	1.198
50	3.00×10^{-5}	1.361
(iii) Near-UV Radiation. Initial cell concentration: 5x10^{8} CFU/ml		
15	9.00×10^{-1}	1.411
30	7.41×10^{-1}	1.828
45	5.50×10^{-1}	1.944
60	4.57×10^{-1}	2.288
75	2.80×10^{-1}	2.049
90	1.46×10^{-1}	2.813
105	5.40×10^{-2}	2.170
120	7.00×10^{-3}	2.042
150	5.00×10^{-5}	2.072

TABLE 22.

Data pertaining to Figure 49.

GROWTH TIME	OPTICAL DENSITY at 470 nm.			
(h)	ZERO K^+	4 mM K^+	8 mM K^+	16 mM K^+
0	0.022	0.022	0.023	0.023
0.5	0.026	0.030	0.028	0.027
1.0	0.031	0.030	0.032	0.032
1.5	0.034	0.034	0.033	0.034
2.0	0.033	0.038	0.037	0.037
2.5	0.037	0.042	0.042	0.042
3.0	0.044	0.047	0.049	0.047
3.5	0.053	0.057	0.060	0.060
4.0	0.072	0.073	0.076	0.078
4.5	0.090	0.088	0.099	0.100
5.0	0.127	0.119	0.127	0.130
5.5	0.168	0.155	0.162	0.171
6.0	0.230	0.204	0.212	0.225
6.5	0.294	0.260	0.277	0.290
7.0	0.380	0.370	0.420	0.360
7.5	0.560	0.500	0.530	0.580
8.0	0.720	0.580	0.560	0.660
8.5	1.020	0.820	0.880	0.900
9.0	1.240	1.090	1.100	1.030
9.5	1.780	1.400	1.420	1.420
10.0	2.150	1.710	1.710	1.710
12.0	3.200	3.170	3.190	2.940
24.0	3.850	4.500	4.360	3.740

TABLE 23.

Data pertaining to Figure 50.

NEAR -UV RADIATION TIME	SURVIVING FRACTIONS on minimal media after growth in differing concentrations of Potassium.							
	ZERO K^+		4 mM K^+		8 mM K^+		16 mM K^+	
(Min)	Low salt	High salt	Low salt	High salt	Low salt	High salt	Low salt	High salt
0	$\underline{9.53\times10^{6}}$	$\underline{6.63\times10^{6}}$	$\underline{1.35\times10^{7}}$	$\underline{1.18\times10^{7}}$	$\underline{1.35\times10^{7}}$	$\underline{1.30\times10^{7}}$	$\underline{1.07\times10^{7}}$	$\underline{1.00\times10^{7}}$
30	2.76×10^{-1}	4.42×10^{-1}	8.15×10^{-1}	5.79×10^{-1}	7.05×10^{-1}	4.72×10^{-1}	8.26×10^{-1}	6.05×10^{-1}
60	7.13×10^{-3}	5.00×10^{-5}	2.27×10^{-1}	1.18×10^{-1}	3.84×10^{-1}	7.88×10^{-1}	4.97×10^{-1}	2.89×10^{-1}
80	1.12×10^{-3}	-	1.02×10^{-1}	5.20×10^{-4}	1.34×10^{-1}	2.06×10^{-3}	1.53×10^{-1}	2.15×10^{-3}
100	1.05×10^{-5}	-	7.54×10^{-3}	6.50×10^{-5}	1.21×10^{-2}	5.60×10^{-5}	9.16×10^{-3}	3.30×10^{-5}
120	-	-	2.08×10^{-4}	2.80×10^{-5}	1.99×10^{-4}	1.03×10^{-5}	7.77×10^{-4}	2.50×10^{-5}

UNDERLINED VALUES = VIABLE COUNTS.

TABLE 24

Data pertaining to Figure 51.

TIME OF IRRADIATION (min)	$^{86}Rb^{+}$ LEAKAGE dpm TEST.	dpm CONTROL
(i) Far - UV Radiation. Fluence rate : 4.78×10^{-2} $Jm^{-2}sec^{-1}$		
	Initial cell concentration : 1×10^{8} CFU/ml.	
0	4.54×10^{1}	4.54×10^{1}
7	8.57×10^{1}	9.87×10^{1}
14	1.268×10^{2}	1.331×10^{2}
21	1.544×10^{2}	1.703×10^{2}
28	1.772×10^{2}	2.199×10^{2}
35	2.169×10^{2}	2.273×10^{2}
42	2.383×10^{2}	2.621×10^{2}
49	2.587×10^{2}	2.867×10^{2}
56	3.077×10^{2}	3.105×10^{2}
(ii) Near- UV Radiation. Initial cell concentration: 1×10^{8} CFU/ml.		
0	7.50×10^{1}	7.50×10^{1}
30	2.615×10^{2}	2.393×10^{2}
60	4.389×10^{2}	3.448×10^{2}
90	8.192×10^{2}	4.476×10^{2}
120	1.4098×10^{3}	5.375×10^{2}
150	2.1221×10^{3}	6.318×10^{2}
180	2.6342×10^{3}	6.969×10^{2}
210	2.9660×10^{3}	7.862×10^{2}
240	3.1224×10^{3}	8.616×10^{2}

TABLE 25.

Data pertaining to Figure 52.

TREATMENT TIME (min)	SURVIVING FRACTION (Low salt minimal medium)	$^{86}Rb^{+}$ LEAKAGE dpm Test/Control
(i) MILD-HEAT (52° C) Initial cell concentration: $1x10^{8}$ CFU/ml.		
4	$8.61x10^{-1}$	1.603
6	$5.92x10^{-1}$	2.506
8	$2.95x10^{-1}$	3.074
12	$5.84x10^{-2}$	3.782
16	$3.04x10^{-2}$	3.981
(ii) FAR-UV RADIATION (254 nm). Fluence rate: $4.78x10^{-2}$ $Jm^{-2}sec^{-1}$. Initial cell concentration: $1x10^{8}$ CFU/ml.		
7	$5.12x10^{-1}$	0.868
14	$1.49x10^{-1}$	0.953
21	$8.41x10^{-3}$	0.907
28	$9.60x10^{-5}$	0.806
35	$2.40x10^{-5}$	0.954
42	$1.00x10^{-6}$	0.909
(iii) NEAR-UV RADIATION. Initial cell concentration: $1x10^{8}$ CFU/ml.		
30	$8.37x10^{-1}$	1.093
60	$7.81x10^{-1}$	1.273
90	$4.96x10^{-1}$	1.830
120	$1.57x10^{-2}$	2.623
150	$3.03x10^{-4}$	3.360
180	$6.53x10^{-5}$	3.780
210	$4.00x10^{-6}$	3.770

TABLE 26

Data pertaining to Figure 53.

HOLDING TIME (min)	$^{86}Rb^{+}$ LEAKAGE -dpm. TEMPERATURE OF HOLDING (°C)			
	37	28	20	0
0	7.50×10^{1}	7.50×10^{1}	7.50×10^{1}	7.50×10^{1}
30	2.48×10^{2}	2.15×10^{2}	1.42×10^{2}	2.53×10^{2}
60	4.80×10^{2}	3.33×10^{2}	2.06×10^{2}	3.86×10^{2}
90	6.83×10^{2}	4.19×10^{2}	2.63×10^{2}	5.24×10^{2}
120	8.29×10^{2}	4.87×10^{2}	3.02×10^{2}	6.38×10^{2}
180	1.00×10^{3}	6.58×10^{2}	4.09×10^{2}	7.86×10^{2}

TABLE 27.

Data pertaining to Figure 54(a,b,c and d).

FLUENCE (Jm^{-2})	dpm TEST/CONTROL	FLUENCE (Jm^{-2})	dpm TEST/CONTROL
54a 254 nm			
$1.00x10^2$	1.028	$2.50x10^3$	1.789
$5.00x10^2$	1.130	$3.00x10^3$	3.540
$1.00x10^3$	1.203	$4.00x10^3$	5.090
$2.00x10^3$	1.495	$5.00x10^3$	6.710
54b 270 nm			
$2.00x10^2$	1.099	$7.25x10^2$	2.410
$3.00x10^2$	1.356	$8.00x10^2$	2.440
$5.00x10^2$	1.739	$9.00x10^2$	2.480
$6.00x10^2$	1.989	$1.00x10^3$	2.872
54c 280 nm			
$1.00x10^2$	1.108	$6.00x10^2$	1.592
$2.00x10^2$	1.147	$8.00x10^2$	3.510
$4.00x10^2$	1.626	$1.00x10^3$	4.892
54d 290 nm			
$2.00x10^2$	1.009	$1.40x10^3$	2.050
$5.00x10^2$	1.095	$2.00x10^3$	4.000
$7.50x10^2$	1.189	$3.00x10^3$	5.480
$1.00x10^3$	1.570	$4.00x10^3$	6.280

TABLE 28.

Data pertaining to Figure 55 (a,b,c and d).

FLUENCE (Jm^{-2})	dpm TEST/CONTROL	FLUENCE (Jm^{-2})	dpm TEST/CONTROL
55a 300 nm			
$5.00x10^2$	1.014	$5.00x10^3$	1.973
$1.00x10^3$	1.015	$6.00x10^3$	2.185
$2.00x10^3$	1.653	$7.50x10^3$	6.820
$3.00x10^3$	1.606	$1.00x10^4$	8.196
$4.00x10^3$	1.853		
55b 305 nm			
$4.00x10^3$	1.060	$9.00x10^3$	4.137
$6.00x10^3$	2.197	$1.00x10^4$	4.260
$7.00x10^3$	3.165	$1.10x10^4$	5.173
$8.00x10^3$	3.154	$1.50x10^4$	6.280
55c 310 nm			
$1.00x10^4$	1.471	$1.40x10^5$	2.572
$3.00x10^4$	2.103	$1.45x10^5$	3.730
$5.00x10^4$	1.781	$1.82x10^5$	5.040
$1.00x10^5$	2.410	$2.70x10^5$	5.200
$1.20x10^5$	2.890		
55d 313 nm			
$2.00x10^4$	1.333	$1.40x10^5$	2.980
$4.00x10^4$	1.492	$1.60x10^5$	4.720
$6.00x10^4$	1.433	$1.80x10^5$	3.470
$7.00x10^4$	1.601	$2.00x10^5$	4.480
$8.00x10^4$	2.670	$2.40x10^5$	5.360
$1.00x10^5$	1.912	$3.00x10^5$	5.410

TABLE 29.

Data pertaining to Figure 56 (a,b,c and d).

FLUENCE (Jm^{-2})	dpm TEST/CONTROL	FLUENCE (Jm^{-2})	dpm TEST/CONTROL
56a 325 nm			
$2.50x10^4$	1.219	$1.25x10^5$	1.906
$4.00x10^4$	1.517	$1.60x10^5$	3.041
$8.00x10^4$	1.741	$2.40x10^5$	3.183
$1.00x10^5$	1.775		
56b 334 nm			
$1.00x10^5$	1.100	$4.00x10^5$	3.050
$2.00x10^5$	1.752	$4.50x10^5$	3.840
$3.00x10^5$	2.150	$5.60x10^5$	3.104
56c 365 nm			
$7.50x10^4$	1.165	$6.00x10^5$	1.673
$1.50x10^5$	1.395	$7.00x10^5$	1.904
$3.00x10^5$	1.611	$9.00x10^5$	3.450
$4.00x10^5$	1.514	$1.10x10^6$	4.890
$4.50x10^5$	1.428	$1.50x10^6$	5.260
$5.00x10^5$	1.389		
56d 405 nm			
$1.00x10^5$	1.289	$5.00x10^5$	2.442
$2.00x10^5$	1.982	$7.50x10^5$	2.863
$2.50x10^5$	2.055	$1.00x10^6$	2.241
$3.00x10^5$	1.765	$1.25x10^6$	2.634

TABLE 30.

Data pertaining to Figure 57.

TIME OF IRRADIATION (min)	SURVIVING FRACTION (low salt minimal medium)	$^{86}Rb^{+}$ LEAKAGE dpm TEST/CONTROL
(A) K-12 SR 385.		
0	$\underline{5.57\times10^{7}}$	initial count = 182
30	8.74×10^{-1}	1.606
60	4.95×10^{-1}	1.957
90	2.10×10^{-2}	2.600
120	2.99×10^{-4}	3.224
150	4.80×10^{-6}	4.430
180	-	3.737
(B) K-12 SR 246.		
0	$\underline{9.67\times10^{7}}$	initial count = 261
30	1.18×10^{-2}	1.453
60	1.45×10^{-4}	1.901
90	6.20×10^{-5}	2.270
120	1.55×10^{-5}	3.226
150	3.62×10^{-6}	3.898
180	-	4.011
(C) K-12 AB1157.		
0	$\underline{5.27\times10^{7}}$	initial count = 188
30	1.05×10^{0}	1.290
60	7.02×10^{-1}	1.659
90	5.86×10^{-1}	2.246
120	1.21×10^{-1}	3.210
150	1.12×10^{-2}	3.895
180	6.65×10^{-4}	6.014
(D) B/r.		
0	$\underline{5.70\times10^{7}}$	initial count = 46.4
30	8.59×10^{-1}	1.977
60	6.84×10^{-1}	1.803
90	6.14×10^{-1}	1.968
120	1.93×10^{-1}	2.580
150	2.02×10^{-2}	2.771
180	2.10×10^{-3}	3.076

UNDERLINED VALUES = VIABLE COUNTS

TABLE 31.

Data pertaining to Figure 58.

WAVELENGTH	LEAKAGE		LETHALITY	
(nm)	FLUENCE (Jm^{-2}) for dpm Test/Control of 2.0	1/FLUENCE m^2/incident quantum	FLUENCE(Jm^{-2}) F_{37}	$1/F_{37}$ m^2/incident quantum
254	2.75×10^{3}	2.840×10^{-22}	4.10×10^{1}	1.907×10^{-20}
260	1.00×10^{3}	7.640×10^{-22}	4.40×10^{1}	1.736×10^{-20}
270	5.50×10^{2}	1.338×10^{-21}	4.10×10^{1}	1.795×10^{-20}
280	7.00×10^{2}	1.013×10^{-21}	3.90×10^{1}	1.819×10^{-20}
290	1.25×10^{3}	5.270×10^{-22}	9.50×10^{1}	7.209×10^{-21}
300	4.50×10^{3}	1.472×10^{-22}	1.25×10^{3}	5.298×10^{-22}
305	7.00×10^{3}	9.300×10^{-23}	4.60×10^{3}	1.415×10^{-22}
310	7.00×10^{4}	9.150×10^{-24}	1.10×10^{5}	5.824×10^{-24}
313	9.50×10^{4}	6.679×10^{-24}	1.60×10^{5}	3.966×10^{-24}
317	1.00×10^{5}	6.265×10^{-24}	2.20×10^{5}	2.848×10^{-24}
325	1.40×10^{5}	4.360×10^{-24}	2.60×10^{5}	2.350×10^{-24}
328	2.10×10^{5}	2.883×10^{-24}	4.10×10^{5}	1.477×10^{-24}
334	3.00×10^{5}	1.980×10^{-24}	4.00×10^{5}	1.486×10^{-24}
365	7.00×10^{5}	7.770×10^{-25}	1.30×10^{6}	4.185×10^{-25}
405	2.50×10^{5}	1.962×10^{-24}	1.80×10^{6}	2.725×10^{-25}

TABLE 32

Data pertaining to Figure 59 (a and b)

FIGURE 59a

NEAR-UV RADIATION TIME (min)	SURVIVING FRACTION (low salt minimal medium)	$^{86}Rb^{+}$ LEAKAGE dpm TEST/CONTROL
0	1.0	1.0
30	8.37×10^{-1}	1.093
60	7.81×10^{-1}	1.273
90	4.96×10^{-1}	1.830
120	1.57×10^{-2}	2.623
150	3.03×10^{-4}	3.360
180	6.53×10^{-5}	3.780
210	4.00×10^{-6}	3.770

FIGURE 59b.

FAR-UV RADIATION FLUENCE (Jm^{-2})	SURVIVING FRACTION (low salt minimal medium)	$^{86}Rb^{+}$ LEAKAGE dpm TEST/CONTROL
0	1.0	1.0
3.0×10^{1}	5.12×10^{-1}	0.868
6.0×10^{1}	1.49×10^{-1}	0.953
9.0×10^{1}	8.41×10^{-3}	0.907
1.20×10^{2}	9.60×10^{-5}	0.806
1.50×10^{2}	2.40×10^{-5}	0.954
1.80×10^{2}	1.00×10^{-6}	0.909
5.00×10^{2}	-	1.130
1.00×10^{3}	-	1.179
2.00×10^{3}	-	1.513
2.50×10^{3}	-	1.714
3.00×10^{3}	-	3.550
4.00×10^{3}	-	5.090
4.50×10^{3}	-	6.951
5.00×10^{3}	-	7.160

TABLE 33

Data pertaining to Figure 60.

TIME OF IRRADIATION (Min)	SURVIVING FRACTION	
	Low salt minimal medium	High salt minimal medium
(i) 24 HOUR CULTURE.		
0	$\underline{1.38\times10^{7}}$	$\underline{1.17\times10^{7}}$
20	8.33×10^{-1}	8.46×10^{-1}
40	6.21×10^{-1}	2.02×10^{-1}
50	5.24×10^{-1}	7.69×10^{-2}
60	3.23×10^{-1}	1.19×10^{-2}
70	1.71×10^{-1}	1.05×10^{-3}
80	6.54×10^{-2}	1.50×10^{-4}
90	1.30×10^{-2}	-
100	2.15×10^{-3}	-
(ii) 3 HOUR CULTURE.		
0	$\underline{1.28\times10^{7}}$	$\underline{1.27\times10^{7}}$
30	8.80×10^{-1}	8.80×10^{-1}
60	6.95×10^{-1}	1.52×10^{-1}
70	5.55×10^{-1}	3.90×10^{-2}
80	3.78×10^{-1}	7.80×10^{-3}
90	2.28×10^{-1}	8.10×10^{-4}
100	1.22×10^{-1}	-
110	3.85×10^{-2}	-
120	5.44×10^{-3}	-
130	1.50×10^{-4}	-
(iii) 6 HOUR CULTURE.		
0	$\underline{2.21\times10^{7}}$	$\underline{2.27\times10^{7}}$
30	7.03×10^{-1}	6.50×10^{-1}
60	5.00×10^{-1}	2.07×10^{-1}
80	1.99×10^{-1}	2.90×10^{-2}
90	1.41×10^{-1}	1.19×10^{-2}
100	3.15×10^{-2}	2.32×10^{-3}
110	9.80×10^{-3}	1.00×10^{-4}
120	1.38×10^{-3}	-

UNDERLINED VALUES = VIABLE COUNTS

TABLE 34

Data pertaining to Figure 61.

GROWTH in Minimal medium (h)	LOW SALT MINIMAL MEDIUM Initial count/ml $X10^7$	Surviving Fraction	HIGH SALT MINIMAL MEDIUM Initial count/ml $X10^7$	Surviving Fraction
0 (24)	1.86	$3.93x10^{-1}$	1.76	$4.26x10^{-2}$
0.5	1.10	$2.44x10^{-1}$	1.15	$3.86x10^{-2}$
1.0	1.55	$7.33x10^{-1}$	1.58	$7.62x10^{-2}$
1.5	1.43	$6.48x10^{-1}$	1.33	$3.44x10^{-1}$
2.0	1.08	$8.47x10^{-1}$	1.21	$5.63x10^{-1}$
2.5	1.29	$8.03x10^{-1}$	1.11	$2.95x10^{-1}$
3.0	1.60	$6.71x10^{-1}$	1.44	$3.17x10^{-1}$
3.5	1.96	$7.53x10^{-1}$	1.85	$4.56x10^{-1}$
4.0	2.17	$5.82x10^{-1}$	1.96	$3.29x10^{-1}$
4.5	2.40	$6.80x10^{-1}$	2.23	$4.62x10^{-1}$
5.0	1.66	$7.35x10^{-1}$	1.97	$2.75x10^{-1}$
5.5	1.95	$5.76x10^{-1}$	1.88	$2.81x10^{-1}$
6.0	2.44	$6.89x10^{-1}$	2.39	$2.66x10^{-1}$

TABLE 35.

Data pertaining to Figure 62.

GROWTH in Minimal medium (h)	VIABLE COUNT /ml $X10^7$	OPTICAL DENSITY (at 470 nm)
0	1.82	0.026
0.25	1.67	0.023
0.5	1.74	0.025
0.75	1.88	0.026
1.0	1.91	0.028
1.25	1.69	0.030
1.5	1.84	0.035
1.75	1.93	0.039
2.0	1.96	0.042
2.25	1.88	0.050
2.5	2.04	0.052
2.75	2.26	0.061
3.0	3.01	0.067
3.25	3.30	0.079
3.5	4.07	0.090
3.75	4.87	0.110
4.0	5.23	0.116
4.25	5.83	0.140
4.5	8.17	0.159
4.75	8.60	0.175
5.0	11.23	0.200
5.25	10.57	0.226
5.5	12.50	0.252
5.75	14.27	0.297
6.0	18.67	0.336

TABLE 36

Data pertaining to Figure 63.

GROWTH in minimal medium.	LOW SALT PLATES Initial count /ml.	Surviving Fraction.	HIGH SALT PLATES Initial count /ml.	Surviving Fraction.	OPTICAL DENSITY (470 nm)
(h)	$X10^7$		$X10^7$		
0	1.41	$1.97x10^{-2}$	1.18	$3.88x10^{-4}$	0.031
1.0	0.95	$3.78x10^{-2}$	0.62	$1.86x10^{-3}$	0.034
2.0	1.05	$4.71x10^{-1}$	1.09	$1.55x10^{-2}$	0.038
3.0	0.85	$2.46x10^{-1}$	0.74	$3.83x10^{-2}$	0.045
4.0	0.52	$5.08x10^{-1}$	0.47	$2.32x10^{-1}$	0.056
5.0	0.20	$3.14x10^{-1}$	0.16	$5.50x10^{-2}$	0.093
6.0	0.31	$8.39x10^{-1}$	0.31	$2.67x10^{-1}$	0.135
7.0	0.79	$2.99x10^{-1}$	0.65	$4.85x10^{-2}$	0.210
8.0	0.97	$5.14x10^{-1}$	0.99	$4.76x10^{-2}$	0.329
9.0	0.79	$4.01x10^{-1}$	0.90	$3.73x10^{-2}$	0.500
10.0	0.78	$3.70x10^{-1}$	0.75	$3.31x10^{-2}$	0.780
11.0	0.96	$2.92x10^{-1}$	0.84	$5.30x10^{-2}$	1.370
12.0	1.06	$9.53x10^{-2}$	0.95	$5.60x10^{-2}$	1.770
13.0	-	-	-	-	2.300
14.0	0.71	$3.27x10^{-1}$	0.55	$6.70x10^{-3}$	1.930
15.0	-	-	-	-	1.990
16.0	0.34	$8.50x10^{-2}$	0.23	$1.77x10^{-2}$	1.940
17.0	-	-	-	-	1.740
18.0	0.36	$8.07x10^{-2}$	0.26	$3.86x10^{-3}$	1.620
19.0	-	-	-	-	2.090
20.0	0.94	$2.08x10^{-1}$	0.81	$1.02x10^{-2}$	1.730
21.0	-	-	-	-	1.830
22.0	0.91	$2.92x10^{-1}$	0.75	$2.19x10^{-2}$	1.670
23.0	-	-	-	-	2.520
24.0	1.41	$1.97x10^{-2}$	1.18	$3.88x10^{-4}$	2.180
25.0	-	-	-	-	2.090

TABLE 37.

Data pertaining to Figure 64.

TIME OF IRRADIATION (min)	SURVIVING FRACTION	
	Low salt minimal medium.	High salt minimal medium.
(i) 24 HOUR CULTURE.		
0	$\underline{1.35\times10^{7}}$	$\underline{1.23\times10^{7}}$
20	6.75×10^{-1}	7.15×10^{-1}
40	4.80×10^{-1}	1.27×10^{-1}
50	3.13×10^{-1}	1.00×10^{-2}
60	1.23×10^{-1}	7.59×10^{-4}
70	3.67×10^{-2}	5.15×10^{-5}
80	3.74×10^{-3}	-
90	3.45×10^{-4}	-
100	1.70×10^{-5}	-
(ii) 6 HOUR CULTURE.		
0	$\underline{2.17\times10^{7}}$	$\underline{2.36\times10^{7}}$
20	1.07×10^{0}	8.06×10^{-1}
30	-	7.27×10^{-1}
40	7.89×10^{-1}	6.27×10^{-1}
50	6.26×10^{-1}	5.04×10^{-1}
60	5.75×10^{-1}	2.54×10^{-1}
70	2.89×10^{-1}	3.85×10^{-2}
80	5.10×10^{-2}	8.90×10^{-4}
90	1.34×10^{-3}	3.80×10^{-5}
100	3.40×10^{-5}	-
110	1.60×10^{-5}	-

UNDERLINED VALUES = VIABLE COUNTS.

TABLE 38.

Data pertaining to Figure 65.

TIME OF IRRADIATION (min)	SURVIVING FRACTION: Low salt minimal medium.	SURVIVING FRACTION: High salt minimal medium.
(i) TEMPERATURE OF IRRADIATION : 0°C.		
0	$\underline{7.17\times10^{6}}$	$\underline{4.33\times10^{6}}$
10	7.74×10^{-1}	8.05×10^{-1}
20	3.90×10^{-1}	2.33×10^{-1}
30	2.36×10^{-1}	8.84×10^{-2}
40	9.06×10^{-2}	1.80×10^{-2}
50	4.02×10^{-2}	7.60×10^{-4}
60	1.27×10^{-2}	7.39×10^{-4}
70	1.83×10^{-3}	3.40×10^{-4}
80	1.46×10^{-4}	1.10×10^{-5}
(ii) TEMPERATURE OF IRRADIATION : 28°C.		
0	$\underline{3.87\times10^{6}}$	$\underline{3.33\times10^{6}}$
30	7.41×10^{-1}	8.05×10^{-1}
40	7.23×10^{-1}	6.29×10^{-1}
52	6.38×10^{-1}	4.58×10^{-1}
60	4.57×10^{-1}	2.30×10^{-1}
70	2.29×10^{-1}	7.76×10^{-2}
80	9.60×10^{-2}	8.80×10^{-3}
90	1.46×10^{-2}	8.50×10^{-4}
100	1.58×10^{-3}	1.00×10^{-4}
110	6.60×10^{-4}	-

UNDERLINED VALUES = VIABLE COUNTS.

TABLE 39.

Data pertaining to Figure 66.

TIME OF IRRADIATION (min)	SURVIVING FRACTION: Low salt minimal medium.	SURVIVING FRACTION: High salt minimal medium.
(i) 24 HOUR CULTURE.		
0	$\underline{1.03\times10^{7}}$	$\underline{8.03\times10^{6}}$
10	9.90×10^{-1}	8.38×10^{-1}
20	7.57×10^{-1}	2.74×10^{-1}
30	5.05×10^{-1}	2.49×10^{-3}
40	1.21×10^{-1}	2.78×10^{-4}
50	3.85×10^{-3}	7.90×10^{-5}
60	7.30×10^{-4}	-
(ii) 6 HOUR CULTURE.		
0	$\underline{1.63\times10^{7}}$	$\underline{1.47\times10^{7}}$
10	9.40×10^{-1}	8.66×10^{-1}
20	4.42×10^{-1}	3.49×10^{-1}
30	4.28×10^{-1}	2.54×10^{-1}
40	2.03×10^{-1}	1.01×10^{-1}
50	1.10×10^{-1}	2.70×10^{-2}
60	5.10×10^{-2}	5.32×10^{-3}
70	1.30×10^{-2}	2.20×10^{-4}
80	1.89×10^{-3}	2.30×10^{-5}
90	1.10×10^{-4}	-
100	4.90×10^{-5}	-

UNDERLINED VALUES = VIABLE COUNTS.

TABLE 40.

Data pertaining to Figure 67.

GROWTH in minimal medium.	INITIAL COUNT ml^{-1} $X10^7$	SURVIVING FRACTION minimal media Low salt	High salt
0	1.45	$6.70x10^{-3}$	$4.36x10^{-4}$
1.0	0.46	$1.64x10^{-1}$	$6.22x10^{-2}$
2.0	0.51	$1.44x10^{-1}$	$4.98x10^{-2}$
3.0	0.75	$3.06x10^{-1}$	$2.15x10^{-1}$
4.0	0.39	$2.56x10^{-1}$	$1.14x10^{-1}$
5.0	1.63	$3.59x10^{-1}$	$9.30x10^{-2}$
6.0	1.97	$5.89x10^{-1}$	$3.11x10^{-1}$
7.0	1.56	$4.19x10^{-1}$	$3.68x10^{-1}$
8.0	0.62	$1.79x10^{-1}$	$5.68x10^{-2}$
9.0	3.24	$7.74x10^{-1}$	$6.78x10^{-1}$
10.0	2.70	$6.96x10^{-1}$	$7.07x10^{-1}$
11.0	1.23	$7.69x10^{-1}$	$5.88x10^{-1}$
12.0	1.25	$5.73x10^{-1}$	$4.67x10^{-1}$

TABLE 41.

Data pertaining to Figure 68.

TIME OF IRRADIATION (min)	SURVIVING FRACTION: Low salt minimal medium.	SURVIVING FRACTION: High salt minimal medium.
(i) 24 HOUR CULTURE.		
0	$\underline{2.22\times10^{7}}$	$\underline{1.91\times10^{7}}$
45	6.06×10^{-1}	7.16×10^{-1}
90	3.53×10^{-1}	2.79×10^{-1}
100	1.97×10^{-1}	1.03×10^{-1}
110	6.60×10^{-2}	5.16×10^{-2}
120	2.93×10^{-2}	4.06×10^{-3}
130	1.58×10^{-2}	4.70×10^{-4}
140	1.98×10^{-3}	2.02×10^{-4}
150	2.19×10^{-4}	-
(ii) 4 HOUR CULTURE.		
0	$\underline{1.22\times10^{7}}$	$\underline{1.32\times10^{7}}$
45	1.15×10^{0}	3.22×10^{-1}
90	2.46×10^{-1}	1.44×10^{-2}
100	5.75×10^{-2}	3.78×10^{-3}
110	1.15×10^{-2}	7.00×10^{-4}
120	1.92×10^{-3}	-

UNDERLINED VALUES = VIABLE COUNTS.

TABLE 42.

Data pertaining to Figure 69.

GROWTH in minimal medium	LOW SALT MINIMAL MEDIUM. Initial count /ml	Surviving Fraction	HIGH SALT MINIMAL MEDIUM. Initial count /ml	Surviving Fraction	OPTICAL DENSITY (470 nm)
(h)	$X10^7$		$X10^7$		
0	1.48	$4.10x10^{-1}$	1.49	$3.30x10^{-1}$	0.024
0.5	-	-	-	-	0.025
1.0	0.84	$7.41x10^{-1}$	0.82	$7.05x10^{-1}$	0.027
1.5	-	-	-	-	0.031
2.0	1.15	$3.72x10^{-1}$	1.24	$1.05x10^{-1}$	0.047
2.5	-	-	-	-	0.093
3.0	1.46	$3.44x10^{-2}$	1.19	$1.06x10^{-2}$	0.137
3.5	-	-	-	-	0.210
4.0	1.45	$3.25x10^{-1}$	1.47	$3.22x10^{-3}$	0.332
4.5	-	-	-	-	0.480
5.0	1.29	$5.66x10^{-1}$	1.24	$1.91x10^{-1}$	0.670
5.5	-	-	-	-	0.760
6.0	1.68	$9.19x10^{-1}$	1.65	$7.51x10^{-1}$	0.830
6.5	-	-	-	-	0.960
7.0	0.93	$9.46x10^{-1}$	0.89	$1.05x10^{0}$	1.170
7.5	-	-	-	-	1.470
8.0	1.10	$1.14x10^{0}$	1.14	$1.44x10^{0}$	1.580
8.5	-	-	-	-	1.800
9.0	0.86	$1.47x10^{0}$	0.96	$1.16x10^{0}$	1.830
9.5	-	-	-	-	2.040
10.0	1.09	$3.77x10^{-1}$	0.98	$2.23x10^{-1}$	2.450
11.0	1.07	$7.11x10^{-1}$	1.12	$7.75x10^{-1}$	2.500
12.0	1.39	$8.29x10^{-1}$	1.39	$8.63x10^{-1}$	2.420
14.0	1.21	$8.02x10^{-1}$	1.21	$7.81x10^{-1}$	2.560
16.0	1.00	$7.48x10^{-1}$	0.94	$6.66x10^{-1}$	2.250
18.0	1.12	$7.01x10^{-1}$	0.94	$6.99x10^{-1}$	2.160

TABLE 43.

Data pertaining to Figure 70.

TIME OF IRRADIATION (min)	SURVIVING FRACTION	
	Low salt minimal medium.	High salt minimal medium.
(i) 24 HOUR CULTURE.		
0	$\underline{1.53\times10^{7}}$	$\underline{1.53\times10^{7}}$
30	8.58×10^{-1}	7.09×10^{-1}
60	3.91×10^{-1}	5.46×10^{-3}
75	8.27×10^{-2}	2.20×10^{-4}
90	8.08×10^{-3}	-
100	1.39×10^{-3}	-
110	2.20×10^{-4}	5.40×10^{-5}
(ii) 6 HOUR CULTURE.		
0	$\underline{1.89\times10^{7}}$	$\underline{1.78\times10^{7}}$
20	9.55×10^{-1}	4.44×10^{-1}
40	5.98×10^{-1}	7.74×10^{-2}
60	3.03×10^{-1}	3.10×10^{-3}
75	4.40×10^{-2}	2.40×10^{-4}
90	2.86×10^{-3}	-
100	2.30×10^{-4}	-

UNDERLINED VALUES = VIABLE COUNTS.

TABLE 44.

Data pertaining to Figure 71.

GROWTH in minimal medium (h)	INITIAL COUNT ml^{-1} $X10^7$	SURVIVING FRACTION LOW SALT minimal medium	SURVIVING FRACTION HIGH SALT minimal medium	OPTICAL DENSITY (470 nm)
0	1.35	$2.74x10^{-1}$	$1.12x10^{-3}$	0.023
0.5	-	-	-	0.026
1.0	0.82	$7.02x10^{-1}$	$3.52x10^{-1}$	0.029
1.5	-	-	-	0.027
2.0	0.93	$4.53x10^{-1}$	$1.28x10^{-1}$	0.039
2.5	-	-	-	0.031
3.0	1.82	$3.78x10^{-1}$	$9.23x10^{-2}$	0.054
3.5	-	-	-	0.067
4.0	0.67	$1.31x10^{-1}$	$2.68x10^{-2}$	0.093
4.5	-	-	-	0.132
5.0	1.35	$1.03x10^{-1}$	$8.90x10^{-2}$	0.190
5.5	-	-	-	0.280
6.0	2.18	$1.56x10^{-1}$	$2.50x10^{-3}$	0.394
6.5	-	-	-	0.540
7.0	1.74	$1.15x10^{-1}$	$3.80x10^{-4}$	0.820
7.5	-	-	-	1.140
8.0	1.23	$9.10x10^{-2}$	$4.43x10^{-3}$	1.660
8.5	-	-	-	2.110
9.0	1.03	$1.08x10^{-1}$	$5.80x10^{-4}$	2.570
9.5	-	-	-	2.810
10.0	1.18	$4.38x10^{-2}$	$7.34x10^{-4}$	2.970
10.5	-	-	-	3.120
11.0	0.97	$1.05x10^{-1}$	$5.18x10^{-4}$	3.280
11.5	-	-	-	3.520
24.0	-	-	-	3.450

TABLE 45.

Data pertaining to Figure 72.

TIME OF IRRADIATION (min)	SURVIVING FRACTION: Low salt minimal medium.	SURVIVING FRACTION: High salt minimal medium.
(i) 24 HOUR CULTURE.		
0	$\underline{2.27\times10^{7}}$	$\underline{2.09\times10^{7}}$
20	8.28×10^{-1}	6.52×10^{-1}
40	5.07×10^{-1}	2.35×10^{-1}
60	3.31×10^{-1}	2.84×10^{-2}
80	1.09×10^{-1}	2.11×10^{-3}
100	3.79×10^{-2}	2.44×10^{-4}
120	6.31×10^{-3}	6.20×10^{-5}
(ii) 3.5 HOUR CULTURE.		
0	$\underline{2.62\times10^{7}}$	$\underline{3.00\times10^{7}}$
20	9.71×10^{-1}	4.73×10^{-1}
40	4.28×10^{-1}	3.28×10^{-2}
60	9.72×10^{-2}	2.73×10^{-3}
80	1.52×10^{-2}	5.52×10^{-4}
100	2.64×10^{-3}	2.02×10^{-4}
120	9.20×10^{-4}	8.30×10^{-5}

UNDERLINED VALUES = VIABLE COUNTS.

TABLE 46.

Data pertaining to Figure 73.

GROWTH in minimal medium (h)	LOW SALT MINIMAL MEDIUM. Initial count /ml $X10^7$	Surviving Fraction	HIGH SALT MINIMAL MEDIUM. Initial count /ml $X10^7$	Surviving Fraction	OPTICAL DENSITY (470 nm)
0	1.29	$5.92x10^{-1}$	1.46	$2.31x10^{-2}$	0.024
0.5	-	-	-	-	0.021
1.0	-	-	-	-	0.024
1.75	-	-	-	-	0.041
2.0	0.48	$2.62x10^{-1}$	0.52	$1.70x10^{-2}$	0.050
2.5	-	-	-	-	0.063
3.0	0.85	$2.08x10^{-1}$	0.95	$6.47x10^{-3}$	0.114
3.5	-	-	-	-	0.156
4.0	0.94	$2.09x10^{-1}$	1.00	$8.04x10^{-3}$	0.231
4.5	-	-	-	-	0.335
5.0	0.80	$2.85x10^{-1}$	0.80	$4.16x10^{-2}$	0.460
5.5	-	-	-	-	0.660
6.0	1.94	$3.52x10^{-1}$	1.79	$4.59x10^{-2}$	0.800
6.5	-	-	-	-	0.960
7.0	1.21	$1.73x10^{-1}$	1.23	$3.67x10^{-2}$	1.250
7.5	-	-	-	-	1.610
8.0	1.37	$4.95x10^{-1}$	1.37	$1.57x10^{-1}$	1.900
8.5	-	-	-	-	2.190
9.0	1.41	$7.53x10^{-2}$	1.54	$5.32x10^{-3}$	2.520
10.0	1.28	$4.96x10^{-2}$	1.24	-	2.600
11.0	1.33	$5.24x10^{-2}$	1.25	$1.72x10^{-3}$	-
12.0	1.59	$7.79x10^{-1}$	1.66	$5.75x10^{-1}$	2.430
14.0	1.34	$6.15x10^{-1}$	1.23	$5.80x10^{-1}$	2.390
16.0	1.15	$3.38x10^{-1}$	1.19	$2.29x10^{-1}$	2.340
18.0	1.11	$4.70x10^{-1}$	1.23	$1.38x10^{-1}$	2.680
20.0	1.09	$8.06x10^{-1}$	1.10	$4.17x10^{-1}$	2.410
22.0	1.06	$7.75x10^{-1}$	1.00	$6.83x10^{-2}$	2.830
24.0	1.29	$5.92x10^{-1}$	1.46	$2.31x10^{-2}$	2.890

TABLE 47.

Data pertaining to Figure 75.

TIME OF IRRADIATION	Semi-enriched medium (SEM)		Histidine supplemented medium. (HSM)	
(min)	Low salt	High salt	Low salt	High salt
(i) SURVIVAL DATA.	SURVIVING FRACTIONS			
0	$\underline{4.12\times10^{7}}$	$\underline{3.90\times10^{7}}$	$\underline{3.97\times10^{7}}$	$\underline{4.30\times10^{7}}$
30	7.85×10^{-1}	7.56×10^{-1}	8.73×10^{-1}	6.05×10^{-1}
45	6.51×10^{-1}	8.70×10^{-2}	6.00×10^{-1}	8.30×10^{-2}
60	4.45×10^{-1}	1.24×10^{-2}	4.32×10^{-1}	8.50×10^{-3}
75	1.54×10^{-1}	8.90×10^{-4}	1.42×10^{-1}	6.23×10^{-4}
90	2.86×10^{-2}	4.90×10^{-4}	3.45×10^{-2}	1.80×10^{-4}
(ii) INDUCED MUTATION FREQUENCY DATA.				
0				
30				
45	NO MUTANTS OBSERVED ON ANY PLATES.			
60				
75				
90				

UNDERLINED VALUES = VIABLE COUNTS.

TABLE 48.

Data pertaining to Figure 76.

TIME OF IRRADIATION (min)	CORRECTED TIME (min)	SEMI-ENRICHED MEDIUM (SEM)			HISTIDINE SUPPLEMENTED MEDIUM (HSM)		
		SEM	Low salt SEM	High salt SEM	HSM	Low salt HSM	High salt HSM
(i) SURVIVAL DATA.		SURVIVING FRACTIONS					
0	0	$\underline{4.58\times10^{8}}$	$\underline{5.07\times10^{8}}$	$\underline{5.27\times10^{8}}$	$\underline{5.43\times10^{8}}$	$\underline{4.97\times10^{8}}$	$\underline{4.97\times10^{8}}$
10	9.1	8.28×10^{-1}	8.78×10^{-1}	9.97×10^{-1}	9.17×10^{-1}	9.21×10^{-1}	8.22×10^{-1}
20	18.3	1.00×10^{0}	1.02×10^{0}	9.44×10^{-1}	9.00×10^{-1}	9.68×10^{-1}	1.02×10^{0}
30	27.5	9.93×10^{-1}	1.04×10^{0}	1.02×10^{0}	9.77×10^{-1}	8.98×10^{-1}	9.83×10^{-1}
40	36.6	8.18×10^{-1}	8.88×10^{-1}	6.80×10^{-1}	7.79×10^{-1}	8.18×10^{-1}	7.42×10^{-1}
50	45.8	5.44×10^{-1}	6.70×10^{-1}	5.10×10^{-1}	5.31×10^{-1}	7.46×10^{-1}	4.31×10^{-1}
60	55.0	5.00×10^{-2}	5.90×10^{-2}	-	6.50×10^{-2}	2.44×10^{-1}	-

UNDERLINED VALUES = VIABLE COUNTS

(ii) INDUCED MUTATION FREQUENCY DATA.		INDUCED MUTATION FREQUENCIES					
0	0	40,35,30 *			20,16,18 *		
10	9.1	2.39×10^{-7}	NO	NO	2.38×10^{-7}	NO	NO
20	18.3	7.91×10^{-7}	MUTANTS	MUTANTS	6.61×10^{-7}	MUTANTS	MUTANTS
30	27.5	1.07×10^{-6}	DETECTED	DETECTED	7.32×10^{-7}	DETECTED	DETECTED
40	36.6	1.78×10^{-6}			1.53×10^{-6}		
50	45.8	3.65×10^{-6}			1.27×10^{-6}		
60	55.0	7.91×10^{-7}			3.07×10^{-6}		

* = PLATE MUTANTS FOR UNIRRADIATED CELLS

TABLE 49.

Data pertaining to Figure 77.

TIME OF IRRADIATION (min)	CORRECTED TIME (min)	HSM	HSM PLUS sodium chloride (100 mM)	HSM PLUS sodium chloride (200 mM)	HSM HALF STRENGTH inorganic salts	HSM LOW SALT PLUS $MgSO_4.7H_2O$ (0.81 mM)	HSM LOW SALT PLUS NH_4Cl (18.7 mM)
(i) **SURVIVAL DATA.**				SURVIVING FRACTIONS			
0	0	$\underline{8.13\times10^{8}}$	$\underline{7.50\times10^{8}}$	$\underline{7.20\times10^{8}}$	$\underline{8.25\times10^{8}}$	$\underline{8.17\times10^{8}}$	$\underline{7.83\times10^{8}}$
10	8.7	9.11×10^{-1}	8.24×10^{-1}	8.30×10^{-1}	8.34×10^{-1}	8.17×10^{-1}	8.13×10^{-1}
20	17.4	8.50×10^{-1}	8.36×10^{-1}	7.98×10^{-1}	8.11×10^{-1}	8.53×10^{-1}	8.87×10^{-1}
30	26.1	6.86×10^{-1}	6.54×10^{-1}	4.25×10^{-1}	9.07×10^{-1}	7.56×10^{-1}	8.68×10^{-1}
40	34.8	6.84×10^{-1}	4.46×10^{-1}	1.08×10^{-1}	6.71×10^{-1}	7.24×10^{-1}	6.52×10^{-1}
50	43.5	4.78×10^{-1}	2.40×10^{-1}	1.82×10^{-2}	5.73×10^{-1}	6.52×10^{-1}	5.44×10^{-1}
60	52.2	2.88×10^{-1}	5.10×10^{-2}	1.44×10^{-3}	3.18×10^{-1}	3.82×10^{-1}	2.87×10^{-1}
70	60.9	3.00×10^{-2}	2.20×10^{-3}	8.10×10^{-4}	6.40×10^{-2}	9.50×10^{-2}	3.80×10^{-2}

UNDERLINED VALUES = VIABLE COUNTS

(ii) **INDUCED MUTATION FREQUENCY DATA.**				INDUCED MUTATION FREQUENCIES			
0	0	11,11,11 *	8,7,7, *	4,3,3, *			
10	8.7	5.32×10^{-7}	2.94×10^{-7}	2.45×10^{-7}	NO	NO	NO
20	17.4	6.61×10^{-7}	4.72×10^{-7}	2.08×10^{-7}	MUTANTS	MUTANTS	MUTANTS
30	26.1	4.83×10^{-7}	7.60×10^{-7}	6.32×10^{-7}	DETECTED	DETECTED	DETECTED
40	34.8	1.19×10^{-6}	5.71×10^{-7}	1.41×10^{-6}			
50	43.5	1.34×10^{-6}	-	1.68×10^{-5}			
60	52.3	2.12×10^{-6}	-	1.77×10^{-5}			
70	60.9	4.70×10^{-6}	-	-			

* = PLATE MUTANTS FOR UNIRRADIATED CELLS.

TABLE 50.

Data pertaining to Figure 78.

TIME OF IRRADIATION (min)	CORRECTED TIME (min)	MOPS HSM	MOPS HSM PLUS sodium chloride (50 mM)	TENFOLD-DILUTED MOPS HSM	TENFOLD-DILUTED MOPS HSM PLUS sodium chloride (50 mM)
(i) **SURVIVAL DATA.**			SURVIVING FRACTIONS		
0	0	$\underline{6.12\times10^{8}}$	$\underline{6.22\times10^{8}}$	$\underline{6.16\times10^{8}}$	$\underline{6.19\times10^{8}}$
20	18.3	8.56×10^{-1}	8.32×10^{-1}	8.90×10^{-1}	8.74×10^{-1}
30	27.5	8.26×10^{-1}	8.26×10^{-1}	9.20×10^{-1}	8.76×10^{-1}
40	36.6	8.35×10^{-1}	1.00×10^{0}	8.70×10^{-1}	9.22×10^{-1}
50	45.8	9.32×10^{-1}	8.02×10^{-1}	7.60×10^{-1}	8.43×10^{-1}
60	55.0	-	-	7.20×10^{-1}	8.24×10^{-1}
		UNDERLINED VALUES = VIABLE COUNTS.			
(ii) **INDUCED MUTATION FREQUENCY DATA.**			INDUCED MUTATION FREQUENCIES		
0	0	10,11,6, *	13,10,8, *		
20	18.3	3.28×10^{-7}	2.92×10^{-7}	NO	NO
30	27.5	3.20×10^{-7}	5.56×10^{-7}	MUTANTS	MUTANTS
40	36.6	5.18×10^{-7}	5.70×10^{-7}	DETECTED	DETECTED
50	45.8	4.23×10^{-7}	7.61×10^{-7}		
60	55.0	-	-		

* = PLATE MUTANTS FOR UNIRRADIATED CELLS.

TABLE 51.

Data pertaining to Figure 79.

TIME OF IRRADIATION (min)	CORRECTED TIME (min)	HSM	HSM PLUS sodium chloride (25 mM)	HSM PLUS sodium chloride (50 mM)	HSM PLUS sodium chloride (75 mM)
(i) **SURVIVAL DATA.**			SURVIVING FRACTIONS		
0	0	$\underline{6.73\times10^{8}}$	$\underline{6.05\times10^{8}}$	$\underline{6.45\times10^{8}}$	$\underline{6.42\times10^{8}}$
20	18.3	8.95×10^{-1}	9.52×10^{-1}	9.90×10^{-1}	8.97×10^{-1}
30	27.5	7.67×10^{-1}	7.46×10^{-1}	7.57×10^{-1}	7.08×10^{-1}
40	36.6	6.57×10^{-1}	5.79×10^{-1}	4.72×10^{-1}	3.78×10^{-1}
45	41.2	-	-	-	1.62×10^{-1}
50	45.8	4.20×10^{-1}	3.70×10^{-1}	2.22×10^{-1}	1.29×10^{-1}
60	55.0	2.18×10^{-1}	1.87×10^{-1}	9.20×10^{-2}	-
		UNDERLINED VALUES = VIABLE COUNTS			
(ii) **INDUCED MUTATION FREQUENCY DATA.**			INDUCED MUTATION FREQUENCIES.		
0	0	11,24,16, *	13,14,15, *	8,14,6, *	8,12,8, *
20	18.3	4.25×10^{-7}	2.68×10^{-7}	3.61×10^{-7}	2.31×10^{-7}
30	27.5	4.83×10^{-7}	4.19×10^{-7}	5.48×10^{-7}	3.59×10^{-7}
40	36.6	6.19×10^{-7}	4.23×10^{-7}	6.16×10^{-7}	6.17×10^{-7}
45	41.2	-	-	-	5.13×10^{-7}
50	45.8	6.22×10^{-7}	5.62×10^{-7}	1.00×10^{-6}	1.04×10^{-6}
60	55.0	1.58×10^{-6}	1.06×10^{-6}	2.02×10^{-6}	-

* PLATE MUTANTS FOR UNIRRADIATED CELLS.

Appendix B.

STATISTICAL ANALYSIS.

Least Squares Regression Analysis.

When a linear relationship is assumed to exist between two variables it is usual to fit a straight line by a least squares regression analysis. The simplest statistical model for this assumes that the independent variable (x) is known without error of measurement and that the corresponding measured values of the dependent variable (y) are scattered normally from their true values. Hence each value of y_i of the dependent is normally distributed about the mean, with a variance σ^2.

The method of least squares obtains estimates of c and m in the equation $y = mx + c$ such that the sum of the squares of the deviations of the observations y_i from their mean is a minimum.

These values are:-

$$m = \frac{n\Sigma x_i y_i - \Sigma x_i \Sigma y_i}{n \Sigma x_i^2 - \left[\Sigma x_i\right]^2}$$

$$= \frac{\sum (x_i - \bar{x})(y_i - \bar{y})}{\sum (x_i - \bar{x})^2}$$

$$c = \frac{\sum y_i - m \sum x_i}{n}$$

$$= \bar{y} - m\bar{x}$$

n is the number of points on the line.

B I B L I O G R A P H Y

ADELBERG, E.A. and BURNS, S.N. (1960)
J. Bacteriol. 79, 321-330.
Genetic variation in the sex factor of Escherichia coli.

AHMED, A.H. (1983)
PhD Thesis, University of Bath.

ALBRIGHT, F.R., WHITE, D.A. and LENNARZ, W.J. (1973)
J. Biol. Chem. 248, 3968-3977.
Studies on enzymes involved in the catabolism of phospholipids in Escherichia coli.

ALLWOOD, M.C. and RUSSELL, A.D. (1967)
Appl. Microbiol. 15, 1266-1269.
Mechanism of thermal injury in Staphylococcus aureus.
1. Relationship between viability and leakage.

ANANTHASWAMY, H.N., HARTMAN, P.S. and EISENSTARK, A. (1979)
Photochem. Photobiol. 29, 53-56.
Synergistic lethality of phage T7 by near-UV radiation and hydrogen peroxide : An action spectrum.

ANDERSON, E.H. (1946)
Proc. Natl. Acad. Sci. (USA) 32, 120-128.
Growth requirements of virus-resistant mutants of Escherichia coli strain B.

ASCENZI, J.M. and JAGGER, J. (1979)
Photochem. Photobiol. 30, 661-666.
Ultraviolet action spectrum (238-405 nm) for inhibition of glycine uptake in E. coli.

BACHMANN, B. (1972)
Bacteriol. Rev. 36, 525-557.
Pedigrees of some mutant strains of Escherichia coli.

BACHMANN, B.J. and BROOKS-LOW, K. (1980)
Microbiol. Rev. 44, 1-56.
Linkage map of Escherichia coli K-12. Edition 6.

BARRAN, L.R., D'AOUST, J.Y., LABELLE, J.L., MARTIN, W.G. and SCHNEIDER, H. (1974)
Biochem. Biophys. Res. Commun. 56, 522-528.
Differential effects of visible light on active transport in E. coli.

BEUKERS, R., IJLSTRA, J. and BERENDS, W. (1960)
Rec. Trav. Chim. 79, 101-104.
The effect of UV on some components of the nucleic acids. 6) The origin of the UV sensitivity of DNA.

BLUMBERG, P.M. and STROMINGER, J.L. (1974)
Bacteriol. Rev. 38, 291-335
Interaction of penicillin with the bacterial cell: Penicillin-binding proteins and penicillin-sensitive enzymes.

BOYCE, R.P. and HOWARD-FLANDERS (1964)
Proc. Natl. Acad. Sci. (USA) 51, 293-301.
Release of ultraviolet light-induced thymine dimers from DNA in E. coli K-12.

BRAGG, P.D. (1971)
Can. J. Biochem. 49, 492-495.
Effect of near-ultraviolet light on the respiratory chain of Escherichia coli.

BRIDGES, B.A. and MOTTERSHEAD, R.P. (1978)
Mutat. Res. 52, 151-159.
Mutagenic DNA repair in Escherichia coli. VII. Constitutive and inducible manifestations.

BROWN, M.S. and WEBB, R.B. (1972)
Mutat. Res. 15, 348-352.
Photoreactivation of 365 nm inactivation in Escherichia coli.

BRUCE, A.K. (1958)
J. Gen. Physiol. 41, 693-702.
Response of potassium retentivity and survival of yeast to far-ultraviolet, near-ultraviolet and visible, and X-radiation.

BURCHARD, R.P. and DWORKIN, M. (1966)
J. Bacteriol. 91, 535-545.
Light-induced lysis and carotenogenesis in Myxococcus xanthus.

BUSTA, F.F. and JEZESKI, J.J. (1963)
Appl. Microbiol. 11, 404-407.
Effect of sodium chloride concentration in an agar medium on growth of heat-shocked Staphylococcus aureus.

CABRERA-JUÁREZ, E. and ESPINOSA-LARA, M. (1974)
J. Bacteriol. 117, 960-964.
Lethal and mutagenic action of black light (325-400 nm) on Haemophilus

influenzae in the presence of air.

CABRERA-JUÁREZ, E. and SETLOW, J.K. (1977)
Biochem. Biophys. Acta. 475, 315-322.
Formation of a thymine photoproduct in transforming DNA by near-UV irradiation.

CABRERA-JUÁREZ, E., SETLOW, J.K., SWENSON, P.A. and PEAK, M.J. (1976)
Photochem. Photobiol. 23, 309-313.
Oxygen-independent inactivation of Haemophilus influenzae transforming DNA by monochromatic radiation: action spectrum, effect of histidine and repair.

CHILDS, C.B. (1962)
Applied Optics 1, 711-716.
Low pressure mercury arc for ultraviolet calibration.

CHENG, L., KELLOGG, E.W. and PACKER, L. (1981)
Photochem. Photobiol. 34, 125-129.
Photoinactivation of catalase.

CLARK, C.W. and ORDAL, Z.J. (1969)
Appl. Microbiol. 18 , 332-336.
Thermal injury and recovery of Salmonella typhimurium and its effect on enumeration procedures.

CLAYTON, R.K. (1971)
Damage and repair of damage by light.
In Light and living matter Vol.2, pp. 190-194. McGraw-Hill, New Jersey.

COOK, J.S. (1975)
Photopathology of the erythrocyte membrane.
In Pathobiology of cell membranes.(Edited by B.F. Trump and A. Arstilla) Vol.1, pp. 199-213. Academic Press, New York.

CRONAN, J.E. Jr. (1968)
J. Bacteriol. 95, 2054-2061.
Phospholipid alterations during growth of Escherichia coli.

CRONAN, J.E. Jr. and GELMANN. E.P. (1975)
Bacteriol. Rev. 39, 232-256.
Physical properties of membrane lipids: biological relevance and regulation.

CRONAN, J.E. Jr. (1978)
Ann. Rev. Biochem. 47, 163-189.
Molecular biology of bacterial membrane lipids.

D'AOUST, J.Y., GIROUX, J., BARRAN, L.R., SCHNEIDER, H. and MARTIN, W.G. (1974)
J. Bacteriol. 120, 799-804.
Some effects of visible light on E. coli.

DALY, J.J., BAKER, M.L. and BURTON, S.B. (1981)
Photochem. Photobiol. 33, 191-195.
The sensitivity of Trichomonas vaginalis and Trichomonas gallinae to ultraviolet radiation.

DAVIS, B.D., DULBECCO, R., EISEN, H.N. and GINSBERG, H.S. (1980)
In Microbiology 3rd Ed. pp. 73-110. Harper and Row, Hagerstown.

DE MORAES, E.C. and TYRRELL, R.M. (1983)
Photochem. Photobiol. 38, 57-63.
Mutational interactions between near-UV radiation and DNA damaging agents in Escherichia coli: The role of near-UV-induced modifications in growth and macromolecular synthesis.

DEMPLE, B., HALBROOK, J. and LINN, S. (1983)
J. Bacteriol. 153, 1079-1082.
Escherichia coli xth mutants are hypersensitive to hydrogen peroxide.

DIAMOND, R.J. and ROSE, A.H. (1970)
J. Bacteriol. 102, 311-319.
Osmotic properties of spheroplasts from Saccharomyces cerevisiae grown at different temperatures.

DOUGHTY, C.J. and HOPE, A.B. (1973)
J. Membrane Biol. 13, 185-198.
Effects of ultraviolet radiation on the membranes of Chara corallina.

DOYLE, R.J. and KUBITSCHEK, H.E. (1976)
Photochem. Photobiol. 24, 291-293.
Near-ultraviolet light inactivation of an energy-independent membrane transport system in Saccharomyces cerevisiae.

DURHAM, N.M. and WYSS, O. (1956)
J. Bacteriol. 72, 95-100.
An example of non-inherited radiation resistance.

EGAN, A.F. and RUSSELL, R.R.B. (1973)
Genet. Res. 21, 139-152.
Conditional mutants affecting the cell envelope of Escherichia coli K-12.

EISENSTARK, A. (1970)
Mutat. Res. 10, 1-6.
Sensitivity of Salmonella typhimurium recombinationless (rec) mutants to visible and near-visible light.

EISENSTARK, A. (1971)
Mutagenic and lethal effects of visible and near-ultraviolet light on bacterial cells.
In Advances in Genetics 16, pp. 167-198. Academic Press, London.

EPSTEIN, W. and DAVIES, M. (1970)
J. Bacteriol. 101, 836-843.
Potassium-dependent mutants of Escherichia coli K-12.

FONG, F., PETERS, J., PAULING, C. and HEATH, R.L. (1975)
Biochim. Biophys. Acta. 387, 451-460.
Two mechanisms of near-ultraviolet lethality in Saccharomyces cerevisiae: A respiratory capacity-dependent and an irreversible inactivation.

FORBES, P.D., DAVIES, R.E., D'ALOISIO, L.C. and COLE, C. (1976)
Photochem. Photobiol. 24, 613-615.
Emission spectrum differences in fluorescent Blacklight lamps.

GALE, E.F., CUNDLIFFE, E., REYNOLDS, P.E., RICHMOND, M.H. and WARING, M.J. (1981)
In The Molecular Basis of Antimicrobial Action 2nd Ed. pp. 137-143. Wiley, London.

GARROD, L.P., LAMBERT, H.P. and O'GRADY, F. (1981)
In Antibiotic and Chemotherapy, 5th Ed. pp. 155-168. Churchill Livingstone, Edinburgh.

GATES, F.L. (1930)
J. Gen. Physiol. 14, 31-42.
A study of the bactericidal action of UV light. III. The absorption of ultraviolet light by bacteria.

GILLIES, N.E., OBIOHA, F.I. and RATNAJOTHI, N.H. (1979)
Int. J. Radiat. Biol. 36, 587-594.
An oxygen dependent X-ray lesion in Escherichia coli strain B/r

detected by penicillin.

GINSBERG, D.M. and JAGGER, J. (1965)
J. Gen. Microbiol. 40, 171-184.
Evidence that initial ultraviolet lethal damage in Escherichia coli strain 15 T⁻ A⁻ U⁻ is independent of growth phase.

GRAU, F.H. (1978)
Appl. Environ. Microbiol. 36, 230-236.
Significance of the inactivation of transport in thermal death of Escherichia coli.

GREEN, M.H.L., ROTHWELL, M.A. and BRIDGES, B.A. (1972)
Mutat. Res. 16, 225-234.
Mutation to prototrophy in Escherichia coli K-12 : Effect of broth on UV-induced mutation in strain AB 1157 and four excision-deficient mutants.

GROSS, J. and GROSS, M. (1969)
Nature (London) 224, 1166-1168.
Genetic analysis of an E. coli strain with a mutation affecting DNA polymerase.

HANAWALT, P.C. (1966)
Photochem. Photobiol. 5, 1-12.
The UV sensitivity of bacteria : Its relation to the DNA replication cycle.

HANAWALT, P.C., FRIEDBERG, E.C. and FOX, C.F. (1978)
In DNA Repair Mechanisms, Academic Press, New York.

HARIHARAN, P.V. and CERUTTI, P.A. (1977)
Biochem. 16, 2791-2795.
Formation of products of the 5,6,-dihydroxydihydrothymine type by ultraviolet light in HeLa cells.

HARRISON, A.P.Jr. (1967)
Ann. Rev. Microbiol. 21, 143-156.
Harmful effects of light, with some comparisons with other adverse physical agents.

HARTMAN, P.S. and EISENSTARK, A. (1978)
J. Bacteriol. 133, 769-774.
Synergistic killing of E. coli by near-UV radiation and hydrogen peroxide : Distinction between recA-repairable and recA-nonrepairable damage.

HARTMAN, P.S., EISENSTARK, A. and PAUW, P.G. (1979)
Proc. Natl. Acad. Sci. (USA) 76, 3228-3232.
Near-ultraviolet radiation plus H_2O_2 inactivation of phage T7 :DNA-protein crosslinks prevent DNA injection.

HATCHARD, C.G. and PARKER, C.A. (1956)
Roy. Soc.(London) Proc., A235, 518-536.
A new sensitive chemical actinometer. II. Potassium ferrioxalate as a standard chemical actinometer.

HAYES, F.N. and GOULD, R.G. (1952)
Science 117, 480-482.
Liquid scintillation counting of tritium labelled water and organic compounds.

HELMSTETTER, C.E. and URETZ, R.B. (1963)
Biophys. J. 3, 35-47.
X-ray and ultraviolet sensitivity of synchronously dividing Escherichia coli.

HILL, R.F. and FEINER, R.R. (1964)
J. Gen. Microbiol. 35, 105-114.
Further studies of UV sensitive mutants of E. coli strain B.

HODGES, N.D.M. (1979)
PhD thesis, University of Bath.

HOLLAENDER, A. (1943)
J. Bacteriol. 46, 531-541.
Effect of long ultraviolet and short visible radiation (3500 to 4900 ^{o}A) on Escherichia coli.

HOWARD-FLANDERS, P., BOYCE, R.P. and THERIOT, L. (1966)
Genetics 53, 1119-1136.
Three loci in Escherichia coli that control the excision of pyrimidine dimers and certainother mutagen products from DNA.

HURST, A., HUGHES, A., BEARE-ROGERS, J.L. and COLLINS-THOMPSON, D.L. (1973)
J. Bacteriol. 116, 901-907.
Physiological studies on recovery of salt tolerance by Staphylococcus aureus after sub-lethal heating.

HURST, A., HUGHES, A., COLLINS-THOMPSON, D.L. and SHAH, B.G. (1974)
Can. J. Microbiol. 20, 1153-1158.

Relationship between loss of magnesium and loss of salt tolerance after sublethal heating of Staphylococcus aureus.

HURST, A., HENDRY, G.S., HUGHES, A. and PALEY, B. (1976)
Can. J. Microbiol. 22, 677-683.
Enumeration of sublethally heated Staphylococci in some dried foods.

IANDOLO, J.J. and ORDAL, Z.J. (1966)
J. Bacteriol. 91, 137-142.
Repair of thermal injury of Staphylococcus aureus.

INOUYE, M. (1979)
In Bacterial outer membranes. Biogenesis and functions. pp. 1-12. John Wiley & sons, New York.

ITO, A. and ITO, T. (1983)
Photochem. Photobiol. 37, 395-401.
Possible involvement of membrane damage in the inactivation by broad-band near-UV radiation in Saccharomyces cerevisiae cells.

JAGGER, J. (1967)
In Introduction to research in ultraviolet photobiology. pp. 137-139
Prentice-Hall Inc., Englewood Cliffs New Jersey.

JAGGER, J. (1972)
Growth delay and photoprotection induced by near-ultraviolet light. In Research Progress in Organic, Biological and Medicinal Chemistry
Edited by U. Gallo and L. Santamaria. Vol. 3, North-Holland, Amsterdam.

JAGGER, J. (1981)
Photochem. Photobiol. 34, 761-768.
Yearly Review: Near-UV radiation effects on microorganisms.

JAGGER, J., WISE, W.C. and STAFFORD, R.S. (1964)
Photochem. Photobiol. 3, 11-24.
Delay in growth and division induced by near ultraviolet radiation in Escherichia coli B and its role in photoprotection and liquid holding recovery.

JAGGER, J., FOSSUM, T. and McCAUL, S. (1975)
Photochem. Photobiol. 21, 379-382.
Ultraviolet irradiation of suspensions of micro-organisms : Possible errors involved in the estimation of average fluence per cell.

KAPUSCINSKI, R.B. and MITCHELL, R. (1981)

Appl.& Environ. Microbiol. 41, 670-674.
Solar radiation induces sublethal injury in Escherichia coli in seawater.

KASHKET, E.R. and BRODIE, A.F. (1962)
J. Bacteriol. 83, 1094-1100.
Effects of near-ultraviolet irradiation on growth and oxidative metabolism of bacteria.

KELNER, A. (1949)
J. Bacteriol. 58, 511-522.
Photoreactivation of UV irradiated E. coli with special reference to the dose reduction principle and to UV induced mutation.

KEYSE, S.M. (1983)
PhD Thesis, University of Bath.

KEYSE, S.M., MOSS, S.H. and DAVIES, D.J.G. (1983)
Photochem. Photobiol. 37, 307-312.
Action spectra for inactivation of normal and xeroderma pigmentosum human skin fibroblasts by ultraviolet radiations.

KLAMEN, D.L. and TUVESON, R.W. (1982)
Photochem. Photobiol. 35, 167-173.
The effect of membrane fatty acid composition on the near-UV (300-400 nm) sensitivity of Escherichia coli K1060.

KLEIN, R.A. (1970)
Biochem. Biophys. Acta. 210, 486-489.
The detection of oxidation in liposome preparations.

KOCH, A.L., DOYLE, R.J. and KUBITSCHEK, H.E. (1976)
J. Bacteriol. 126, 140-146.
Inactivation of membrane transport in Escherichia coli by near-ultraviolet light.

KUBITSCHEK, H.E. (1967)
Science 155, 1545-1546.
Mutagenesis by near-ultraviolet light.

KUBITSCHEK, H.E. and PEAK, M.J. (1980)
Photochem. Photobiol. 31, 55-58.
Action spectrum for growth delay induced by near-ultraviolet light in E. coli B/r K.

KUBITSCHEK, H.E. and DOYLE, R.J. (1981)
Photochem. Photobiol. 33, 695-702.
Growth delay induced in Escherichia coli by near-ultraviolet radiation : Relationship to membrane transport functions.

KUBITSCHEK, H.E., FINNEY, A.C. and KRISCH, R.E. (1973)
Photochem. Photobiol. 18, 365-370.
Constancy of the UV sensitivity of E. coli during the cell cycle.

LAKCHAURA, B.D., FOSSUM, T. and JAGGER, J. (1976)
J. Bacteriol. 125, 111-118.
Inactivation of Adenosine 5'- Triphosphate synthesis and reduced-form Nicotinamide Adenine Dinucleotide Dehydrogenase activity in E. coli by near-UV and violet radiations.

LAMOLA, A.A. (1977)
Photodegradation of biomembranes. In Research in Photobiology, Edited by A. Castellani. pp. 53-63. Plenum Press, New York.

LEA, D.E. (1955)
In Actions of radiation on living cells. 2nd Ed., Cambridge University Press, New York.

LEHMANN, A.R. and BRIDGES, B.A. (1977)
Essays in Biochem. 13, 71-117.
DNA repair.

LEHMANN, A.R. and KARRAN, P. (1981)
Int. Rev. Cytology. 72, 101-146.
DNA Repair.

LEY, R.D., SEDITA, B.A. and BOYE, E. (1978)
Photochem. Photobiol. 27, 323-327.
DNA polymerase 1-mediated repair of 365 nm-induced single-strand breaks in the DNA of Escherichia coli.

LUCKIESH, M. (1946)
In Applications of Germicidal, Erythemal and Infrared energy. Van Nostrand, New York.

MACKAY, D., EISENSTARK, A., WEBB, R.B. and BROWN, M.S. (1976)
Photochem. Photobiol. 24, 337-343.
Action spectra for lethality in recombinationless strains of Salmonella typhimurium and Escherichia coli.

MADDEN, J.J., BOATWRIGHT, D.T. and JAGGER, J. (1981)
Photochem. Photobiol. 33, 305-311.
Action spectra for modification of E. coli B/r menaquinone by near-UV and visible radiations (313-578 nm).

MANDAL, T.K. and CHATTERJEE, S.N. (1980)
Radiat. Res. 83, 290-302.
Ultraviolet and sunlight-induced lipid peroxidation in liposomal membrane.

MARR, A.G. and INGRAHAM, J.L. (1962)
J. Bacteriol. 84, 1260-1267.
Effect of temperature on the composition of fatty acids in Escherichia coli.

MARTIN, S.E., FLOWERS, R.S. and ORDAL, Z.J. (1976)
Appl. & Environ. Microbiol. 32, 731-734.
Catalase :Its effect on microbial enumeration.

MATHEWS, M.M. and SISTROM, W.R. (1959)
Nature (London) 184, 1892-1893.
Function of carotenoid pigments in non-photosynthetic bacteria.

MATHEWS, M.M. and KRINSKY, N.I. (1965)
Photochem. Photobiol. 4, 813-817.
The relationship between carotenoid pigments and resistance to radiation in non-photosynthetic bacteria.

MERLIE, J.P. and PIZER, L.I. (1973)
J. Bacteriol. 116, 355-366.
Regulation of phospholipid sysnthesis in Escherichia coli by guanosine tetraphosphate.

MOROWITZ, H. (1950)
Science 111, 229-230.
Absorption effects in volume irradiation of micro-organisms.

MORTON, R.A. and HAYNES, R.H. (1969)
J. Bacteriol. 97, 1379-1385.
Changes in the ultraviolet sensitivity of Escherichia coli during growth in batch cultures.

MOSS, S.H. and DAVIES, D.J.G. (1974)
J. Bacteriol. 120, 15-23.
Interrelationship of repair mechanisms in ultraviolet-irradiated Escherichia coli.

MOSS, S.H. and SMITH, K.C. (1981)
Photochem. Photobiol. 33, 203-210.
Membrane damage can be a significant factor in the inactivation of Escherichia coli by near-ultraviolet radiation.

MUNAKATA, N. and RUPERT, C.S. (1972)
J. Bacteriol. 111, 192-198.
Genetically controlled removal of spore photoproduct from DNA of UV irradiated B. subtilis spores.

MURPHY, T.M. and WILSON, C. (1982)
Plant Physiol. 70, 709-713.
UV-stimulated K^+ efflux from Rose cells.

NEIDHARDT, F.C., BLOCH, P.L. and SMITH, D.F. (1974)
J. Bacteriol. 119, 736-747.
Culture medium for Enterobacteria.

OLCERST, R.B., BELMAN, S., EISENBUD, M., MUMFORD, W.W. and RABINOWITZ, J.R. (1980)
Radiat. Res. 82, 244-256.
The increased passive efflux of sodium and rubidium from rabbit erythrocytes by microwave radiation.

OLDMIXON, E. and BRAUN, V. (1978)
Biochim. Biophys. Acta. 506, 111-118.
Changes in fluorescence of 8-anilino-1-naphthalene sulfonate after bacteriophage T5 infection of Escherichia coli. Initial fluorescence rise coincides with onset of rubidium efflux.

OVERATH, P., SCHAIRER, H.V. and STOFFEL, W. (1970)
Proc. Natl. Acad. Sci. (USA), 67, 606-612.
Correlation of in vivo and in vitro phase transitions of membrane lipids in Escherichia coli.

PEAK, M.J. (1970)
Photochem. Photobiol. 12, 1-8.
Some observations on the lethal effects of near-UV light on Escherichia coli, compared with the lethal effects of far-ultraviolet light.

PEAK, M.J. and PEAK, J.G. (1978)
Radiat. Res. 76, 325-330.
Action spectra for ultraviolet and visible light inactivation of phage T7 : Effect of host-cell reactivation.

PEAK, M.J. and PEAK, J.G. (1982)
Photochem. Photobiol. 35, 675-680.
Single-strand breaks induced in Bacillus subtilis DNA by ultraviolet light : Action spectrum and properties.

PEAK, M.J., PEAK, J.G. and WEBB, R.B. (1973)
Mutat. Res. 20, 129-135.
Inactivation of transforming DNA by ultraviolet light : 1. Near-UV action spectrum for marker inactivation.

PEAK, M.J., PEAK, J.G. and NERAD, L. (1983a)
Photochem. Photobiol. 37, 169-172.
The role of 4-thiouridine in lethal effects and in DNA backbone breakage caused by 334 nm ultraviolet light in Escherichia coli.

PEAK, M.J., PEAK, J.G. and TUVESON, R.W. (1983b)
Photochem. Photobiol. 38, 541-543.
Ultraviolet action spectra for aerobic and anaerobic inactivation of Escherichia coli strains specifically sensitive and resistant to near ultraviolet radiations.

PETERS, J. (1977)
Nature (London), 267, 546-548.
In vivo photoinactivation of Escherichia coli ribonucleotide reductase by near-ultraviolet light.

PETERS, J. and JAGGER, J. (1981)
Nature (London), 289, 194-195.
Inducible repair of near-UV radiation lethal damage in E. coli.

PIERSON, M.D., TOMLINS, R.I. and ORDAL, Z.J. (1971)
J. Bacteriol. 105, 1234-1236.
Biosynthesis during recovery of heat-injured Salmonella typhimurium.

POLAKIS, S.E., GUCHHAIT, R.B. and LANE, M.D. (1973)
J. Biol. Chem. 248, 7957-7966.
Stringent control of fatty acid synthesis in Escherichia coli. Possible regulation of Acetyl coenzyme A by ppGpp.

RAMABHADRAN, T.V. and JAGGER, J. (1975)
Photochem. Photobiol. 21, 227-233.
Evidence against DNA as the target for 334 nm-induced growth delay in Escherichia coli.

RAMABHADRAN, T.V., FOSSUM, T. and JAGGER, J. (1976)
Photochem. Photobiol. 23, 315-321.

In vivo induction of 4-thiouridine - cytidine adducts in tRNA of *E. coli* B/r by near-ultraviolet radiation.

RAYMAN, M.K., ARIS, B. EL DEREA, H.B. (1978)
Can. J. Microbiol. **24**, 883-885.
Effects of compounds which degrade H_2O_2 on enumeration of heat-stressed cells of *S. senftenberg*.

REDPATH, J.L. and PATTERSON, L.K. (1978)
Radiat. Res. **75**, 443-447.
The effect of membrane fatty acid composition on the radiosensitivity of *E. coli* K1060.

ROBB, F.T., HAUMAN, J.H. and PEAK, M.J. (1978)
Photochem. Photobiol. **27**, 465-469.
Similar spectra for the inactivation by monochromatic light of two distinct leucine transport systems in *Escherichia coli*.

ROBB, F.T. and PEAK, M.J. (1979)
Photochem. Photobiol. **30**, 379-383.
Inactivation of the lactose permease of *Escherichia coli* by monochromatic UV light.

ROGERS, H.J., PERKINS, H.R. and WARD, J.B. (1980)
In *Microbial cell walls and membranes*. Chapman and Hall Ltd., London.

ROSENSTEIN, B.S. and DUCORE, J.M. (1983)
Photochem. Photobiol. **38**, 51-55.
Induction of DNA strand breaks in normal human fibroblasts exposed to monochromatic ultraviolet and visible wavelengths in the 240-546 nm range.

ROSHCHUPKIN, D.I., PELENITSYN, A.B., POTAPENKO, A.Y., TALITSKY, V.V. and VLADIMIROV, Y.A. (1975)
Photochem. Photobiol. **21**, 63-69.
Study of the effects of ultraviolet light on biomembranes- IV. The effect of oxygen on UV-induced haemolysis and lipid photoperoxidation in rat erythrocytes and liposomes.

RUPP, W.D. and HOWARD-FLANDERS, P. (1968)
J. Molec. Biol. **31**, 291-304.
Discontinuities in the DNA synthesized in an excision deficient strain of *Escherichia coli* following ultraviolet irradiation.

RUSSELL, A.D. and HARRIES, D. (1967)
Appl. Microbiol. **15**, 407-410.

Some aspects of thermal injury in Escherichia coli.

RYALS, J., HSU, R.Y., LIPSETT, M.N. and BREMER, H. (1982)
J. Bacteriol. 151, 899-904.
Isolation of single-site Escherichia coli mutants deficient in thiamine and 4-thiouridine syntheses : Identification of a nuv C mutant.

SAMMARTANO, L.J. and TUVESON, R.W. (1983)
J. Bacteriol. 156, 904-906.
Escherichia coli xth A mutants are sensitive to inactivation by broad spectrum near-UV (300-400 nm) radiation.

SCHERRER, R. and GERHARDT, P. (1973)
J. Bacteriol. 114, 888-890.
Influence of magnesium ions on porosity of the Bacillus megaterium cell wall and membrane.

SETLOW, R.B. and CARRIER, W.L. (1964)
Proc. Natl. Acad. Sci. (USA), 51, 226-231.
The disappearance of thymine dimers from DNA, an error correcting mechanism.

SHARMA, R.C. and JAGGER, J. (1981)
Photochem. Photobiol. 33, 173-177.
Ultraviolet (254-405 nm) action spectrum and kinetic studies of alanine uptake in Escherichia coli B/r.

SHARMA, R.C., WINGO, R.J. and JAGGER, J. (1981)
Photochem. Photobiol. 34, 529-533.
Roles of the rel A^+ gene and of 4-thiouridine in near-UV (334 nm) radiation inhibition of induced synthesis of tryptophanase in Escherichia coli B/r.

SIEGEL, S.M. and CORN, C. (1974)
Physiol. Plant 31, 267-270.
Thermal and ionic factors in the ultraviolet photolysis of plant cell membranes.

SILBERT, D.F. (1975)
Ann. Rev. Biochem. 44, 315-335.
Genetic modification of membrane lipid.

SINGER, S.J. and NICOLSON, G.L. (1972)
Science 175, 720-731.
The fluid mosaic model of the structure of cell membranes.

SMITH, K.C. (1977)
Ultraviolet radiation effects on molecules and cells. In The Science of Photobiology. pp. 113-142. Plenum Press, New York.

SPROTT, G.D., MARTIN, W.G. and SCHNEIDER, H. (1976)
Photochem. Photobiol. 24, 21-27.
Differential effects of near-UV and visible light on the active transport and other membrane processes in Escherichia coli.

SPROTT, G.D. and USHER, J.R. (1977)
Can. J. Microbiol. 23, 1683-1688.
The electrochemical proton gradient and phenylalanine transport in E. coli irradiated with near-ultraviolet light.

STORM, D.R. and STROMINGER, J.L. (1974)
J. Biol. Chem. 249, 1823-1827.
Binding of bacitracin to cells and protoplasts of Micrococcus lysodeikticus.

STORM, D.R. and TOSCANO, W.A. Jr. (1979)
In Antibiotics - Mechanism of action of antimicrobial agents. Edited by F.E. Hahn. Vol.5, pp. 1-17. Springer-Verlag, New York.

SUTHERLAND, B.M. (1977)
Photochem. Photobiol. 25, 413-414.
Symposium on molecular mechanisms in photoreactivation : Fundamentals of photoreactivation.

SUTHERLAND, J.C. and GRIFFIN, K.P. (1981)
Radiat. Res. 86, 399-409.
Absorption spectrum of DNA for wavelengths greater than 300 nm.

SWENSON, P.A. (1976)
Physiological responses of E. coli to far-UV radiation. In Photochemical and Photobiological Reviews, Edited by K.C. Smith, Vol. 1, pp. 269-387. Plenum Press, New York.

SWENSON, P.A. and SCHENLEY, R.L. (1974)
J. Bacteriol. 117, 551-559.
Evidence relating cessation of respiration, cell envelope changes, and death in ultraviolet-irradiated Escherichia coli B/r cells.

TABER, H., POMERANTZ, B.J. and HALFENGER, G.M. (1978)
Photochem. Photobiol. 28, 191-196.
Near-ultraviolet induction of growth delay studied in a menaquinone-deficient mutant of Bacillus subtilis.

THOMAS, G. and FAVRE, A. (1975)
Biochem. Biophys. Res. Commun. 66, 1454-1461.
4-Thiouridine as the target for near-ultraviolet induced growth delay in Escherichia coli.

TOMLINS, R.I. and ORDAL, Z.J. (1971)
J. Bacteriol. 105, 512-518.
Requirements of Salmonella typhimurium for recovery from thermal injury.

TOMLINS, R.I. and ORDAL, Z.J. (1976)
Thermal injury and inactivation in vegetative bacteria. In Inhibition and inactivation of vegetative microbes. Edited by F.A. Skinner and W.B. Hugo. pp.153-190. Academic Press, New York.

TOMLINS, R.I., VAALER, G.L. and ORDAL, Z.J. (1972)
Can. J. Microbiol. 18, 1015-1021.
Lipid biosynthesis during the recovery of Salmonella typhimurium from thermal injury.

TSAI, S.C. and JAGGER, J. (1981)
Photochem. Photobiol. 33, 825-834.
The roles of the rel^+ gene and of 4-thiouridine in killing and photoprotection of Escherichia coli by near-ultraviolet radiation.

TURNER, M.A. and WEBB, R.B. (1981)
J. Bacteriol. 147, 410-417.
Comparative mutagenesis and interaction between near-ultraviolet (313-405 nm) and far-ultraviolet (254 nm) radiation in Escherichia coli strains with differing repair capabilities.

TUVESON, R.W. (1980)
Photochem. Photobiol. 32, 703-705.
Genetic control of near-UV sensitivity independent of excision deficiency (uvrA6) in Escherichia coli K-12.

TUVESON, R.W. (1981)
Photochem. Photobiol. 33, 919-923.
The interaction of a gene (nur) controlling near-UV sensitivity and the pol A1 gene in strains of E. coli K-12.

TUVESON, R.W. and JONAS, R.B. (1979)
Photochem. Photobiol. 30, 667-676.
Genetic control of near-UV (300-400 nm) sensitivity independent of the rec A gene in strains of Escherichia coli K-12.

TUVESON, R.W. and VIOLANTE, E.V. (1982)
Photochem. Photobiol. 35, 845-847.
The effects of liquid holding on near-UV (300-400 nm) irradiated Escherichia coli strains differing in near and far-UV radiation sensitivity.

TUVESON, R.W., PEAK, J.G. and PEAK, M.J. (1983)
Photochem. Photobiol. 37, 109-112.
Single-strand DNA breaks induced by 365 nm radiation in E. coli strains differing in sensitivity to near and far UV.

TYRRELL, R.M. (1973)
Photochem. Photobiol. 17, 69-73.
Induction of pyrimidine dimers in bacterial DNA by 365 nm radiation.

TYRRELL, R.M. (1976)
Photochem. Photobiol. 23, 13-20.
Rec A^+-dependent synergism between 365 nm and ionising radiation in log-phase Escherichia coli : A model for oxygen-dependent near-UV inactivation by disruption of DNA repair.

TYRRELL, R.M. (1978a)
Photochem. Photobiol. 27, 571-579.
Solar dosimetry with repair deficient bacterial spores : Action spectra, photoproduct measurements and a comparison with other biological systems.

TYRRELL, R.M. (1978b)
Mutat. Res. 52, 25-35.
Mutagenic interaction between near-(365 nm) and far-(254 nm) ultraviolet radiation in repair-proficient and excision-deficient strains of Escherichia coli.

TYRRELL, R.M. (1978c)
Radiation synergism and antagonism. In Photochemical and Photobiological Reviews Vol.3. pp. 35-113. Edited by K.C. Smith. Plenum Press, New York.

TYRRELL, R.M. (1980)
Photochem. Photobiol. 31, 37-46.
Mutation induction by, and mutational interaction between monochromatic wavelength radiations in the near-UV and visible ranges.

TYRRELL, R.M. and WEBB, R.B. (1973)
Mutat. Res. 19, 361-364.
Reduced dimer excision in bacteria following near ultraviolet (365 nm) radiation.

TYRRELL, R.M. and PEAK, M.J. (1978)
J. Bacteriol. 136, 437-440.
Interactions between UV radiation of different energies in the inactivation of bacteria.

TYRRELL, R.M., MOSS, S.H. and DAVIES, D.J.G. (1972)
Mutat. Res. 16, 1-12.
The variation in UV sensitivity of four K-12 strains of Escherichia coli as a function of their stage of growth.

TYRRELL, R.M., WEBB, R.B. and BROWN, M.S. (1973)
Photochem. Photobiol. 18, 249-254.
Destruction of photoreactivating enzyme by 365 nm radiation.

TYRRELL, R.M., LEY, R.D. and WEBB, R.B. (1974)
Photochem. Photobiol. 20, 395-398.
Induction of single-strand breaks (alkali-labile bonds) in bacterial and phage DNA by near UV (365 nm) radiation.

WAGNER, S., TAYLOR, W.D., KEITH, A. and SNIPES, W. (1980)
Photochem. Photobiol. 32, 771-779.
Effects of acridine plus near ultraviolet light on Escherichia coli membranes and DNA in vivo.

WAGNER, S., FELDMAN, A. and SNIPES, W. (1982)
Photochem. Photobiol. 35, 73-81.
Recovery from damage induced by acridine plus near-ultraviolet light in Escherichia coli.

WATANABE, T., ITO, A. and ITO, T. (1982)
Photochem. Photobiol. 36, 599-602.
Early effects of near-ultraviolet radiation on yeast cells : Changes in cell size.

WEBB, R.B. (1977)
Lethal and mutagenic effects of near-ultraviolet radiation. In Photochemical and Photobiological Reviews, Edited by K.C. Smith. Vol. 2. pp. 169-261. Plenum Press, New York.

WEBB, R.B. (1978)
J. Bacteriol. 133, 860-866.
Near-UV mutagenesis : Photoreactivation of 365 nm-induced mutational lesions in Escherichia coli WP2s.

WEBB, R.B. and LORENZ, J.R. (1970)
Photochem. Photobiol. 12, 283-289.

Oxygen dependence and repair of lethal effects of near-ultraviolet and visible light.

WEBB, R.B. and MALINA, M.M. (1970)
Photochem. Photobiol. 12, 457-468.
Mutagenic effects of near ultraviolet and visible radiant energy on continuous cultures of E. coli.

WEBB, R.B. and BROWN, M.S. (1976)
Photochem. Photobiol. 24, 425-432.
Sensitivity of strains of Escherichia coli differing in repair capability to far-UV, near-UV and visible radiations.

WEBB, R.B. and BROWN, M.S. (1979a)
Radiat. Res. 80, 82-91.
Oxygen dependence of sensitization to 254 nm radiation by prior exposure to 365 nm radiation of Escherichia coli K-12 differing in DNA repair capability.

WEBB, R.B. and BROWN, M.S. (1979b)
Photochem. Photobiol. 29, 407-409.
Action spectra for oxygen-dependent and independent inactivation of Escherichia coli WP2s from 254 to 460 nm.

WEBB, R.B. and BROWN, M.S. (1979c)
Int. J. Radiat. Biol. 36, 671-676.
Lethality by 365 nm radiation in Escherichia coli K-12 AB 2480 in the presence of maximal photoreactivation under aerobic and anaerobic conditions.

WEBB, R.B. and PEAK, M.J. (1981)
Mutat. Res. 91, 177-182.
The effect of stray light in the 300-320 nm range and the role of cyclobutyl pyrimidine dimers in 365 nm lethality.

WEBB, R.B. and TURNER, M.A. (1981)
Mutat. Res. 84, 227-237.
Mutation induction by monochromatic 254 nm and 365 nm radiation in strains of Escherichia coli that differ in repair capability.

WEBB, R.B. and TUVESON, R.W. (1982)
Photochem. Photobiol. 36, 525-530.
Differential sensitivity to inactivation of nur and nur^+ strains of Escherichia coli at six selected wavelengths in the UVA, UVB and UVC ranges.

WEBB, R.B., BROWN, M.S. and TYRRELL. R.M. (1976)
Mutat. Res. 37, 163-172.
Lethal effects of pyrimidine dimers induced at 365 nm in strains of E. coli differing in repair capability.

WEBB, R.B., BROWN, M.S. and TYRRELL, R.M. (1978)
Radiat. Res. 74, 298-311.
Synergism between 365 and 254 nm radiations for inactivation of Escherichia coli.

WEBB, R.B., BROWN, M.S. and LEY, R.D. (1982)
Photochem. Photobiol. 35, 697-703.
Nonreciprocal synergistic lethal interaction between 365 nm and 405 nm radiation in wild type and uvrA strains of Escherichia coli.

WINGO, R.J., FOSSUM, T., LUO, S. and JAGGER, J. (1980)
Photochem. Photobiol. 32, 353-360.
Reduction by near-ultraviolet (334 nm) light of E. coli capacity for phage growth depends upon the rel gene and 4-thiouridine.

WRIGHT, L.A.Jr., MURPHY, T.M. and TRAVIS, R.L. (1981)
Photochem. Photobiol. 33, 343-348.
The effect of ultraviolet radiation on wheat root vesicles enriched in plasma membrane.

YATVIN, M.B. (1976)
Int. J. Radiat. Biol. 30, 571-575.
Evidence that survival of γ-irradiated Escherichia coli is influenced by membrane fluidity.

YOUNGS, D.A. AND SMITH, K.C. (1976)
J. Bacteriol. 125, 102-110.
Genetic control of multiple pathways of post-replicational repair in uvrB strains of Escherichia coli K-12.

YOUNGS, D.A., VAN der SCHUEREN, E. and SMITH, K.C. (1974)
J. Bacteriol. 117, 717-725.
Separate branches of the uvr gene-dependent excision repair process in UV irradiated E. coli K-12 cells. Their dependence upon growth medium and the polA,recA, recB and exrA genes.